UNIVERSITÀ DEGLI STUDI DELL'AQUILA

Dipartimento di Scienze Fisiche e Chimiche

Dottorato di Ricerca in Scienze Fisiche e Chimiche - XXXVII ciclo

Developing sustainable strategies for the construction of heterocycles and cyano-functionalization

SSD Chem05/A Organic Chemistry

Dottorando

Valerio Morlacci

Coordinatore del corso

Prof. Massimiliano Aschi

Tutor

Prof.ssa Laura Palombi

AA. 2023/2024

To my family

The work described in this thesis has been carried out at:

DSFC-Dipartimento di Scienze Fisiche e Chimiche
Università degli Studi dell'Aquila
L'Aquila, Italy

Faculty of Engineering and Science
School of Science
University of Greenwich
Chatham Maritime, UK

Summary

Abstract

This thesis presents the development of novel synthetic methods for the preparation of various nitrogen-containing heterocycles and polyheterocycles, utilizing greener and more sustainable methodologies. It also explores new electrochemical cyanation protocols that employ safer cyanide sources and/or milder reaction conditions.

The **Introduction** emphasizes the significance of heterocyclic compounds in everyday chemistry, briefly discussing their applications in pharmaceuticals and industry.

Chapter 1 introduces the isoindolinone core and its biological properties. The importance of cascade procedures in the synthesis of isoindolinone derivatives is also highlighted, with a particular focus on electrochemical methods. The chapter first details an electro-induced cascade reaction for synthesizing 3-*N*-aryl-substituted isoindolinones using catalytic amounts of current and supporting electrolyte. The method was then extended to synthesize isoindolinone-containing polyheterocycles exploiting the second reactivity of suitable electrophilic moieties at the *ortho*-position of the reagents. Finally, the chapter concludes by describing a one-pot cascade protocol for preparing a *C*-10-substituted batracylin analog using Cs_2CO_3, as the solely catalyst. A preliminary photophysical characterization of the attained analog is also reported.

Publications described in this chapter:

1) V. Morlacci, T. Caruso, M. Chiarini, A. Arcadi, M. Aschi, L. Palombi. Electrochemical-Induced Cascade Reaction of 2-Formyl Benzonitrile with Anilines: Synthesis of *N*-Aryl Isoindolinones. *Molecules* **2022**, *27*, 8199.
2) V. Morlacci, T. Caruso, M. Chiarini, V. Marsicano, A. Arcadi, L. Palombi. On Route to Diverse Nitrogen-Bridged Polyhetero-cycles with an *N*(acyl), *N*(aryl)-acetal Core. *ChemistrySelect* **2023,** *8*, e202301439.

3) V. Morlacci, M. Aschi, M. Chiarini, A. Massa, A. Arcadi, L. Palombi. Ethyl 2-(12-Oxo-10,12-dihydroisoindolo[1,2-b] Quinazolin-10-yl) Acetate. *Molbank* 2023, *2*, M1628.

Chapter 2 discusses the importance of nitrile group in organic chemistry, outlining the limitations of traditional cyanation protocols and the consequent need for safer cyanide sources and greener methods. Two novel electrochemical cyanation reactions are described: the cyanation of chalcones and imines through the catalytic electrochemical activation of acetone cyanohydrin, as cyanating agent; the exploration of the 5-aminotetrazole as a novel and safer CN surrogate, capable of generating both electrophilic and nucleophilic cyanide for the cyanation of a large range of substrates. This latter method was also optimized in flow-electrochemical systems.

Publications described in this chapter:

1) V. Morlacci, C. Momoli, M. Ndrita, M. Aschi, A. Arcadi, L. Palombi. Electrocatalytic Hydrogen Evolution Reaction Enabling Cyanation of Electron-poor Carbons with Acetone Cyanohydrin. *Eur. J. Org. Chem.* 2024, *27*, e202400236.
2) V. Morlacci, M. Milia, J. Saiter, I. P. Bhela, M. Leech, K. Lam. eCyanation Using 5-Aminotetrazole As a Safer Electrophilic and 2 Nucleophilic Cyanide Source. *JACS Au* 2024 (published)

Chapter 3 explores the advantages of combining of the Pictet-Spengler and Ugi four-component reactions for the first synthesis of 4-imidazolidinone-tetrahydro-β-carboline hybrids by means of TMSOTf as an effective mediator.

Publication described in this chapter:

1) V. Morlacci, A. Arcadi, M. Aschi, M. Chiarini, N. Demitri, D. Lamba, C. Momoli, L. Palombi, V. Vece. Diastereoselective Synthesis of High Functionalized 4-Imidazolidinone-Tetrahydro-β-Carboline Hybrids via Divergent Post-Ugi Transformation. *Adv. Synth. Cat.* 2024, *366*, 2376-2381.

Introduction

Heterocyclic compounds

Heterocyclic compounds are defined by IUPAC as "*cyclic compounds having as ring members atoms of at least two different elements* ",[1] primarily nitrogen, sulfur, and oxygen,[2] although other heteroatoms are also commonly found.[3] These compounds have a leading role in nature, with more than half of all natural products being heterocyclic systems. For instance, the presence of pyrimidine and purine bases in DNA and RNA, vitamin and coenzyme precursors, and amino acids such as proline and tryptophan, underscores the crucial role of heterocyclic compounds in everyday life.

Heterocyclic compounds find applications across various fields, including polymeric materials,[4] sensors,[5] and dyes.[6] However, their most significant use is in the medicinal and pharmaceutical industries (**Figure 1**).[7]

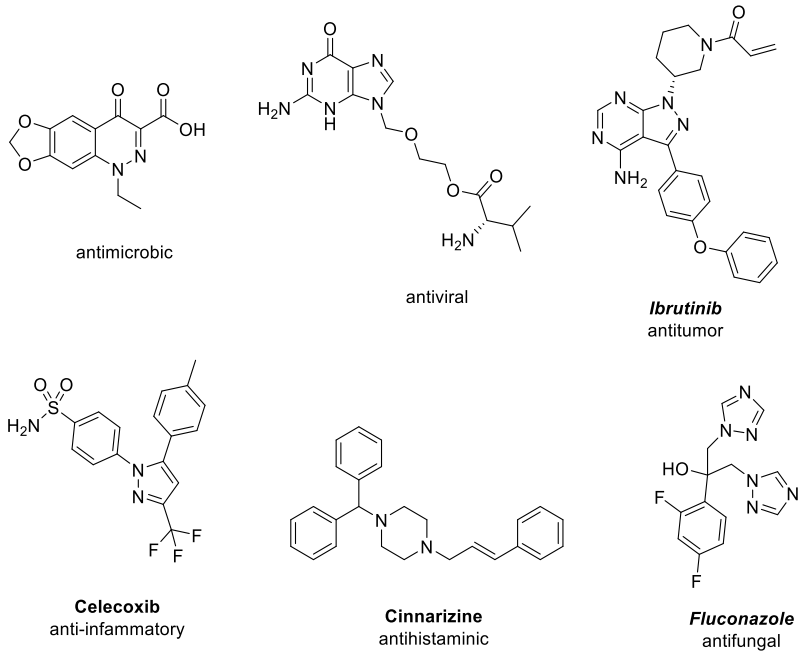

Figure 1: Examples of biological active heterocyclic compounds.

They are widely used for their antifungal,[8] anti-inflammatory,[9] antimicrobical,[10] antiviral,[11] antitumor[12] and antihistamine[13] properties. These biological activities also make heterocycles valuable in veterinary products and agrochemicals. Additionally, their unique reactivity has led to their application as organo- and photocatalysts, chiral auxiliaries and metal ligands.[14] These pivotal characteristics have consistently motivated organic chemists to develop innovative methods for synthesizing heterocycles and expanding their diversity. In light of these considerations, heterocycles have been the primary focus of my research. In particular, I mainly focused on exploring the chemical space of the heterocyclic cores shown in **Figure 2**, either as synthetic targets or as starting materials.

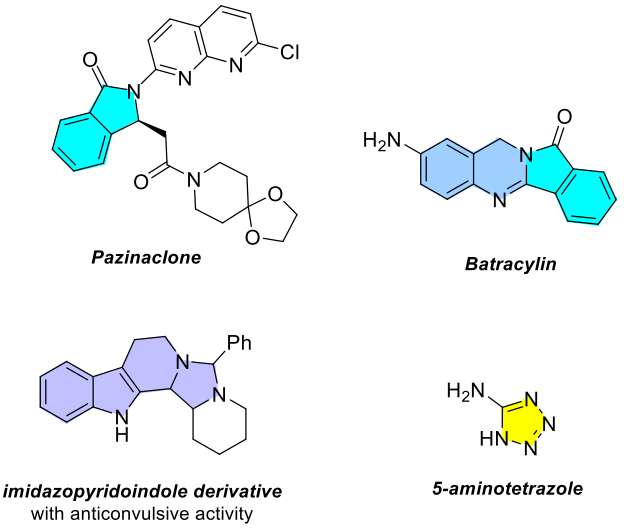

Figure 2: Biological active core described in this dissertation.

Chapter I: Chemical and electrochemical cascade reactions for the preparation of C3-*N*-substituted isoindolinones

1.2 Isoindolinones

Among nitrogen-containing heterocycles,[15] isoindolinones are undoubtedly a privileged scaffold, exhibiting a wide range of biological activities, including antiviral,[16] anxiolytic,[17] antifungal,[18] antioxidant,[19] anticancer[20] and anti-infammatory[21] activities. Examples of biologically active isoindolinone derivatives are reported in **Figure 3**.

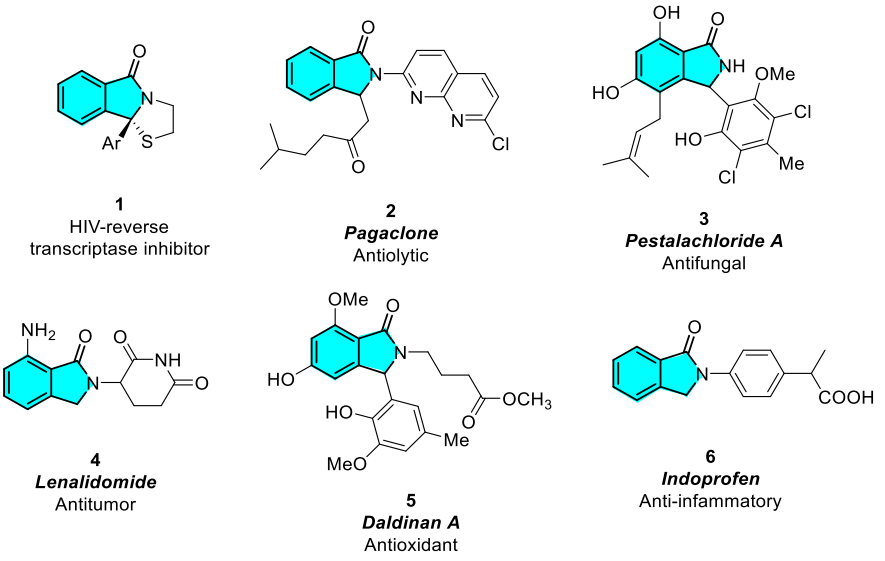

Figure 3: Examples of isoindolinone derivatives with biological activities.

Compound **1** with thio-substituent in position 3 has shown interesting results as HIV-reverse transcriptase inhibitor.[22] Pagaclone **2** and Lenalidomide **4** are utilized in clinical trials. The first serves as an anxiolytic compound and acts as a partial agonist of the GABA-A receptors,[23] while the second, a derivative of Thalidomide, is an anticancer drug employed in the treatment of multiple myeloma.[24] Indoprofen **6** is a nonsteroidal analgesic anti-infiammatory drug with notable effects on increasing SMN2-luciferase reporter protein and endogenous SMN protein levels.[25]

Given their significance in medicinal chemistry, in the last decades many efforts have been made to develop new procedures for the synthesis of isoindolinone

derivatives, including enantioselective organocatalytic, transition metal, and Lewis acid catalyzed methods.[26,27] Finally, special attention has been devoted to the preparation of isoindolinone-based products through green methodologies, including electrosynthesis,[28] photochemistry,[29] and flow chemistry,[30] to discover new synthetic pathways that minimize solvent and reagent use and improve reaction atom economy.

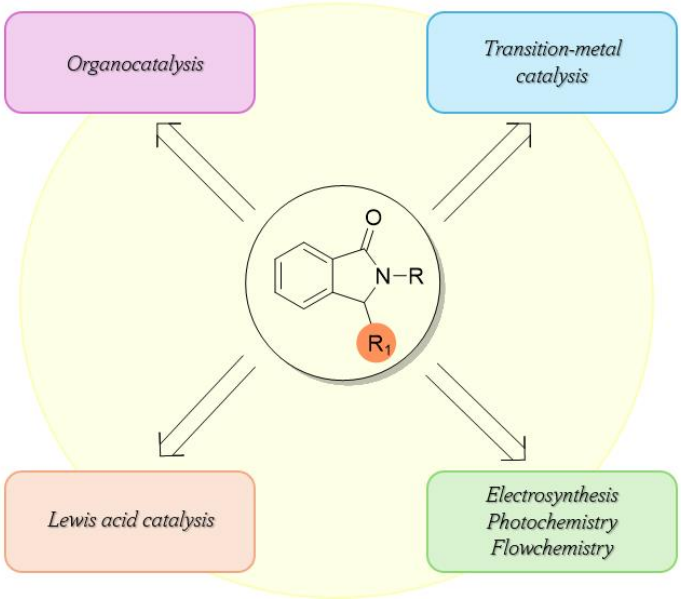

Figure 4: General methodologies for the preparation of isoindolinones.

1.3 Isoindolinones Synthesis though tandem reactions

In connection with these advanced techniques, the goal of many research groups has been to develop "cascade" pathways for the preparation of these compounds. A cascade process, called also "domino" or "tandem", consists in multiple organic transformations occurring sequentially without changing the reaction conditions.[31] Each step in the cascade reaction depends on the previous one, with at least two

conversions necessary for a valid cascade sequence. For this reason, cascade reactions are considered part of "green chemistry" due to their excellent atom economy and efficiencies in time, resources and waste reduction.[32] Since the Robinson's pioneering example of a cascade reaction[33] demonstrating the first one-pot synthesis of tropilone **9** (**Scheme 1**), numerous studies have focused on simplifying the synthesis of complex compounds, particularly natural products that were previously obtained through multi-step reaction sequences.[34]

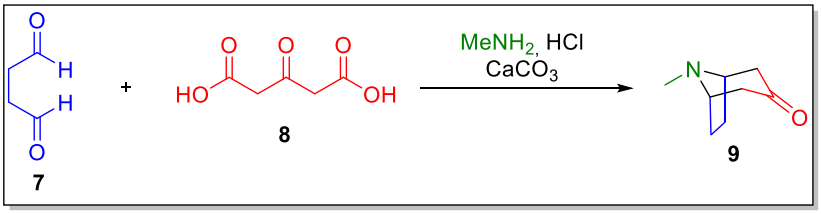

Scheme 1: Robinson's one-pot synthesis of tropilone.

Several examples of transition metal-catalyzed tandem approaches to the preparation of isoindolinone products were reported. Palladium,[35] such as nickel,[36] cobalt,[37] rhodium,[38] zinc[39] and ruthenium[40] have been used in different cascade procedures leading to various *C*-3 substituted isoindolinones with excellent results. For example, in 2013, Zhao *et al.* reported for the first time an efficient synthetic procedure for the preparation of hydroxyl isoindolinones by means of palladium catalysis (**Scheme 2a**).[41] In addition, Li and coworkers developed a Rh catalyzed method for the synthesis of 3-alkylideneisoindolinones through the reaction of *ortho*-amidation of ketoximes with isocyanates, via *C*-H functionalization (**Scheme 2b**).[42] Another interesting synthesis of isoindolinones starting from *ortho*-cyanobenzaldehyde and 1,3-dicarbonyl compounds catalyzed by cobalt (II) chloride has been proposed by Shi (**Scheme 2c**).[43]

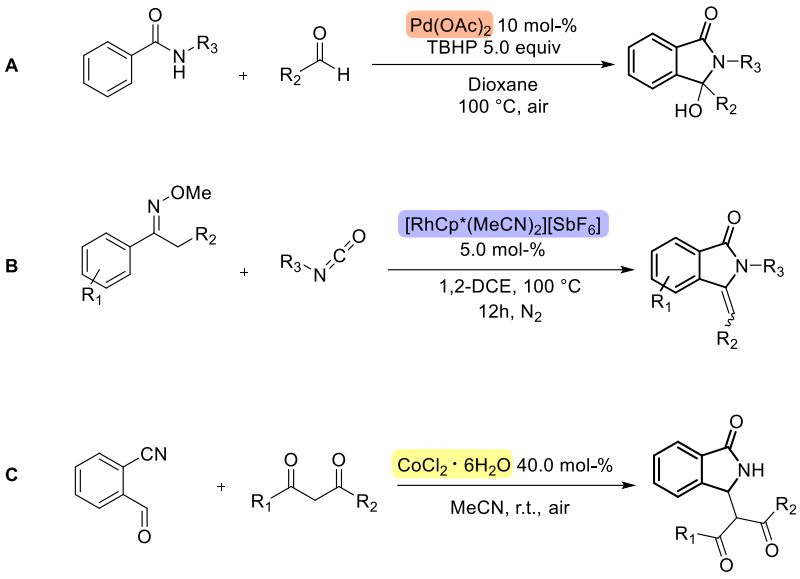

Scheme 2: Examples of transition metal catalyzed isoindolinones synthesis.

However, considering the growing focus on developing more eco-friendly procedures, methodologies based on electrochemistry,[44] photochemistry,[45] or flow chemistry[46] have emerged in literature as viable alternatives, enabling the synthesis of various isoindolinone derivatives through efficient cascade processes.

In the last 15 years numerous publications have explored the use of electrochemistry to activate or facilitate tandem mechanism reactions for the synthesis of functionalized isoindolinones. In this field, the electrochemical synthesis of isoindolinones proposed by Palombi[47] and coworkers in 2012 represents pioneering work, highlighting the possibility to prepare different compounds with catalytic amount of current and supporting electrolyte, maximizing the reaction atom economy (**Scheme 3**). In this work *C*-3 substituted isoindolinones were obtained by reacting 2-formylbenzonitrile with carbon nucleophiles in a divided cell electrochemical set-up, using sub-stoichiometric cathodic current.

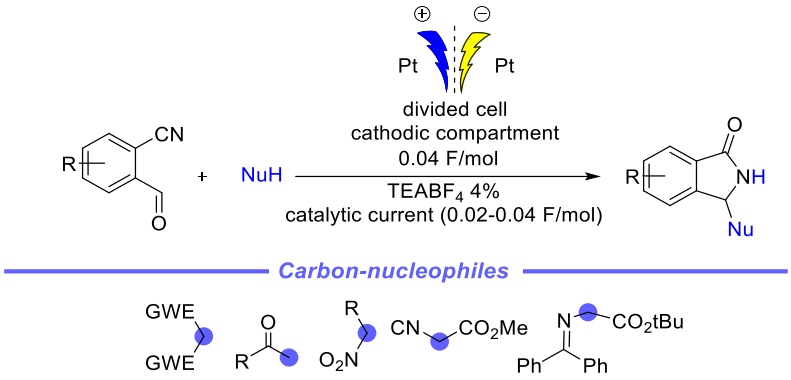

Scheme 3: Electrocatalytic tandem reaction for the synthesis of *C*-3 substituted isoindolinones.

Similar electrochemical conditions, herein and thereafter,[48] achieved the extension of the process to other carbon nucleophiles for the one-pot *C*- and *N*-functionalization of isoindolinones with various electrophiles, accessing highly functionalized related structures (**Scheme 4**). These results offer an excellent alternative for the synthetic preparation of various isoindolinone derivatives. In addition, the high tolerance of different functionalities under electrochemical conditions and the minimization of the number and quantity of chemical species in the reaction solutions make this approach particularly advantageous.

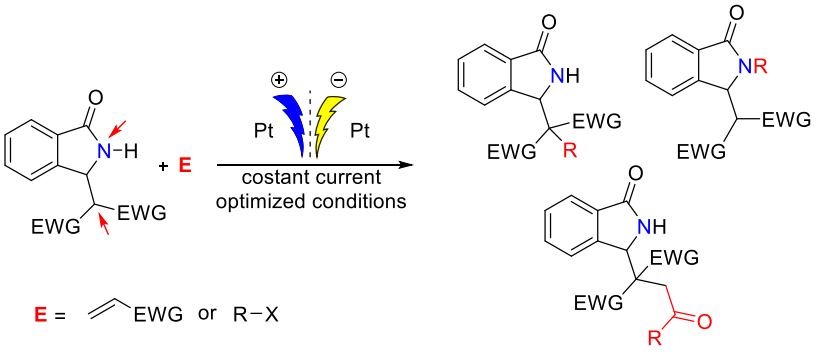

Scheme 4: Electrochemical carbon and nitrogen functionalization.

Moreover, the electrochemical activation proved to be effective to induce tandem hemiaminal-heterocyclization-*aza*-Mannich reaction of 2-formylbenzonitriles with

primary and secondary alkyl-amines (**Scheme 5**).[49] The application of this method, in a divided cell cathode compartment, allowed the total conversion of the starting material (95 % yield) with a catalytic amount of current (0.025 F/mol) and Pt as working electrode, reducing drastically the amount of amine used in the literature procedures.[50]

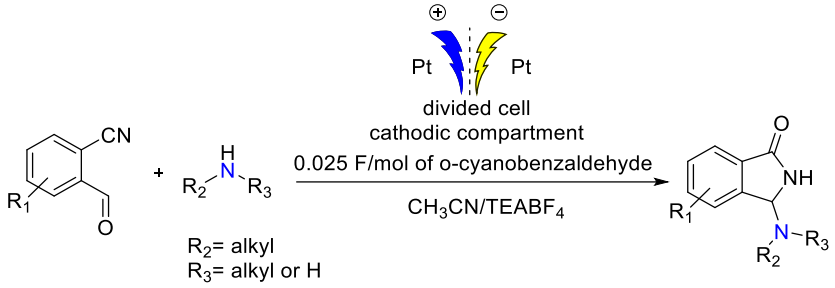

Scheme 5: Electrocatalytic synthesis of *C*-3 *N*-substituted isoindolinones.

Subsequently, new convenient electrochemically-based tandem processes have been developed by several research groups. Huang and coworkers proposed an interesting synthesis of *N*-substituted isoindolinones via cathodic reduction/amidation of 2-carboxybenzaldehydes and amines (**Scheme 6**).[51] The reaction works very well using both aromatic and aliphatic amines, with a simple electrochemical set-up.

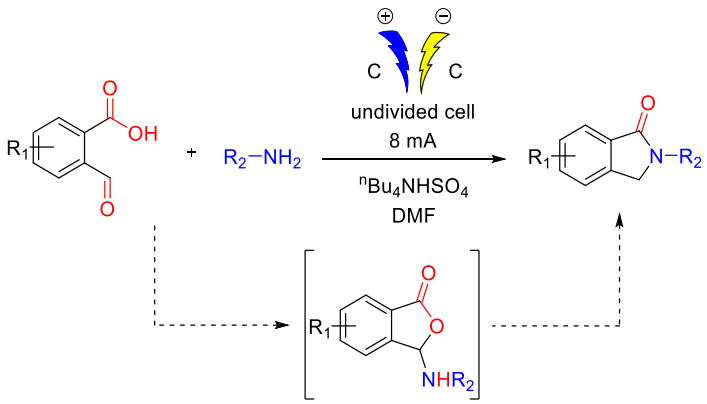

Scheme 6: Cathodic reduction/amidation for the synthesis of *N*-substituted isoindolinones.

Another interesting example showing the simultaneous functionalization of both the position 3 and the nitrogen atom was reported by Lei.[52] In this case, different isoindolinone derivatives have been isolated from *o*-alkyl benzoic acids and nitriles through an electrochemical-induced benzyl C-H amidation (**Scheme 7**).

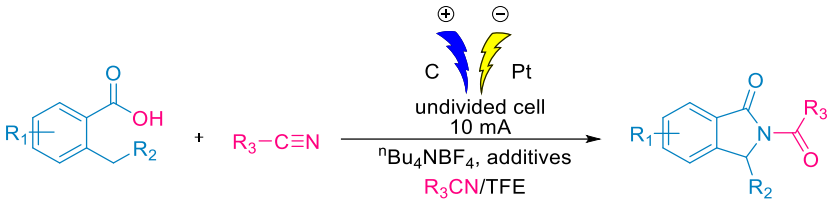

Scheme 7: Electrochemical C-H amidation.

The reactions were efficiently carried out in an undivided electrochemical set-up. Noteworthy, the methodology proved to be suitable for gram-scale process. Moreover, Xiang *et al.* developed an interesting alternative way to generate *N*-protected isoindolinones *via* direct reduction of imides to efficiently afford both *C*-3 substituted hydroxyisoindolinones and *N*-substituted isoindolinone derivatives simply tuning the electrolysis time (**Scheme 8**).[53] In addition, the mild conditions made the method compatible with the presence of reduction-sensitive functional groups, including alkenes, alkynes, epoxides, halides and ketones.

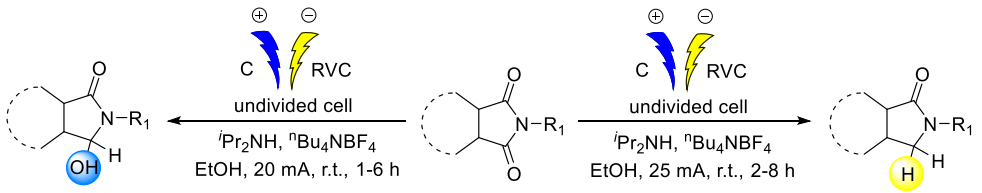

Scheme 8: Electrochemical reduction of imides.

Recently, Ye and coworkers reported an efficient electrochemical intramolecular 5-*exo*-dig *aza*-cyclization of 2-alkynylbenzamides to give the highly stereoselective synthesis of mono- and trifluorinated isoindolin-1-one derivatives.[54] This work

highlights the unique capability of synthetic electrochemistry in controlling reaction selectivity, obtaining two different products simply changing the current intensity (Scheme 9).

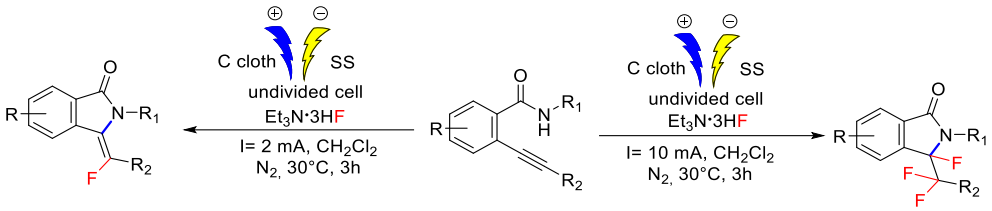

Scheme 9: Mono- and trifluorinated synthesis of isoindolin-1-one derivatives.

To improve the scalability of the reaction and to minimize the number of species in solution and their corresponding amounts, electrochemistry has also been integrated with flow setups. In this context, an example of electrochemical tandem synthesis of isoindolinones in a flow chemical reactor was proposed by Wirth et *al*. in 2017.[55] They developed a second-generation electro-flow microreactor with platinum as the cathode and boron-doped diamond (BDD) as the anode, separated by fluorinated ethylene propylene (FEP). Using benzyltrimethylammonium hydroxide as a base and TEMPO as a mediator, they obtained the desired *N*-aryl/alkyl isoindolinones starting from **10**. Additionally, the presence of an electron-withdrawing group on the alkene moieties led directly to the corresponding reduced product (**Scheme 10**). Then, the reaction flow setup has been optimized by increasing the reactor temperature to 85 °C at a pressure of 2.8 bar to achieve complete conversion of the TEMPO-embedded product to the reduced alkylidene-substituted product. Furthermore, the corresponding alcohols were obtained by using a Zn cartridge and acetic acid. The use of a flow reactor represents a valid example of developing greener procedures as it significantly reduces the need for additives and supporting electrolytes in the reaction.

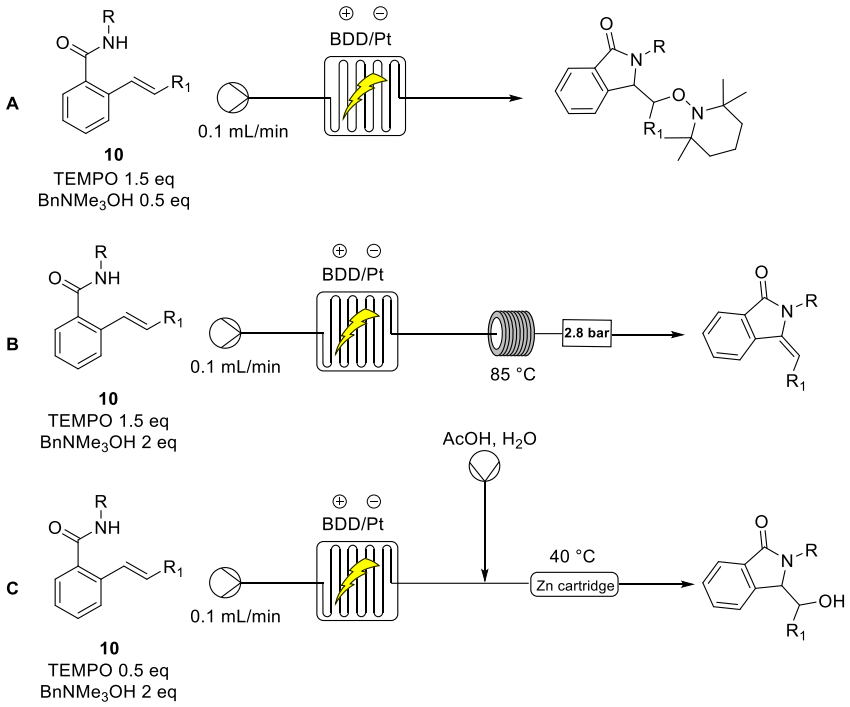

Scheme 10: Electrochemical synthesis of isoindolinones in flow-microreactor.

1.4 Part I: Electrochemically-Induced Cascade Reaction of 2-formyl Benzonitrile with Anilines: Synthesis of N-Aryl Isoindolinones

In drug design, the incorporation of multiple pharmacophores within a single molecular structure has emerged as a powerful strategy to enhance therapeutic efficacy and overcome limitations associated with single-target drugs, thereby increasing the potential for achieving synergistic effects and improving drug selectivity. Given the diverse previously described pharmacological activities associated with isoindolinones, their functionalization with other bio-active substructures (for ex., an *N*-aryl system) could in fact introduce new biological properties or enhance existing ones.[56]

The aminophenyl group is found in many natural compounds and several well-known commercialized pharmaceutical products (Figure 5) with antipyretic activity (Example: Paracetamol **11**), antihistaminic activity (Example: Chlorphenamine Maleate **12**), antibiotic activity (Example: Sulfanilamide **13**) and central nervous system (CNS) activity (Example: Nefazodone **14**).

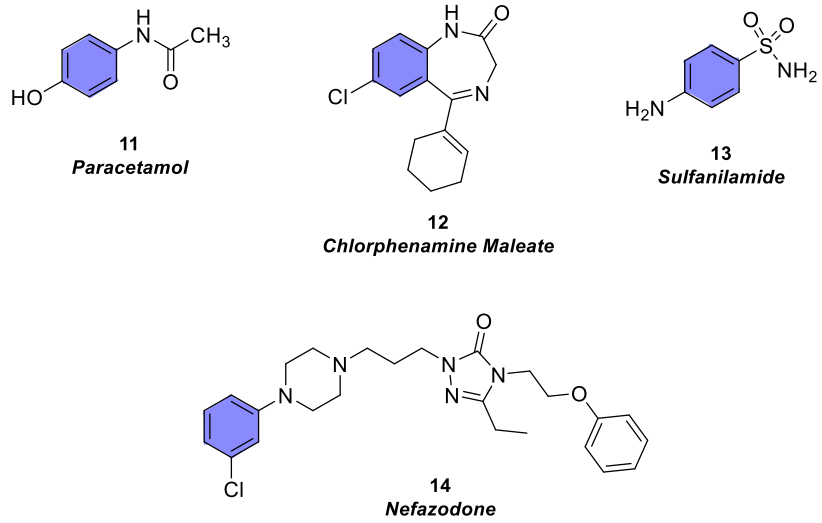

Figure 5: Aniline containing biological active compounds.

Considering that, during the first period of my PhD I focused on the synthesis of phenylamino-containing isoindolinones **15,** which have only been accessed so far using multistep reactions (**Figure 6**).[57]

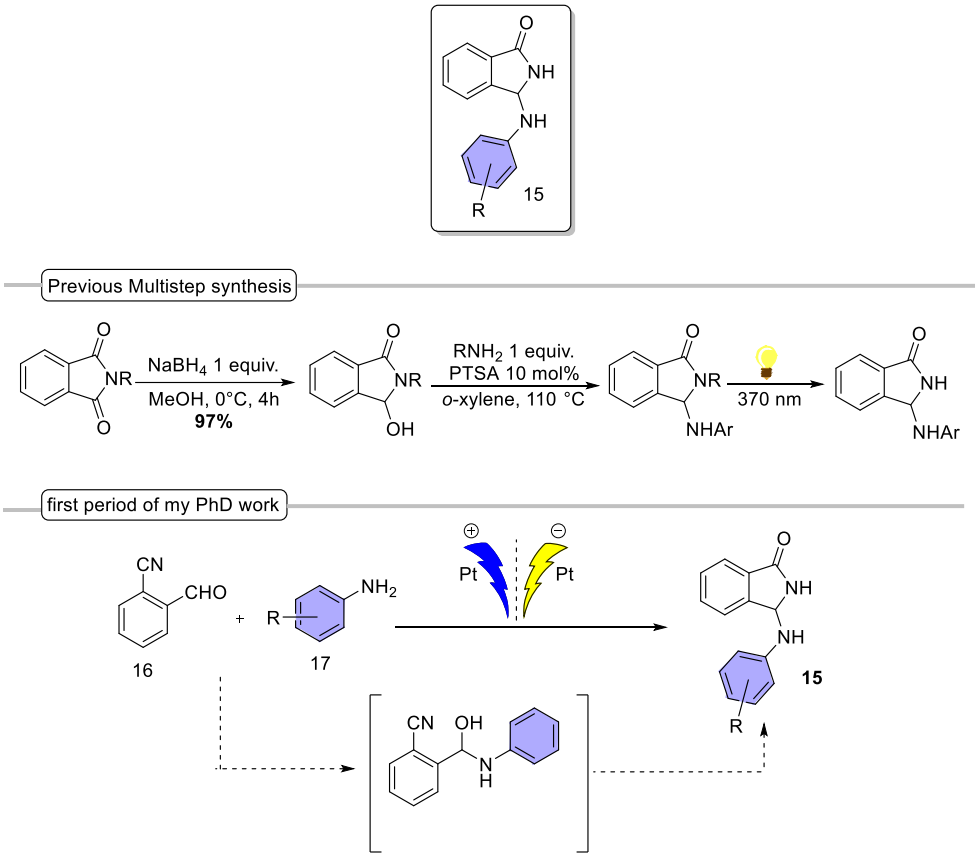

Figure 6: Synthesis of *C*-3 *N*-aryl substituted isoindolinones.

Based on the above-mentioned results on *C*-3 *N*-substituted isoindolinones through electrocatalytic activation,[48] I explored the possibility to use aromatic amines in a similar tandem process with 2-formylbenzonitrile **16** in order to develop the first direct access to **15**. With respect to alkylamines, anilines should be considered more challenging substrates because they have lower nucleophilicity and strong tendency to eliminate water (**Scheme 11**).[58]

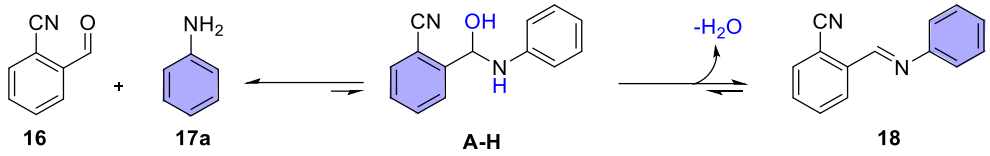

Scheme 11: Imine formation.

1.4 Results and discussion

The investigation started using aniline, 2-bromoaniline or 2-iodoaniline as model compounds in the reaction with 2-formylbenzonitrile **16** under different electrochemical set-up and conditions.

As shown in **Table 1**, the optimized conditions led to a 91% yield in the corresponding product **15a** using aniline as nucleophile (**Entry 1**). In contrast, with 2-halogenated anilines **17b** (**Entry 8**) and **17c** (**Entry 11**), the isolated yields were lower (80% and 57% respectively), likely due to side reactions involving cathodic dehalogenation.[59] Variations from the standard conditions resulted in a drop of the final yield for all the three products. With CH_3CH_2CN instead of CH_3CN, the yield with aniline drastically decreased to 22% (**Entry 5**) while the use of DMF as solvent led to a 37% yield (**Entry 6**). Significantly, a change in current intensity resulted in lower yield. The data in **Table 1** also demonstrate that 2-formylbenzonitrile is sensitive to the cathodic environment, as it cannot be recovered after the electrolysis, even when a low amount of charge of 0.06 F/mol (**Entry 9**) is applied. As a result, any deviation in current quantity from the optimal conditions leads not only to a decrease in yield but also to reduced selectivity. In fact, doubling the current intensity (8 mA instead of 4 mA), the final yield was 61%. Similarly, modifications to the electrochemical setup, such as altering the porosity of the glass septum, changing electrode materials, or using an undivided cell instead of a divided one, caused a drop of the yield.

Table 1: Optimization of the reaction conditions.[a]

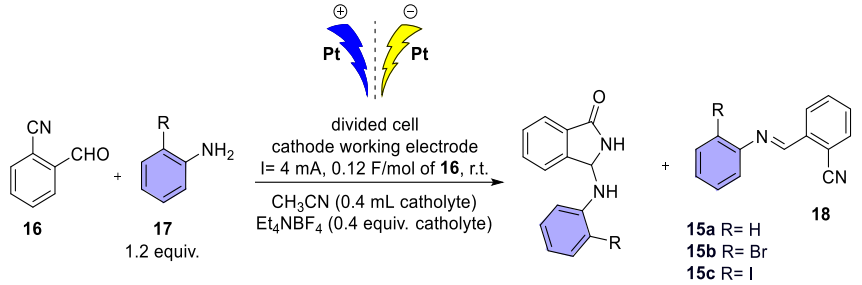

Entry	Variations from Standard Conditions	16 %Conv[b]	17 %Conv[c]	15 %Yield[d]	18 %Yield[d]
1	None	>98	**17a** 80	**15a** 91	**18a** -
2	Undivided cell	>98	**17a** 25	**15a** traces	**18a** 25
3	No electricity[e]	57	**17a** 48	**15a** -	**18a** 57[f]
4	I= 8 mA, CH_3CN: 0.6 mL	>98	**17a** 61	**15a** 68	**18a** -
5	CH_3CH_2CN instead of CH_3CN	>98	**17a** 51	**15a** 22	**18a** 28
6	DMF instead of CH_3CN	>98	**17a** 74	**15a** 37	**18a** -
7	MeOH instead of CH_3CN	>98	**17a** <2	**15a** -	**18a** traces
8	None	>98	**17b** 70	**15b** 80	**18b** -
9	Q= 0.06 F/mol	>98	**17b** 61	**15b** 47	**18b** -
10	Ratio **16:17b**= 1.2:1	>98	**17b** 67	**15b** 61	**18b** -
11	None	>98	**17c** 62	**15c** 57	**18c** -
12	CH_3CN: 0.8 mL	>98	**17c** 44	**15c** 31	**18c** -
13	Q= 0.35 F/mol	>98	**17c** >98	**15c** 38	**18c** -
14	Electrolysis at 0 °C	>98	**17c** 72	**15c** 38	**18c** -

[a]After the electrolysis the anolyte was removed, and the reaction prolonged under stirring for 6h at r.t. [b]Conversions have been determined by ^{1}H-NMR analysis of the crude mixture. [c]Conversions have been determined based on recovered 17a-c (isolated). [d]Isolated Yield. [e]Solvent: CD_3CN. [f]Conversion of **16** and yield of **18** were established by ^{1}H-NMR analysis after 6h.

Subsequently, I evaluated the scope and the limitations of this electrochemical method by testing the series of compounds reported in **Table 2**.

Table 2: Substrate scope of 3-*N*-Aryl substituted isoindolinones.[a,b]

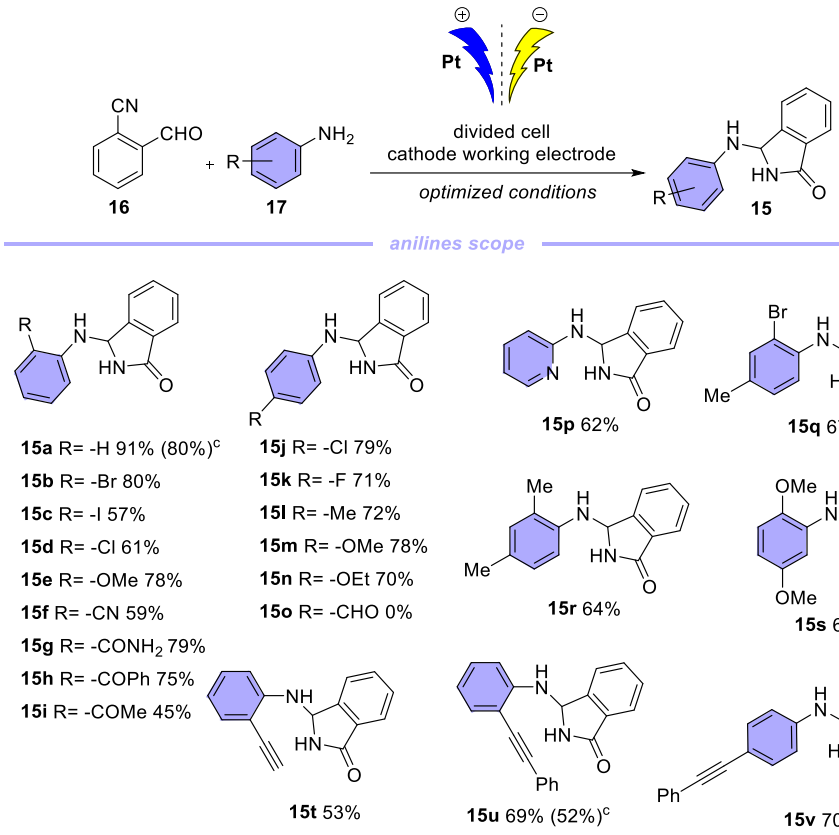

[a]Standard conditions (see Table 1). [b]Isolated Yield. [c]Isolated yield by chemical reaction, 1 eq of K_2CO_3 as base, CH_3CN, 72 h, r.t.

As shown in the Table above, a variety of substituents on the aniline molecule have been examined to assess the influence of changes in electron density of the benzene ring. The results show that the electrochemical conditions were generally compatible with almost all the different substituted anilines. Notably, halogen-substituted anilines produced high yields, demonstrating the selectivity for the desired products. The reaction also performed with 2-ketoanilines, yielding a good 75% yield for **15h** and a moderate but still acceptable 45% yield for **15i**. Additionally, when 2-aminopyridine was used as the starting material, the reaction resulted in 62% yield of the hybrid pyridine-

isoindolinone product. For *ortho*- and *para*-alkynyl anilines, the reactions led to the desired products with moderate yields and complete conversion of the starting materials. Remarkably, the reaction gave interesting products that could be useful for further molecular diversification in the presence of functionalities on the aniline moieties such as -CN and -$CONH_2$. Noteworthy, compared to heterogeneous basic catalysis (as indicated by **15a** and **15u** in **Table 2**, data in parentheses), the electrochemical method proved superior in both efficiency and reaction time. However, no product was obtained when aniline **15o** with the *p*-formyl substituent was used as a nucleophile, likely due to the low tolerance and subsequent decomposition of the formyl group. Furthermore, significant decomposition of the starting aldehyde occurred under electrochemical conditions, resulting in the formation of the corresponding imine through heterogeneous basic catalysis, when the 2- the 5-bromo-2-formylbenzonitrile was used instead of the formylbenzonitrile.

To gain further insight into the electro-induced reaction mechanism, I conducted the following control experiments on the general reaction between 2-formylbenzonitrile and aniline under various conditions (**Scheme 12**).

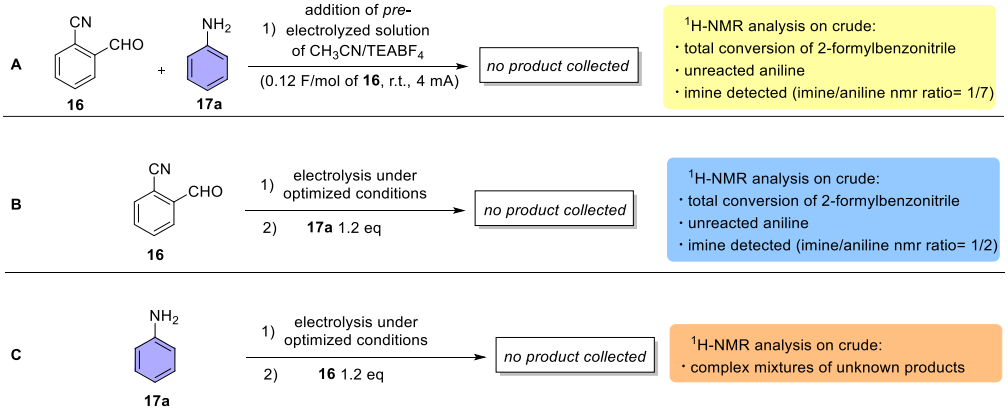

Scheme 12: Control experiments of reaction model under different conditions.

^{1}H-NMR on the crude mixtures of the three experiments outlined in **Scheme 12** clearly indicated that the presence of both reagents during the electrolysis is a strict prerequisite to achieve the desired product. When either 2-formylbenzonitrile or aniline was added after electrolysis, or when the pre-electrolyzed solution was directly used, the result was either the formation of an imine side product or a complex decomposition mixture that was difficult to interpret. Consequently, the second phase of our study focused on investigating the uncatalyzed nucleophilic addition of aniline to 2-cyanobenzaldehyde in acetonitrile through quantum-chemical investigations, in collaboration with Prof. Massimiliano Aschi (**Figure 7**).

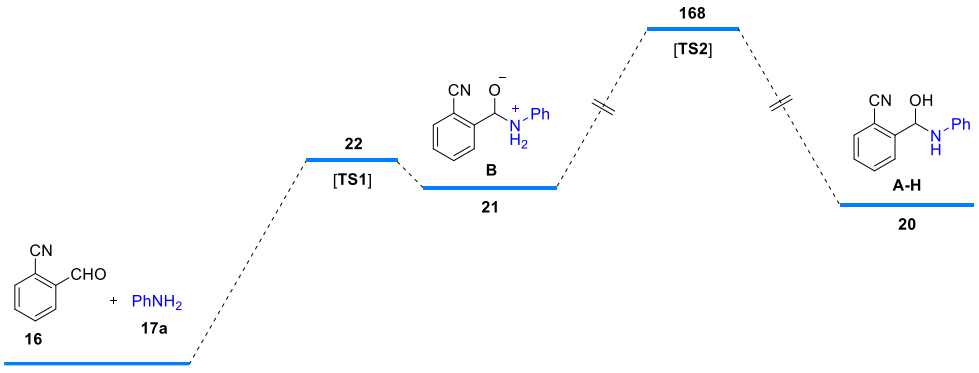

Figure 7: Uncatalyzed hemiaminal formation in CH_3CN with standard free-energy values (kJ/mol in CH_3CN at 298 K).

Not surprisingly, the uncatalyzed nucleophilic attack of **17a** to **16** to produce the hemiaminal **A-H** is predicted as a disfavored process both kinetically and thermodynamically. For this reason, in order to identify the fundamental step of the electro-activation leading to the desired product, we considered both the catholyte solution and the intermediate **B**, formed after the nucleophilic attack of the aniline, as potentially affected by the applied potential. In these studies, we report the energetic of the possible electro-reductive processes of all the species involved in the reaction, conventionally referring to the thermodynamics of the reaction as initiated by $[CH_3CN]^{\bullet-}$, being the solvent the most present species in solution (**Figure**

8). The ΔG° values clearly indicate that the 2-formylbenzonitrile has the highest oxidizing power. However, a subsequent reaction initiated by $16^{\bullet-}$ (**Equations 5 and 7**) is thermodynamically strongly disfavored. Zwitterionic intermediate **B** is likewise easily reduced (**Equation 4**). However, this channel also reveals itself as totally ineffective due to the strongly thermodynamic driving force leading to $\mathbf{B}_{(sol)}^{-}$ dissociation (**reverse of Equation 7**). Therefore, these data suggest that the electrochemical process acting as the reaction trigger is the formation of $^{-}CH_2CN_{(sol)}$ which follows the hydrogen evolution reaction (HER) (**Equation 1**). The electrogenerated strong base $^{-}CH_2CN_{(sol)}$ might undergo acid-base reaction with either the aniline **17a** (to form the strong nucleophilic aryl amide anion) (**Equation 8**) and, concurrently, with the zwitterion **B** (**Equation 9**).

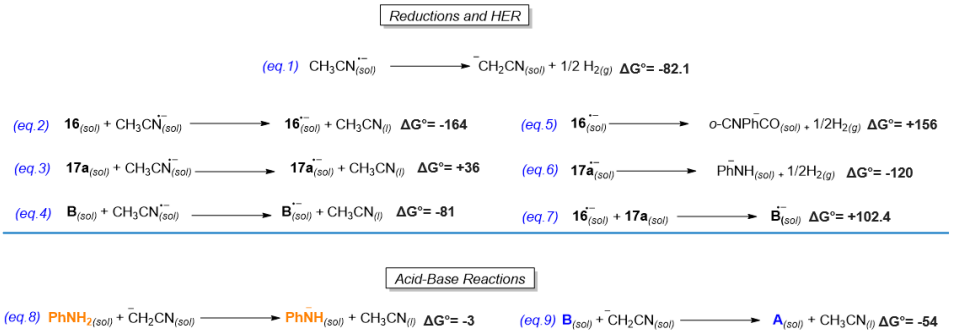

Figure 8: Standard free energy (kJ/mol) at 298 K of the plausible channels initiated by the Pt-electroreduction.

The proposed reaction pathway is depicted in **Figure 9**. As illustrated, following the electrochemically initiated process and the formation of the critical anionic intermediate **A**, a series of unimolecular H- and HO- transfers occurs, resulting in **D**, which evolves without barrier to **F**, the conjugate base of the final product. Subsequently, a thermodynamically guided (ΔG° = −50 kJ/mol) acid-base reaction between **F** and CH_3CN leads to the formation of **15a**, with the base $^{-}CH_2CN$ being regenerated to restart the catalytic cycle. It is also plausible that the acid-base

reaction between the electrogenerated base $^{-}CH_2CN$ and zwitterion **B** contributes to the formation of intermediate **A**, without involving directly the reaction partners. Additionally, it should be noted that DFT calculations have excluded the potential alternative pathway involving the closure of **A** and rearrangement of intermediate **G**, since this rearrangement step would require a higher activation energy.

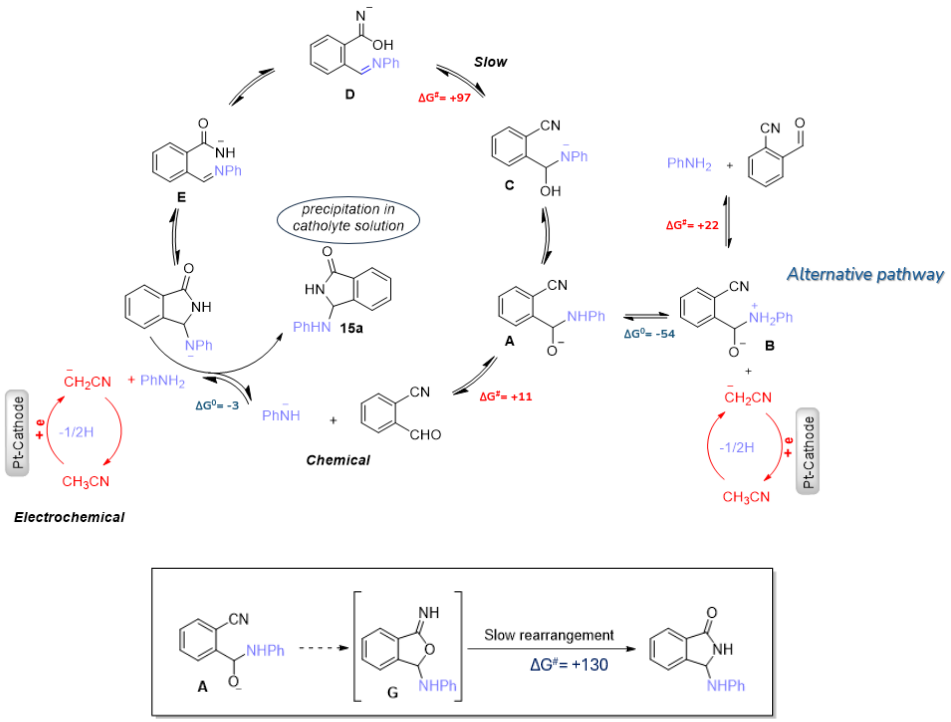

Figure 9: Proposed reaction pathways at 298 K in acetonitrile based on DFT calculations.

1.5 Isoindolinone-containing polyheterocycles

The oxo-isoindole nucleus is often found in polycyclic molecules, both natural and synthetic, with high therapeutic potential as antivirals, antimicrobicals, antipsychotic and antitumoral agents.[60] Some examples are reported in **Figure 10**.

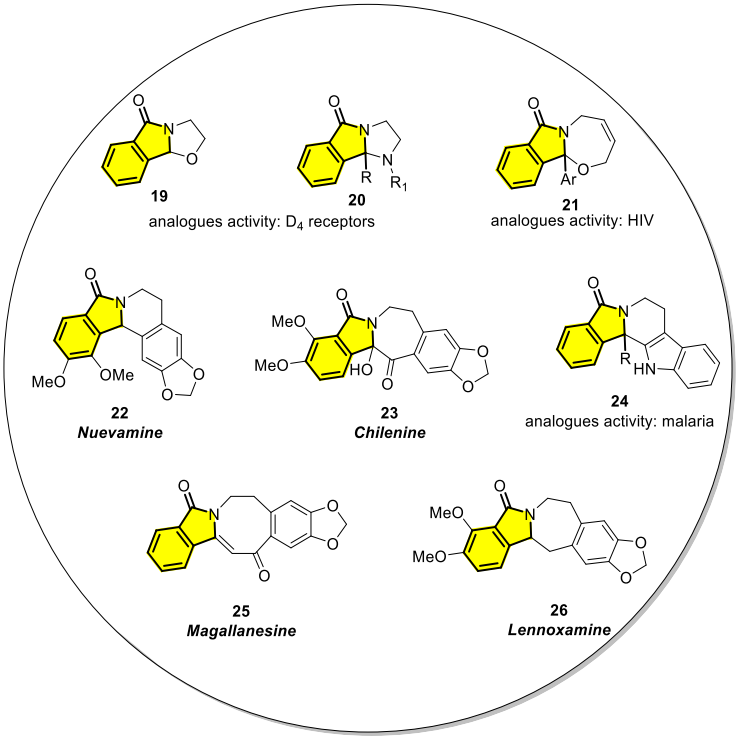

Figure 10: Representative examples of polyhetocycles containing fused C_3-*N* bridged oxo-isoindole.

Isoindolinone derivatives **20** represent an interesting class of respiratory syncytial virus (RSV) inhibitors. Chilenine **23** was the first isoindolobenzazepine alkaloid isolated from *Berberis empetrifolia* in 1982.[61] Subsequently, different derivatives have been isolated from *Berberidaceae* species, such as Magallanesine **25** and Lennoxamine **26**. After their isolation, many synthetic procedures of these molecules have been developed, to produce high functionalized derivatives.[62]

The interest in these products has driven research aimed at discovering new, straightforward synthetic methodologies. Recently, one-pot approaches including

transition metal-promoted processes have been proposed. For example, Zhou and coworkers have developed an *ortho*-C-H imidation of benzaldehydes catalyzed by monodentate transient direct group assisted Ruthenium (II) catalyst (**Scheme 13**).[63]

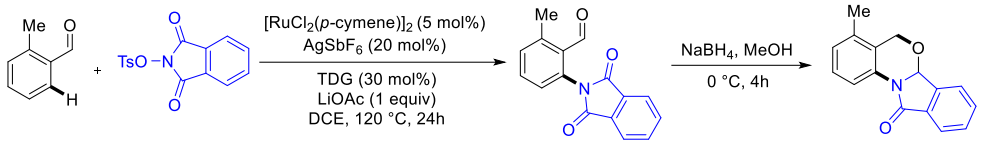

Scheme 13: Ruthenium-catalyzed synthesis of tetracyclic isoindolinone.

By using Palladium catalysis, Singh *et al.* developed a radical-induced catalyzed C-H activation for the synthesis of 4H-benzo[*d*][1,3]oxazin-4-one **27** starting from toluenes, aldehydes and benzyl alcohols, using TBHP as oxidant (**Scheme 14**).[64]

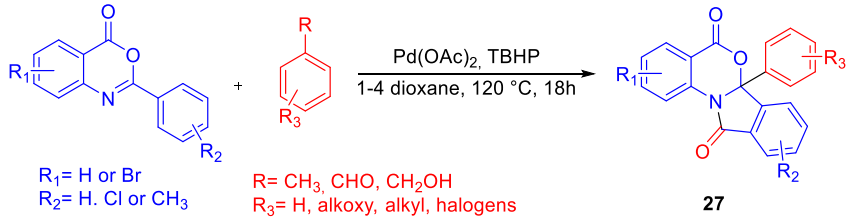

Scheme 14: Palladium-catalyzed synthesis of 4H-Benzo[*d*][1,3]oxazin-4-one.

Palladium catalysis has shown to be very efficient in promoting the one-pot synthesis of polyheterocyclic derivatives. Pal and coworkers reported in fact another palladium-catalyzed methodology to obtain 11-substituted-6*H*-isoindolo[2,1-a]indol-6-ones **29** through a sequential intramolecular Heck reaction starting from *N*-allyl substituted *N*-arylbenzamide derivatives **28**.[65] They also evaluated the biological activities of these new products, that have shown promising antiproliferative properties against several cancer cell lines *in vitro* (**Scheme 15**).

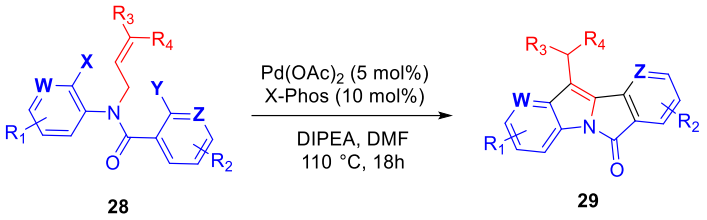

Scheme 15: Palladium-catalyzed synthesis of 11-substituted 6H-isoindolo[2,1-a]indol-6-ones.

Another intriguing example of a metal-catalyzed one-pot synthesis of polycyclic isoindolinones has been developed by Li.[66] As shown in **Scheme 16**, new isoindolinones derivatives have been prepared starting from 2-formylbenzonitrile, through a Copper-catalyzed divergent cyclization using hypervalent iodine.

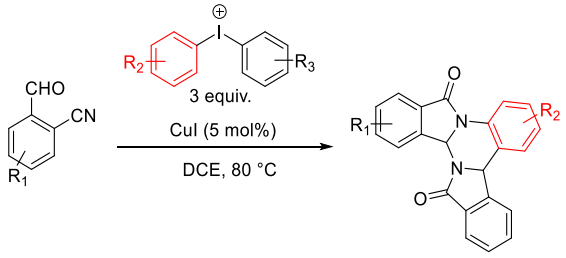

Scheme 16: Copper-catalyzed polycyclic isoindolinones synthesis.

Likewise, greener procedures have been developed avoiding the use of metals and/or acids, bases or non-conventional catalysts. For ex., Eisler and coworkers reported a sequential intramolecular cyclization starting from compounds **30** in presence of TBAF (**Scheme 17**).[67] Interestingly, changing the reaction conditions such as solvent and temperature, or the substituent on the alkynyl group, is possible to obtain selectively the derivative **32** though a 7-*endo-dig* cyclization and the product **31** via a 6-*exo-dig* closure.

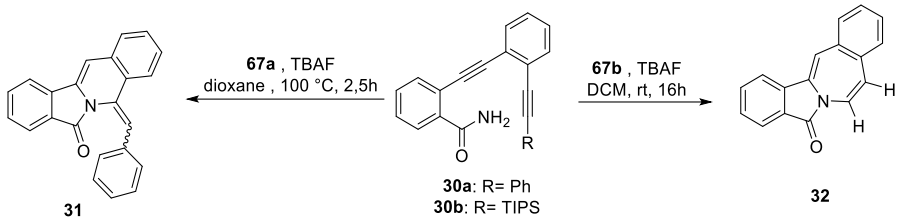

Scheme 17: Multiple cyclizations for base-catalyzed synthesis of fused isoindolinones.

Liu reported a peculiar methodology for preparing new tetracyclic benzodiazepine-fused isoindolinones pseudo natural products **33** using mesoporous silica nanoparticles as catalyst and AcOH as solvent, with satisfactory results also in gram-scale reaction.[68] In addition, the catalyst has been recycled several times without significant loss of catalytic activity (**Scheme 18**).

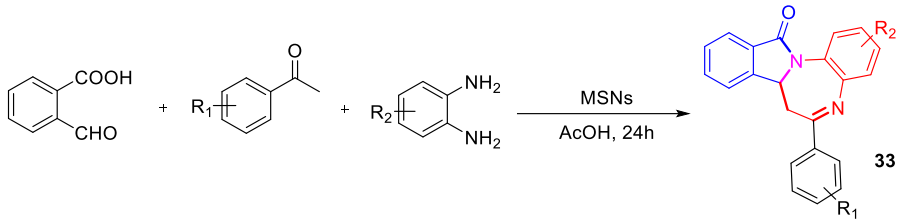

Scheme 18: Benzodiazepine-fused isoindolinones synthesis.

Enantioenriched tricyclic isoindolinones **34** have been obtained as single diastereoisomers by Massa and co-workers through a sequential tandem organocatalyzed synthesis of isoindolinones followed by base-catalyzed Michael addition to acrylaldehyde.[69] Notably, electrochemical conditions also proven effective for a diastereoselective access to tricyclic isoindolinones **34** (**Scheme 19**).[48]

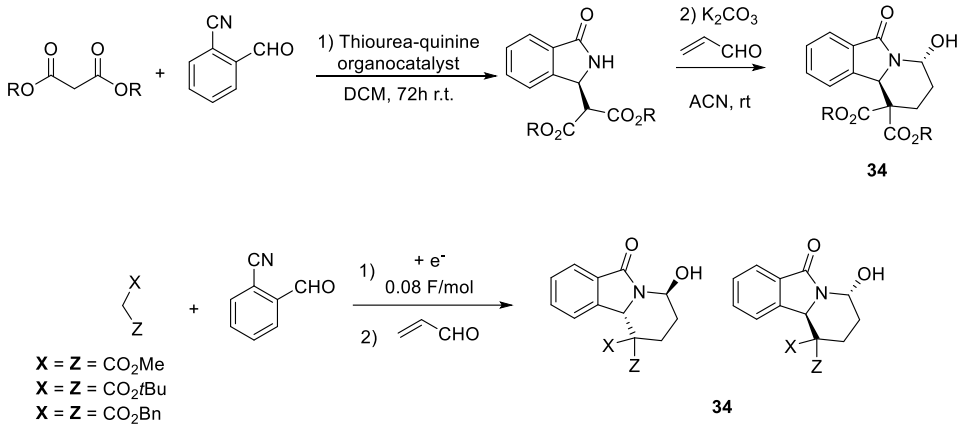

Scheme 19: One-pot electro-induced generation of tricyclic isoindolinones.

These entries led to unprecedented tricyclic isoindolinone derivatives with hemiaminal functionality, an interesting scaffold for further investigations.

Part II: On Route to Diverse Nitrogen-Bridged Polyhetero-cycles with an N(acyl), N(aryl)-acetal Core

Building on our previous work on the electro-induced synthesis of 3-*N*-substituted isoindolinones, we decided to further investigate the synthetic potential of this process. Our goal was to achieve a sequential one-pot cyclization of the isoindolinone NH with suitable electrophilic moieties at the *o*-position of the *N*-aryl subunits (**Scheme 20**).

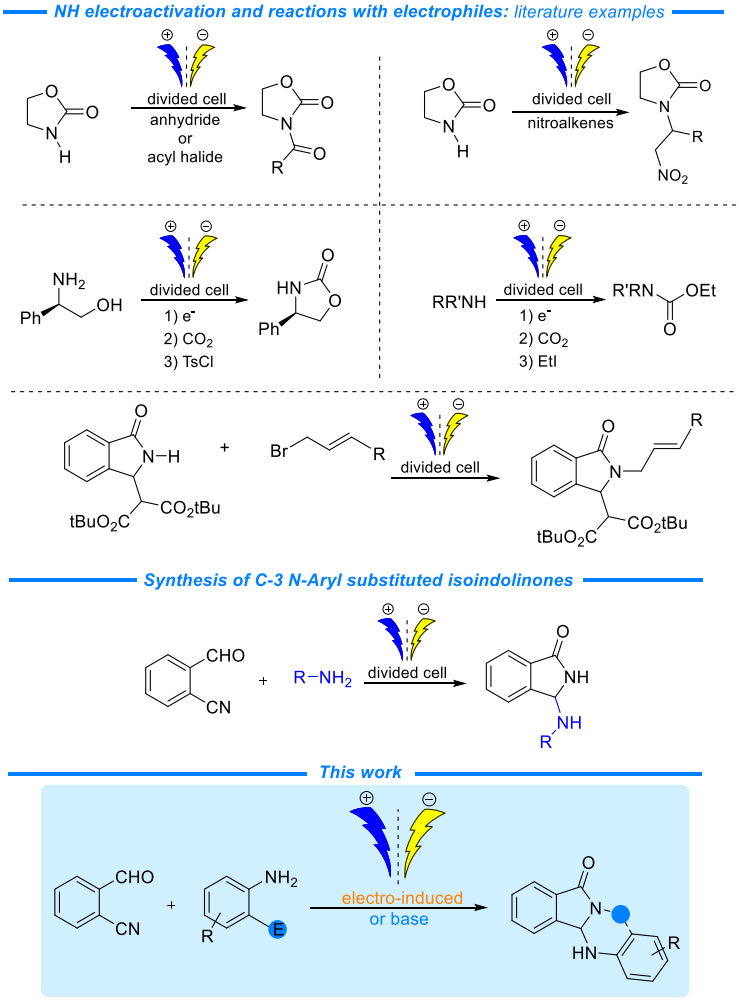

Scheme 20: Previous works vs this work.

Indeed, previous reports demonstrated that, under cathodic constant current the -NH group of amines, oxazolidinones and isoindolinones can smoothly undergo reaction with electrophiles such as carbon dioxide, nitroalkenes, acyl- or alkyl-halides.[70]

1.6 Results and discussion

I started the investigation taking as reference the reaction conditions previously optimized for the electro-induced synthesis of 3-*N*-substituted isoindolinones and using *o*-substituted anilines **35** with different carbonyl functionalities in *o*-position as reaction partners of **16** (**Table 3**).

Table 3: Study of reactivity of anilines having *o*-carbonyl functionalities.

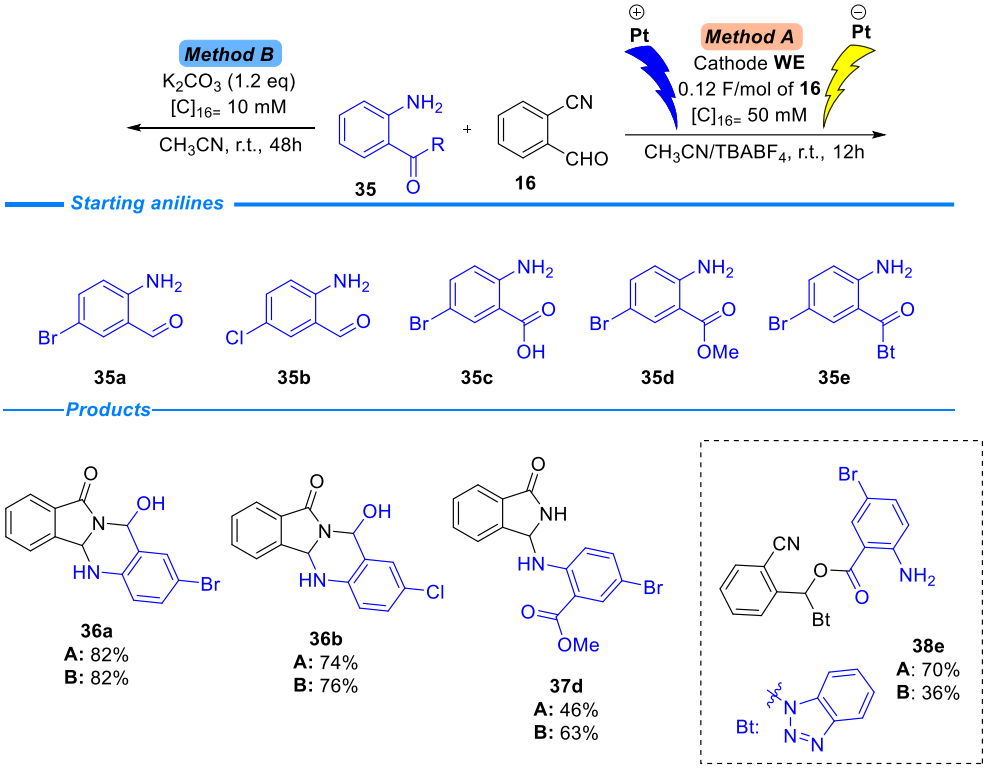

Pleasantly, with the electrochemical optimized conditions, the reaction worked quite well with the *o*-formylanilines **35a** and **35b**, directly giving the tetracyclic products **36a** and **36b** with 82% and 75% yield, respectively. The reaction chemo-selectivity is particularly good, considering the presence of a formyl group and a halogen-atom on the aniline ring, both susceptible of electroreduction to the electrochemical medium. Disappointingly, tetracyclic products have not been collected by using acid, ester and benzotriazole amide functionalities. The results shown in fact that with the acid derivatives **35c** no reactivity was observed, while with the *o*-ester aniline **35d** only the corresponding isoindolinone **37d** was obtained. Surprisingly, the aniline **35e** lead to the 1-benzotriazole ester **38e** as major product with 70%.[71]

To better evaluate the effectiveness of the electrochemical methodology (**Method A**) and any specific features of electroactivation, the reactions were consistently repeated under traditional basic conditions (**Method B**). As shown in **Table 3**, in comparison to the base-mediated process (**Method B**), despite the costs for the eChem apparatus, electrochemical promotion (**Method A**) involved shorter reaction times, a lower amount of solvent, catalytic amount of supporting electrolyte, and a simpler work-up that avoided the extraction step. On the other hand, the limitations encountered with substrates **35c-e** were also observed when using traditional base-mediated reaction.

Subsequently, the reaction was assessed using Michael acceptor functionalities as electrophilic centers at the *o*-position of the aniline molecules. In fact, although the *aza*-Michael addition represents one of the most straightforward and exploited process to form C-N bond, this reaction can be challenging, especially if internal electro-poor alkenes are used as acceptors or scarcely reactive *N*-nucleophiles (for ex. amides, as in our case) are involved. In addition, metal catalysis,[72] strongly basic/acid catalysis[73] and in general harsh pressure/temperature conditions[74] are often required to contrast the reaction reversibility.[75] Therefore, a series of *o*-

substituted anilines **35f-l** was prepared and tested in the reaction with **16** under standard electrochemical conditions (**Table 4**). The reactions with anilines **35f** and **35g** only gave isoindolinones with the free NH. Moreover, despite a high conversion of the starting materials, the isoindolinone derivatives **37f** and **37g** were isolated at only 19% and 42% yield, respectively. In contrast, using traditional base-catalyzed method, **37f** and **37g** were obtained in good 77% and 71% yields. Therefore, the decomposition of the anilines **35f** and **35g** is likely due to the low tolerance of the electron-deficient alkenyl functionalities to the cathodic environment.[70]

Pleasantly, interesting results were obtained using *o*-functionalized anilines with an inone moiety as Michael acceptor. In these cases, the electrochemical method proved to be an effective tool for tandem addition/cyclization/rearrangement and subsequent *aza*-Michael reaction, providing the tetracyclic keto-enamides **39** as a single diastereoisomer Z and yields ranging from 40% and 68%, albeit a variable amount of the corresponding acyclic isoindolinones were detected by ^{1}H-NMR analysis, in some cases (**Entry 39j**, **39k** and **39l**, acyclic isoindolinone yield in parentheses). This incomplete conversion could not be avoided after changing electrochemical parameters such as the current quantity or increasing the temperature and/or the reaction time. Further electrolysis on the crude mixture was also detrimental.

Table 4: Study of reactivity of anilines having *o*-Michael acceptors functionalities.

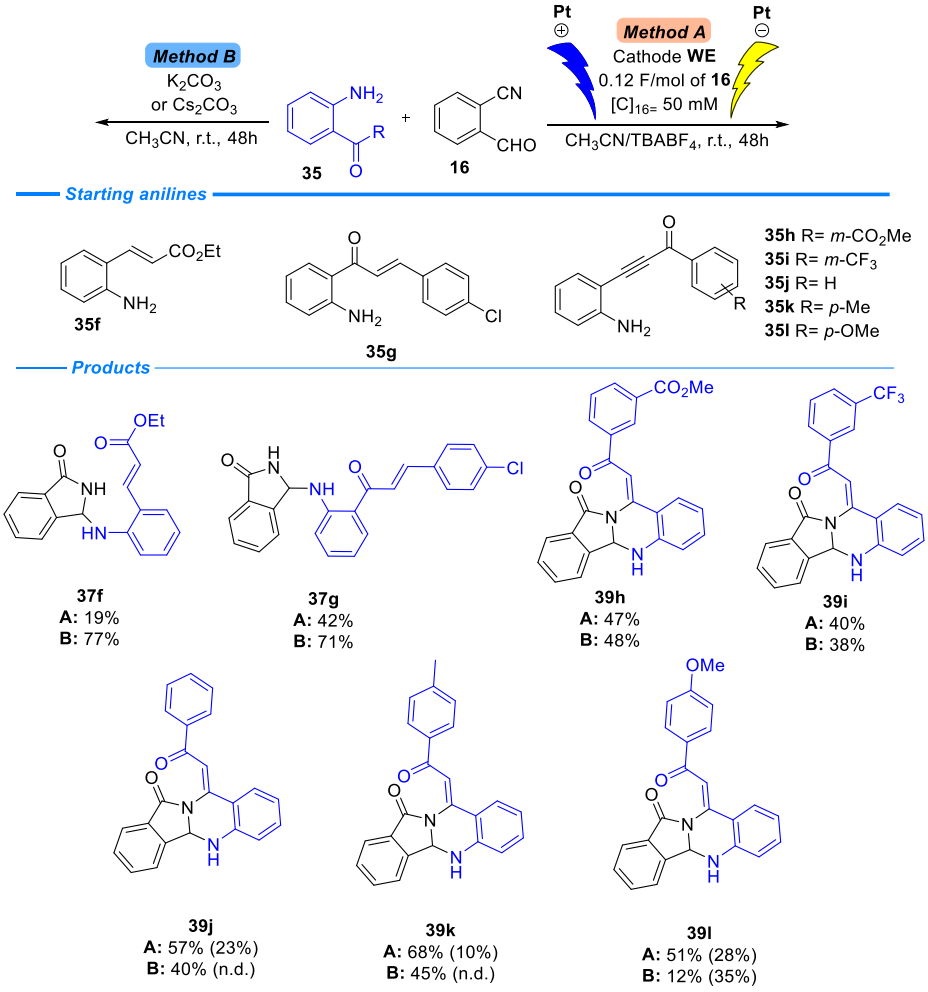

The primary challenge of cyclization likely stems from the precipitation of the open intermediate **37**, which may hinder the subsequent *aza*-Michael addition. Indeed, control experiments conducted by performing the electrolysis on isolated isoindolinones **37l-k**, resulted in their quantitative conversion into the final tetracyclic products (**Scheme 21b**). This result confirms that the electro-induced process leading to the tetracyclic derivative is controlled by a complex thermodynamic system involving the species in solid phase and in solution.

Otherwise, open intermediates **37f** and **37g** failed in producing the corresponding tetracyclic products, both under chemical and electrochemical conditions (**Scheme 21b**).

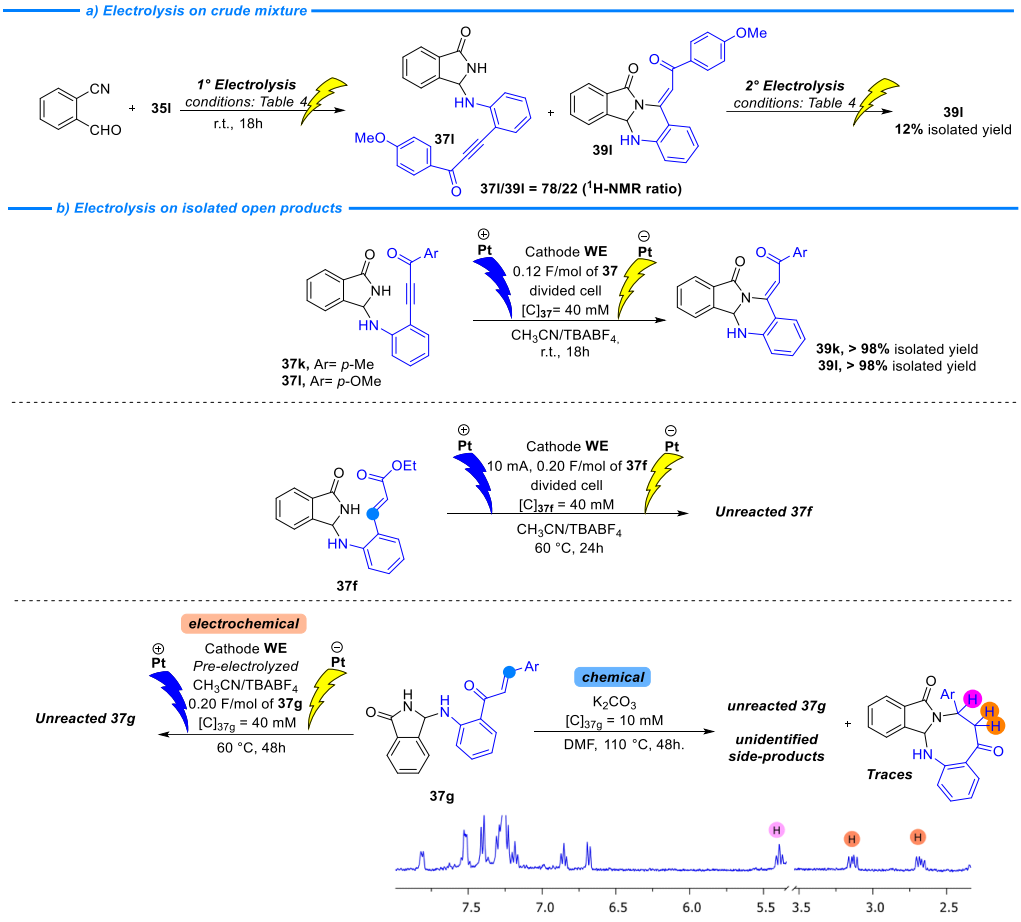

Scheme 21: Attempts of cyclization with a second electrolysis on open products.

1.7 Fused isoindoloisoquinolinones and isoindoloquinolinones

Isoquinolinones and quinolinones have garnered considerable interest due to their diverse biological activities. Numerous derivatives have demonstrated significant potential as antimalarial, antimicrobial, anti-inflammatory, and therapeutic agents (**Figure 11**).[76]

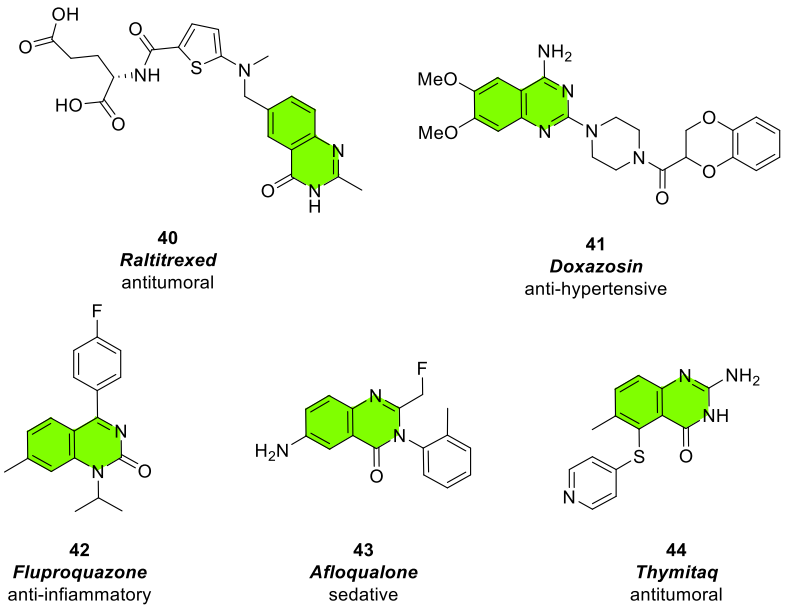

Figure 11: Biologically active Isoquinolinones and quinolinones.

For instance, Raltitrexed **40** has exhibited strong antitumor efficacy, particularly as a chemotherapeutic agent for advanced colorectal cancer.[77] Doxazosin **41** is an antihypertensive drug noted for its effectiveness and safety in treating benign prostatic hyperplasia and is also utilized in medical expulsion therapy for distal ureteric calculi.[78] Fluproquazone **42** also possesses potent analgesic properties, demonstrated in studies on soft-tissue injuries and osteoarthritis, along with notable anti-inflammatory activity.[79] Additionally, quinazolinones and their derivatives serve as key building blocks for various natural alkaloids found across numerous plant families, as well as in microorganisms and animals.[80] In recent years, various

research groups have concentrated on synthesizing fused polycyclic structures containing different heterocyclic cores with the goal to assess whether the integration of two or more biologically active cores could enhance pharmaceutical efficacy (**Figure 12**).

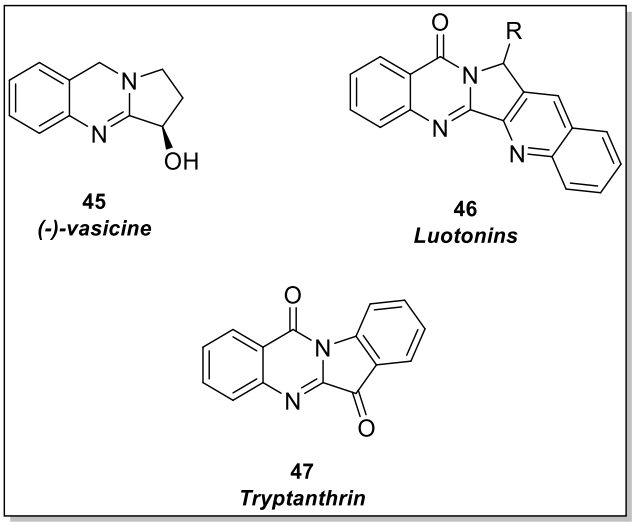

Figure 12: Fused isoindoloisoquinolinones and isoindoloquinolinones.

Part III: One-pot access to a novel batracylin analog

An intriguing example of isoindoloquinazolinone-containing polyheterocycle is the molecule **48**, known as Batracylin. Initially synthesized by Bayer AG (Leverkusen, Germany) as a potential pharmacodynamic agent and later acquired through the NCI Liaison Office (Brussels, Belgium), this molecule has demonstrated promising antitumor activity in both *in vivo* and *in vitro* preclinical studies. It has been tested against solid tumors, in particular for the treatment of colon adenocarninoma 38, demonstrating a significant inhibition of the tumor growth and so representing a valid alternative for the cisplatin- and doxorubicin-resistant tumors.[81] Subsequently, due to the low water solubility of Batracylin, which limits its oral administration,

extensive research has been conducted to develop effective analogues. The modifications mainly involved the introduction of various substituents onto the isoindoloquinalozinone core, including halogens, -NH_2, -CO_2Me and -OMe, as well as acylation with amino acids, dipeptides, tripeptides.[82] In particular, most of these structural modifications concerned the aromatic rings A and D functionalization,[83] the replacement of the nitrogen atom in position 5,[84] the derivatization of amino group[85] in position 8 and the alkylation or arylation in position 10 (**Figure 13**).[86]

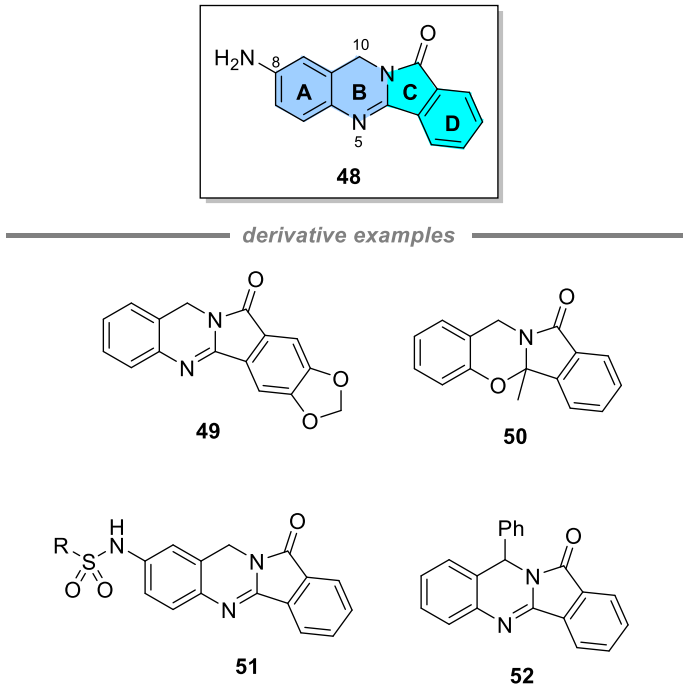

Figure 13: Batracylin and derivatives.

However, to the best of our knowledge, there are no reported examples of functionalization at position 10 with functional group other than alkyl or aryl.

During our investigation on the synthesis of isoindolinone-containing tetraheterocycles, we serendipitously discovered a straightforward access to the derivative **53**, presenting an ester functionality on the batracylin skeleton (**Figure 14**).

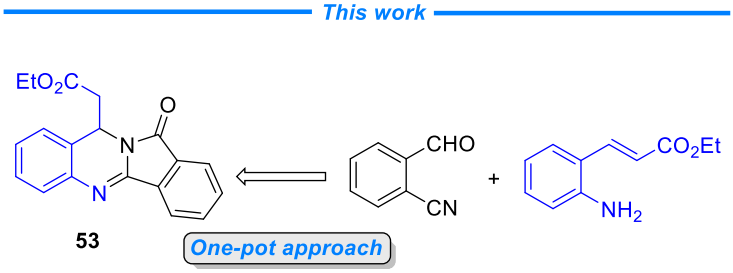

Figure 14: This work.

1.8 Results and discussion

Despite the fact that, when reacted with **16**, aniline **35f** gave almost exclusively the open isoindolinone **37f** either using electricity or K_2CO_3 catalyzed reaction (**Scheme 22a**), was observed the direct formation of dihydroisoindoloquinazolinone **53** when Cs_2CO_3 was used as base (**Scheme 22b**). Despite the modest 24% yield, it is worth noting that the derivative **53** was obtained *via* a one-pot cascade reaction, without the use of any external oxidant or the need to isolated intermediates.

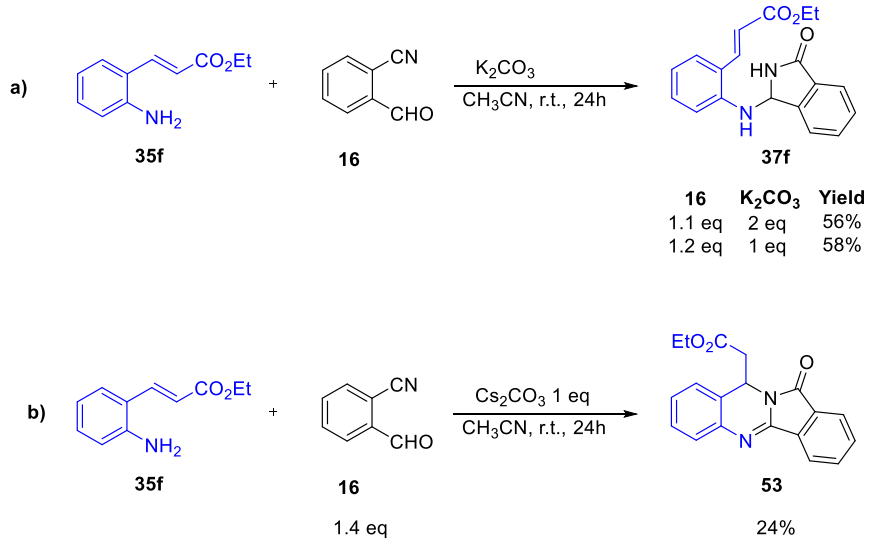

Scheme 22: One-pot synthesis of the dihydroisoindolo-quinazolin-12-one derivative **53.**

To rationalize the cascade reaction sequence leading to product **53**, I carried out a series of control experiments. When the open isoindolinone **37f** was submitted to the reaction conditions reported in **Scheme 23, eq. 1**, the *aza*-Michael reaction occurred, essentially producing the tetrahydro derivative **54** as mixture 1/1 of diastereoisomers while the desired product was only present in traces. Conversely, the conversion of **37f** in **53** increased significantly when the *aza*-Michael cyclization was performed in the presence of aldehyde **16** (**Scheme 23, eq. 2**). This entry clearly demonstrates that the starting aldehyde **16** is involved in the oxidative dehydrogenation process leading to **53**.[87] However, increasing the amount of aldehyde did not improve the final yield.

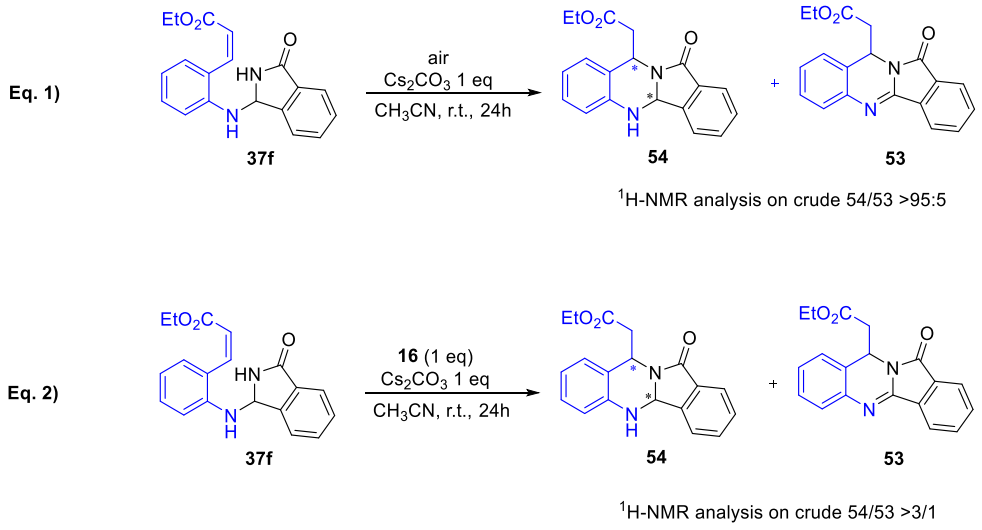

Scheme 23: Control experiments.

A preliminary photophysical characterization of isoindoloquinazolinone **53** by UV-vis absorption and fluorescence spectroscopy in solution[88] highlighted the remarkable photoluminescent properties of this compound, making it also interesting for potential applications in the development of fluorescent materials. Moreover, to shed light on the character of the involved electronic transitions, the experimental spectra were also modelled through quantum-chemical calculations. As shown in

Figure 15, the calculated UV absorption and emission spectra are perfectly stackable with the experimental values. Quantum-chemical calculation revealed that the main absorption peak at 354 nm can be characterized by HOMO → LUMO and HOMO-1 → LUMO, essentially corresponding to π-π* transitions, while the intense emission band at 439 nm is due to π*-π transitions, dominated by LUMO→ HOMO orbitals.

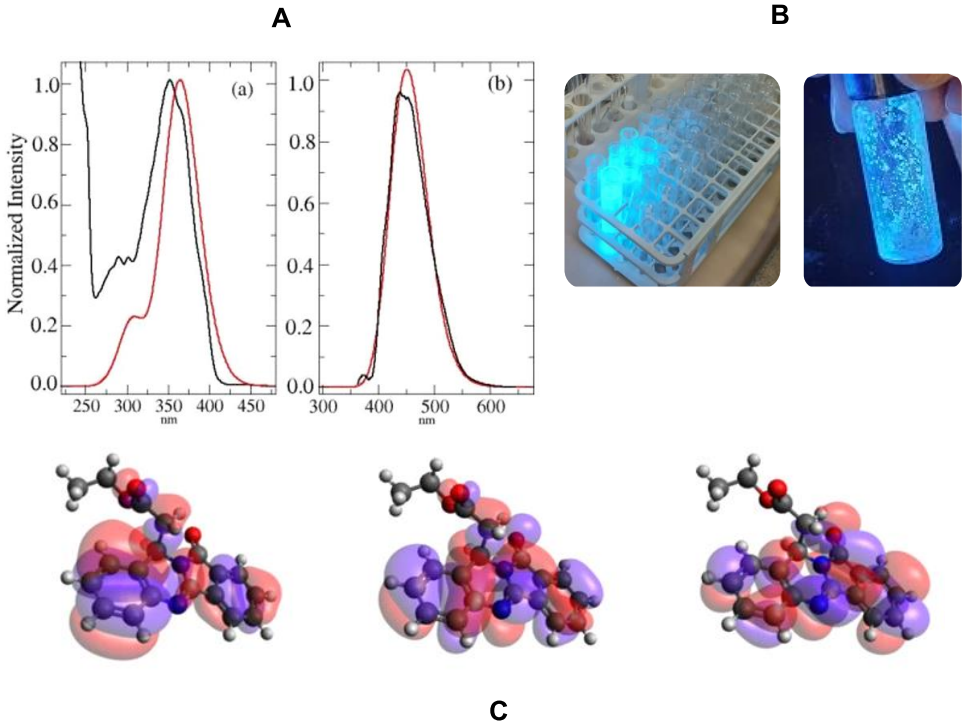

Figure 15: a) Experimental (black, in DCM) and calculated (red, in vacuum) UV absorption spectrum of **53** (spectra on the left); experimental (black, in DCM) and calculated (red, in vacuum) UV emission spectrum spectra of **53** (spectra on the right); b) Picture of fluorescence effect in liquid and solid phase; c) Frontier orbitals mainly involved in the absorption and emission spectra. HOMO-1, HOMO and LUMO representations are reported from left to right.

1.9 Conclusions

In conclusion, in the first period of my PhD, I successfully accomplished unprecedent tandem processes for the direct synthesis of isoindolinones bearing *N*-aryl groups in position 3 and isoindolinone fused tetracyclic structures, including the promising batracylin analogous **53**. During these studies, advantageous electrochemical procedures have been set up. Among the significant advantages of the electrocatalytic method, the following stand out:

- *Mild reaction conditions*
- *Use of catalytic amounts of current and supporting electrolyte*
- *Short reaction and electrolysis times*
- *Good tolerance for various functional groups*

In addition, the presence of editable functional groups on the aniline aromatic rings makes these products suitable for further elaboration of the structures. In fact, applying the same electrochemical procedure on *ortho*-functionalized anilines, unprecedented tetracylic amino-aminals and ketoenamides with *N*(Acyl) and *N*(aryl)-Acetal core can be obtained through a sequential cyclization involving of the amidic nitrogen. The comparison between chemical and electrochemical procedure evidently highlighted the significant advantages of the electro-approach, including higher yield, milder solution and simple purification procedure.

Finally, a practical synthesis for the derivative **53** a potential batracylin analogous with also relevant photoluminescent properties was developed though a one-pot five-step process using Cs_2CO_3 as base. Despite the moderate yield, general atom economy and external oxidant-free conditions make this approach particularly sustainable and eco-friendly.

1.10 Experimental section Part I

Electrochemical reactions were conducted using Hewlett Packard DC Power Supply Mod. E3612A in constant current mode, in a U-divided glass cell separated through a porous G-3 glass plug. Platinum spirals (apparent area 1 cm^2) were used as anode and cathode (distance between the electrodes 1 cm). Before use, Pt electrodes were treated with a Piranha solution (sulfuric acid/hydrogen peroxide 3:1) for 1 min, washed with double-distilled water and sonicated three times for 5 min with double-distilled water, acetone, and isopropanol. The reactions were monitored by thin layer chromatography (TLC) using Merck Silica Gel 60 F254 plates and were visualized by fluorescence quenching at 254 nm. Column chromatographic purification of products was carried out using silica gel 60 (70–230 mesh, Merck). The NMR spectra were recorded on Bruker Avance 400 spectrometers (400 MHz, ^1H; 101 MHz, ^{13}C). Spectra were referenced to residual $CHCl_3$ (7.26 ppm, ^1H; 77.00 ppm, ^{13}C), MeOD (3.31 ppm, ^1H; 49 ppm, ^{13}C) or DMSO (2.50 ppm, ^1H; 39.5 ppm, ^{13}C) when indicated. Yields are given for isolated products showing one spot on a TLC plate and seldom impurities detectable in the NMR spectrum. High-resolution mass spectra (HRMS) were acquired using a Bruker SolariX XR Fourier transform ion cyclotron resonance mass spectrometer (Bruker Daltonik GmbH, Bremen, Germany) equipped with a 7 T refrigerated actively shielded superconducting magnet. The samples were ionized in positive ion mode using an electrospray (ESI) ionization source or the MALDI ion source. All chemicals and solvents were obtained from commercial sources and were used without further purification. Pt electrodes (wires, wire, diam. 0.5 mm, 99.99% trace metals basis) were purchased from Sigma-Aldrich.

Experimental procedures and characterization data of products 15

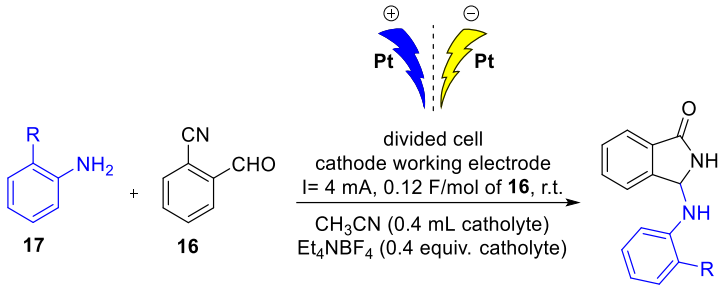

A solution of **16** (0.2 mmol), **17** (0.24 mmol), and tetraethylammonium tetrafluoroborate (Et_4NBF_4) (0.08 mmol) in MeCN (0.4 mL) is added in the cathodic compartment of a U-divided cell equipped with platinum spirals (apparent area 1 cm^2) as cathode (WE, working electrode) and anode (CE, counter electrode). Catholyte was constituted by a solution of Et_4NBF_4 (0.1 mmol) in MeCN (0.5 mL). Electrolysis was conducted under galvanostatic conditions (4 mA, 0.12 electrons/molecule of **16**) at r.t. At the end of the electrolysis, TLC analysis showed disappearance of **16** and the reaction was in any case prolonged at r.t. under magnetic stirring for 6 h. The mixture was then concentrated in vacuum and directly purified by silica gel chromatography (Hexane: Ethyl Acetate from 4:1 to 3:2) to afford the desired products **15a**–**15v.**

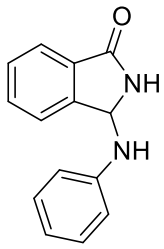

3-(phenylamino) isoindolin-1-one (**15a**): Prepared following general procedure using **16** (0.2 mmol, 26 mg) and aniline **17a** (0.24 mmol, 22 mg). The crude was purified directly by flash chromatography to give a white solid **15a** (41 mg, 91%). **^{1}H-NMR** (400 MHz, $CDCl_3$) δ = 7.87 (d, J = 7.5 Hz, 1H, Ar), 7.62 (d, J = 4.1 Hz, 2H, Ar), 7.60–7.52 (m, 1H, Ar), 7.28 (d, J = 7.9 Hz, 2H, Ar), 6.89 (t, J = 7.4 Hz, 1H, Ar), 6.79 (d, J = 8.0 Hz, 2H, Ar), 6.60 (s, 1H, CONH), 6.19 (d, J = 10.7 Hz, 1H, CH), 4.11 (d, J = 10.7 Hz, 1H, NH). **^{13}C-NMR** (101 MHz, DMSO) δ = 168.8; 146.8; 145.7; 132.6; 131.8; 129.0; 128.8; 123.7; 122.5; 117.3; 113.5; 64.7. **HRMS** (MALDI) m/z calcd for $C_{14}H_{13}N_2O$ [M + H^+] 225.1022, found 225.1009, m/z calcd for $C_{14}H_{12}N_2ONa$ [M + Na^+] 247.0841, found 247.0827.

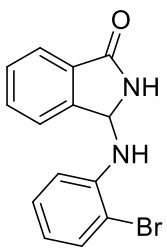

3-((2-bromophenyl) amino) isoindolin-1-one (**15b**): Prepared following general procedure using **16** (0.2 mmol, 26 mg) and 2-bromoaniline **17b** (0.24 mmol, 41 mg). The crude was purified directly by flash chromatography to give a yellow solid **15b** (48 mg, 80%). **^{1}H-NMR** (400 MHz, $CDCl_3$) δ = 7.88 (d, J = 7.3 Hz, 1H, Ar); 7.67–7.53 (m, 3H, Ar); 7.49 (d, J = 8.0 Hz, 1H, Ar); 7.30–7.16 (m, 1H, Ar); 6.94 (s, 1H, CONH); 6.89 (d, J = 8.1 Hz, 1H, Ar), 6.73 (t, J = 7.7 Hz, 1H, Ar); 6.17 (d, J = 9.7 Hz, 1H, CH); 4.85 (d, J = 9.7 Hz, 1H, NH). **^{13}C-NMR** (101 MHz, $CDCl_3$) δ = 169.6; 144.2; 142.6; 133.3; 132.8; 132.0; 129.9; 128.8; 124.0; 123.4; 120.5; 112.7; 111.2; 65.4. **HRMS** (MALDI) m/z calcd for $C_{14}H_{12}BrN_2O$ [M + H^+] 303.0127, found 303.0110.

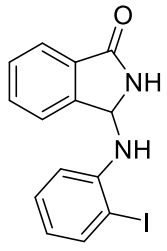

3-((2-iodophenyl) amino) isoindolin-1-one (**15c**): Prepared following general procedure using **16** (0.2 mmol, 26 mg) and 2-iodoaniline **17c** (0.24 mmol, 52 mg). The crude was purified directly by flash chromatography to give a yellow solid **15c** (40 mg, 57%). **^{1}H-NMR** (400 MHz, $CDCl_3$) δ = 7.89 (dd, J = 7.4, 1.2 Hz, 1H, Ar); 7.74 (dd, J = 7.9, 1.5 Hz, 1H, Ar); 7.68–7.55 (m, 3H, Ar); 7.29 (d, J = 7.7 Hz, 1H, Ar); 6.83 (d, J = 8.1 Hz, 1H, Ar); 6.74 (s, 1H, CONH); 6.61 (t, J = 7.6 Hz, 1H, Ar); 6.17 (d, J = 9.6 Hz, 1H, CH); 4.69 (d, J = 9.6 Hz, 1H, NH). **^{13}C-NMR** (101 MHz, $CDCl_3$) δ = 169.5; 145.0; 144.2; 139.9; 132.8; 131.9; 130.0; 129.8; 124.0; 123.4; 121.3; 112.1; 87.0; 65.8. **HRMS** (MALDI) m/z calcd for $C_{14}H_{12}IN_2O$ [M + H^+] 350.9988, found 350.9966.

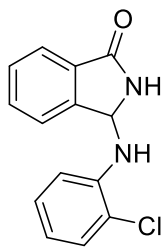

3-((2-chlorophenyl) amino) isoindolin-1-one (**15d**): Prepared following general procedure using **16** (0.2 mmol, 26 mg) and 2-chloroaniline **17d** (0.24 mmol, 30 mg). Th crude was purified directly by flash chromatography to give a yellow solid **15d** (31 mg, 61%). **^{1}H-NMR** (400 MHz, $CDCl_3$) δ = 7.86 (dt, J = 7.5, 1.1 Hz, 1H, Ar); 7.66–7.51 (m, 3H, Ar); 7.49 (s, 1H, CONH); 7.33–7.22 (m, 1H, Ar); 7.23–7.13 (m, 1H, Ar); 6.92 (dd, J = 8.3, 1.4 Hz, 1H, Ar); 6.77 (td, J = 7.7, 1.4 Hz, 1H, Ar); 6.16 (d, J = 9.7 Hz, 1H, CH); 4.85 (d, J = 9.7 Hz, 1H, NH). **^{13}C-NMR** (101 MHz, $CDCl_3$) δ = 169.6; 144.3; 141.6; 132.8; 132.0; 130.0; 129.9; 128.1; 124.0; 123.4; 120.7; 120.0; 112.6; 65.2. **HRMS** (MALDI) m/z calcd for $C_{14}H_{12}ClN_2O$ [M + H^+] 259.0632, found 259.0617.

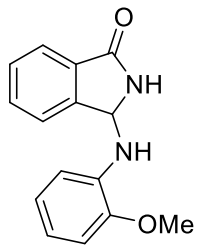

3-((2-methoxyphenyl) amino) isoindolin-1-one (**15e**): Prepared following general procedure using **16** (0.2 mmol, 26 mg) and 2-methoxyaniline **17e** (0.24 mmol, 29 mg). The crude was purified directly by flash chromatography to give a yellow solid **15e** (39 mg, 78%). **^{1}H-NMR** (400 MHz, $CDCl_3$) δ = 7.87 (d, J = 7.4 Hz, 1H, Ar); 7.68–7.49 (m, 3H, Ar); 6.98–6.79 (m, 4H, Ar); 6.72 (s, 1H, CONH); 6.19 (d, J = 8.0 Hz, 1H, CH); 4.74 (d, J = 8.0 Hz, 1H, NH); 3.80 (s, 3H, OCH_3). **^{13}C-NMR** (101 MHz, $CDCl_3$) δ = 169.5; 147.7; 144.8; 135.2; 132.5; 132.0; 129.7; 123.9; 123.6; 121.4; 119.4; 111.4; 110.5; 65.4; 55.5. **HRMS** (MALDI) m/z calcd for $C_{15}H_{15}N_2O_2$ [M + H^+] 255.1128, found 255.1112.

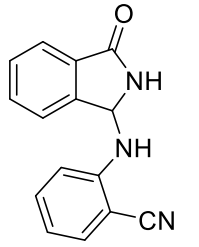

2-((3-oxoisoindolin-1-yl) amino) benzonitrile (**15f**): Prepared following general procedure using **16** (0.2 mmol, 26 mg) and 2-cyanoaniline **17f** (0.24 mmol, 28 mg). The crude was purified directly by flash chromatography to give a yellow solid **15f** (29 mg, ^{59}%). **^{1}H-NMR** (400 MHz, $CDCl_3$) δ = 7.88 (d, J = 7.3 Hz, 1H, Ar); 7.69–7.55 (m, 3H, Ar); 7.47 (m, 2H, Ar); 7.11 (s, 1H, CONH); 6.94–6.83 (m, 2H, Ar); 6.21 (d, J = 9.2 Hz, 1H, CH); 5.07 (d, J = 9.2 Hz, 1H, NH). **^{13}C-NMR** (101 MHz, $CDCl_3$) δ = 169.7; 147.8; 143.5; 134.6; 133.4; 133.0; 131.8; 130.2; 124.2; 123.4; 119.3; 117.1; 112.0; 98.4; 64.8. **HRMS** (MALDI) m/z calcd for $C_{15}H_{12}N_3O$ [M + H^+] 250.0974, found 250.0962.

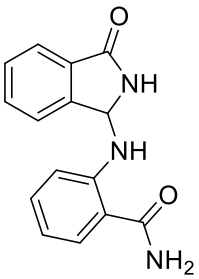

2-((3-oxoisoindolin-1-yl) amino) benzamide (**15g**): Prepared following general procedure using **16** (0.2 mmol, 26 mg) and 2-aminobenzamide **17g** (0.24 mmol, 32 mg). The crude was purified directly by flash chromatography to give a white solid **15g** (42 mg, 79%). **^{1}H-NMR** (400 MHz, MeOD) δ = 7.79 (d, J = 7.5 Hz, 1H, Ar); 7.71–7.61 (m, 2H, Ar); 7.57 (t, J = 7.5 Hz, 1H, Ar); 7.45 (d, J = 7.6 Hz, 1H, Ar); 7.19 (t, J = 7.7 Hz, 1H, Ar); 6.76 (d, J = 8.3 Hz, 1H, Ar); 6.72 (s, 1H, CH); 6.57 (t, J = 7.6 Hz, 1H, Ar). **^{13}C NMR** (101 MHz, DMSO-d_6) δ 169.4; 168.9; 150.1; 145.4; 132.6; 132.2; 131.9; 128.9; 128.5; 123.5; 122.5; 116.4; 114.4; 113.4; 60.4. **HRMS** (MALDI) m/z calcd for $C_{15}H_{14}N_3O_2$ [M + H^+] 268.1080, found 268.1145

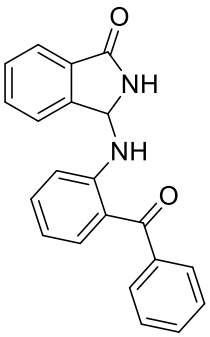

3-((2-benzoylphenyl) amino) isoindolin-1-one (**15h**): Prepared following general procedure using **16** (0.2 mmol, 26 mg) and 2-aminobenzophenone **17h** (0.24 mmol, 47 mg). The crude was purified directly by flash chromatography to give a yellow solid **15h** (49 mg, 75%). **^{1}H-NMR** (400 MHz, $CDCl_3$) δ = 8.81 (d, J = 8.4 Hz, 1H, NH); 7.88 (d, J = 7.4 Hz, 1H, Ar); 7.68–7.38 (m, 10H, Ar); 7.07 (s, 1H, CONH); 6.99 (d, J = 8.4 Hz, 1H, Ar); 6.75 (t, J = 7.6 Hz, 1H, Ar); 6.26 (d, J = 8.4 Hz, 1H, CH). **^{13}C-NMR** (101 MHz, $CDCl_3$) δ = 199.4; 169.7; 149.2; 144.3; 139.7; 135.7; 135.1; 132.8; 131.9; 131.5; 129.9; 129.3; 128.2; 124.0; 123.4; 119.5; 116.6; 112.0; 64.3. **HRMS** (MALDI) m/z calcd for $C_{21}H_{17}N_2O_2$ [M + H$^+$] 329.1284, found 329.1264.

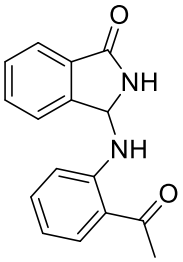

3-((2-acetylphenyl) amino) isoindolin-1-one (**15i**): Prepared following general procedure using **16** (0.2 mmol, 26 mg) and 2-aminoacetophenone **17i** (0.24 mmol, 32 mg). The crude was purified directly by flash chromatography to give a yellow solid **15i** (24 mg, 45%). **^{1}H-NMR** (400 MHz, $CDCl_3$) δ = 9.35 (d, J = 8.4 Hz, 1H, NH); 7.88 (d, J = 7.3 Hz, 1H, Ar); 7.84 (dd, J = 8.1, 1.5 Hz, 1H, Ar); 7.66–7.54 (m, 3H, Ar); 7.47–7.40 (m, 1H, Ar); 6.89 (d, J = 8.4 Hz, 1H, Ar); 6.84–6.77 (m, 1H, Ar); 6.72 (s, 1H, CONH); 6.22 (d, J = 8.4 Hz, 1H, CH); 2.59 (s, 3H, CH_3). **^{13}C-NMR** (101 MHz, $CDCl_3$) δ = 201.3; 169.6; 148.7; 144.4; 135.3; 133.1; 132.8; 129.8, 124.0; 123.3; 119.4; 116.9; 111.9; 64.1; 28.1. **HRMS** (MALDI) m/z calcd for $C_{16}H_{15}N_2O_2$ [M + H$^+$] 267.1128, found 267.1111.

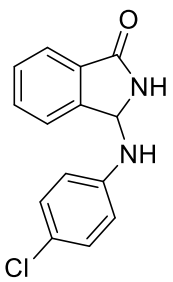

3-((4-chlorophenyl) amino) isoindolin-1-one (**15j**): Prepared following general procedure using **16** (0.2 mmol, 26 mg) and 4-chloroaniline **17j** (0.24 mmol, 30 mg). The crude was purified directly by flash chromatography to give a white solid **15j** (40 mg, 79%). **^{1}H-NMR** (400 MHz, MeOD) δ = 7.79 (d, J = 7.5 Hz, 1H, Ar); 7.70–7.60 (m, 2H, Ar); 7.57 (t, J = 7.3 Hz, 1H, Ar); 7.13 (d, J = 8.4 Hz, 2H, Ar); 6.77 (d, J = 8.4 Hz, 2H, Ar); 6.19 (s, 1H, CH). **^{13}C-NMR** (101 MHz, MeOD) δ = 172.5; 146.9; 146.8; 133.7; 133.4; 130.5; 130.0; 124.9; 124.2; 124.2; 116.5; 67.3. **HRMS** (MALDI) m/z calcd for $C_{14}H_{12}ClN_2O$ [M + H$^+$] 259.0632, found 259.0618.

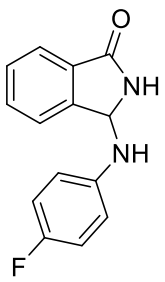

3-((4-fluorophenyl) amino) isoindolin-1-one (**15k**): Prepared following general procedure using **16** (0.2 mmol, 26 mg) and 4-fluoroaniline **17k** (0.24 mmol, 26 mg). The crude was purified directly by flash chromatography to give a yellow solid **15k** (34 mg, 71%). **^{1}H-NMR** (400 MHz, MeOD) δ = 7.78 (d, J = 7.5 Hz, 1H, Ar); 7.65 (d, J = 6.4 Hz, 2H, Ar); 7.56 (t, J = 7.0 Hz, 1H, Ar); 6.90 (t, J = 8.6 Hz, 2H, Ar); 6.84–6.73 (m, 2H, Ar); 6.16 (s, 1H, CH). **^{13}C-NMR** (101 MHz, MeOD) δ = 178.4; 165.9; 163.6; 155.1; 152.9; 142.1; 141.4; 138.6; 133.3; 132.1; 124.9; 124.7; 124.3; 74.9. **HRMS** (MALDI) m/z calcd for $C_{14}H_{12}FN_2O$ [M + H$^+$] 243.0928, found 243.0913.

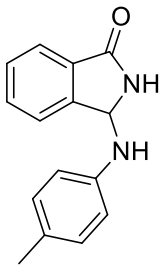

3-(*p*-tolylamino)isoindolin-1-one (**15l**): Prepared following general procedure **A** using **16** (0.2 mmol, 26 mg) and *p*-toluidine **17l** (0.24 mmol, 26 mg). The crude was purified directly by flash chromatography to give a white solid **15l** (34 mg, 72%). **^{1}H-NMR** (400 MHz, $CDCl_3$) δ = 7.85 (d, J = 7.4 Hz, 1H, Ar); 7.65–7.51 (m, 3H, Ar); 7.07 (d, J = 7.8 Hz, 2H, Ar); 6.70 (d, J = 7.8 Hz, 2H, Ar); 6.64 (s, 1H, CONH); 6.14 (d, J = 8.6 Hz, 1H, CH); 3.96 (d, J = 8.6 Hz, 1H, NH); 2.28 (s, 3H, CH_3). **^{13}C-NMR** (101 MHz, $CDCl_3$) δ = 169.5; 144.7; 143.0; 132.5; 132.0; 130.3; 129.8; 129.6; 123.9; 123.5; 114.7; 66.3; 20.5. **HRMS** (MALDI) m/z calcd for $C_{15}H_{15}N_2O$ [M + H$^+$] 239.1178, found 239.1166.

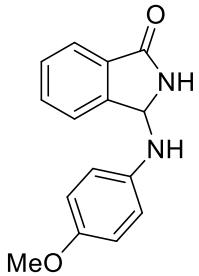

3-((4-methoxyphenyl) amino) isoindolin-1-one (**15m**): Prepared following general procedure using **16** (0.2 mmol, 26 mg) and 4-methoxyaniline **17m** (0.24 mmol, 29 mg). The crude was purified directly by flash chromatography to give a brown solid **15m** (39 mg, 78%). **^{1}H-NMR** (400 MHz, $CDCl_3$) δ = 7.85 (d, J = 7.4 Hz, 1H, Ar); 7.65–7.49 (m, 3H, Ar); 6.84 (d, J = 8.7 Hz, 2H, Ar); 6.75 (d, J = 8.7 Hz, 2H, Ar); 6.67 (s, 1H, CONH); 6.06 (s, 1H, CH); 3.89–3.77 (m, 4H, OCH_3 + NH). **^{13}C-NMR** (101 MHz, $CDCl_3$) δ = 169.5; 154.1; 144.7; 139.0; 132.5; 131.9; 129.7; 123.9; 123.6; 116.6; 115.3; 67.2; 55.7. **HRMS** (MALDI) m/z calcd for $C_{15}H_{15}N_2O_2$ [M + H$^+$] 255.1128, found 255.1119.

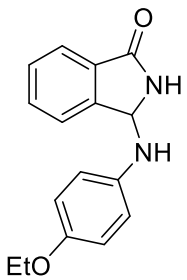

3-((4-ethoxyphenyl) amino) isoindolin-1-one (**15n**): Prepared following general procedure using **16** (0.2 mmol, 26 mg) and 4-ethoxyaniline **17n** (0.24 mmol, 33 mg). The crude was purified directly by flash chromatography to give a yellow solid **15n** (37 mg, 70%). **^{1}H-NMR** (400 MHz, $CDCl_3$) δ = 7.85 (d, J = 7.4 Hz, 1H, Ar); 7.64–7.48 (m, 3H, Ar); 6.86–6.81 (m, 2H, Ar); 6.77–6.71 (m, 2H, Ar); 6.65 (s, 1H, CONH); 6.07 (s, 1H, CH); 3.99 (q, J = 7.0 Hz, 2H, CH_2); 3.81 (s, 1H, NH); 1.40 (t, J = 7.0 Hz, 3H, CH_3). **^{13}C-NMR** (101 MHz, $CDCl_3$) δ = 169.5; 153.4; 144.7; 138.9; 132.5; 131.9; 129.7; 123.9; 123.6; 116.6; 116.1; 67.2; 64.0. **HRMS** (MALDI) m/z calcd for $C_{16}H_{17}N_2O_2$ [M + H^+] 269.1284, found 269.1271.

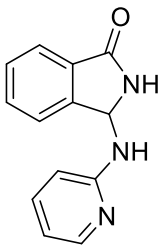

3-(pyridin-2-ylamino) isoindolin-1-one (**15p**): Prepared following general procedure using **16** (0.2 mmol, 26 mg) and 2-aminopyridine **17p** (0.24 mmol, 22 mg). The crude was purified directly by flash chromatography to give a yellow solid **15p** (28 mg, 62%). **^{1}H-NMR** (400 MHz, $CDCl_3$) δ = 8.23–8.12 (m, 1H, Ar); 7.83 (d, J = 7.5 Hz, 1H, Ar); 7.60 (d, J = 4.1 Hz, 2H, Ar); 7.57–7.42 (m, 2H, Ar); 7.06 (s, 1H, CONH); 6.79–6.70 (m, 1H, Ar); 6.57 (d, J = 8.8 Hz, 1H, CH); 6.51 (d, J = 8.3 Hz, 1H, Ar); 4.93 (d, J = 8.8 Hz, 1H, NH). **^{13}C-NMR** (101 MHz, $CDCl_3$) δ = 169.2; 157.1; 148.1; 144.7; 137.8; 132.5; 132.4; 129.7; 124.4; 123.9; 123.2; 115.1; 109.8; 63.4. **HRMS** (MALDI) m/z calcd for $C_{13}H_{12}N_3O$ [M + H^+] 226.0974, found 226.0971.

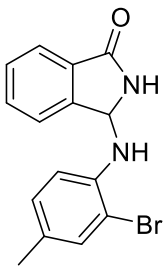

3-((2-bromo-4-methylphenyl) amino) isoindolin-1-one (**15q**): Prepared following general procedure using **16** (0.2 mmol, 26 mg) and 2-bromo-4-methylaniline **17q** (0.24 mmol, 44 mg). The crude was purified directly by flash chromatography to give a yellow solid **15q** (42 mg, 67%). **^{1}H-NMR** (400 MHz, $CDCl_3$) δ = 7.87 (d, J = 7.4 Hz, 1H, Ar); 7.61 (m, 2H, Ar); 7.57 (d, J = 7.4 Hz, 1H, Ar); 7.31 (s, 1H, Ar); 7.03 (d, J = 8.2 Hz, 1H, Ar); 6.94 (s, 1H, CONH); 6.79 (d, J = 8.2 Hz, 1H, Ar); 6.12 (d, J = 9.8 Hz, 1H, CH); 4.68 (d, J = 9.8 Hz, 1H, NH); 2.25 (s, 3H, CH_3). **^{13}C-NMR** (101 MHz, $CDCl_3$) δ = 169.6; 144.4; 140.2; 133.5; 132.7; 131.9; 130.4; 129.9; 129.3; 123.9; 123.4; 113.0; 111.3; 65.8; 20.1. **HRMS** (MALDI) m/z calcd for $C_{15}H_{14}N_2OBr$ [M + H^+] 317.0284, found 317.0265.

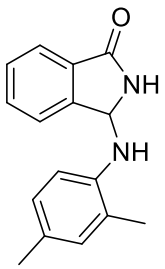

3-((2,4-dimethylphenyl) amino) isoindolin-1-one (**15r**): Prepared following general procedure using **16** (0.2 mmol, 26 mg) and 2,4-dimethylaniline **17r** (0.24 mmol, 29 mg). The crude was purified directly by flash chromatography to give a yellow solid **15r** (32 mg, 64%). **^{1}H-NMR** (400 MHz, $CDCl_3$) δ = 7.87 (d, J = 7.4, 1H, Ar), 7.68–7.58 (m, 2H, Ar), 7.56 (m, 1H, Ar), 7.05–6.90 (m, 2H, Ar), 6.82 (m, 2H, Ar + CONH), 6.16 (s, 1H, CH), 3.86 (s, 1H, NH), 2.27 (s, 3H, CH_3), 2.11 (s, 3H, CH_3). **^{13}C-NMR** (101 MHz, $CDCl_3$) δ = 169.6; 145.1; 141.2; 132.7; 132.0; 129.9; 129.3; 127.8; 124.3; 124.0; 123.6; 112.1; 112.0; 66.2; 20.5; 17.6. **HRMS** (MALDI) m/z calcd for $C_{16}H_{17}N_2O$ [M + H^+] 253.1335, found 253.1325.

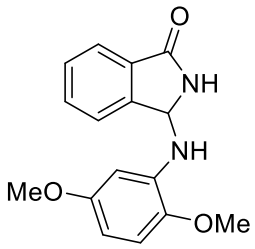

3-((2,5-dimethoxyphenyl)amino) isoindolin-1-one (**15s**): Prepared following general procedure using **16** (0.2 mmol, 26 mg) and 2,5-dimethoxyaniline **17s** (0.24 mmol, 36 mg). The crude was purified directly by flash chromatography to give a white solid **15s** (34 mg, 61%). **^{1}H-NMR** (400 MHz, $CDCl_3$) δ = 7.86 (d, J = 7.4 Hz, 1H, Ar); 7.67–7.48 (m, 3H, Ar); 6.80 (s, 1H, CONH); 6.73 (d, J = 8.8 Hz, 1H, Ar); 6.46 (d, J = 2.8 Hz, 1H, Ar); 6.31 (dd, J = 8.8, 2.8 Hz, 1H, Ar); 6.14 (d, J = 10.2 Hz, 1H, CH); 4.77 (d, J = 10.2 Hz, 1H, NH); 3.75 (d, J = 1.3 Hz, 6H, OCH_3). **^{13}C-NMR** (101 MHz, $CDCl_3$) δ = 169.5; 154.7; 144.7; 142.1; 136.2; 132.5; 132.1; 129.7; 123.9; 123.5; 111.1; 101.9; 99.6; 65.2; 56.0; 55.7. **HRMS** (MALDI) m/z calcd for $C_{16}H_{17}N_2O_3$ [M + H^+] 285.1233, found 285.1216.

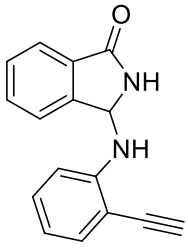

3-((2-ethynylphenyl) amino) isoindolin-1-one (**15t**): Prepared following general procedure using **16** (0.2 mmol, 26 mg) and 2-((trimethylsilyl)ethynyl)aniline **17t** (0.24 mmol, 45 mg). The crude was purified directly by flash chromatography to give a yellow solid **15t** (26 mg, 53%). **^{1}H-NMR** (400 MHz, $CDCl_3$) δ = 7.89 (d, J = 7.3 Hz, 1H, Ar); 7.68–7.60 (m, 2H, Ar); 7.60–7.54 (m, 1H, Ar); 7.41 (dd, J = 7.7, 1.6 Hz, 1H, Ar); 7.28 (d, J = 1.6 Hz, 1H, Ar); 6.88–6.77 (m, 2H, Ar); 6.72 (s, 1H, CONH); 6.22 (d, J = 9.6 Hz, 1H, CH); 5.11 (d, J = 9.6 Hz, 1H, NH); 3.33 (s, 1H, CH). **^{13}C-NMR** (101 MHz, $CDCl_3$) δ = 169.5, 146.9; 144.4; 133.4; 132.8; 131.9; 130.5; 129.9; 124.0; 123.4; 118.9; 110.8; 108.5; 83.7; 79.8; 65.1. **HRMS** (MALDI) m/z calcd for $C_{16}H_{13}N_2O$ [M + H^+] 249.1022, found 249.1008.

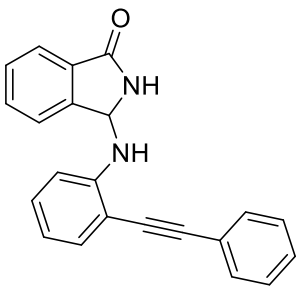

3-((2-(phenylethynyl) phenyl) amino) isoindolin-1-one (**15u**): Prepared following general procedure using **16** (0.2 mmol, 26 mg) and 2-(phenylethynyl) aniline **17u** (0.24 mmol, 46 mg). The crude was purified directly by flash chromatography to give a yellow solid **15u** (44 mg, 69%). **^{1}H-NMR** (400 MHz, $CDCl_3$) δ = 7.89 (d, J = 7.4 Hz, 1H, Ar); 7.68–7.63 (m, 2H, Ar); 7.62–7.54 (m, 1H, Ar); 7.45 (d, J = 7.6 Hz, 1H, Ar); 7.40–7.35 (m, 2H, Ar); 7.32–7.26 (m, 4H, Ar); 6.88–6.80 (m, 3H, Ar + CONH); 6.23 (d, J = 9.5 Hz, 1H, CH); 5.13 (d, J = 9.5 Hz, 1H, NH). **^{13}C-NMR** (101 MHz, $CDCl_3$) δ = 169.6; 146.1; 144.6; 132.9; 132.8; 132.0; 131.5; 130.1; 129.9; 128.5; 128.4; 128.4; 124.0; 123.3; 122.8; 119.1; 111.1; 109.8; 95.8; 85.1; 65.4. **HRMS** (MALDI) m/z calcd for $C_{22}H_{17}N_2O$ [M + H^+] 325.1335, found 325.1318.

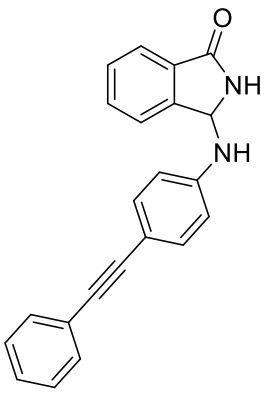

3-((4-(phenylethynyl) phenyl) amino) isoindolin-1-one (**15v**): Prepared following general procedure using **16** (0.2 mmol, 26 mg) and 4-(phenylethynyl) aniline **17v** (0.24 mmol, 46 mg). The crude was purified directly by flash chromatography to give a yellow solid **15v** (45 mg, 70%). **^{1}H-NMR** (400 MHz, DMSO) δ = 9.06 (s, 1H, CONH); 7.70 (d, J = 7.4 Hz, 1H, Ar); 7.68–7.60 (m, 1H, Ar); 7.61–7.52 (m, 2H, Ar); 7.48 (d, J = 7.4 Hz, 2H, Ar); 7.38 (q, J = 8.2, 7.3 Hz, 3H, Ar); 7.31 (d, J = 8.2 Hz, 2H, Ar); 6.85 (d, J = 9.3 Hz, 1H, CH); 6.81 (d, J = 8.3 Hz, 2H, Ar); 6.24 (d, J = 9.3 Hz, 1H, NH). **^{13}C-NMR** (101 MHz, DMSO) δ = 169.3; 147.9; 145.8; 133.0; 132.9; 132.5; 131.4; 129.7; 129.1; 128.4; 124.3; 123.7; 123.1; 113.9; 110.7; 91.2; 87.6; 64.7. **HRMS** (MALDI) m/z calcd for $C_{22}H_{17}N_2O$ [M + H^+] 325.1335, found 325.1314.

1.11 Experimental section Part II

Electrochemical reactions were conducted using Hewlett Packard DC Power Supply Mod. E3612A in constant current mode, in a U-divided glass cell separated through a porous G-3 glass plug. Platinum spirals (apparent area 1 cm^2) were used as anode and cathode (distance between the electrodes 1 cm). Before using, Pt electrodes were treated with a Piranha solution (sulfuric acid/hydrogen peroxide 3:1) for 1 min, washed with double-distilled water and sonicated three times for 5 min with double-distilled water, acetone, and isopropanol. The reactions were monitored by thin layer chromatography (TLC) using Merck Silica Gel 60 F254 plates and were visualized by fluorescence quenching at 254 nm. Column chromatographic purification of products was carried out using silica gel 60 (70–230 mesh, Merck). The NMR spectra were recorded on Bruker Avance 400 spectrometers (400 MHz, ^1H; 101 MHz, ^{13}C). Spectra were referenced to residual $CHCl_3$ (7.26 ppm, ^1H; 77.00 ppm, ^{13}C), MeOD (3.31 ppm, ^1H; 49 ppm, ^{13}C) or DMSO (2.50 ppm, ^1H; 39.5 ppm, ^{13}C) when indicated. Yields are given for isolated products showing one spot on a TLC plate and seldom impurities detectable in the NMR spectrum. High-resolution mass spectra (HRMS) were acquired using a Bruker SolariX XR Fourier transform ion cyclotron resonance mass spectrometer (Bruker Daltonik GmbH, Bremen, Germany) equipped with a 7 T refrigerated actively shielded superconducting magnet. The samples were ionized in positive ion mode using an electrospray (ESI) ionization source or the MALDI ion source. All chemicals and solvents were obtained from commercial sources and were used without further purification. Pt electrodes (wires, wire, diam. 0.5 mm, 99.99% trace metals basis) were purchased from Sigma-Aldrich. The substrates **35** were synthesized according to previously described methods.

Experimental procedures and characterization data of compounds 36, 37 and 39:

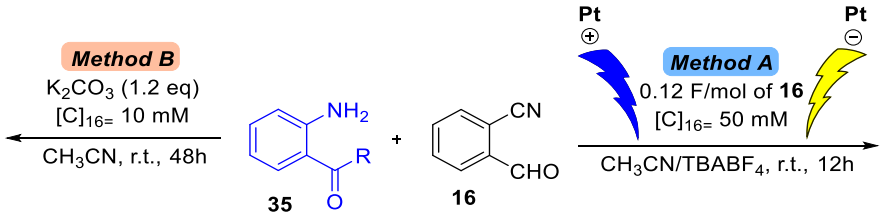

Method A: A solution of 2-cyanobenzaldehyde **16** (0.026 g, 0.2 mmol), aniline **35** (0.24 mmol) and tetrabutylammoniumtetrafluoroborate (Bu_4NBF_4) (0.008 g, 0.024 mmol) in MeCN (0.4 mL) is added in the cathodic compartment of a U-divided cell equipped with platinum spirals (apparent area 1 cm^2) as cathode (WE, working electrode) and anode (CE, counter electrode). Anolyte was constituted by a solution of Bu_4NBF_4 (0.033 g, 0.1 mmol) in MeCN (0.5mL). Electrolysis was conducted under galvanostatic conditions (4mA, 0.12 electrons/molecule of **16**) at r.t. At the end of the electrolysis, TLC analysis showed disappearance of **16** and the reaction was in any case prolonged at r.t. (or 60°C, for substrate **37l**) under magnetic stirring . The mixture was then concentrated in vacuum and directly purified by silica gel chromatography (Hexane/Ethyl Acetate from 4:1 to 3:2) to afford the product **36-37-39**.

Method B: In a round-bottom flask 2-cyanobenzaldehyde **16** (0.026 g, 0.2 mmol), aniline **35** (0.24 mmol) and K_2CO_3 (0.028 g, 0.2 mmol) are dissolved in acetonitrile (2 mL). After 48h (reaction monitored by TLC), the reaction was diluted with CH_2Cl_2 (1 mL) and evaporated under reduced pressure. The residue was purified by flash chromatography over silica gel eluting with *n*-Hexane/AcOEt (Hexane/Ethyl Acetate from 4:1 to 3:2) to give the product **36-37-39**.

General procedure for the two-steps synthesis of 39l:

I step: In a round-bottom flask 2-cyanobenzaldehyde **16** (0.026 g, 0.2 mmol), aniline **35l** (0.060 g, 0.24 mmol) and K_2CO_3 (0.028 g, 0.2 mmol) are dissolved in acetonitrile (2 mL). After 18h (reaction monitored by TLC), the reaction was diluted with CH_2Cl_2 (1 mL) and evaporated under reduced pressure. The residue was purified by flash chromatography over silica gel eluting with *n*-Hexane/AcOEt (Hexane/Ethyl Acetate from 4:1 to 3:2) to give product 3-((2-(3- (4 methoxyphenyl) -3-oxoprop-1-yn-1-yl) phenyl) amino) isoindolin-1 one (**37l**) as a yellow solid (0.027 g, 35% yield).

II Step: A suspension of **37l** (0.027 g, 0.07 mmol) in Acetonitrile/ $TBABF_4$ (0.18 mL/0.003 g, 0.008 mmol) was electrolyzed in the cathodic compartment of a U-divided cell equipped with platinum spirals (apparent area 1 cm^2) as cathode (WE, working electrode) and anode (CE, counter electrode). Anolyte was constituted by a solution of Bu_4NBF_4 (0.017 g, 0.05 mmol)

in MeCN (0.20 mL). Electrolysis was conducted under galvanostatic conditions (4mA, 0.12 electrons/molecule of **37l**) at r.t. The mixture was stirred at r.t. for 18h. The mixture was then concentrated in vacuum and directly purified by silica gel chromatography (Hexane/Ethyl Acetate 4:1) to afford the product (Z)-10-(2-(4-methoxyphenyl)-2 oxoethylidene)-5,10-dihydro isoindolo[1,2-b]quinazolin-12(4bH) one (**39l**) as a yellow solid (0.027 g, 100% yield).

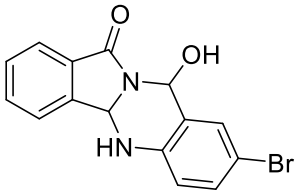

8-bromo-10-hydroxy-4b,5-dihydroisoindolo[1,2-b] quinazolin-12(10H)-one (**36a**): The product **36a** (**A** 0,054 g, 82 %; **B** 0,054 g, 82 %) was obtained as white solid. **^{1}H-NMR** (400 MHz, MeOD) δ = 7.86 (d, J = 7.6 Hz, 1H); 7.81 (d, J = 7.6 Hz, 1H); 7.73 (t, J = 7.5, 1H); 7.62 (t, J = 7.5 Hz, 1H); 7.55 (d, J = 2.3 Hz, 1H); 7.27 (dd, J = 8.7, 2.3 Hz, 1H); 6.77 (d, J = 8.7 Hz, 1H); 6.34 (s, 1H, CH); 5.72 (s, 1H, CH). **^{13}C-NMR** (101 MHz, DMSO) δ = 165.1; 142.9; 142.5; 132.4; 131.8; 131.6; 131.3; 129.5; 123.8; 123.5; 123.4; 108.9; 68.7; 62.0. **HRMS** (MALDI) m/z calculated for $C_{15}H_{12}BrN_2O_2$ [M+H$^+$] 330.9881, found 331.0076.

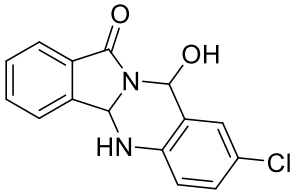

8-chloro-10-hydroxy-4b,5-dihydroisoindolo[1,2-b] quinazolin-12(10H)-one (**36b**): The product **36b** (**A** 0,042 g, 74%; **B** 0,043 g, 76%) was obtained as white solid. **^{1}H-NMR** (400 MHz, MeOD) δ = 7.86 (d, J = 7.6 Hz, 1H); 7.81 (d, J = 7.6 Hz, 1H); 7.73 (t, J = 7.5 Hz, 1H); 7.62 (t, J = 7.5 Hz, 1H); 7.41 (d, J = 2.1 Hz, 1H); 7.15 (dd, J = 8.7, 2.3 Hz, 1H); 6.82 (d, J = 8.7 Hz, 1H); 6.33 (s, 1H, CH); 5.72 (s, 1H, CH). **^{13}C-NMR** (101 MHz, MeOD) δ = 167.7; 143.33; 141.9; 132.6; 131.8; 130.9; 129.4; 129.2; 128.8; 128.6; 128.5; 123.8; 123.5; 123.1; 122.7; 117.6; 69.4; 63.0. **HRMS** (MALDI) m/z calculated for $C_{15}H_{12}ClN_2O_2$ [M+H$^+$] 287.0587, found 287.0579.

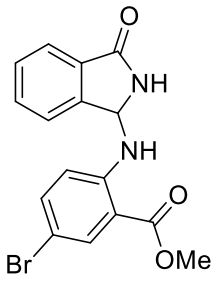

methyl 5-bromo-2-((3-oxoisoindolin-1-yl) amino) benzoate (**37d**): The product **37d** (**A** 0,033 g, 46%; **B** 0,045 g, 63%) was obtained as white solid. **^{1}H-NMR** (400 MHz, DMSO-d_6) δ = 9.20 (s, 1H, NH); 8.07 (d, J = 8.3 Hz, 1H); 7.93 (s, 1H); 7.73 (d, J = 7.4 Hz, 1H); 7.67 (d, J = 7.0 Hz, 1H); 7.65 – 7.56 (m, 3H); 7.08 (d, J = 9.3 Hz, 1H, CH); 6.39 (d, J = 8.4 Hz, 1H, NH); 3.78 (s, 3H, OCH_3). **^{13}C-NMR** (101 MHz, DMSO-d_6) δ = 169.3; 167.5; 148.5; 145.3; 137.5; 133.4; 133.0; 132.7; 130.1; 123.9; 123.5;116.2; 112.9;

107.7; 64.2; 52.7. **HRMS** (MALDI) m/z calculated for $C_{16}H_{14}BrN_2O_3$ [M+H$^+$] 361.0188, found 361.0221.

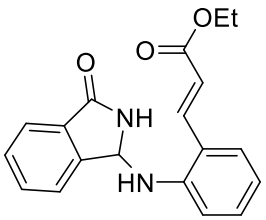

Ethyl 3-(2-((3-oxoisoindolin-1-yl) amino) phenyl) acrylate (37f): The product **37f** (**A** 0,012 g, 19%; **B** 0,049 g, 77%) was obtained as yellow solid. **^{1}H-NMR** (400 MHz, $CDCl_3$) δ = 7.85 (s, 1H), 7.79 (d, J = 15.7 Hz, 1H, CH), 7.63 (d, J = 5.5 Hz, 2H), 7.56 (t, J = 7.2 Hz, 1H), 7.46 (d, J = 7.7 Hz, 1H), 7.33 (t, J = 7.7 Hz, 1H), 7.02 (s, 1H, NH), 6.93 (dt, J = 10.4, 5.8 Hz, 2H), 6.33 (d, J = 15.7 Hz, 1H, CH), 6.13 (d, J = 10.2 Hz, 1H, CH), 4.46 (d, J = 10.2 Hz, 1H, NH), 4.20 (q, J = 7.1 Hz, 2H, CH_2), 1.29 (t, J = 7.1 Hz, 3H, CH_3). **^{13}C-NMR** (101 MHz, $CDCl_3$) δ = 169.6; 166.9; 144.3; 144.0; 139.4; 132.7; 131.9; 131.5; 129.9; 128.6; 124.0; 123.6; 122.7; 120.5; 119.9; 113.9; 66.1; 60.6; 14.3. **HRMS** (MALDI) m/z calculated for $C_{19}H_{19}N_2O_3$ [M+H$^+$] 323.1396, found 323.1403.

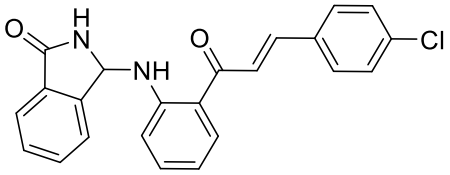

3-((2-(3-(4-chlorophenyl) acryloyl) phenyl) amino) isoindolin-1-one (37g): The product **37g** (**A** 0,032 g, 42%; **B** 0,055 g, 71%) was obtained as orange solid. **^{1}H-NMR** (400 MHz, DMSO-d_6) δ = 9.48 (d, J = 8.3 Hz, 1H, NH), 9.30 (s, 1H, NH), 8.33 (d, J = 8.2 Hz, 1H), 8.08 (d, J = 15.5 Hz, 1H, CH), 7.94 (d, J = 8.3 Hz, 2H), 7.81 (d, J = 7.3 Hz, 1H), 7.74 (d, J = 7.1 Hz, 1H), 7.72 – 7.63 (m, 3H), 7.57 (d, J = 8.2 Hz, 3H), 7.23 (d, J = 8.5 Hz, 1H), 6.89 (t, J = 7.6 Hz, 1H), 6.48 (d, J = 8.3 Hz, 1H, CH). **^{13}C-NMR** (101 MHz, DMSO) δ = 191.9; 169.3; 150.1; 145.7; 142.1; 135.7; 135.3; 134.3; 133.0; 132.8; 130.9; 130.1; 129.4; 124.4; 123.9; 123.4; 119.4; 116.8; 113.7; 64.1. **HRMS** (MALDI) m/z calculated for $C_{23}H_{18}ClN_2O_2$ [M+H$^+$] 389.1057, found 389.1023.

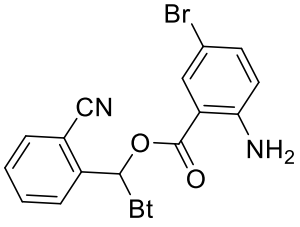

(1H-benzo[d] [1,2,3] triazol-1-yl) (2-cyanophenyl) methyl 2-amino-5-bromobenzoate (**38e**): The product **38e** (**A** 0,062 g, 70%; **B** 0,032 g, 36%) was obtained as yellow solid. **^{1}H-NMR** (400 MHz, $CDCl_3$) δ = 8.78 (s, 1H); 8.17 (d, J = 8.1 Hz, 1H); 8.10 (d, J = 8.4 Hz, 1H); 8.05 (s, 1H); 7.93 – 7.86 (m, 1H); 7.82 (t, J = 8.0 Hz, 1H); 7.75 (d, J = 7.7 Hz, 1H); 7.64 – 7.56 (m, 2H); 7.44 (t, J = 7.9 Hz, 1H); 7.40 – 7.32 (m, 1H); 6.56 (d, J = 8.6 Hz, 1H); 5.80 (s, 2H, NH_2). **^{13}C-NMR** (101 MHz, $CDCl_3$) δ = 164.6; 150.4;

145.6; 138.2; 137.7; 133.5; 133.4; 133.0; 132.8; 130.3; 128.7; 128.4; 124.8; 120.2; 118.6; 116.3; 111.3; 110.2; 109.2; 107.5. **HRMS** (MALDI) m/z calculated for $C_{21}H_{15}BrN_5O_2$ [M+H$^+$] 448.0409, found 448.0377.

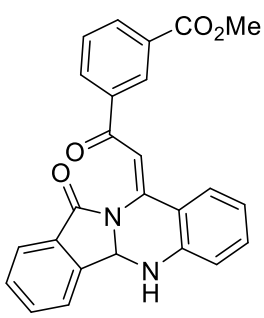

(Z)-methyl 3-(2-(12-oxo-4b,5-dihydroisoindolo[1,2-b] quinazolin-10 (12H)-ylidene) acetyl) benzoate (**39h**): The product **39h** (**A** 0,038 g, 47%; **B** 0,039 g, 48%) was obtained as orange solid. **^{1}H-NMR** (400 MHz, $CDCl_3$) δ = 8.67 (s, 1H); 8.26 (d, J = 7.9 Hz, 1H); 8.19 (d, J = 7.3 Hz, 1H); 7.87 (d, J = 7.1 Hz, 2H); 7.65 (s, 2H); 7.55 (t, J = 7.4 Hz, 2H); 7.33 (t, J = 7.9 Hz, 1H); 7.04 (s, 1H, CH); 7.00 (m, 1H); 6.84 (d, J = 7.6 Hz, 1H); 5.94 (s, 1H, CH); 4.68 (s, 1H, NH); 3.93 (s, 3H, OCH_3). **^{13}C-NMR** (101 MHz, $CDCl_3$) δ = 190.6; 166.7; 164.1; 143.5; 141.1; 139.3; 137.3; 133.1; 133.1; 132.9; 132.3; 131.9; 130.3; 130.1; 129.7; 128.6; 125.3; 125.3; 122.3; 121.2; 117.9; 117.2; 105.9; 67.5; 52.3. **HRMS** (MALDI) m/z calculated for $C_{25}H_{19}N_2O_4$ [M+H$^+$] 411.1345, found 411.1375.

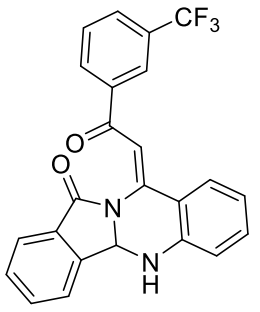

(Z)-10-(2-oxo-2-(3-(trifluoromethyl) phenyl) ethylidene)-4b,5-dihydroisoindolo[1,2-b] quinazolin-12(10H)-one (**39i**): The product **39i** (**A** 0,033 g, 40%; **B** 0,032 g, 38%) was obtained as orange solid. **^{1}H-NMR** (400 MHz, $CDCl_3$) δ = 8.26 (s, 1H); 8.22 (d, J = 7.7 Hz, 1H); 7.82 (t, J = 8.3 Hz, 2H); 7.74 (m, 1H); 7.66 – 7.45 (m, 4H); 7.30 (t, J = 7.6 Hz, 1H); 6.99 (m, 1H); 6.96 (s, 1H, CH); 6.81 (d, J = 8.0 Hz, 1H); 5.86 (s, 1H, CH); 4.79 (s, 1H, NH). **^{13}C-NMR** (101 MHz, $CDCl_3$) δ = 190.0; 164.1; 143.4; 141.0; 139.8; 137.6; 133.2; 132.3; 132.0; 131.8; 130.9; 130.6; 130.2; 128.9; 128.5; 128.5; 125.3; 125.3; 122.3; 121.3; 118.0; 117.3; 105.6; 67.5. **HRMS** (MALDI) m/z calculated for $C_{24}H_{16}F_3N_2O_2$ [M+H$^+$] 421.1164, found 421.1202.

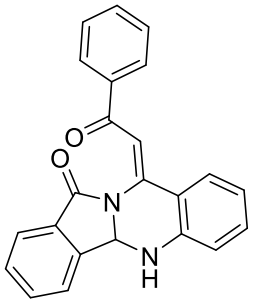

(Z)-10-(2-oxo-2-phenylethylidene)-4b,5-dihydroisoindolo[1,2-b] quinazolin-12(10H)-one (39j): The product **39j** (**A** 0,040 g, 57%; **B** 0,028 g, 40%) was obtained as yellow solid. **^{1}H-NMR** (400 MHz, $CDCl_3$) δ = 8.04 (d, J = 7.7 Hz, 2H); 7.81 (m, 2H); 7.59 (m, 2H); 7.53 – 7.41 (m, 4H); 7.29 – 7.23 (m, 1H); 7.04 (s, 1H, CH); 6.95 (t, J = 7.6 Hz, 1H); 6.79 (d, J = 11.9 Hz, 1H); 5.83 (s, 1H, CH), 4.86 (s, 1H, NH). **^{13}C-NMR** (101 MHz, $CDCl_3$) δ = 191.4; 164.0; 143.2; 141.1; 139.2; 136.6; 133.0; 132.5; 132.1; 131.6; 130.1; 128.5; 128.3; 125.4; 125.1; 122.2; 121.3; 118.0; 117.7; 106.7; 67.5. **HRMS** (MALDI) m/z calculated for $C_{23}H_{17}N_2O_2$ [M+H$^+$] 353.1262, found 353.1284.

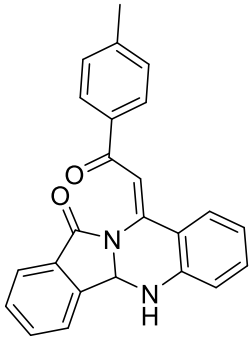

(Z)-10-(2-oxo-2-(*p*-tolyl) ethylidene)-4b,5-dihydroisoindolo[1,2-b] quinazolin-12(10H)-one (**39k**): The product **39k** (**A** 0,050 g, 69%; **B** 0,033 g, 45%) was obtained as yellow solid. **^{1}H-NMR** (400 MHz, $CDCl_3$) δ = 7.95 (d, J = 7.8 Hz, 2H); 7.79 (t, J = 7.4 Hz, 2H); 7.64 – 7.51 (m, 2H); 7.46 (m 1H); 7.28 – 7.19 (m, 3H); 7.04 (s, 1H, CH); 6.93 (t, J = 7.7 Hz, 1H); 6.78 (d, J = 8.1 Hz, 1H); 5.79 (s, 1H, CH); 4.89 (s, 1H, NH); 2.39 (s, 3H, CH_3). **^{13}C-NMR** (101 MHz, $CDCl_3$) δ = 191.1; 164.1; 143.4; 142.8; 141.2; 136.6; 136.4; 132.9; 132.5; 131.5; 129.9; 129.0; 128.7; 125.2; 125.0; 122.3; 121.0; 118.0; 117.6; 106.7; 67.5; 21.6. **HRMS** (MALDI) m/z calculated for $C_{24}H_{19}N_2O_2$ [M+H$^+$] 367.1430, found 367.1441.

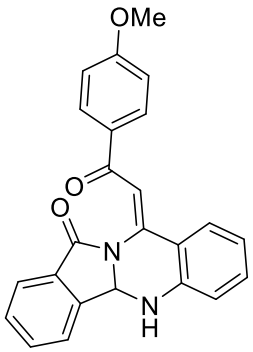

(Z)-10-(2-(4-methoxyphenyl)-2-oxoethylidene)-4b,5-dihydroisoindolo[1,2-b] quinazolin-12(10H)-one (**39l**): The product **39l** (**A** 0,039 g, 51%; **B** 0,009 g, 12%) was obtained as yellow solid. **^{1}H-NMR** (400 MHz, $CDCl_3$) δ = 8.04 (d, J = 8.8 Hz, 2H); 7.86 – 7.77 (m, 2H); 7.67 – 7.56 (m, 2H); 7.54 – 7.46 (m, 1H); 7.27-7.25 (m, 1H); 7.04 (s, 1H, CH); 6.95 (m, 3H); 6.81 (d, J = 8.0 Hz, 1H); 5.86 (s, 1H, CH); 3.85 (s, 3H, OCH_3). **^{13}C-NMR** (101 MHz, DMSO) δ = 189,0; 163.9; 162.8; 145.4; 142.2; 136.7; 133.5; 132.3; 132.0; 131.9; 130.9; 130.4; 125.7; 124.4; 119.7; 117.1; 115.7; 113.9; 106.5; 67.3; 55.9. **HRMS** (MALDI) m/z calculated for $C_{24}H_{19}N_2O_3$ [M+H$^+$] 383.1376, found 383.1390.

1.12 Experimental section Part III

The reactions were monitored via thin layer chromatography (TLC) using Merck Silica Gel 60 F254 plates and were visualized through fluorescence quenching at 254 nm. Column chromatographic purification of products was carried out using silica gel 60 (70–230 mesh, Merck, Milan, Italy). The NMR spectra were recorded on Bruker Avance 400 spectrometers (400 MHz, ^{1}H; 101 MHz, ^{13}C). Spectra were referenced to residual $CHCl_3$ (7.26 ppm, ^{1}H; 77.00 ppm, ^{13}C) or CH_2Cl_2 (5.32 ppm, ^{1}H; 54.0 ppm, ^{13}C) when indicated. Yields are given for isolated products showing one spot on a TLC plate and no significant impurities detectable in the NMR spectrum. High-resolution mass spectra (HRMS) were acquired using a Xevo G2-XS QTof (Waters Corporation, Milford, CT, USA). The samples were ionized in positive ion mode using an electrospray (ESI) ionization source. All chemicals and solvents were obtained from commercial sources and were used without further purification. Aniline **35f** were prepared according to the reported procedures and gave spectra and analytical data as reported. All chemicals and solvents were obtained from commercial sources and were used without further purification.

Experimental Procedure and characterization data of Compound 53:

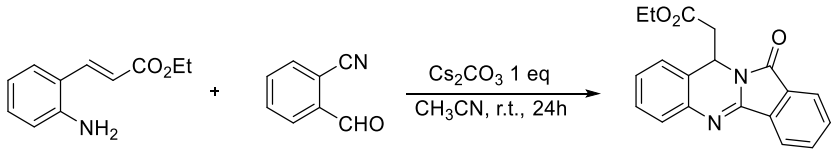

In a round-bottom flask, ethyl (E)-3-(2-aminophenyl) acrylate **35f** (0.100 g, 0.523 mmol), 2-cyanobenzaldehyde **16** (0.096 g, 0.732 mmol), and Cs_2CO_3 (0.170 g, 0.523 mmol) are dissolved in acetonitrile (3.5 mL). After 24 h (reaction monitored by TLC), acetonitrile was evaporated under reduced pressure. The residue was directly purified by flash chromatography over silica gel eluting with *n*-hexane/AcOEt (hexane ethyl acetate from 4:1 to 3:2) to produce Ethyl 2-(12-oxo-10,12-dihydroisoindolo [1,2-b] quinazolin-10-yl) acetate **53** (0.040 g, 24% Yield) as a white solid. **^{1}H-NMR** (400 MHz, CD_2Cl_2) = 8.05 (dt, J = 7.5, 1.0 Hz, 1H); 7.91–7.84 (m, 1H); 7.72 (dtd, J = 21.4, 7.4, 1.2 Hz, 2H); 7.49–7.43 (m, 1H); 7.36 (ddd, J = 7.7, 4.9, 3.9 Hz, 1H); 7.32–7.22 (m, 2H); 5.74 (dd, J = 5.7, 3.9 Hz, 1H, CH); 3.91 (qd, J = 7.1,

2.1 Hz, 2H,CH_2); 3.20 (dd,J=15.3, 5.7Hz, 1H, CH); 2.83 (dd,J=15.3, 3.9 Hz, 1H, CH); 0.99 (t, J = 7.1 Hz, 3H, CH_3). **^{13}C-NMR** (101 MHz, CD_2Cl_2) = 170.2; 167.4; 149.9; 141.4; 135.3; 133.8; 132.8; 131.1; 129.7; 128.3; 128.3; 127.3; 125.3; 123.8; 122.8; 61.3; 49.3; 41.2; 14.2. **HRMS** (ESI) m/z calculated for $C_{19}H_{17}N_2O_3$ [M+H$^+$] 321.1233, found 321.1239.

Experimental Procedure and characterization data of Compound 37f:

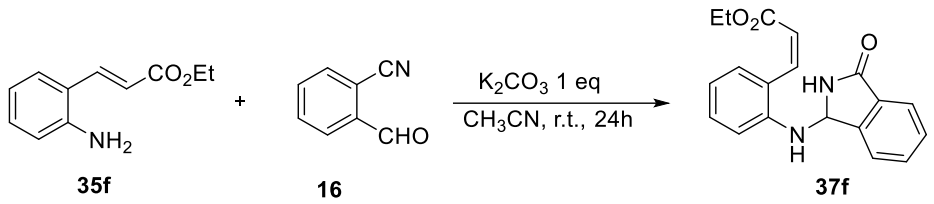

In a round-bottom flask, 2-cyanobenzaldehyde **16** (0.075 g, 0.572 mmol), ethyl (E)-3 (2-aminophenyl) acrylate **35f** (0.131 g, 0.686 mmol), and K_2CO_3 (0.079 g, 0.572 mmol) are dissolved in acetonitrile (3.8 mL). After 24 h (reaction monitored by TLC), the reaction was diluted with CH_2Cl_2 (5 mL) and evaporated under reduced pressure. The residue was purified with flash chromatography over silica gel eluting with *n*-Hexane/AcOEt (Hexane/ethyl Acetate from 4:1 to 3:2) to produce ethyl 3-(2-((3-oxoisoindolin-1-yl) amino) phenyl) acrylate **37f** (0.107 g, 58 % Yield) as a yellow solid. **^{1}H-NMR** (400 MHz, $CDCl_3$) = 7.85 (s, 1H), 7.79 (d, J = 15.7 Hz, 1H, CH), 7.63 (d, J = 5.5 Hz, 2H), 7.56 (t, J = 7.2 Hz, 1H), 7.46 (d, J = 7.7 Hz, 1H), 7.33 (t, J = 7.7 Hz, 1H), 7.02 (s, 1H, NH), 6.93 (dt, J = 10.4, 5.8 Hz, 2H), 6.33 (d, J = 15.7 Hz, 1H, CH), 6.13 (d, J = 10.2 Hz, 1H, CH), 4.46 (d, J = 10.2 Hz, 1H, NH), 4.20 (q, J = 7.1 Hz, 2H, CH2), 1.29 (t, J = 7.1 Hz, 3H, CH3). **^{13}C-NMR** (101 MHz, $CDCl_3$) = 169.6; 166.9; 144.3; 144.0; 139.4; 132.7; 131.9; 131.5; 129.9; 128.6; 124.0; 123.6; 122.7; 120.5; 119.9; 113.9; 66.1; 60.6; 14.3. **HRMS** (ESI) m/z calculated for $C_{19}H_{19}N_2O_3$ [M+H$^+$] 323.1396, found 323.1403.

1.13 Reference Chapter I

1) https://goldbook.iupac.org/terms/view/H02798
2) **a)** A. Gomtsyan. Heterocycles in drugs and drug discovery. *Chem. Heterocycl. Comp*. **2012**, *48*, 7-10; **b)** R. Dua, S. Shrivastava, S. K. Sonwane, S. K. Srivastava. Pharmacological Significance of Synthetic Heterocycles Scaffold: A Review. *Adv. Biol. Res.* **2011**, *5*, 120-144.
3) **a)** T. K. Wood, W. E. Piers, B. A. Keay, M. Parvez. 1-Borabarrelene Derivatives via Diels–Alder Additions to Borabenzenes. *Org. Lett.* **2006**, *8*, 2875-2878; **b)** T. P. Clark, C. Landis. Recent developments in chiral phospholane chemistry. *Tetrahedron Asymmetry* **2004**, *15*, 2123-2137; **c)** L. Aubouy, P. Gerbier, N. Huby, G. Wantz, L. Vignau, L. Hirsch, J. M. Janot. Synthesis of new dipyridylphenylaminosiloles for highly emissive organic electroluminescent devices. *New. J. Chem.* **2004**, *28*, 1086-1090. **d)** H. D. Hartough. Thiophene and Its Derivatives. The Chemistry of Heterocyclic Compounds. John Wiley & Sons, **2009**.
4) R. R. Gupta, M. Kumar, V. Gupta. Heterocyclic Chemistry. Volume I: Principles, Three- and Four-Membered Heterocycles. Springer Berlin, Heidelberg, **1998**.
5) M. -C. Ríos, N. -F, Bravo, C. -C. Sánchez, J. Portilla. Chemosensors based on *N*-heterocyclic dyes: advances in sensing highly toxic ions such as CN^- and Hg_2^+. *RSC Adv.* **2021**, *11*, 34206-34234.
6) S. S. Murphree. Heterocyclic Dyes: Preparation, Properties, and Applications. *Prog. Heterocycl. Chem.* **2011**, 22, 21-58.
7) E. Kabir, M. Uzzaman. A review on biological and medicinal impact of heterocyclic compounds. *Results Chem*. **2022,** *4*, 100606-100617.
8) C. Ryu, R. Lee, N. Y. Kim, Y. H. Kim, A. L. Song. Synthesis and antifungal activity of benzo[*d*]oxazole-4,7-diones. *Bioorg. Med. Chem. Lett.* **2009**, *19*, 5924-5926.
9) M. H. M. Abdel-Azim, M. A. Aziz, S. M. Mouneir, A. F. El-Farargy, W. S. Shehab. Ecofriendly synthesis of pyrano[2,3-*d*]pyrimidine derivatives and related heterocycles with anti-inflammatory activities. *Arch. Pharm.* **2020**, *353*, 1-13.

10) Y. F. Mustafa. Synthesis, characterization and antibacterial activity of novel heterocycle, coumacine, and two of its derivatives. *Saudi Pharm. J.* 2018, *26*, 870–875.

11) B. K. Banik. Beta-lactams. Novel Synthetic Patways and Applications. Spinger International Publishing AG 2017.

12) L. Yurttaş, Y. Özkay, G. Akalin-Çiftçi, S¸. Ulusoylar-Yildirim. Synthesis and anticancer activity evaluation of *N*-[4-(2-methylthiazol-4-yl)phenyl]acetamide derivatives containing (benz)azole moiety. *J. Enzyme Inhib. Med. Chem.* 2014, *29*, 175-184.

13) M. Gobinath, N. Subramanian, V. Alagarsamy, S. Nivedhitha, V. R. Solomon. Design and Synthesis of 1-Substituted-4-(4-Nitrophenyl)-[1,2,4]triazolo[4,3-*a*]quinazolin-5(4*H*)-ones as a New Class of Antihistaminic Agents. Russ. *J. Bioorganic Chem.* 2020, *46*, 403-408.

14) H. P. A. Khan, T. K. Chakraborty. Diversity-Oriented Approach to *N*-Heterocyclic Compounds from α-Phenyl-β-enamino Ester via a Mitsunobu-Michael Reaction Sequence. *J. Org. Chem.* 2018, *83*, 2027-2039.

15) N. Kerru, L. Gummidi, S. Maddila, K. K. Gangu, S. B. Jonnalagadda. A Review on Recent Advances in Nitrogen-Containing Molecules and Their Biological Applications. *Molecules* 2020, *9*, 1909-1951.

16) a) I. Pendrak, S. Barney, R. Wittrock, D. M. Lambert, W. D. Kingsbury. Synthesis and Anti-HSV Activity of A-Ring-Deleted Mappicine Ketone Analog. *J. Org. Chem.* 1994, *59*, 2623-2625; b) E. De Clercq. Toward Improved Anti-HIV Chemotherapy: Therapeutic Strategies for Intervention with HIV Infections. *J. Med. Chem.* 1995, *38*, 2491-2517.

17) I. Takahashi, T. Kawakami, E. Hirano, H. Yokota, H. Kitajima. Novel Phthalimidine Synthesis. Mannich Condensation of *o*-Phthalaldehyde with Primary Amines using 1,2,3-1*H*-Benzotriazole and 2-Mercaptoethanol as Dual Synthetic Auxiliaries. *Synlett* 1996, 4, 353-355.

18) A. M. Pirttilä, A. C. Frank. Endophytes of Forest Trees. Biology and Applications. Forestry Sciences Springer, 2011, *86*, 302-624.

19) I. -K. Lee, S. -E. Kim, J. -H. Yeom, D. W. Ki, M. -S. Lee, J. -G. Song, Y. -S. Kim, S. -J. Seok, B. -S. Yun. Daldinan A, a novel isoindolinone antioxidant from the ascomycete Daldinia concentrica. *J. Antibiot.* 2012, *65*, 95-97.

20) E. C. Taylor, P. Zhou, L. D. Jenning, Z. Mao, B. Hu, J. -G. Jun. Novel synthesis of a conformationally-constrained analog of DDATHF. *Tetrahedron Lett.* 1997, *38*, 521-524.

21) A. Buttinoni, M. Ferrari, M. Colombo, R. Ceserani. Biological activity of indoprofen and its optical isomers. *J. Pharm. Pharmacol.* 1983, *35*,603–604.

22) A. Mertens, H. Zilch, B. Koenig, W. G. Schaefer, T. Poll, W. Kampe, H. Seidel, U. Leser, H. Leinert. Selective non-nucleoside HIV-1 reverse transcriptase inhibitors. New 2,3-dihydrothiazolo[2,3-*a*]isoindol-5(9b*H*)-ones and related compounds with anti-HIV-1 activity. *J. Med. Chem.* 1993, *36*. 2526-2535.

23) A. F. Cavaney, B. Giordani, G. M. Haig. Preliminary effects of Pagoclone, a partial $GABA_A$ agonist, on neuropsychological performance. *Neuropsychiatr Dis Treat.* 2008, *4*, 277-282.

24) C. -W. Zhang, Y. -N. Wang, X. -L. Ge. Lenalidomide use in multiple myeloma. *Mol. Clin. Oncol.* 2024, *20*, 1-13.

25) M. R. Lunn, D. E. Root, A. M. Martino, S P. Flaherty, B. P. Kelley, D. D. Coovert, A. H. Burghes, N. thi Man, G. E. Morris, J. Zhou, E. J. Androphy, C. J. Sumner, B. R. Stockwell. Indoprofen Upregulates the Survival Motor Neuron Protein through a Cyclooxygenase-Independent Mechanism. *Chem. Biol.* 2004, *11*, 1489-1493.

26) **a)** A. Di Mola, L. Palombi, A. Massa. An Overview on asymmetric synthesis of 3-substituted isoindolinones. *Targets Heterocycl. Syst.* 2014, *18*, 113-140; **b)** J. Suć, I. Dokli, M. Gredičak. Chiral Brønsted acid-catalysed enantioselective synthesis of isoindolinone-derived N (acyl), S-acetals. *Chem. Commun.* 2016, *52*, 2071-2074; **c)** L. Serusi, A. Massa, C. Tedesco, A. Capobianco, L. Palombi. The First Highly Enantioselective Synthesis of 3-Sulfinyl-Substituted Isoindolinones Having Adjacent Carbon and Sulfur Stereocenters. *J. Org. Chem.* 2021, *86*, 10630-10639; **d)** C. Min, Y. Lin, D. Seidel. Catalytic Enantioselective Synthesis of Mariline A and Related Isoindolinones through a Biomimetic Approach. *Angew. Chem. Int. Ed.* 2017, *56*, 15353-15357; **e)** L. Serusi, L. Palombi, G. Pierri, A. Di Mola, A. Massa. Asymmetric Cascade *Aza*-Henry/Lactamization Reaction in the Highly Enantioselective Organocatalytic Synthesis of 3-(Nitromethyl)isoindolin-1-ones from α-Amido Sulfones. *J. Org. Chem.* 2022, *87*, 8420-8428.

27) R. Savela, C. Méndez-Gálvez. Isoindolinone Synthesis via One-Pot Type Transition Metal Catalyzed C–C Bond Forming Reactions. *Chem. Eur. J.* 2021, *27*, 5344-5378.

28) P. W. Seavill, J. D. Wilden. The preparation and applications of amides using electrosynthesis. *Green Chem.* 2020, *22*, 7737-7759.

29) A. Kemp, M. Durand, D. Wall, P. Szieber, M. I. Hermanns, M. Oelgemöller. Synthesis of 1*H*-isoindolin-1-ones via a simple photodecarboxylative addition of carboxylates to phthalimides and evaluation of their antibiotic activity. *Photochem. Photobiol. Sci.* 2024, *23*, 1353-1360.

30) S. Mumtaz, M. J. Robertson, M. Oelgemöller. Continuous Flow Photochemical and Thermal Multi-Step Synthesis of Bioactive 3-Arylmethylene-2,3-Dihydro-1*H*-Isoindolin-1-Ones. *Molecules* 2019, *24*, 4527.

31) L. F. Tietze. Domino Reactions in Organic Synthesis. *Chem. Rev.* 1996, *96*, 115-136.

32) M. Trost. Atomökonomische Synthesen – eine Herausforderung in der Organischen Chemie: die Homogenkatalyse als wegweisende Methode. *Angew. Chem.* 1995, *107*, 285-307.

33) R. Robinson. A Synthesis of Tropinone. *J. Chem. Soc. Trans.* 1917, *111*, 762-768.

34) a) K. C. Nicolaou, J. S. Chen. The art of total synthesis through cascade reactions. *Chem. Soc. Rev.* 2009, *38*, 2993-3009; b) K. Nicolaou, N. Petasis, R. Zipkin, J. Uenishi. The endiandric acid cascade. Electrocyclizations in organic synthesis. I. Stepwise, stereocontrolled total synthesis of endiandric acids A and B. *J. Am. Chem. Soc*. 1982, *104*, 5555-5557; c) W. S. Johnson, M. B. Gravestock, B. E. McCarry. Acetylenic bond participation in biogenetic-like olefinic cyclizations. II. Synthesis of dl-progesterone. *J. Am. Chem. Soc.* 1971, *93*, 4332-4334.

35) Y. -J. Liu, H. Xu, W. -J. Kong, M. Shang, H. -X. Dai, J. -Q. Yu. Overcoming the limitations of directed C–H functionalizations of heterocycles. *Nature* 2014, *515*, 389-393.

36) W. Hao, J. Tian, W. Li, R. Shi, Z. Huang, A. Lei. Nickel-Catalyzed Oxidative C–H/N–H Isocyanide Insertion: An Efficient Synthesis of Iminoisoindolinone Derivatives. *Chem. Asian J.* 2016, *11*, 1664-1667.

37) L. -B. Zhang, X. -Q. Hao, Z. -J. Liu, X. -X. Zheng, S.-K. Zhang, J. -L. Niu, M. -P. Song. Cobalt(II)-Catalyzed C sp^2-H Alkynylation/Annulation with Terminal Alkynes: Selective Access to 3-Methyleneisoindolin-1-one. *Angew. Chem. Int. Ed.* 2015, *54*, 10012-10015.

38) B. Gao, S. Liu, Y. Lan, H. Huang. Rhodium-Catalyzed Cyclocarbonylation of Ketimines via C–H Bond Activation. *Organometallics* **2016**, *35*,1480-1487.

39) S. Dhanasekaran, A. Kayet, A. Suneja, V. Bisai, V. K. Singh. Unified Approach to Isoindolinones and THIQs via Lewis Acid Catalyzed Domino Mukaiyama–Mannich Lactamization/Alkylations: Application in the Synthesis of (±)-Homolaudanosine. *Org. Lett.* **2015**, *17*, 2780-2783.

40) A. Bechtoldt, C. Tirler, K. Raghuvanshi, S. Warratz, C. Kornhaaß, L. Ackermann. Ruthenium Oxidase Catalysis for Site-Selective C–H Alkenylations with Ambient O_2 as the Sole Oxidant. *Angew. Chem. Int. Ed.* **2016**, *55*, 264-267.

41) Q. Yu, N. Zhang, J. Huang, S. Lu, Y. Zhu, X. Yu, K. Zhao. Efficient Synthesis of Hydroxyl Isoindolones by a Pd-Mediated C-H Activation/Annulation Reaction. *Chem. Eur. J.* **2013**, *19*, 11184-11188.

42) B. Zhou, W. Hou, Y. Yang, Y. Li. Rhodium(III)-Catalyzed Amidation of Aryl Ketone *O*-Methyl Oximes with Isocyanates by C-H Activation: Convergent Synthesis of 3-Methyleneisoindolin-1-ones. *Chem. Eur. J.* **2013**, *19*, 4701-4706.

43) M. Liu, J. Li, Q. Zhang, D. Shi. $COCl_2{\cdot}6H_2O$-Promoted Pinner-Dimroth tandem reaction: facile synthesis of 3-substituted isoindolinones. *Heterocycles* **2015**, *97*,1465-1472.

44) M. K. Yadav, S. Chowdhury. Electrochemical cascade reactions: an account of recent developments for this modern strategic tool in the arsenal of chemical synthesis. *Green Chem.* **2023**, *25*, 10144-10181.

45) L. Song, X. Tian, K. Farshadfar, F. Shiri, F. Rominger, A. Ariafard, A. S. K. Hashmi. An unexpected synthesis of azepinone derivatives through a metal-free photochemical cascade reaction. *Nat. Commun.* **2023**, *14*, 1-8.

46) D. Liang, Q. -Q. Zhou, J. Xuan. Multiple-cycle photochemical cascade reactions. *Org. Biomol. Chem.* **2024**, *22*, 2156-2174.

47) P. Antico, V. Capaccio, A. Di Mola, A. Massa, L. Palombi. Electrochemically Initiated Tandem and Sequential Conjugate Addition Processes: One-Pot Synthesis of Diverse Functionalized Isoindolinones. *Adv. Synth. Catal.* **2012**, *354*, 1717-1724.

48) L. Palombi, A. Di Mola, C. Vignes, A. Massa. Combined electrochemical/chemical methods for the synthesis and the molecular diversifying of isoindolinone-based heterocyclic scaffolds. *Mol. Divers.* **2014**, *18*, 323-333.

49) L. Palombi, A. Di Mola, A. Massa. Quick and easy access to *N*-Mannich bases of 1-isoindolinones by catalytic electroactivation of primary and secondary amines and tandem reaction with 2-formylbenzonitriles. *New J. Chem.* **2015**, *39*, 81-84.

50) R. Sato, T. Senzaki, T. Goto, M. Saito. Novel synthesis of 3-(*N*-substituted amino)-1-isoindolenones from 2-Cyanobenzaldehyde with Amines. *Chem. Lett.* **1984**, 1599-1602.

51) Z. Zou, G. Cai, W. Chen, C. Zou, Y. Li, H. Wu, L. Chen, J. Hu, Y. Li, Y. Huang. Metal-Free Cascade Formation of Intermolecular C–N Bonds Accessing Substituted Isoindolinones under Cathodic Reduction. *J. Org. Chem.* **2021**, *86*, 15777-15784.

52) M. Yu, Y. Gao, L. Zhang, Y. Zhang, Y. Zhang, H. Yi, Z. Huang, A. Lei. Electrochemical-induced benzyl C–H amination towards the synthesis of isoindolinones via aroyloxy radical-mediated C–H activation. *Green Chem.* **2022**, *24*, 1445-1450.

53) Y. Bai, L. Shi, L. Zheng, S. Ning, X. Che, Z. Zhang, J. Xiang. Electroselective and Controlled Reduction of Cyclic Imides to Hydroxylactams and Lactams. *Org. Lett.* **2021**, *23*, 2298-2302.

54) C. -L. Ding, Q. Xu, S. Wu, Y. Zhong, X. He, Y. Lin, Y. Li, K. -Y. Ye. Current-Controlled Electrochemical Approach Toward Mono- and Trifluorinated Isoindolin-1-one Derivatives. *Org. Lett.* **2024**, *26*, 8, 1645-1651.

55) A. A. Folgueiras-Amador, K. Philipps, S. Guilbaud, J. Poelakker, T. Wirth. An Easy-to-Machine Electrochemical Flow Microreactor: Efficient Synthesis of Isoindolinone and Flow Functionalization. *Angew. Chem. Int. Ed.* **2017**, *56*, 15446-15450.

56) S. M. Sicardi, J. L. Martiarena, M. T. Iglesias. Mutagenic and analgesic activities of aniline derivatives. *J. Pharm. Sci.* **1991**, *80*, 761-764.

57) **a)** H. Surya Prakash Rao, J. Prabhakaran, U. Kaloor. Facile and High-Yielding Synthesis of C(3)-Aminoisoindolinones Under Metal Catalyst-Free Conditions. *Chem. Select.* **2022**, *7*, e20210442; **b)** H. Surya Prakash Rao, J. Prabhakaran. Palladium-catalyzed intramolecular C–N coupling: Facile synthesis of tetracyclic C(3)-aminoisoindolinones. *Synthetic Communications* **2022**, *52*, 1448-1456.

58) **a)** F. Brotzel, Y. C. Chu, H. J. Mayr. Nucleophilicities of primary and secondary amines in water. *J. Org. Chem.* **2007**, *72*, 3679-3688; **b)** R. Appel, S. Chelli, T. Tokuyasu, K. Troshin, H.J. Mayr. Electrophilicities of Benzaldehyde-Derived Iminium Ions:

Quantification of the Electrophilic Activation of Aldehydes by Iminium Formation. *J. Am. Chem. Soc.* 2013, *135*, 6579-6587.

59) D. Formenti, F. Ferretti, F. K. Scharnagl, M. Beller. Reduction of Nitro Compounds Using 3d-Non-Noble Metal Catalysts. *Chem. Rev.* 2019, *119*, 2611-2680.

60) S. Samanta, S. A. Ali, A. Bera, S. Giri, K. Samanta. Transition metal-free advanced synthetic approaches for isoindolinones and their fused analogues. *New J. Chem*. 2022, *46*, 7780-7830.

61) V. Fajardo, V. Elango, B. K. Cassels, M. Shamma. Chilenine: an isoindolobenzazepine alkaloid. *Tetrahedron Lett.* 1982, *23*, 39-42.

62) K. Speck, T. Magauer. The chemistry of isoindole natural products. *Beilstein J. Org. Chem.* 2013, *9*, 2048-2078.

63) Y. Wu, N. Liu, M. Qi, H. Qiao, X. Lu, L. Ma, Y. Zhou, F. -L. Zhang. Monodentate Transient Directing Group Assisted Ruthenium(II)-Catalyzed Direct *ortho*-C–H Imidation of Benzaldehydes for Diverse Synthesis of Quinazoline and Fused Isoindolinone. *Org. Lett*. 2021, *23*, 3923-3927.

64) P. Kumar, M. Gupta, V. Bahadur, V. S. Parmar, B. K. Singh. Radical-Induced, Palladium-Catalyzed C–H Activation: An Approach to Functionalize 4H-benzo[*d*][1,3]oxazin-4-one Derivatives by Using Toluenes, Aldehydes, and Benzyl Alcohols. *Eur. J. Org. Chem.* 2018, *13*, 1552-1558.

65) S. B. Nallapati, R. Adepu, M. A. Ashfaq, B. Y. Sreenivas, K. Mukkanti, M. Pal. A Pd-catalyzed direct entry to 11-substituted 6*H*-isoindolo[2,1-a]indol-6-one derivatives as potential anticancer agents. *RSC Adv.* 2015, *5*, 88686-88691.

66) L. Liu, J. Qiang, S. -H. Bai, H. -L. Sung, C. -B. Miao, J. Li. Direct Access to Isoindolin-1-one Scaffolds by Copper-Catalyzed Divergent Cyclizations of 2-Formylbenzonitrile and Diaryliodonium Salts. *Adv. Synth. Cat.* 2017, *8*, 1283-1289.

67) G. Infante, S. Eisler. Accessing Extended Fused Isoindolinones Via Sequential Anionic Intramolecular Cyclizations. *Chem. Eur. J.* 2021, *27*, 16121-16126.

68) S. Yuan, Y.-L. Yue, D.-Q. Zhang, J.-Y. Zhang, B. Yu, H.-M. Liu. Synthesis of new tetracyclic benzodiazepine-fused isoindolinones using recyclable mesoporous silica nanoparticles *Chem. Commun.* 2020, *56*, 11461-11464.

69) S. Tiso, L. Palombi, C. Vignes, A. Di Mola, A. Massa. Organocatalysts and sequential asymmetric cascade reactions in the synthesis of functionalized isoindolinones and benzoindolizidinones. *RSC Adv.* **2013**, *3*, 19380-19387.

70) **a)** M. Feroci, A. Inesi, L. Palombi, G. Sotgiu. Electrogenerated Base-Induced *N*-Acylation of Chiral Oxazolidin-2-ones. *J. Org. Chem.* **2002**, *67*, 1719-1721; **b)** M. Feroci, A. Inesi, L. Palombi, L. Rossi. Electrochemical generation of chiral oxazolidin-2-ones anions: a new procedure for the highly diastereoselective conjugate addition to nitroalkenes. *Tetrahedron Asymmetry* **2001**, *12*, 2331-2335; **c)** M. Feroci, A. Gennaro, A. Inesi, M. Orsini, L. Palombi. Synthesis of chiral oxazolidin-2-ones by 1,2-amino alcohols, carbon dioxide and electrogenerated acetonitrile anion. *Tetrahedron Lett.* **2002**, *43*, 5863-5865; **d)** M. Feroci, M. A. Casadei, M. Orsini, L. Palombi, A. Inesi. Cyanomethyl Anion/Carbon Dioxide System: An Electrogenerated Carboxylating Reagent. Synthesis of Carbamates under Mild and Safe Conditions. *J. Org. Chem.* **2003**, *68*, 1548-1551.

71) A. R. Katritzky, A. Pastor, M. V. Voronkov. An efficient general synthesis of 1-(benzotriazol-1-yl)alkyl esters. *J. Heterocycl. Chem.* **1999**, *36*, 777-781.

72) M. Kawatsura, J. F. Hartwig. Transition Metal-Catalyzed Addition of Amines to Acrylic Acid Derivatives. A High-Throughput Method for Evaluating Hydroamination of Primary and Secondary Alkylamines. *Organometallics* **2001**, *20*, 1960-1964.

73) W.-Q. Chen, J.-A. Ma. Stabilized Nucleophiles with Electron Deficient Alkenes, Alkynes, and Allenes. *Comprehensive Organic Synthesis* **2014**, *4*, 1-85.

74) S. Azad, T. Kobayashi, K. Nakano, Y. Ichikawa, H. Kotsuki. Efficient Brønsted acid-catalyzed *Aza*-Michael reaction of amides and ureas with α,β-unsaturated enones under high-pressure conditions. *Tetrahedron Lett.* **2009**, *50*, 48-50.

75) A. Gupta, M. L. Condakes. Thermodynamic Understanding of an *Aza*-Michael Reaction Enables Five-Step Synthesis of the Potent Integrin Inhibitor MK-0429. *J. Org. Chem.* **2021**, *86*, 17523-17527.

76) I. Khan, A. Ibrar, N. Abbas, A. Saeed. Recent advances in the structural library of functionalized quinazoline and quinazolinone scaffolds: Synthetic approaches and multifarious applications. *Eur. J. Med. Chem.* **2014**, *76*, 193-244.

77) S. Barni, A. Ghidini, A. Coinu, K. Borgonovo, F. Petrelli. A systematic review of Raltitrexed-based first-line chemotherapy in advanced colorectal cancer. *Anti-Cancer Drugs* **2014**, *25*, 1122-1128.

78) B. Yu, X. Zheng, Z. Sun, P. Cao, J. Zhang, Z. Gao, H. Cao, F. Zhang, W. Wang. The safety and efficacy of Doxazosin in medical expulsion therapy for distal ureteric calculi: A meta-analysis. *Plos One* **2021***, 16,* e0245741.

79) D. Wheatley. Analgesic properties of Fluproquazone. *Rheumatol. Rehabil.* **1982**, *21*, 98-100.

80) **a)** C. Wattanapiromsakul, P. I. Forster, P. G. Waterman. Alkaloids and limonoids from Bouchardatia neurococca: systematic significance. *Phytochemistry* **2003**, *64,* 609-615; **b)** Z. -Z. Ma, Y. Hano, T. Nomura, Y. -J. Chen. Two new pyrroloquinazolinoquinoline alkaloids from Peganum nigellastrum. *Heterocycles* **1997**, *46,* 541-546; **c)** D. Yonghong, X. Rensheng, Y. Yang. A New Quinazolone Alkaloid from Leaves of Dichroa febrifuga. *J. Chin. Pharm. Sci.* **2000**, *9,* 116-118; **d)** J. Plowman, K. D. Paull, G. Atassi, S. D. Harrison Jr, D. J. Dykes, H. J. Kabbe, V. L. Narayanan, O. C. Yoder. Preclinical antitumor activity of batracylin (NSC 320846). *Investig. New Drugs* **1988**, *6*, 147-153.

81) V. A. Rao, K. Agama, S. Holbeck, Y. Pommier. Batracylin (NSC 320846), a Dual Inhibitor of DNA Topoisomerases I and II Induces Histone γ-H2AX as a Biomarker of DNA Damage. *Cancer Res*. **2007**, *67*, 9971-9979.

82) K. Dzierzbicka, W. Januchta, A. Skladanowski. Novel Approaches in the Synthesis of Batracylin and Its Analogs: Rebirth of an Old Player?. *Curr. Med. Chem*. **2012**, *19*, 4475-4487.

83) J. Chen, H. Neumann, M. Beller, X. -F. Wu. Palladium-catalyzed synthesis of isoindoloquinazolinones via dicarbonylation of 1,2-dibromoarenes. *Org. Biomol. Chem.* **2014**, *12*, 5835-5838.

84) W. Li, B. Wan, R. Shi, S. Chen, J. Li, F. Wang, H. Niu, X. -M. Xu, W. -L. Wang. Catalyst-free one-pot cascade cyclization: An efficient synthesis of isoindolobenzoxazinones and isoindoloquinazolinones derivatives. *Tetrahedron* **2022**, *104*, 1-8.

85) M. -C. Tseng, P. -Y. Lai, L. Shi, H. -Y. Li, M. -J. Tseng, Y. -H. Chu. Synthesis of Batracylin and its *N*-sulfonamido analogues in [b-3C-im][NTf_2] ionic liquid. *Tetrahedron* **2014**, *70*, 2629-2633.

86) R. Shankar, M. Balu Wagh, M. V. Madhubabu, N. Vembu, U. K. S. Kumar. A Concise and Cascade Synthesis of Batracylin and Substituted Isoindolo-[1,2-*b*]quinazolin-12(10*H*)-ones. *Synlett* 2011, *6*, 844-848.

87) D. Purohit, K. S. Rawat, S. Parveen, R. P. Vats, C. P. Sharma, A. Goel. One-Pot Synthesis of Functionalized Isoindolinones and Their Bis(isoindolinone)ethane Derivatives. *Eur. J. Org. Chem.* 2022, *47*, e202201128.

88) H. Singh, K. Tiwari, R. Tiwari, S. K. Pramanik, A. Das. Small Molecule as Fluorescent Probes for Monitoring Intracellular Enzymatic Transformations. *Chem. Rev.* 2019, *119*, 11718-11760.

Chapter II: Electrochemical cyanation reactions using safe cyanide sources

2.1 Nitrile group

Nitriles represent an important class of compounds in organic chemistry (**Figure 16**).[89] From a chemical point of view, the nitro group is defined by a sp-hybridized carbon bonded through a triple bond to a nitrogen atom. Due to the nitrogen atom's higher electronegativity relative to carbon, nitriles are reactive in three keyways: they can participate in nucleophilic, electrophilic, and radical reactions.[90]

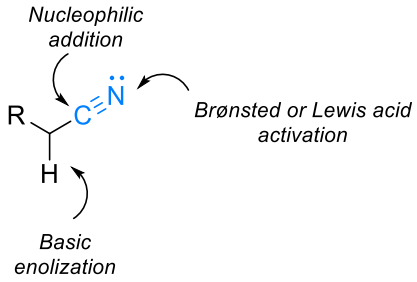

Figure 16: General reactivity of the cyano group.

The high reactivity and unique versatility of nitriles have significantly increased the interest in this chemical scaffold over the past few decades. For instance, nitrile reduction using $LiAlH_4$ or catalytic hydrogenation efficiently transforms the -CN group into an amine. Additionally, through an acid-catalyzed reaction involving protonation and nucleophilic attack by water, the -CN group can be converted into an amide, which can subsequently undergo hydrolysis to form a carboxylic acid derivative. Nitriles are also easily reducible to aldehydes using DIBAL in acidic conditions, and their reaction with Grignard reagents, followed by the addition of water, results in the formation of a ketone. Multiple nucleophilic additions to the -CN group can be also used to synthesize a variety of nitrogen-containing heterocycles (**Figure 17**).

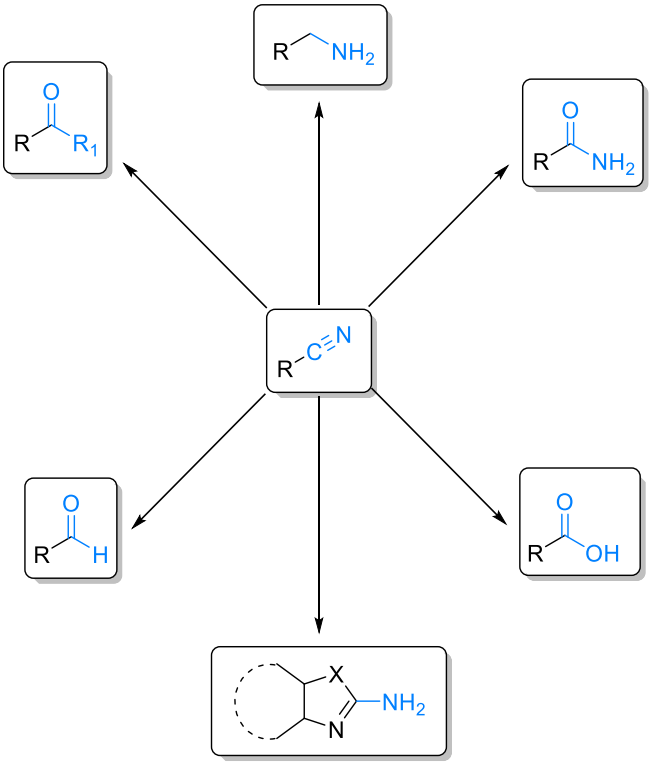

Figure 17: Possible conversions of cyano-group.

For all these reasons, nitrile compounds found application in several fields and are utilized for the preparation of pharmaceuticals,[91] dyes[92] and natural products.[93] Concerning medicinal applications, more than 50 nitrile-containing drugs are currently on the market for a wide range of therapeutic uses. For instance, Paxlovid®[94] **55** (ritonavir-boosted Nirmatrelvir) is used in the treatment of COVID-19. Verapamil[95] **56** is an effective and well-tolerated first-line treatment for patients with mild to moderate essential hypertension. Escitalopram[96] **57** is a selective serotonin reuptake inhibitor (SSRI) prescribed for major depressive disorder and anxiety disorder. Additionally, Tofacitinib[97] **58** is an FDA-approved drug for the treatment of moderate to severe rheumatoid arthritis, psoriatic arthritis and ulcerative colitis (**Figure 18**).

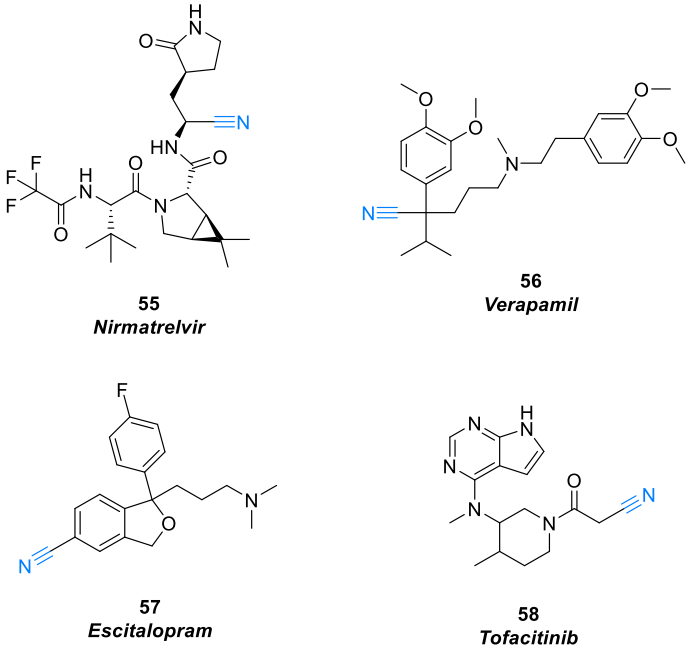

Figure 18: Nitrile-containing drugs.

2.2 Cyanation reactions and cyanide source

Despite the cyano group being a crucial scaffold in synthetic chemistry, cyanation reaction remains challenging due to the high toxicity of hydrogen cyanide (HCN). Its volatility presents significant health hazards, particularly through inhalation, making stringent safety measures essential during handling. In response, the past century has witnessed the development of transition metal-catalyzed cyanation reactions,[98] introducing safer nucleophilic cyanide alternatives, such as metallic salts like CuCN, NaCN, and $Zn(CN)_2$ in order to reduce risks and simplify reaction procedures. Notably, CuCN is used in the well-known Von Braun[99] and Sandmeyer[100] reactions to produce aromatic nitriles (**Figure 19**). However, like HCN, metallic cyanides remain highly toxic and can release HCN in acidic conditions, making their use still hazardous.

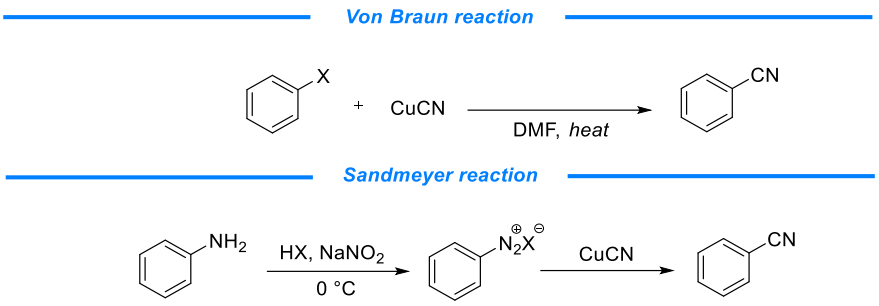

Figure 19: Von Braun and Sandmeyer reactions.

Regarding electrophilic cyanation reactions, commercially available cyanogen bromide (BrCN) is the most commonly used source of CN^+ group. BrCN readily reacts with various nucleophilic groups, including N,[101] O,[102] S[103] and C,[104] enabling a wide range of functionalizations (**Figure 20**).

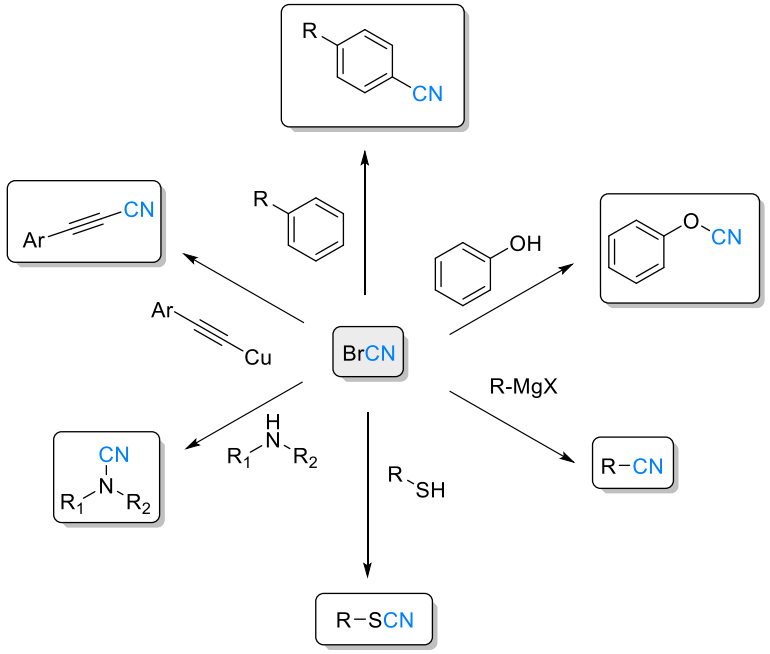

Figure 20: Possible functionalization using BrCN.

However, similarly to HCN, the use of cyanogen bromide has also become highly difficult and has declined due to its acute toxicity, even in small amounts, as well as

its tendency to be easily absorbed through inhalation or skin contact.[105] Additionally, the need to store it at low temperatures to prevent sublimation complicates its transport, making it hazardous. For these reasons, it has been classified as a highly restricted substance in several countries, including China, in recent years.[106]

Due to the limitations associated with the use of HCN, cyanide salts and BrCN, considerable efforts have been made to minimize risks and simplify reagent handling. These efforts have resulted in the design of various cyanide sources that, depending on the electronegativity of the α-atom and the bonding properties, can act as electrophilic, nucleophilic or radical cyanation agents. Among the nucleophilic cyanide surrogates, ferrocyanides **59** are widely used as CN^- donors, particularly in combination with transition metal catalysts like palladium and copper. A notable advancement in the use of these safer cyanide reagents has been proposed by Beller and coworkers in 2004, which opened the possibility to broader applications (**Scheme 24**).[107]

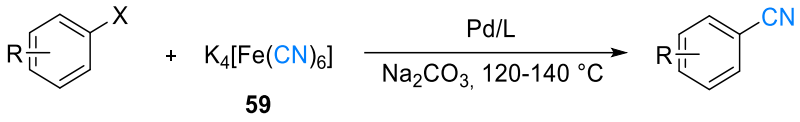

Scheme 24: Palladium-catalyzed cyanation reaction.

Although the procedure risks are particularly limited compared to the cyanide sources previously mentioned, the use of ferrocyanide still require harsh conditions, such as >100°C reaction temperature. Another interesting example of CN^- surrogates are the cyanocarbonyls. In **2012**, Palacios et *al.* presented an enantioselective procedure for the cyanation of α-ketiminophosphonates catalyzed by cinchona Alkaloids and CH_3COCN **60** as cyanide source (**Scheme 25**).[108] With respect to the ferrocyanides, cyanocarbonyls offer the advantage of generating cyanide ions (CN^-) at lower temperatures, simplifying the reaction conditions and making the process well-suited for use in flow-chemistry reactors.

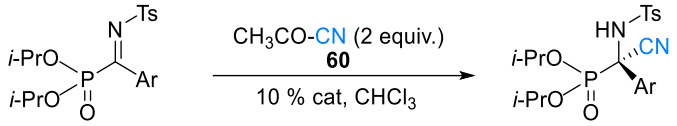

Scheme 25: Enantioselective cyanation of α-ketiminophosphonates.

Cyanohydrins are also valuable nucleophilic cyanide surrogates. Among them, acetone cyanohydrin **61** (ACH) stand out as one of the most convenient options, due to its stability, widespread availability and cost-effectiveness. Consequently, ACH has been widely utilized in various cyanation reactions. A notable example is its application in the asymmetric Strecker reaction in a one-pot procedure using water as solvent, proposed by Giacomini and coworkers (**Scheme 26**).[109]

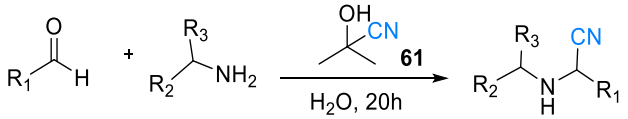

Scheme 26: Asymmetric Strecker reaction using ACH.

Simultaneously, significant efforts have been dedicated to developing electrophilic cyanide surrogates. An example is the 1-cyanoimidazole, first introduced as an electrophilic cyanating agent by Hamilton et *al.* in 2000.[110] In this study, 1-cyanoimidazole **62** has been tested with different nucleophiles, including amines, Grignard reagents and thiols, demonstrating strong potential under various reaction conditions (**Scheme 27**).

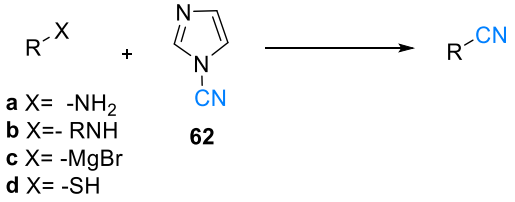

Scheme 27: Electrophilic cyanation using 1-cyanoimidazole.

Electrophilic cyanation can also be achieved using cyanamide derivatives, such as *N*-cyano-*N*-phenyl-*p*-toulenesulfonamide **63** (NCTS). In 2011 Beller et *al.* introduced NCTS as a non-toxic electrophilic cyanating agent for the synthesis of aromatic nitriles.[111] The efficacy of this reagent was demonstrated in two key reactions: the cyanation of aryl bromides through the intermediate formation of Grignard reagents (Scheme 28a) and the cyanation of arylboronic acids via Rhodium catalysis (Scheme 28b).

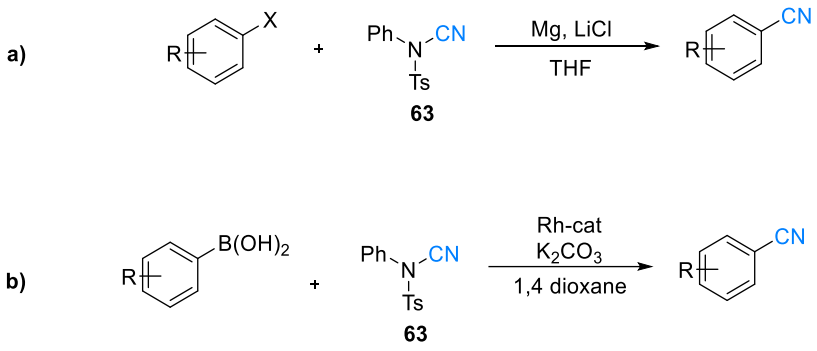

Scheme 28: Electrophilic cyanation using NCTS.

Additionally, cyano chalcogenides, such as cyanate and thiocyanate, represent another class of electrophilic cyanating agents. Among these, phenyl cyanate **64** has been employed by Sato and coworkers, who described the cyanation of various aromatic compounds though initial lithiation with *n*-Butyl Lithium (Scheme 29).[112]

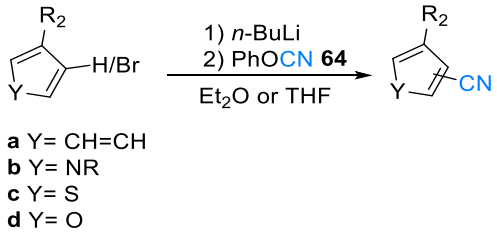

Scheme 29: Electrophilic cyanation with phenyl cyanate.

More recently, Alcarazo's research group has proposed additional notable examples of electrophilic cyanide sources. Both imidazolium thiocyanates[113] **65** and 5-(Cyano)-dibenzothiophenium trifrate[114] **66** has been synthesized in reaction with TMSCN, showing excellent reactivity with a range of nucleophilic substrates, such as thiols, amines, ketones and aromatic compounds (**Figure 21**).

65

a R= Me, X= Br
b R= *i*Pr, X= Cl
c R= *i*Pr, X= Br

66

Figure 21: Sulfur based electrophilic cyanating agent.

Finally, in the last decades radical cyanating agent has been developed, such as tosyl cyanide. In 2011, Inoue et *al.* presented an oxidative photocyanation with benzophenone as organic photocatalyst.[115] In this work, through a photon-induced hydrogen abstraction mechanism, several nucleophilic compounds such as ethers, alcohols, carbamates and aliphatic compounds were successfully cyanated using TsCN **67** as $CN^{\cdot}$ donor (**Scheme 30**).

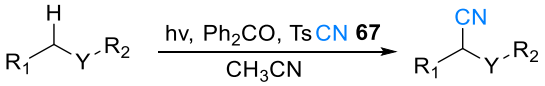

a Y= CR_2
b Y = NR
c Y = O

Scheme 30: Tosyl cyanide as radical CN donor.

An outline summary of the different electrophilic, nucleophilic and radical cyanide sources is provided in **Figure 22**. While the reagents previously discussed offer valid alternatives for cyanation reaction procedures, in term of handling of the starting

material and reaction set-up, it is important to note that many of them are still synthesized using hazardous procedures.

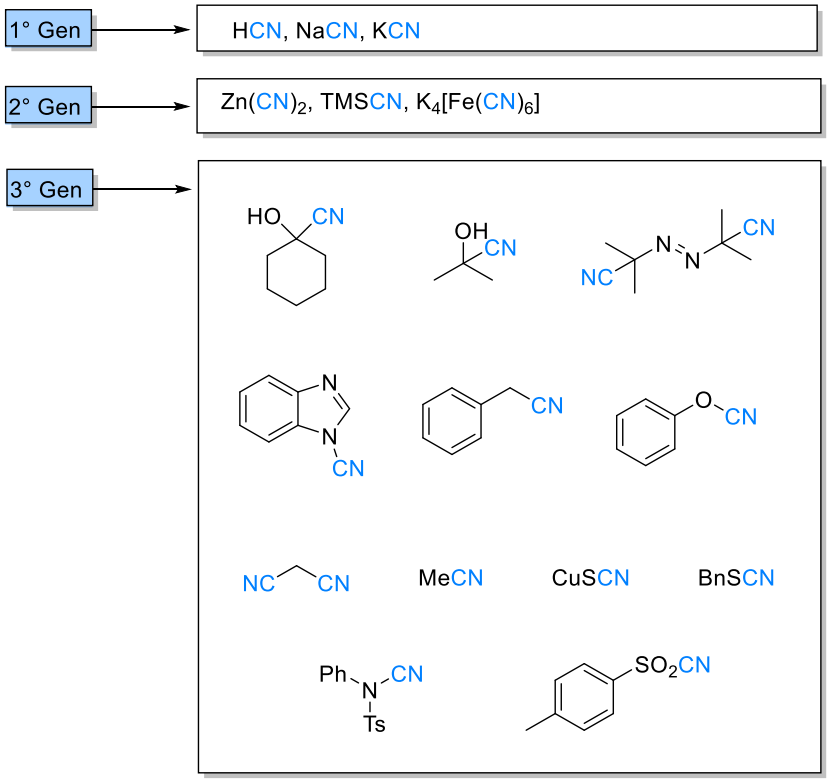

Figure 22: Cyanide sources.

2.3 Electrochemical cyanation reactions.

Alongside the effort to identify new, safer cyanide sources that minimize the risks associated with cyanation reactions, an equally important objective is to improve the efficiency and safety of the procedures based on the reagents introduced thus far. In this context, the use of techniques such as electrochemistry or flow chemistry provides a reliable alternative, representing the perfect connection between safe and eco-friendly methodologies, as they generally offer milder conditions and simple procedures. In fact, in the last decade numerous electrochemical studies have been carried out to synthesize both aromatic and aliphatic nitrile derivatives.[116] Some

recent examples are reported below. In 2021, Cai et *al.* reported an electrochemical strategy for the *N*-cyanation of secondary amines or the α-*C*-cyanation of tertiary amines under transition metal-free solution and with TMSCN as cyanide source.[117] The reactions were carried out in an undivided cell setup with a Glassy Carbon (GC) serving as working electrode for the *N*-cyanation (**Scheme 31a**) and Carbon (C) serving as working electrode for the α-*C*-cyanation (**Scheme 31b**).

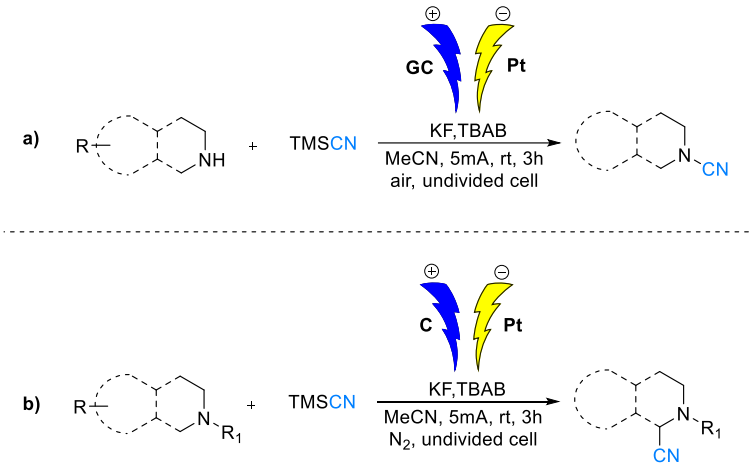

Scheme 31: Electrochemical cyanation reaction using TMSCN.

Another interesting example of electrochemical α-cyanation of secondary amines has been reported by Stahl et *al.*, and this protocol proved to be particularly advantageous for the synthetic modification of pharmaceutical building blocks.[118] Thanks to the use of ABNO (9-azabicyclononane *N*-oxyl) as hydride-transfer mediator, has been possible to proceed at lower potentials, making the procedure also applicable to substrates bearing electrochemical susceptible functional groups. Again, TMSCN has been used for the CN donation, and with the subsequent hydrolysis of the cyanated products, pipecolic acids have been easily obtained in high yields and diasteroselectivity (**Scheme 32**).

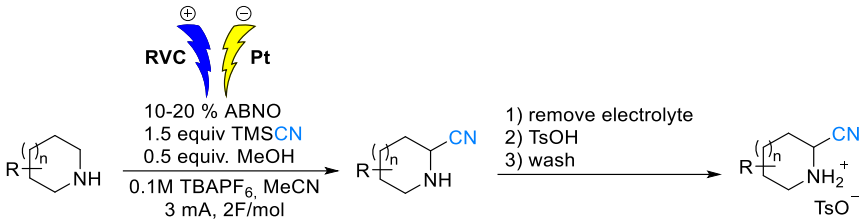

Scheme 32: Electrochemical α-Cyanation of secondary piperidines.

Focusing on different starting material, in 2020, Ding and coworkers reported an interesting cyanosilylation of aldehydes through electrochemically induced intramolecular reaction pathway, with high yield both with aromatic and aliphatic aldehydes, under mild conditions.[119] Also in this case, TMSCN has been used as CN source, with platinum plate as anode working electrode (**Scheme 33**).

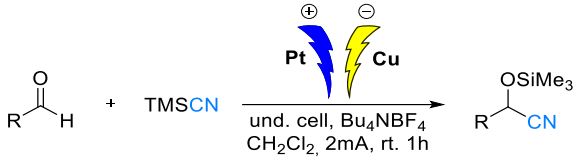

Scheme 33: Electrochemical cyanosilylation of aldehydes.

Regarding the polyfunctionalization, Xu and coworkers have reported in 2024 a peculiar electrochemical azidocyanation of alkenes.[120] The reaction has been conducted using an undivided electrochemical set-up with **RVC** as working electrode and $Cu(acac)_2$ as catalyst (**Scheme 34**). A broad range of alkenes with various substituents was tested, showcasing that the mild conditions applied provide exceptional tolerance to different functional groups.

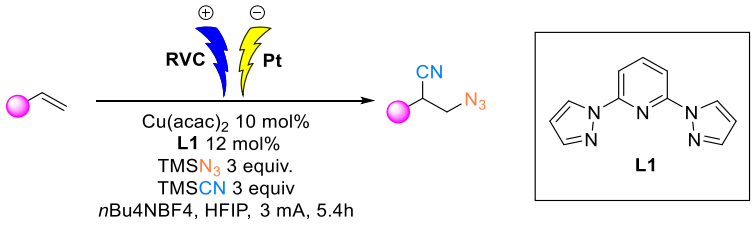

Scheme 34: Electrochemical azidocyanation of alkenes.

In 2020 Sheikhi et *al.* reported an electrochemical synthesis of β-ketonitriles starting from aryl methyl ketones in reaction with KCN and with graphite as working electrode (**Scheme 35**).[121] Remarkably, in this procedure, KI has been employed as both electrochemical mediator and supporting electrolyte, avoiding the need for hazardous and toxic iodine. Furthermore, the scale-up experiment has shown the feasibility of the method for gram-scale productions.

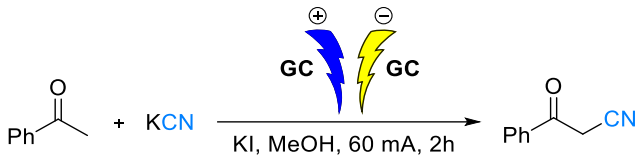

Scheme 35: Electrosynthesis of β-ketonitriles.

Recently, Terent'ev and coworkers reported an interesting cascade process for the preparation of CN-substituted imidazo[1,5-a]pyridines using NH_4SCN as both a supporting electrolyte and a safe cyanating agent.[122] The final products have been also tested *in vitro* as fungicidal, showing potential results against mycelium radial growth in potato-sucrose agar (**Scheme 36**). In this case DMSO has been used as solvent and GC as working electrode.

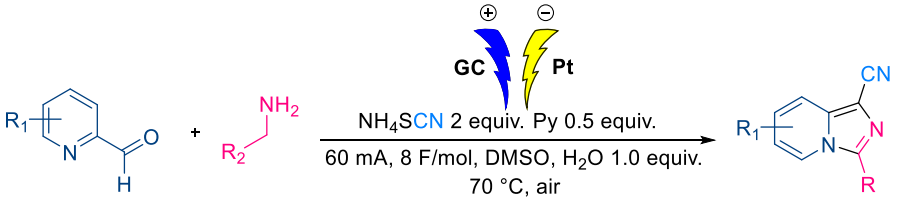

Scheme 36: Cascade synthesis of imidazo[1,5-a]pyridines.

Finally, Gooßen et *al.* reported a peculiar electrochemical C-H activation of electron-rich (Hetero)Arene for their direct cyanation with NaCN (**Scheme 37**).[123] The procedure proposed represent an operationally simple alternative to the traditional method, with good results and perfect reproducibility also in gram-scale synthesis without loss of yield and selectivity.

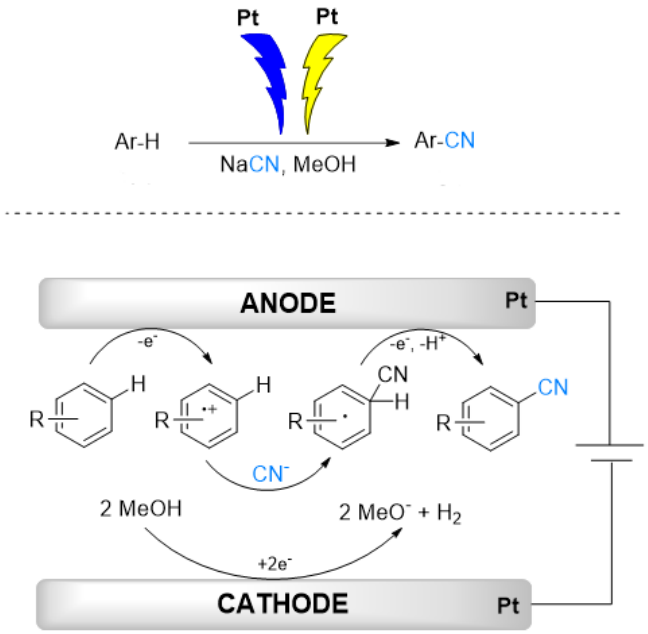

Scheme 37: Electrochemical C-H cyanation of aromatic rings and proposed reaction mechanism.

Part I: Electrocatalytic Hydrogen Evolution Reaction Enabling Cyanation of Electron-poor Carbons with Acetone Cyanohydrin

The numerous examples of electrochemical cyanation reactions shown above clearly demonstrated the reliability of this approach as a viable alternative to avoid the harsh conditions typically used in traditional chemical methods. For this reason, following the research program on cathodic activation of nucleophiles using catalytic amount of current described in the **Chapter I**, was explored the possibility to use electricity for the electroactivation of ACH to enable the cyanation of α,β-unsaturated ketones and imines (**Scheme 38**). In fact, the use of catalytic amount of current and supporting electrolyte and a limited amount of solvent, could represent an important advantage for the development of a greener cyanation procedure.

Indeed, despite the numerous studies on the base-catalyzed activation of ACH as a convenient source of nucleophilic CN^-, to the best of our knowledge, no examples regarding the use of this reagent in an electrochemical environment have been reported in the literature.

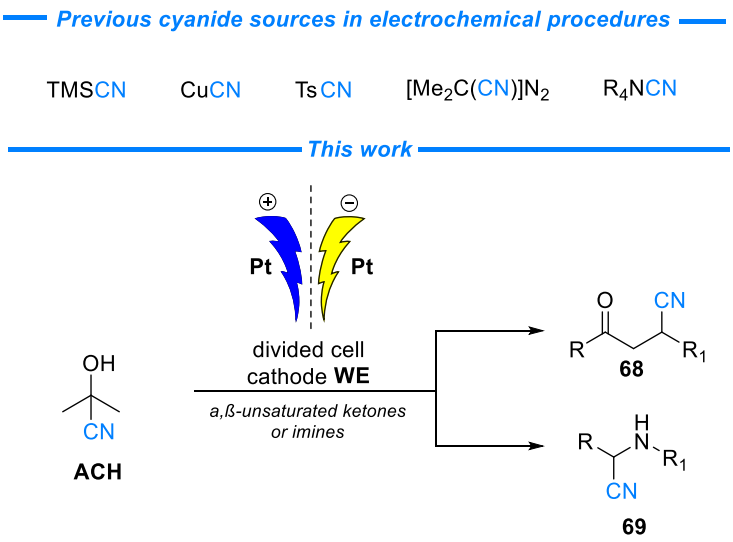

Scheme 38: This work.

2.4 Results and discussion

I firstly focused on the electro-induced CN addition to α,β-unsaturated ketones, optimizing the reaction conditions on chalcone **70a** as model substrate (**Table 5**).

Table 5: Optimization studies of cyanation reaction on α,β-unsaturated ketones.

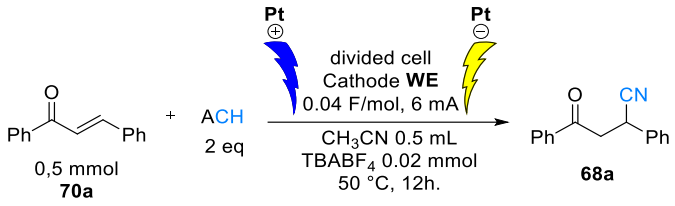

Entry[a]	Deviation from the standard conditions	Yield[b]
1	None	96 %
2	No electricity	-
3	Undivided cell	-
4	DMF instead of CH_3CN	90 %
5[c]	*Ex-cell* reaction	82 %
6	Electrolysis/reaction at r.t.	92 %
7[d]	Solvent-free, ACH (15 equiv.)	30 %
8[d]	0.02 F/mol, CH_3CN (1.5 mL)	72 %
9[d]	0.02 F/mol, CH_3CN (1.5 mL), ACH (3 equiv.)	65 %
10	GC as cathode	18 %
11[d]	0.02 F/mol, CH_3CN (1 mL)	53 %

[a] For the electrolysis using divided cell, the potential is ranging from 9 to 30 V. [b] Isolated yield. [c] **70a** was added post-electrolysis of ACH in CH_3CN. [d] Both electrolysis and reaction were conducted at r.t.

Although ACH did not show any voltammetric peak both in DMF/$TBABF_4$ and CH_3CN/$TBABF_4$, electrolysis is necessary to obtain the desired product (**Table 5**, **Entry 2**). The different entries also suggest that the reaction is initiated by a cathodic reduction process and, subsequently, progresses chemically until the total

conversion of the starting material is completed. Good results have been obtained also proceeding "*ex-cell*" (i.e. by adding the substrate **70a** after the pre-electrolysis of the ACH) with 82 % isolated yield on the desired product (**Table 5, Entry 5**). Furthermore, the reaction was found to be highly dependent on the substrate concentration in acetonitrile (**Table 5, Entry 8 and 11**) and on the electrode material used. (**Table 5, Entry 10**). Finally, it is important to highlight that using catalytic amount of current is particularly beneficial for the reaction result. In fact, with mild electrolysis conditions is possible to use susceptible starting materials, such as α,β-unsaturated ketones, that could undergo to cross coupling or unwanted side products.[124] In this regard, a control experiment in absence of ACH, shows the complete disappearance of **70a** with 0.7 F/mol, under standard conditions.

With the optimized conditions in hand, I started the study of the substrate scope using various α,β-unsaturated carbonyls, as shown in **Table 6**.

Table 6: Substrate scope and limitations of the electrochemical cyanation of α,β unsaturated carbonyls.

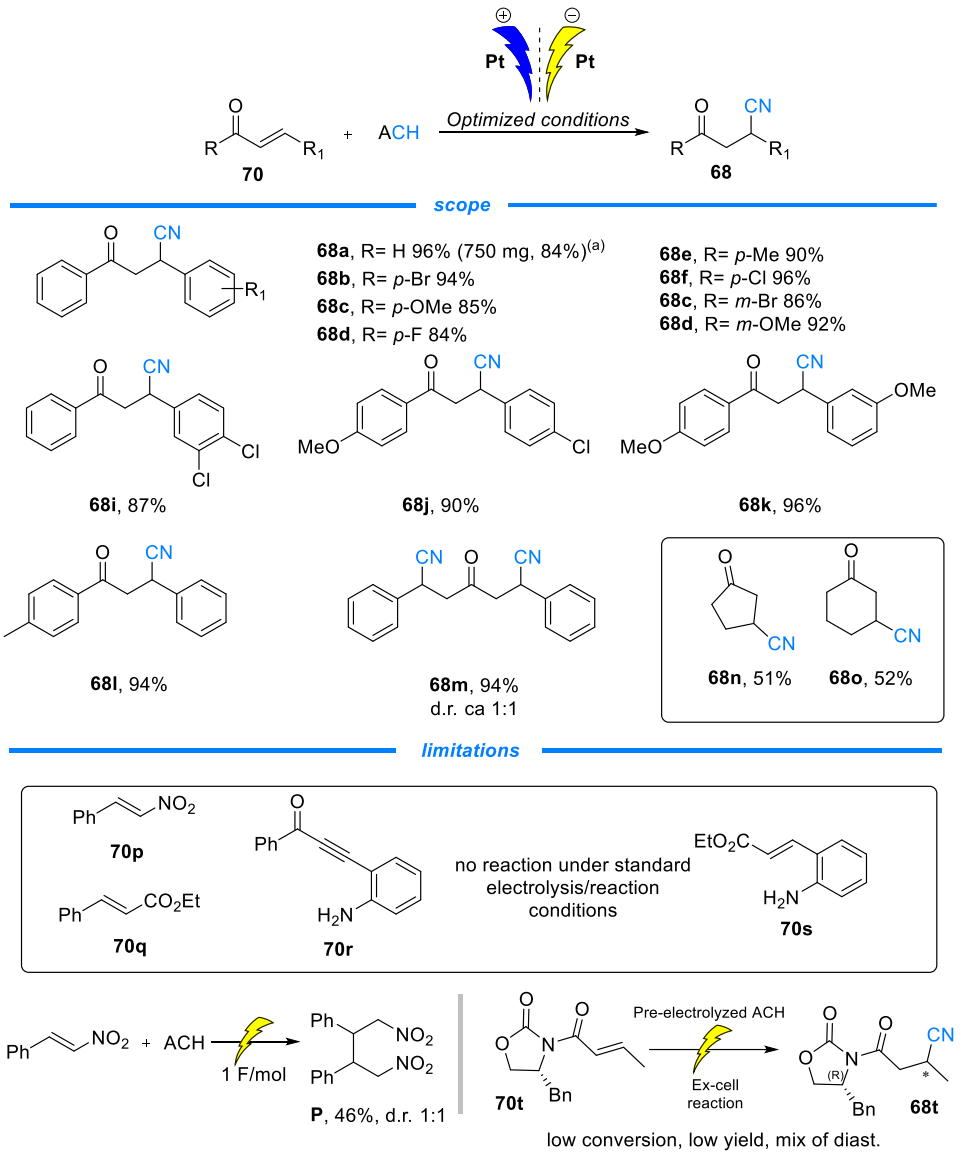

[a]Large scale cyanation on 3.6 mmol of **70a**.

The reaction proceeded smoothly with both alkyl and methoxy substituents on either aromatic ring, leading to the corresponding β-ketonitriles with high isolated yields. Halogen- and polyhalogeno-substituted chalcones proved to be suitable

substrates as well, with 87 % yield in the product **68i**. The reaction with the benzylideneacetone **70m** led to the formation of the double cyanation product **68m** as diastereoisomer mixture in 94 % yield. Under similar reaction conditions, the cyclic starting materials **68n** and **68o** exhibited slightly reduced reactivity/selectivity, resulting in the formation of the desired products with 51 % and 52 % isolated yield respectively. Moreover, the scale-up attempt (3.6 mmol, 750 mg of chalcone) succeeded, yielding the product in a satisfactory 84%—an encouraging result for the batch electrochemical process. While the procedure proved effective for α,β-unsaturated carbonyls, significant limitations were encountered with nitrostyrene **70p** and α,β-unsaturated esters. These substrates were largely recovered unreacted, also by changing a variety of reaction parameters such as current, temperature, and reaction time. Notably, nitrostyrene **70p** underwent considerable hydrodimerization when electrolyzed with a stoichiometric amount of current, yielding the side product **P** as a diastereomeric mixture in a 46% isolated yield. Consequently, to minimize the formation of potential side products from sensitive functional groups during the electrolysis of the challenging functionalized α,β-unsaturated amide **70t**, I conducted the reaction using an "*ex-cell*" procedure with a slight increase in current. However, ^{1}H-NMR analysis of the crude mixture showed only partial conversion of **70t**, with the desired product detected in traces as a diastereomeric mixture.

Subsequently, the generality of the electrocatalytic activation of ACH was further examined in the cyanation of imines to produce α-aminonitriles, which are valuable intermediates in the synthesis of α-aminoacids. Also in this case, an optimization has been done, using imine **71a** as model substrate. Compared to the previous procedure, in this case, optimized conditions involved an even lower amount of current, supporting electrolyte and ACH loading, leading to the corresponding 2-phenyl-2 (phenylamino)acetonitrile **69a** in a good 94% yield. As shown in **Table 7**, also for this reaction the result is dependent on the electrode used for the electrolysis, with best results achieved by utilizing Pt, Pd and Au. (**Table 7, Entry 1, 4,**

5). In addition, **Entry 10** shows that a slight benefit in term of final yield in product (+ 3%) at the expense of a large excess of the cyanating agent, which is clearly not advantageous in terms of the atom economy of the process.

Table 7: Optimization reaction condition for the synthesis of α-aminonitriles.

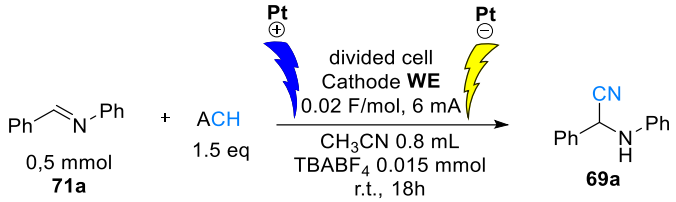

Entry[a]	Deviation from standard conditions	Yield[b]
1	none	94%
2	No electricity	-
3	Undivided cell	-
4	Pd as cathode	91%
5	Au as cathode	90%
6	Glassy Carbon as cathode	22%
7	DMF instead of CH_3CN	87%
8	*ex-cell* reaction	77%
9	Solvent-free, ACH/10 eq	45%
10	ACH 5eq	97%
11	0.05 F/mol, 0.038 mmol of Bu_4NBF_4	94%
12	0.07 F/mol, ACH (5 eq)	96%

[a] For electrolysis using divided cell, the potential is ranging from 9-30 V. [b] Isolated yield. [c] **71a** was added post-electrolysis of ACH in CH_3CN. [d]Both electrolysis and reaction were conducted at r.t.

As shown in **Table 8**, the optimized electrochemical protocol allowed the cyanation of several imines **71a-j** bearing different substituent on the aromatic rings.

Table 8: Substrate scope and limitations of the electrochemical cyanation of α-aminonitriles.

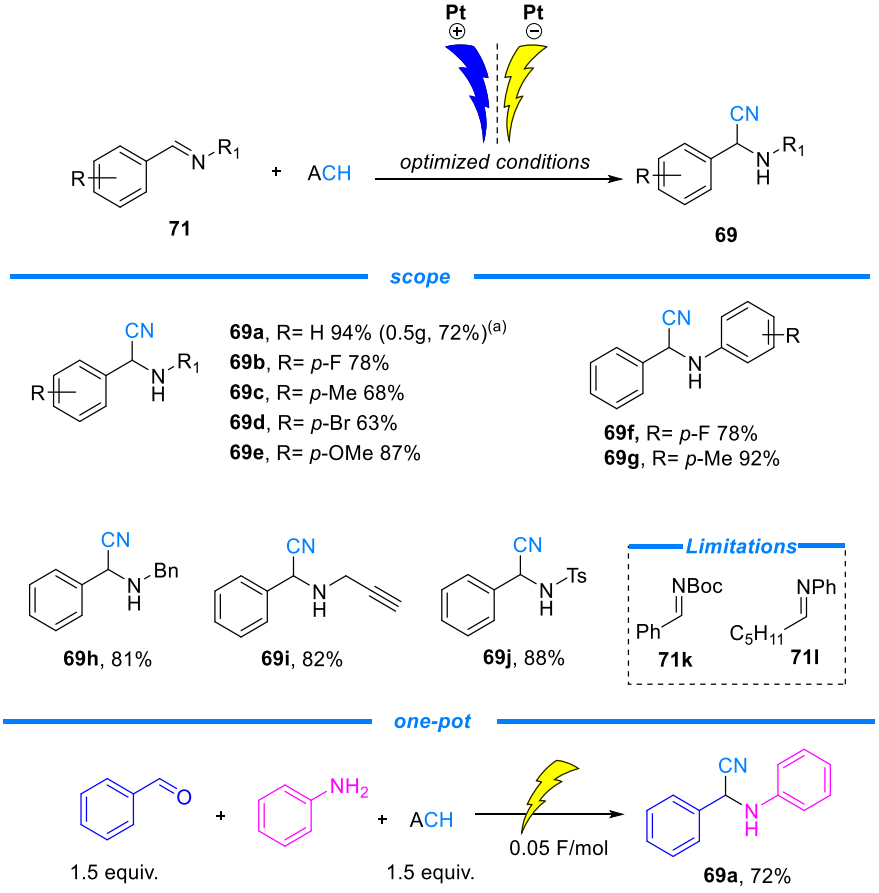

(a)Large scale cyanation of **71a**; One pot reaction: Benzaldehyde (0.32 mmol), aniline (0.21 mmol), ACH (0.32 mmol) in CH_3CN (0.67 mL), $TBABF_4$ (0.006 mmol) were electrolyzed using optimized conditions. Current quantity (0.05 F/mol).

Similarly, the presence of a halogen atom as a substituent did not hinder the achievement of high yields, showing that using catalytic current effectively prevents unwanted reactions and side product formation. Encouragingly, the reaction also performed well with various *N*-protecting groups, such as benzyl (**71h**), propargyl (**71i**), and tosyl (**71j**), producing the desired products with yields up to 88%. However, the reaction failed with the Boc-protected imine **71k** and alkyl derivative **71l**.

Interestingly, the electrochemical activation could also proceed via a one-pot process, directly leading to the final product **69a**, by electrolyzing simultaneously ACH, benzaldehyde and aniline, with 72% yield. Finally, the half gram-scale reaction resulted in a good 72% isolated yield.

DFT computations have been conducted to have an understanding on the electrocatalytic process. Based on the control experiments studies and calculations of the standard free energies and the redox potentials, we can outline an electrochemical-chemical process initiated by the cathodic reduction of acetone cyanohydrin (**Figure 23**).

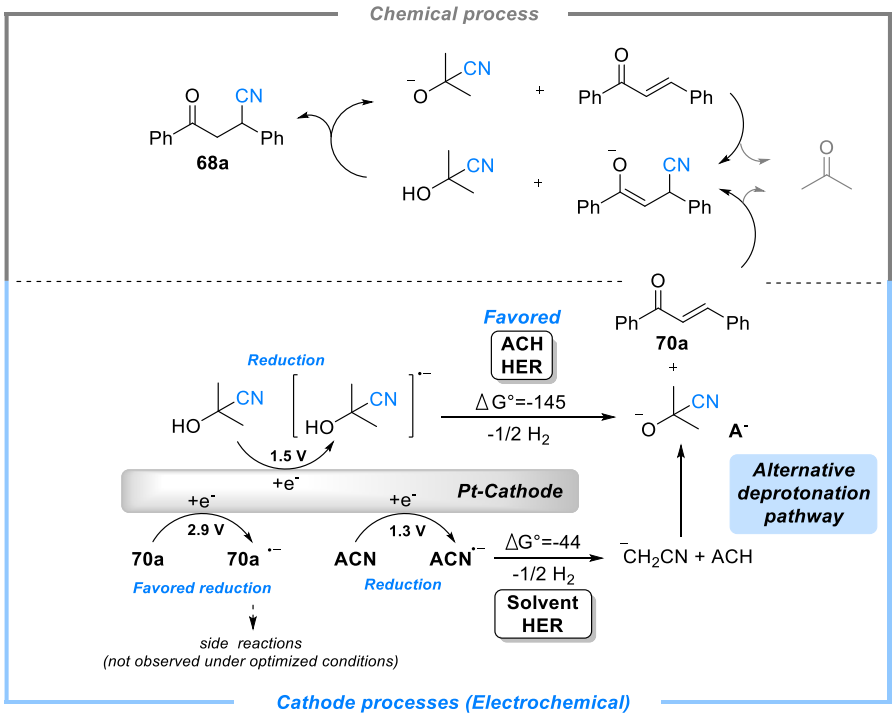

Figure 23: Proposed EC pathway for the electrochemical cyanation process. Standard free energies (ΔG ° (kJ/mol)) are calculated at 25 °C. ΔV are calculated excluding the reference electrode absolute redox potential.

The first reduction to form ACH radical anion is subsequently followed by the thermodynamically high favored HER (ΔG° = -145 kJ/mol), generating the

deprotonated species **A⁻**. Then, the reaction should evolve with a chemical process, by nucleophilic addition of CN^- to the α,β-unsaturated carbonyls or to the imine until the total conversion of the starting material. Surprisingly, according to the experimental data, the DFT calculations assigned the chalcone **70a** as the more reducible species in the reaction system.[124] However, chalcone radical coupling side product is only observed when ACH isn't present during the electrolysis, when an undivided-cell set up was used or finally when the hydrogen evolution reaction is disfavored for the electrode material and its overpotentials (see optimization tables). It is also notable that the reduction and secondary HER of the solvent, while less compared to the direct activation of the cyanating agent, could represent an alternative pathway initiating the process *via* acid-base reaction.[125] Despite the gas evolution during the electrolysis, the voltammetry experiment failed in identifying the reduction peak of ACH. For this reason, direct production of $[ACH]^{\cdot -}$ may be expected only in solvent-free conditions. To further understand the reaction pathway, we evaluated alternative channels for the indirect electrochemical activation of ACH, using DFT calculation. From these calculations resulted that the only plausible alternative involves the solvent activation, used for the electrolysis (**Figure 24**).

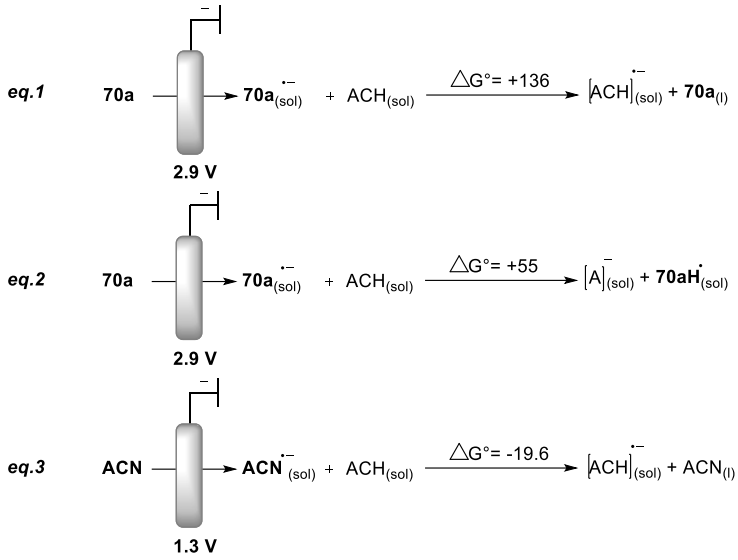

Figure 24: Thermodynamics for indirect electrochemical activation of ACH. Standard free energies (ΔG ° (kJ/mol)) are calculated at 25 C. ΔV are calculated excluding the reference electrode absolute redox potential.

Part II: eCyanation using 5-aminotetrazole as a safer electrophilic and nucleophilic cyanide source

The electrochemical activation of ACH, described in the previous part, certainly represent an interesting alternative as cyanation reactions protocol, with the combination of the electro-mild conditions and the use of a safe and handling cyanating reagent.

During a six-month internship in Prof. Kevin Lam's Research Group (University of Greenwich, Kent, UK) I had the opportunity to further study this interesting synthetic field, developing a new cyanation procedure. Also in this case, an electrochemical methodology has been used but recurring to an unprecedent cyanating agent. By anodic oxidation of 5-aminotetrazole, I was able to successfully generate, *in situ*, either an electrophilic (cyanogen bromide) or nucleophilic cyanide source (CN^-), by simply varying the supporting electrolyte/base system (**Figure 25**). As already stated

in the introduction of this chapter, safety concerns make the use of cyanide source from HCN or cyanide salts particularly dangerous, especially from an industrial point of view. In addition, for the most cyanide surrogates, being still toxic and flammable reagents, particular attention on the storage is required, that could be costly and not without risk.

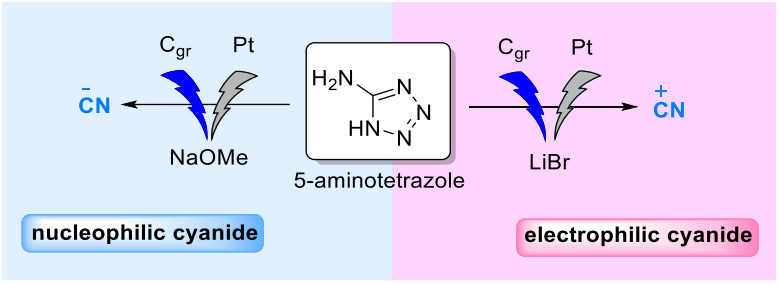

Figure 25: Electrochemical generation of cyanide source.

2.5 Results and discussion

Based on the different studies regarding the thermal decomposition[126] reported in literature and the previous work[127] of the Lam's research group on the anodic oxidation of aminotetrazole derivatives, we began our investigation by examinate the possibility to electrochemically generate an electrophilic cyanide agent. Indeed, the generation of cyanide anions via anodic oxidation, in connection with the electrogenerated Br^{+}, could directly lead to the desired BrCN. With this idea, we started the reaction optimization by using an undivided electrochemical cell and LiBr as bromide source. When the oxidation has been carried out with CH_3CN/H_2O as reaction solvent, the formation of BrCN has been detected by ^{13}C-NMR analysis (**Figure 26**).

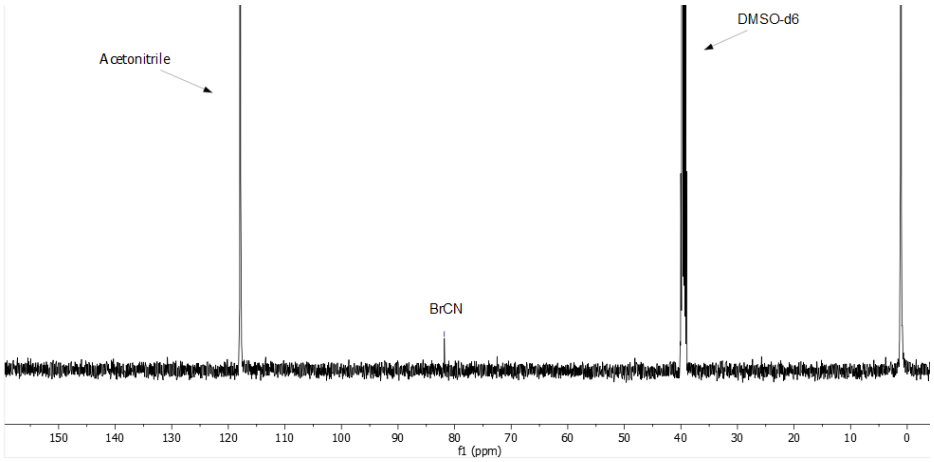

Figure 26: ^{13}C-NMR detection of BrCN.

This interesting result prompted us to investigate the possibility of using the electrogenerated cyanogen bromide in a subsequent reaction in order to achieve synthetic transformations. With this aim, we chose to utilize secondary amines as nucleophilic substrates to optimize the starting material conversion and so the BrCN generation. Optimization studies making with dihexylamine **72a** have shown that cyanogen bromide can be efficiently generate in situ by electrolyzing a solution of 5-aminotetrazole and LiBr in CH_3CN/H_2O 25:1 with a current density of 41.7 $mA{\cdot}cm^{-2}$ for 2.8 F/mol and using a graphite anode and a platinum cathode. The addition of **72a** after the electrolysis led to the desired cyanated product **73a** with 75% isolated yield (**Table 9**). Subsequently, in order to increase the final product formation, 1.5 equivalent of potassium carbonate have been added after the electrolysis, leading to 86% yield after 1h of stirring at room temperature. Changing the solvent, both in the CH_3CN/H_2O ratio and the solvent type, such as methanol and ethanol, drastically decrease the final yield (**Entry 5-6, Table 9**) or the possibility to obtain the product (**Entry 7, Table 9**). With 2 equivalents of LiBr instead 3 equivalents the reaction was reduced to 68% (**Entry 9, Table 9**). Also decreasing the current amount affects the final yield, with 64 % instead 86% yield (**Entry 4, Table 9**). Finally, the procedure seems to be particularly dependent also on the concentration (**Entry 2, Table 9**).

Table 9: Optimization of cyanogen bromide generation.

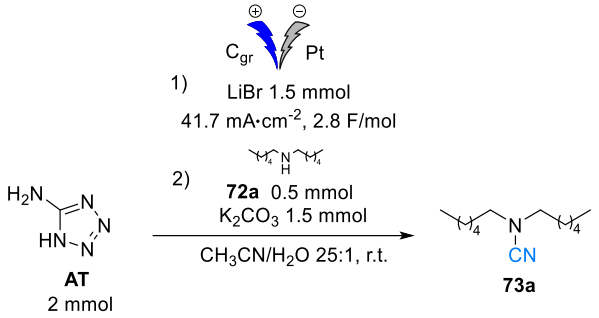

Entry	Deviation from the standard conditions	Yield[(a)]
1	none	86 %
2	5 mL instead of 10 mL	76 %
3	No base	75 %
4	2 F/mol instead of 2.8 F/mol	64 %
5	CH_3CN/H_2O 1:1 instead of CH_3CN/H_2O 25:1	25 %
6	MeOH instead of CH_3CN/H_2O 25:1	22 %
7	EtOH instead of CH_3CN/H_2O 25:1	-
8	$NaHCO_3$ instead of K_2CO_3	82 %
9	1 mmol LiBr instead of 1.5 mmol	68 %

[(a)]Isolated yield

With the optimized reaction conditions in hand, the scope of this novel cyanation methodology was investigated on different secondary amines. As shown in **Table 10**, the electrochemical protocol facilitated the cyanation of a quite representative number of substrates, leading to the corresponding products **73a-g**, in high yields. The reaction also showed good tolerance for functionality such as nitro-group or alkenes, which are usually instable in electrochemical conditions.

Table 10: Substrate scope with secondary amines.

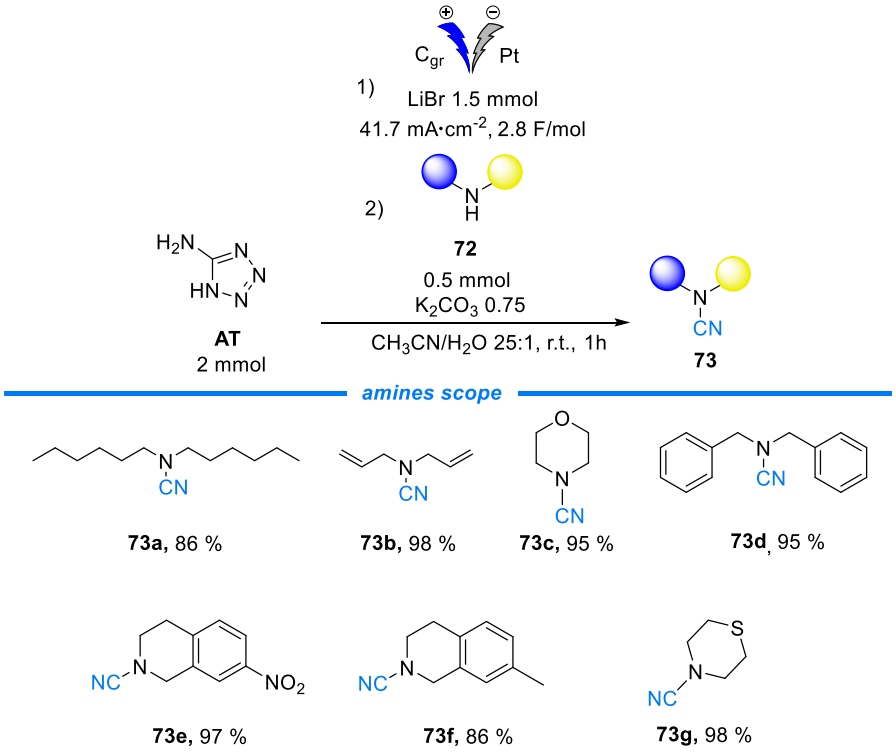

It is worth noting that most of the products were obtained through a simple basic aqueous work-up, without the need for chromatographic purification.

Nicely, providing that Et_3N or DBU were used as base, this electrochemical protocol also proved effective in the cyanation of sulfur nucleophiles, such as thiols (**Table 11**). Indeed, in this case, the use of organic bases was required to limit the formation of the disulphide side product. Triethylamine proved to be the better choice for the cyanation of alkyl thiols, such as decylthiol **74d** and benzylthiol **74a**, leading to the desired products with 56% and 83% yield respectively. Otherwise, with the aromatic thiols, as *p*-methoxybenzenethiol **74c** and *p*-chlorobenzenethiol **74b** the best results have been achieved using DBU.

Table 11: Substrate scope with thiols.

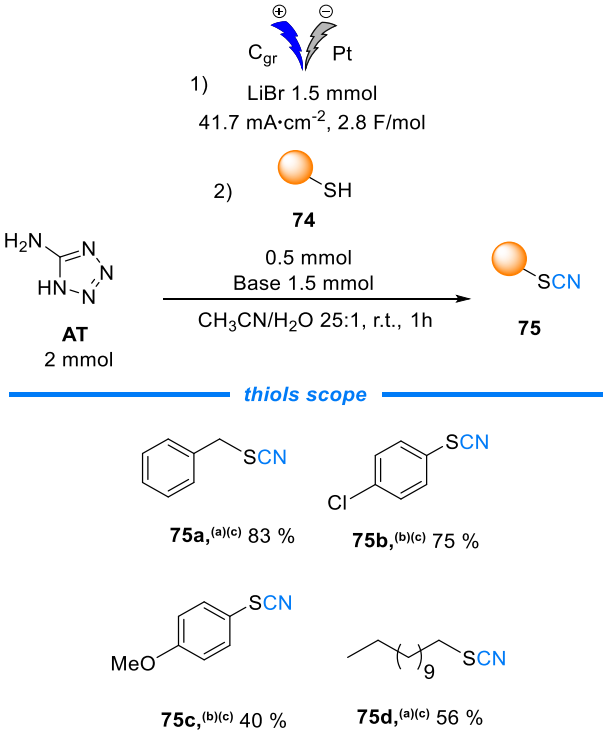

(a) Et_3N, 1.5 mmol. (b) DBU, 1.5 mmol. (c) Thiol added at 0°C.

Finally, to further assess the method, we tested *o*-substituted anilines containing various nucleophilic groups, such as -OH, -SH, and -NH_2, to promote a double nucleophilic attack and directly access heterocyclic compounds. As shown in **Table 12**, leaving the solution to stir at 60 °C for 3 hours, the product **77b** has been obtained with 57% starting from phenyl-diamine **76b**. In addition, the reaction worked successfully with thiophenol **76a** and thiol **76c** derivatives, leading to the desired cyanated products with 80% and 78% isolated yields respectively. In particular the use of 2-(methylamino)phenol **76d** was highly effective, leading to product **77d** with a yield of 70%.

Table 12: Synthesis of heterocyclic compounds.

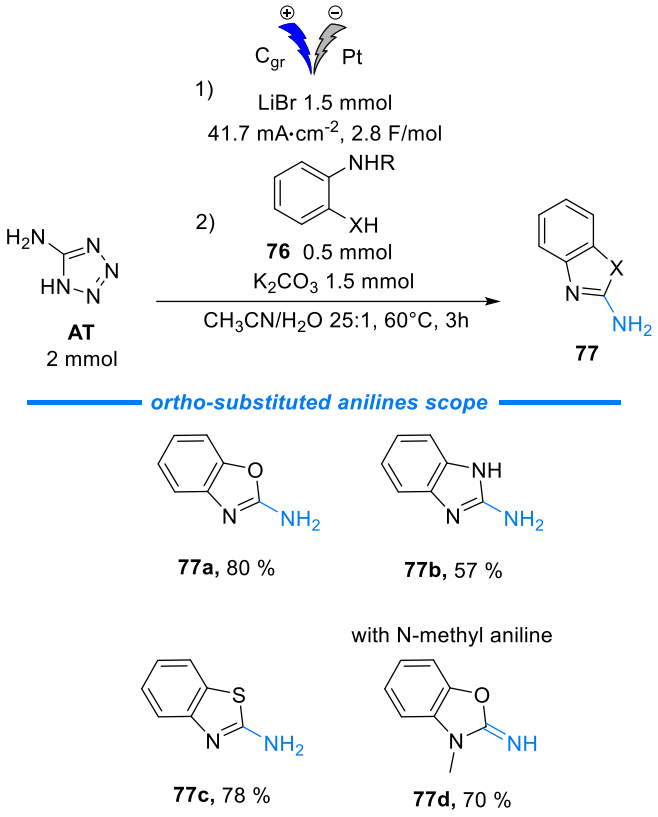

Taking inspiration by the promising results obtained in the electrogeneration of cyanogen bromide, we decided to explore the versatility of the electrochemical strategy for generating nucleophilic cyanide, once again using 5-aminotetrazole (AT) as the cyanide source. To evaluate and optimize this procedure, we selected the electrochemical cyanation of aromatic rings as a model reaction, as summarized in Table 13.

Table 13: Optimization of cyanation reaction of aromatic rings.

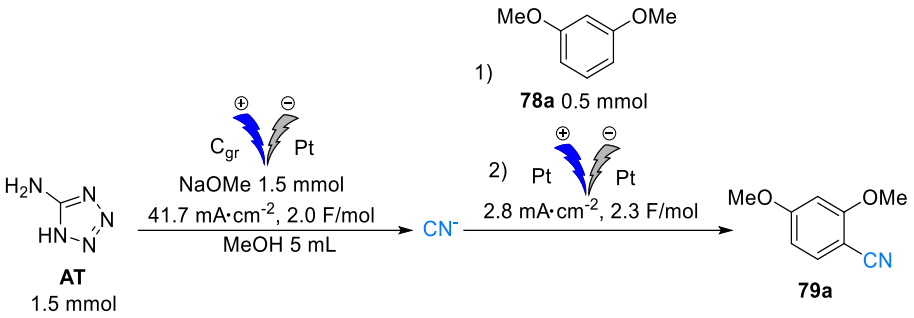

Entry	Deviation from standard conditions	Yield %[(a)]
1	none	83
2	Cgr as anode in the 2° electrolysis	53
3	25 mA instead of 5 mA during the 2° electrolysis	71
4	Cgr as cathode and Pt as anode in the 2° electrolysis	55
5	0.5 eq of NaOMe instead of 3 eq	10
6	NaOH instead of NaOMe	-

[(a)] Isolated yield.

The first reaction step concerns the electrogeneration of cyanide, obtained electrolyzing 3 equivalents of 5-aminotetrazole with 3 equivalents of sodium methoxide in methanol. The electrolysis has been carried out with a current density of J= 41.7 mA·cm^{-2} for 2 F/mol of tetrazole, using a graphite anode and a platinum cathode. In the second step, the graphite anode has been replaced by a platinum

electrode. Then, 1 equivalent of arene is added and the electrolysis is continued at 2.8 mA·cm^{-2} for 2.3 F/mol of arene, achieving the desired aromatic nitrile **79a** with 83% yield (**Table 13, Entry 1**). Replacing the anode electrode after the first electrolysis proved crucial for improving the yield. Performing the cyanation step without replacing the graphite anode resulted in a lower yield of the final product (53%) (**Table 13, Entry 2**). Another critical parameter was the current intensity used during the cyanation step. As shown in **Entry 3**, increasing the current to 25 mA during this cyanation reaction led to a decrease in yield (from 83% to 71%) and a deterioration in selectivity, resulting in the formation of various by-products, including the dimer of the arene as well as the dicyanated product. With the optimized reaction conditions, we explored the scope and limitations of the cyanide generation/aromatic cyanation sequence (**Table 14**).

Table 14: Electrochemical cyanation of electron-rich aromatic rings.

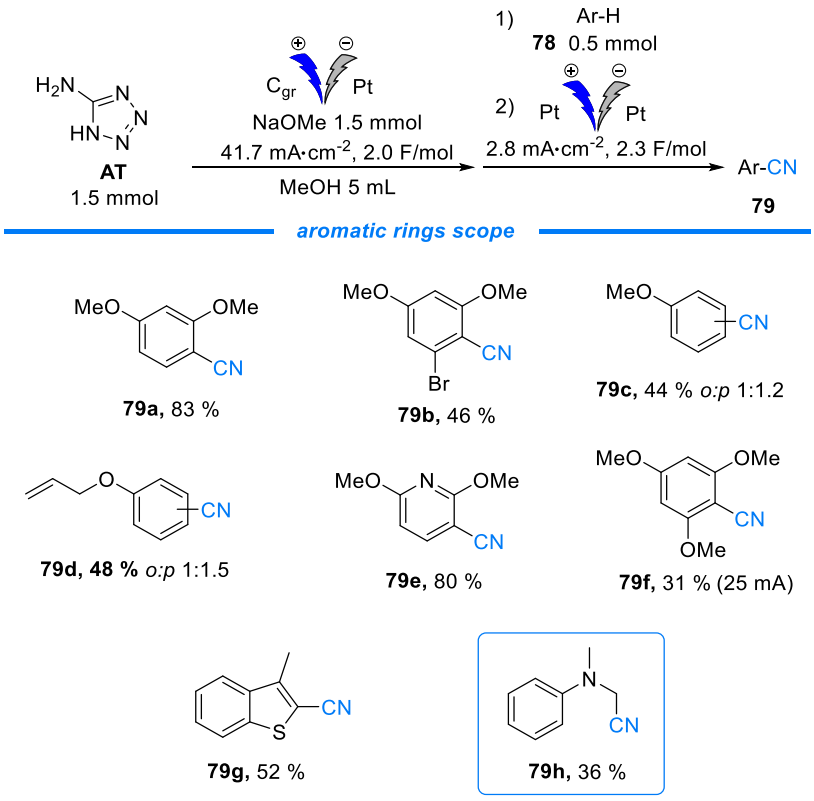

This procedure has been tested with various substituted aromatic compounds, including 2,5-dimethoxypyridine **78e** and 3-methylbenzothiophene **78g**, with 80% and 52% respectively. With 1,2,5-trymethoxybenzene **78f** as starting material, the reaction led to the formation of the desired cyanated derivatives only using 25 mA, with a 31% final yield, due to the simultaneous formation of the dimer side product. In addition, under the optimized reaction conditions, the reaction with *N,N*-dimethylaniline **78h** as starting material directly led to cyanated product **79h** on the methyl group with 36% yield, proceeding predominantly though a Shono-type oxidation.[128]

To further demonstrate the versatility of this the electrochemical cyanation reaction, has been also tested its applicability on a second electrophilic compound class, such

as aldehydes. The reaction has been carried out using the conditions previously optimized for the cyanation of aromatic rings but increasing the amount of starting material to 1 mmol. After the first electrolysis to generate CN^-, the aldehyde was added and the solution was stirred for 1 hour at room temperature, to give the corresponding cyanohydrin **81a-f** with final isolated yield ranging from 68 to 84% (**Table 15**).

Table 15: Cyanation reaction of aldehydes.

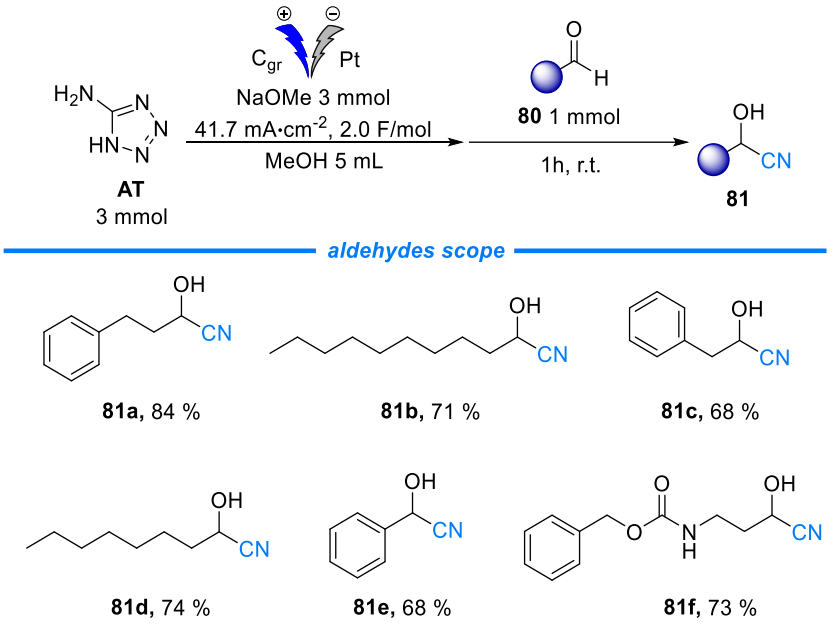

Subsequently, to confirm the validity of this novel methodology, I decided to extend the nucleophilic addition of cyanide to various electrophilic compounds (**Scheme 39**). Firstly, was tested a nucleophilic substitution using benzyl bromide **82a** and *p*-bromo benzyl bromide **82b** as starting material. The reactions have been carried out at 60°C for 5 hours, giving **83a** with 57% yield and **83b** with 71%. Secondary, with a Micheal acceptor such as chalcone **70a** as electrophile, the reaction led to the formation of **68a** with an excellent 80% yield after 5h at 60°C. When nitrostyrene **84** has been used as starting material, the cyanation reaction done at room temperature directly led to the formation of 2-phenylsuccinonitrile **85** in a yield of 74%.[129] In addition, the reaction was also carried out with (*E*)-*N*,1-diphenylmethanimine **71a** as electrophile, leading to the corresponding of α-aminonitrile derivative **69a** with 70% isolated yield.

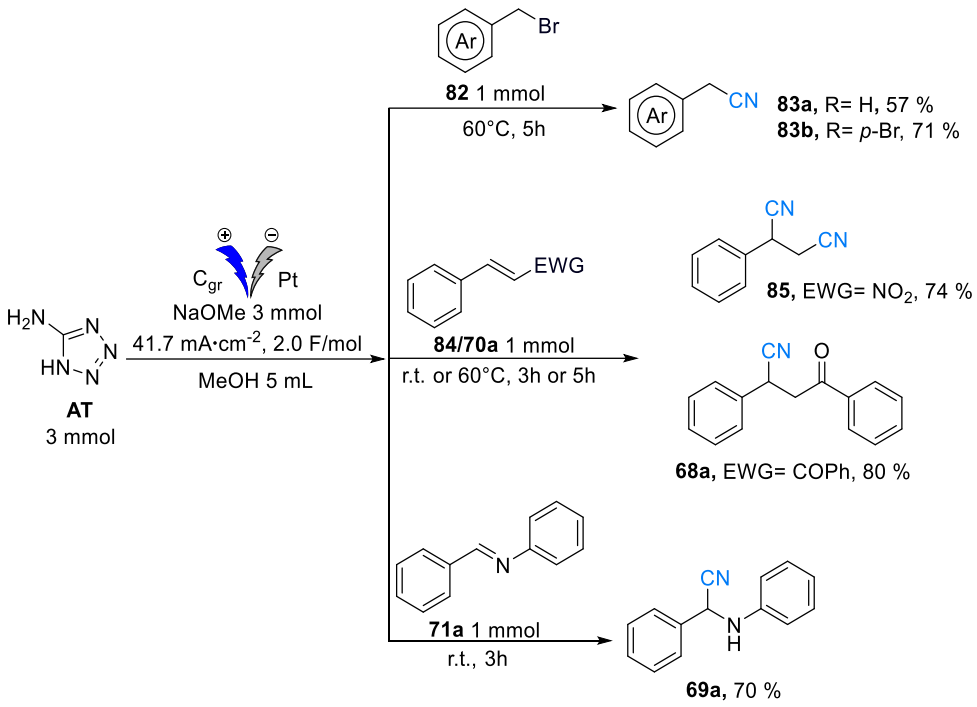

Scheme 39: Cyanation reaction on different electrophilic substrates.

To further demonstrate the scalability and practicality of using 5-aminotetrazole as a safer alternative cyanide source, we explored the transfer of our method to a flow-electrochemical setup. Flow chemistry represents in fact a valid methodology for the rapid electrochemical reaction scale-up,[130] and is particularly effective when two reactions need to be performed back-to-back, as in this case. Notably, the use of a flow-electrochemical setup could be ideal for this method and cyanation reactions in general, as it allows the entire process to occur within a closed system, eliminating any exposure to cyanide during the reaction. In order to test the applicability of this methodology, we started the investigation carrying out the electrolysis to a solution containing lithium bromide 0.045M and aminotetrazole 0.06M, in an electrochemistry flow cell equipped with a carbon graphite anode and a SS cathode (stainless-steel) at a rate of 0.19 mL·min^{-1} and a current density of 5.5 mA·cm^{-2}. The

electrolyzed mixture was directly added to 2.5 mL of a 0.033M solution (solution **B**) of dibenzylamine **72d** and 0.05 M of K_2CO_3 (**Scheme 40**).

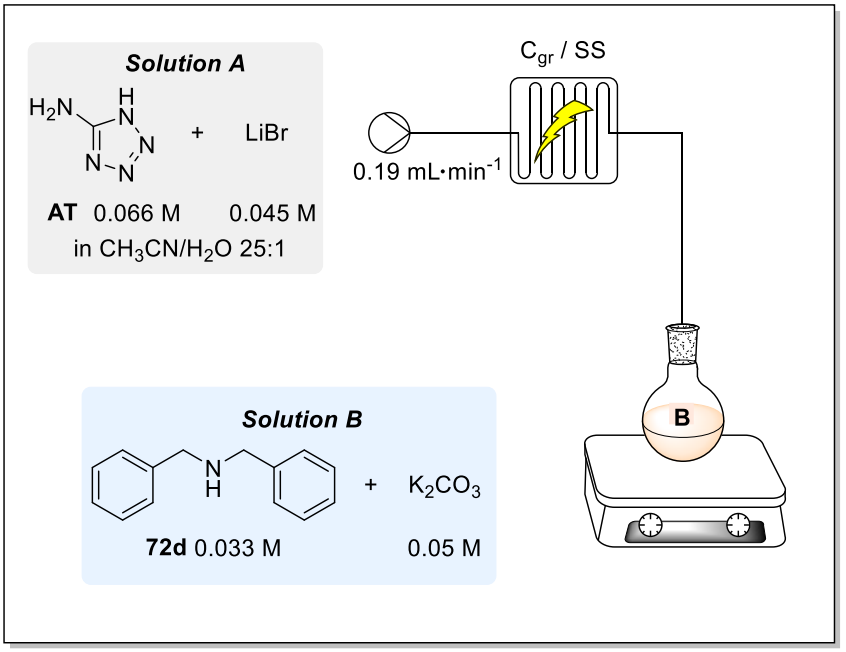

Scheme 40: First attempt to flow-electrochemical experiment.

After stirring at room temperature for 1 hour, the reaction led to the total conversion of the amine starting material, with a quantitative formation of the desired product. The positive results obtained with the first attempt prompted us to further study the reliability for the flow chemistry, trying the two steps coupled in flow. However, the low solubility of potassium carbonate in the solution used previously proved to be a limitation for the process, making necessary the use of a different solvent mixture for the solution **B**, such as CH_3CN/H_2O 10:1. Using a 5 mL reactor and a T-shaped mixer, with the flow of the solution **A** reduced to 0.083 $mL \cdot min^{-1}$, the cyanated product has been obtained with quantitative yield after the collection for 1 hour 47 minutes, corresponding to $3.31 \cdot 10^{-9}$ $Kg \cdot h^{-1} \cdot L^{-1}$, compared to $4.22 \cdot 10^{-8}$ $Kg \cdot h^{-1} \cdot L^{-1}$ in batch (**Scheme 41**). Nevertheless, the batch scale-up

electrosynthesis can be particurarly challenging and limited. For these reasons, the flow-electrochemical method represents a perfect solution for the reaction scale-up, limiting also all the potential risks connected with this reaction type, carrying out the reaction in a closed system.

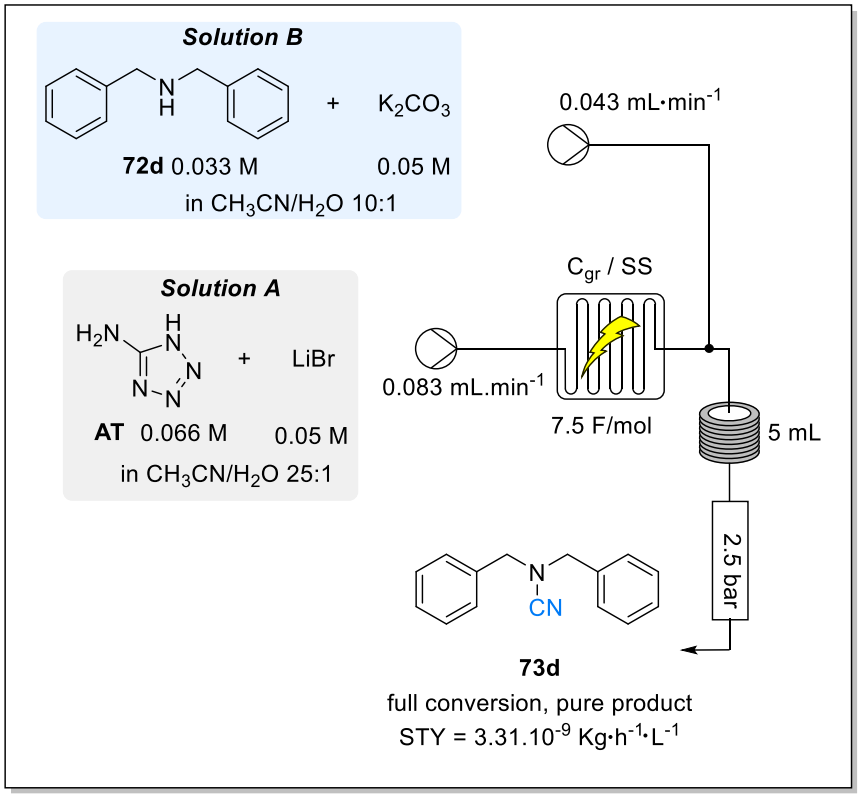

Scheme 41: Two reactions coupled in flow system.

A plausible reaction mechanism for the electrochemical generation of cyanide from 5-aminotetrazole is depicted in **Scheme 42**. After a first tetrazole deprotonation, the anion is anodically oxidized to form an unstable fulvene, which subsequently decomposes losing two nitrogen molecules to form a cyanide anion.

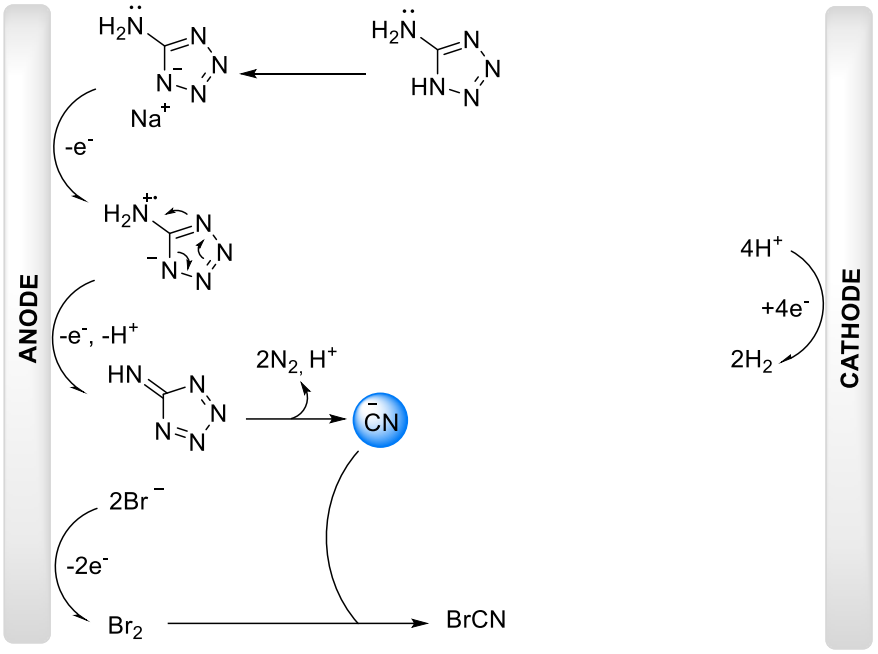

Scheme 42: Plausible reaction mechanism.

2.6 Conclusions

In conclusion, in the second period of my PhD, I successfully developed new electrochemical cyanation reactions procedures. First, by utilizing acetone cyanohydrin as a cyanide surrogate, I established a novel electrochemical method for the cyanation of α,β-unsaturated carbonyls and imines. The protocol has been successfully accomplished using a slight excess of cyanating agent and catalytic amount of current and supporting electrolyte. The hypothesized mechanism, supported by DFT calculations, suggested the involvement of Pt-Cathode hydrogen evolution reaction of the ACH as the key step. The procedure showed an elevated atom economy, accompanied by short electrolysis times and minimal demands on electrochemical equipment, with promising results for the reaction scale-up.

Furthermore, during my Visiting PhD period at the University of Greenwich, I successfully developed new electrochemical procedures for generating electrophilic and nucleophilic cyanide agents from 5-aminotetrazole, as an unprecedented and safe cyanide source. These electrogenerated cyanide agents proved effective in carrying out a wide range of cyanation reactions with good yields and selectivity, also demonstrating reliability in a flow-electrochemical system. Compared to classical cyanation methods, the proposed electrochemical strategy offers a significant improvement, particularly in terms of safety and control in generating otherwise toxic and hazardous reagents. The reaction setup is undeniably safer due to the use of 5-aminotetrazole, a stable and easy-to-store cyanide source.

2.7 Experimental section Part I

Electrochemical reactions were conducted using Hewlett Packard DC Power Supply Mod. E3612A in constant current mode, in a U-divided glass cell separated through a porous G-5 glass plug. Platinum spirals (apparent area 1 cm^2) were used as anode and cathode (distance between the electrodes 1 cm). Before use, Pt electrodes were treated with a Piranha solution (sulfuric acid/hydrogen peroxide 3:1) for 1 min, washed with double-distilled water and sonicated three times for 5 min with double-distilled water, acetone, and isopropanol. The reactions were monitored by thin layer chromatography (TLC) using Merck Silica Gel 60 F254 plates and were visualized by fluorescence quenching at 254 nm. Column chromatographic purification of products was carried out using silica gel 60 (70–230 mesh, Merck). The NMR spectra were recorded on Bruker Avance 400 spectrometers (400 MHz, ^1H; 101 MHz, ^{13}C). Spectra were referenced to residual $CHCl_3$ (7.26 ppm, ^1H; 77.00 ppm, ^{13}C). Yields are given for isolated products showing one spot on a TLC plate and seldom impurities detectable in the NMR spectrum. All chemicals and solvents were obtained from commercial sources and were used without further purification. Pt electrodes (wires, wire, diam. 0.5 mm, 99.99% trace metals basis) were purchased from Sigma-Aldrich.

Experimental procedures and characterization data of products 68

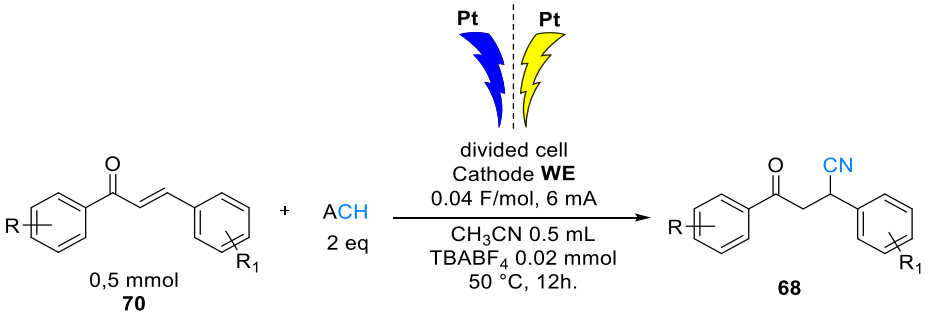

A solution of **70** (0.5 mmol), **ACH** (1 mmol), and tetrabutylammonium tetrafluoroborate (Bu_4NBF_4) (0.02 mmol) in MeCN (0.5 mL) is added in the cathodic compartment of a U-divided cell (glass frit 5G) equipped with platinum spirals (apparent area 1 cm^2) as cathode (WE, working electrode) and anode (CE, counter electrode). Anolyte was constituted by a solution of Bu_4NBF_4 (0.2 mmol) in MeCN (0.5 mL). Electrolysis was conducted under galvanostatic

conditions (6 mA, 0.04 electrons/molecule of **70**) at r.t. At the end of the electrolysis the solution has been left stirring for 12h at 50 °C. The mixture was then concentrated in vacuum and directly purified by silica gel chromatography (Hexane: Ethyl Acetate from 4:1 to 3:2) to afford the desired products **68a**–**68o**.

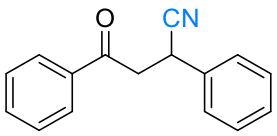

4-oxo-2,4-diphenylbutanenitrile (68a): The product **68a** (0.113 g, 96% yield) was obtained as white solid. **^{1}H-NMR** (400 MHz, $CDCl_3$): δ= 7.96 – 7.89 (m, 2H), 7.64 – 7.55 (m, 1H), 7.51 – 7.27 (m, 7H), 4.57 (dd, J = 7.9, 6.0 Hz, 1H, CH), 3.73 (dd, J = 17.9, 7.9 Hz, 1H, CH), 3.51 (dd, J = 17.9, 6.0 Hz, 1H, CH). **^{13}C-NMR** (101 MHz, $CDCl_3$): δ= 194.6, 135.6, 135.2, 133.9, 129.3, 128.8, 128.4, 128.1, 127.5, 120.6, 44.5, 31.9.

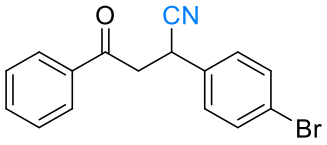

2-(4-bromophenyl)-4-oxo-4-phenylbutanenitrile (68b): The product **68b** (0.148 g, 94% yield) was obtained as white solid. **^{1}H-NMR** (400 MHz, $CDCl_3$): δ= 7.91 (dt, J = 7.2, 1.3 Hz, 2H), 7.64 – 7.53 (m, 1H), 7.52 –7.42 (m, 4H), 7.38 – 7.28 (m, 2H), 4.54 (t, J = 6.9 Hz, 1H, CH), 3.71 (dd, J = 18.0, 7.4 Hz, 1H, CH), 3.50 (dd, J = 18.0, 6.4 Hz, 1H, CH). **^{13}C-NMR** (101 MHz, $CDCl_3$): δ= 194.3, 135.5, 134.2, 134.0, 132.3, 129.2, 128.8, 128.0, 122.4, 120.1, 44.1, 31.3.

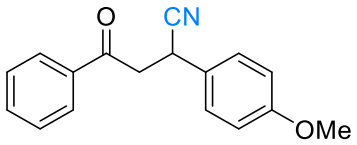

2-(4-methoxyphenyl)-4-oxo-4-phenylbutanenitrile (68c): The product **68c** (0.113 g, 85% yield) was obtained as white solid.**^{1}H-NMR** (400 MHz, $CDCl_3$): δ= 7.91 (d, J = 7.8 Hz, 2H), 7.58 (t, J = 7.4 Hz, 1H), 7.45 (t, J = 7.6 Hz, 2H), 7.34 (d, J = 8.4 Hz, 2H), 6.90 (d, J = 8.5 Hz, 2H), 4.50 (t, J = 7.0 Hz, 1H, CH), 3.79 (s, 3H, CH_3), 3.68 (dd, J = 17.9, 7.8 Hz, 1H, CH), 3.48 (dd, J = 17.9, 6.2 Hz, 1H, CH). **^{13}C-NMR** (101 MHz, $CDCl_3$): δ= 194.7, 159.4, 135.6, 133.7, 128.7, 128.6, 128.0, 127.1, 120.8, 114.5, 55.2, 44.4, 31.0.

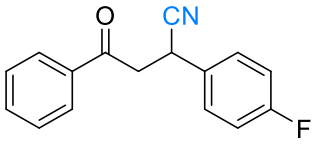

2-(4-fluorophenyl)-4-oxo-4-phenylbutanenitrile (68d): The product **68d** (0.106 g, 84% yield) was obtained as white solid. **^{1}H-NMR** (400 MHz, $CDCl_3$): δ= 7.95 – 7.88 (m, 2H), 7.60 (t, J = 7.5 Hz, 1H), 7.54 – 7.37 (m, 4H), 7.17 – 7.02 (m, 2H), 4.57

(t, J = 6.9 Hz, 1H, CH), 3.71 (dd, J = 17.9, 7.5 Hz, 1H, CH), 3.51 (dd, J = 17.9, 6.4 Hz, 1H, CH). **^{19}F-NMR** (376 MHz, $CDCl_3$): δ= -113.24. **^{13}C-NMR** (101 MHz, $CDCl_3$): δ= 194.4, 162.47 (d, $^{1}J_{C,F}$ = 248.0 Hz, CF), 135.6, 134.0, 131.03 (d, $^{4}J_{C,F}$ = 3.3 Hz), 129.30 (d, $^{3}J_{C,F}$ = 8.4 Hz), 128.8, 128.0, 120.5, 116.19 (d, $^{2}J_{C,F}$ = 22.0 Hz), 44.4, 31.2.

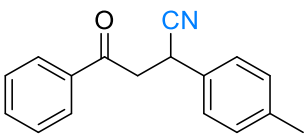

4-oxo-4-phenyl-2-(*p*-tolyl)butanenitrile (68e): The product **68e** (0.112 g, 90% yield) was obtained as white solid. **^{1}H-NMR** (400 MHz, $CDCl_3$): δ= 7.96 – 7.89 (m, 2H), 7.65 – 7.55 (m, 1H), 7.46 (dd, J = 8.4, 7.1 Hz, 2H), 7.38 – 7.29 (m, 2H), 7.20 (d, J = 7.9 Hz, 2H), 4.52 (dd, J = 8.0, 6.0 Hz, 1H, CH), 3.71 (dd, J = 18.0, 8.0 Hz, 1H, CH), 3.49 (dd, J = 18.0, 5.9 Hz, 1H, CH) 2.35 (s, 3H, CH_3). **^{13}C-NMR** (101 MHz, $CDCl_3$): δ= 194.8, 138.3, 135.7, 133.9, 132.3, 129.9, 128.9, 128.1, 127.4, 120.9, 44.6, 31.6, 21.1.

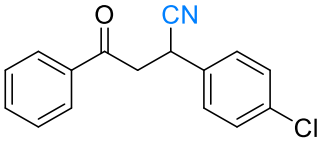

2-(4-chlorophenyl)-4-oxo-4-phenylbutanenitrile (68f): The product **68f** (0.129 g, 96% yield) was obtained as white solid. **^{1}H-NMR** (400 MHz, $CDCl_3$): δ= 7.95 – 7.87 (m, 2H), 7.65 – 7.54 (m, 1H), 7.46 (m, 2H), 7.41 – 7.31 (m, 4H), 4.55 (dd, J = 7.5, 6.3 Hz, 1H, CH), 3.71 (dd, J = 18.0, 7.5 Hz, 1H, CH), 3.51 (dd, J = 18.0, 6.4 Hz, 1H, CH). **^{13}C-NMR** (101 MHz, $CDCl_3$) : δ= 194.4, 135.5, 134.4, 134.1, 133.8, 129.4, 129.0, 128.9, 128.1, 120.4, 44.3, 31.3.

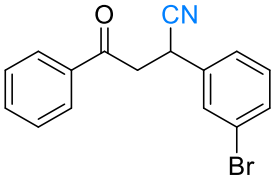

2-(3-bromophenyl)-4-oxo-4-phenylbutanenitrile (68g): The product **68g** (0.135 g, 86% yield) was obtained as white solid. **^{1}H-NMR** (400 MHz, $CDCl_3$): δ= 7.94 – 7.86 (m, 2H), 7.63 – 7.53 (m, 2H), 7.50 – 7.42 (m, 3H), 7.36 (m, 1H), 7.24 (t, J = 7.9 Hz, 1H), 4.52 (dd, J = 7.7, 6.0 Hz, 1H, CH), 3.71 (dd, J = 18.0, 7.8 Hz, 1H, CH), 3.49 (dd, J = 18.0, 6.1 Hz, 1H, CH). **^{13}C-NMR** (101 MHz, $CDCl_3$): δ= 194.2, 137.3, 135.4, 134.0, 131.6, 130.7, 130.6, 128.8, 128.0, 126.2, 123.1, 120.0, 44.2, 31.4.

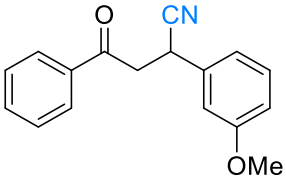

2-(3-methoxyphenyl)-4-oxo-4-phenylbutanenitrile (68h): The product **68h** (0.122 g, 92% yield) was obtained as white solid. **^{1}H-NMR** (400 MHz, $CDCl_3$): δ= 7.96 – 7.88 (m, 2H), 7.63 – 7.54 (m, 1H), 7.51 – 7.41 (m, 2H), 7.35 – 7.26 (m, 1H), 7.00 (m, 1H),

6.97 (m, 1H), 6.87 (m, 1H), 4.52 (dd, J = 8.2, 5.8 Hz, 1H, CH), 3.81 (s, 3H, CH_3), 3.72 (dd, J = 18.0, 8.2 Hz, 1H, CH), 3.50 (dd, J = 18.0, 5.7 Hz, 1H, CH). **^{13}C-NMR** (101 MHz, $CDCl_3$): δ= 194.7, 160.2, 136.7, 135.7, 133.9, 130.4, 128.9, 128.1, 120.6, 119.7, 113.8, 113.3, 55.4, 44.5, 31.9.

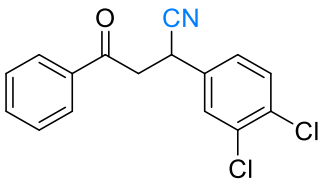

2-(3,4-dichlorophenyl)-4-oxo-4-phenylbutanenitrile (68i): The product **68i** (0.132 g, 87% yield) was obtained as white solid. **^{1}H-NMR** (400 MHz, $CDCl_3$): δ= 7.95 – 7.88 (m, 2H), 7.64 – 7.58 (m, 1H), 7.57 (d, J = 4.0 Hz, 1H), 7.52 – 7.41 (m, 3H), 7.30 (m, 1H), 4.55 (t, J = 6.9 Hz, 1H, CH), 3.72 (dd, J = 18.0, 7.2 Hz, 1H, CH), 3.52 (dd, J = 18.0, 6.5 Hz, 1H, CH). **^{13}C-NMR** (101 MHz, $CDCl_3$): δ= 194.1, 135.38, 135.35, 134.2, 133.4, 132.9, 131.2, 129.7, 128.9, 128.1, 127.0, 119.8, 44.1, 31.1.

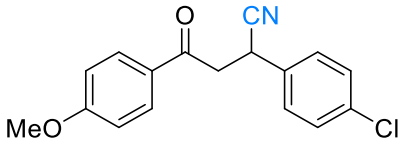

2-(4-chlorophenyl)-4-(4-methoxyphenyl)-4-oxobutanenitrile (68j): The product **68j** (0.135 g, 90% yield) was obtained as white solid. **^{1}H-NMR** (400 MHz, $CDCl_3$): δ= 7.93 – 7.83 (m, 2H), 7.41 – 7.29 (m, 4H), 6.98 – 6.85 (m, 2H), 4.54 (dd, J = 7.5, 6.4 Hz, 1H, CH), 3.85 (s, 3H, CH_3), 3.64 (dd, J = 17.7, 7.5 Hz, 1H, CH), 3.44 (dd, J = 17.8, 6.4 Hz, 1H, CH). **^{13}C-NMR** (101 MHz, $CDCl_3$): δ= 192.8, 164.2, 134.3, 134.0, 130.5, 129.4, 129.0, 128.6, 120.5, 114.0, 55.6, 43.9, 31.4.

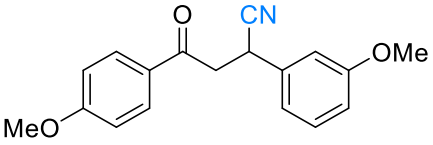

2-(3-methoxyphenyl)-4-(4-methoxyphenyl)-4-oxobutanenitrile (68k): The product **68k** (0.142 g, 96% yield) was obtained as white solid. **^{1}H-NMR** (400 MHz, $CDCl_3$): δ= 7.94 – 7.84 (m, 2H), 7.33 – 7.23 (m, 1H), 7.04 – 6.81 (m, 5H), 4.51 (dd, J = 8.3, 5.8 Hz, 1H, CH), 3.84 (s, 3H, CH_3), 3.79 (s, 3H, CH_3), 3.71 – 3.60 (m, 1H, CH), 3.43 (dd, J = 17.8, 5.8 Hz, 1H, CH). **^{13}C-NMR** (101 MHz, $CDCl_3$): δ) 193.1, 164.1, 160.1, 136.9, 130.5, 130.3, 128.8, 120.8, 119.6, 114.0, 113.7, 113.3, 55.6, 55.4, 44.1, 32.0.

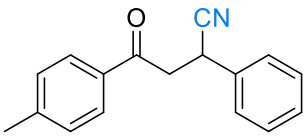

4-oxo-2-phenyl-4-(*p*-tolyl)butanenitrile (68l): The product **68l** (0.117 g, 94% yield) was obtained as white solid. **^{1}H-NMR** (400 MHz, $CDCl_3$): δ= 7.88 – 7.81 (m, 2H), 7.50 – 7.31 (m, 5H), 7.29 – 7.24 (m, 2H), 4.57 (dd, J = 8.2, 5.9 Hz, 1H, CH), 3.71 (dd, J = 17.9, 8.1 Hz, 1H, CH), 3.50 (dd, J = 17.9, 5.9 Hz, 1H, CH), 2.42 (s, 3H, CH_3). **^{13}C-NMR** (101 MHz, $CDCl_3$): δ= 194.3, 144.9, 135.4, 133.3, 129.5, 129.3, 128.4, 128.3, 127.5, 120.8, 44.4, 32.0, 21.7.

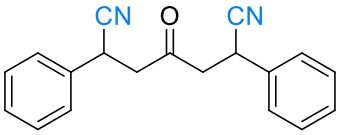

4-oxo-2,6-diphenylheptanedinitrile (68m): The product **68m** (0.136 g, 94% yield) was obtained as mixture of diastereoisomers both as white solids. Less polar diastereoisomer **68m'**: **^{1}H-NMR** (400 MHz, $CDCl_3$): δ= 7.42 – 7.29 (m, 10H), 4.36 (dd, *J* = 8.5, 5.8 Hz, 2H, CH), 3.09 (dd, *J* = 17.9, 8.5 Hz, 2H, CH), 2.97 (dd, *J* = 17.9, 5.8 Hz, 2H, CH). **^{13}C-NMR** (101 MHz, $CDCl_3$): δ= 200.9, 134.4, 129.4, 128.6, 127.3, 120.0, 48.0, 31.6. More polar diastereoisomer **68m''**: **^{1}H-NMR** (400 MHz, $CDCl_3$): δ= 7.43 – 7.26 (m, 10H), 4.34 (t, J = 7.0 Hz, 2H), 3.19 (dd, J = 17.8, 7.2 Hz, 2H), 2.89 (dd, J = 17.8, 6.8 Hz, 2H). **^{13}C-NMR** (101 MHz, $CDCl_3$): δ= 200.5, 134.5, 129.3, 128.6, 127.4, 119.9, 47.8, 31.5.

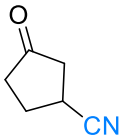

3-oxocyclopentane-1-carbonitrile (68n): The product **68n** (0.028 g, 51% yield) was obtained as yellow solid. **^{1}H-NMR** (400 MHz, $CDCl_3$): δ= 3.20 (m, 1H), 2.68 – 2.58 (m, 1H), 2.56 – 2.39 (m, 3H), 2.37 – 2.19 (m, 2H). **^{13}C-NMR** (101 MHz, $CDCl_3$): δ= 212.8, 120.9, 41.4, 36.7, 27.4, 25.6.

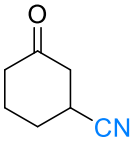

3-oxocyclohexane-1-carbonitrile (68o): The product **68o** (0.032 g, 52% yield) was obtained as yellow solid. **^{1}H-NMR** (400 MHz, $CDCl_3$): δ= 3.06 (m, 1H), 2.70 (m, 1H), 2.61 (m, 1H), 2.48 – 2.39 (m, 2H), 2.26 – 2.13 (m, 2H), 2.10 – 2.00 (m, 1H), 1.93 – 1.81 (m, 1H). **^{13}C-NMR** (101 MHz, $CDCl_3$): δ= 205.5, 120.2, 43.2, 40.7, 28.6, 28.1, 23.7.

Experimental procedures and characterization data of products 69

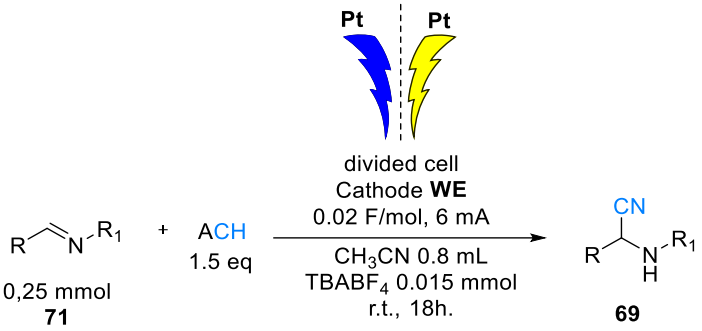

A solution of **71** (0.25 mmol), **ACH** (0.38 mmol), and tetrabutylammonium tetrafluoroborate (Bu_4NBF_4) (0.015 mmol) in MeCN (0.8 mL) is added in the cathodic compartment of a U-divided cell (glass frit 5G) equipped with platinum spirals (apparent area 1 cm^2) as cathode (WE, working electrode) and anode (CE, counter electrode). Anolyte was constituted by a solution of Bu_4NBF_4 (0.15 mmol) in MeCN (0.8 mL). Electrolysis was conducted under galvanostatic conditions (6 mA, 0.02 electrons/molecule of **71**) at r.t. At the end of the electrolysis the solution has been left stirring at r.t. for 18h. The mixture was then concentrated in vacuum and directly purified by silica gel chromatography (Hexane: Ethyl Acetate from 95:5 to 3:2) to afford the desired products **69a**–**69j**.

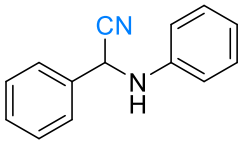

2-phenyl-2-(phenylamino)acetonitrile (69a): The product **69a** (0.049 g, 94% yield) was obtained as brown solid. **^{1}H-NMR** (400 MHz, $CDCl_3$): δ= 7.67 – 7.56 (m, 2H), 7.53 – 7.38 (m, 3H), 7.35 – 7.24 (m, 2H), 6.91 (m, 1H), 6.87 – 6.75 (m, 2H), 5.44 (d, J = 8.3 Hz, 1H, CH), 4.04 (d, J = 8.4 Hz, 1H, NH). **^{13}C-NMR** (101 MHz, $CDCl_3$): δ= 144.7, 133.9, 129.5, 129.5, 129.3, 127.2, 120.3, 118.2, 114.1, 50.2.

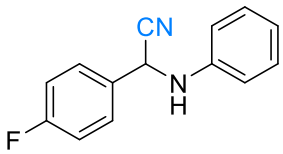

2-(4-fluorophenyl)-2-(phenylamino)acetonitrile (69b): The product **69b** (0.044 g, 78% yield) was obtained as white solid. **^{1}H-NMR** (400 MHz, $CDCl_3$): δ= 7.60 (t, J = 6.8 Hz, 2H), 7.28 (dd, J = 12.0, 5.4 Hz, 2H), 7.16 (m, 2H), 6.92 (t, J = 7.5 Hz, 1H), 6.78 (d, J = 7.9 Hz, 2H), 5.43 (d, J = 8.6 Hz, 1H, CH), 4.02 (d, J = 8.6 Hz, 1H, NH). **^{19}F-NMR** (376 MHz, $CDCl_3$): δ= -111.4. **^{13}C-NMR** (101 MHz, $CDCl_3$): δ= 163.23 (d, $^1J_{H,F}$= 249.4 Hz, CF), 144.4, 129.75

(d, $^{4}J_{H,F}$= 3.3 Hz) 129.6, 129.17 (d, $^{3}J_{H,F}$= 8.8 Hz), 120.5, 118.0, 116.37 (d, $^{2}J_{H,F}$= 22.0 Hz), 114.2, 49.6.

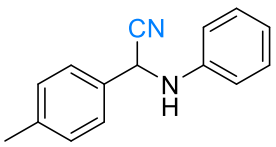

2-(phenylamino)-2-(*p*-tolyl)acetonitrile (69c): The product **69c** (0.038 g, 68% yield) was obtained as white solid. **^{1}H-NMR** (400 MHz, $CDCl_3$): δ= 7.61 (d, J = 6.9 Hz, 2H), 7.48-7.45 (m, 3H), 7.09 (d, J = 7.9 Hz, 2H), 6.71 (m, 2H), 5.41 (d, J = 8.2 Hz, 1H, CH), 3.91 (d, J = 8.7 Hz, 1H, NH), 2.29 (d, J = 2.6 Hz, 3H, CH_3). **^{13}C-NMR** (101 MHz, $CDCl_3$): δ= 142.3, 134.1, 130.0, 129.8, 129.5, 129.3, 127.2, 118.3, 114.4, 50.7, 20.5.

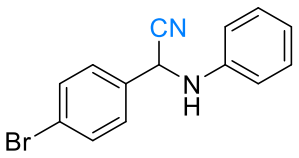

2-(4-bromophenyl)-2-(phenylamino)acetonitrile (69c): The product **69d** (0.045 g, 63% yield) was obtained as white solid. **^{1}H-NMR** (400 MHz, $CDCl_3$): δ= 7.69 – 7.58 (m, 2H), 7.54 – 7.47 (m, 2H), 7.37 – 7.24 (m, 2H), 6.95 (t, *J* = 7.4 Hz, 1H), 6.85 – 6.74 (m, 2H), 5.43 (d, *J* = 8.6 Hz, 1H, CH), 4.08 (d, *J* = 8.6 Hz, 1H, NH). **^{13}C-NMR** (101 MHz, $CDCl_3$): δ= 144.3, 132.9, 132.5, 129.6, 128.8, 123.7, 120.6, 117.7, 114.3, 49.7.

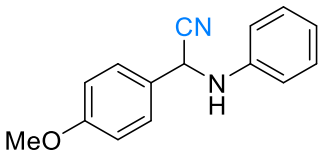

2-(4-methoxyphenyl)-2-(phenylamino)acetonitrile (69e): The product **69e** (0.052 g, 87% yield) was obtained as white solid. **^{1}H-NMR** (400 MHz, $CDCl_3$): δ= 7.58 – 7.49 (m, 2H), 7.36 – 7.26 (m, 2H), 7.02 – 6.97 (m, 2H), 6.93 (m, 1H), 6.80 (d, *J* = 7.6 Hz, 2H), 5.39 (d, *J* = 8.1 Hz, 1H), 4.05 (d, *J* = 8.3 Hz, 1H), 3.87 (s, 3H). **^{13}C-NMR** (101 MHz, $CDCl_3$): δ= 160.3, 144.7, 129.5, 128.6, 125.9, 120.1, 118.4, 114.6, 114.0, 55.4, 49.6.

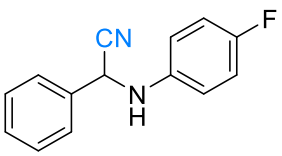

2-((4-fluorophenyl)amino)-2-phenylacetonitrile (69f): The product **69f** (0.044 g, 78% yield) was obtained as white solid. **^{1}H-NMR** (400 MHz, $CDCl_3$): δ= 7.60 (d, J = 6.7 Hz, 2H), 7.47 (d, J = 6.8 Hz, 3H), 7.04 – 6.93 (m, 2H), 6.74 (m, 2H), 5.37 (d, J = 8.6 Hz, 1H, CH), 3.94 (d, J = 8.6 Hz, 1H, NH). ^{19}F NMR (376 MHz, $CDCl_3$): δ= -123.97. **^{13}C-NMR** (101 MHz, $CDCl_3$): δ= 157.35 (d, $^{1}J_{H,F}$= 238.8 Hz, CF), 140.86 (d, $^{4}J_{H,F1}$= 1.9 Hz), 133.7, 129.6, 129.4, 127.2, 118.1, 116.16 (d, $^{2}J_{H,F}$= 22.7 Hz), 115.62 (d, $^{3}J_{H,F}$= 7.7 Hz), 51.0.

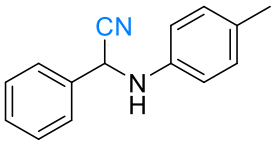

2-phenyl-2-(*p*-tolylamino)acetonitrile (69g): The product **69g** (0.051 g, 92% yield) was obtained as white solid. **^{1}H-NMR** (400 MHz, $CDCl_3$): δ= 7.54 – 7.47 (m, 2H), 7.32-7.28 (m, 4H), 6.92 (t, J = 7.6 Hz, 1H), 6.80 (d, J = 7.9 Hz, 2H), 5.41 (d, J = 8.3 Hz, 1H, CH), 4.02 (d, J = 8.3 Hz, 1H, NH), 2.42 (d, J = 2.7 Hz, 3H, CH_3). **^{13}C-NMR** (101 MHz, $CDCl_3$): δ= 144.7, 139.6, 131.0, 130.0, 129.5, 127.2, 120.2, 118.3, 114.1, 49.9, 21.2.

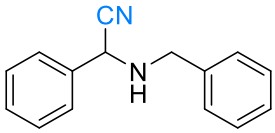

2-(benzylamino)-2-phenylacetonitrile (69h): The product **69h** (0.045 g, 81% yield) was obtained as brown solid. **^{1}H-NMR** (400 MHz, $CDCl_3$): δ= 7.59 – 7.51 (m, 2H), 7.46 – 7.28 (m, 8H), 4.76 (s, 1H, CH), 4.08 (d, J = 12.9 Hz, 1H, CH), 3.97 (d, J = 13.0 Hz, 1H, CH). **^{13}C-NMR** (101 MHz, $CDCl_3$): δ= 138.1, 134.8, 129.0, 128.9, 128.6, 128.4, 127.6, 127.3, 118.7, 53.4, 51.2.

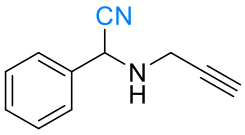

2-phenyl-2-(prop-2-yn-1-ylamino)acetonitrile (69i): The product **69i** (0.035 g, 82% yield) was obtained as brown solid. **^{1}H-NMR** (400 MHz, $CDCl_3$): δ= 7.58 – 7.48 (m, 2H), 7.47 – 7.35 (m, 3H), 4.99 (s, 1H, CH), 3.69 – 3.53 (m, 2H, CH_2), 2.34 (m, 1H, CH). **^{13}C-NMR** (101 MHz, $CDCl_3$): δ= 134.2, 129.4, 129.1, 127.6, 118.4, 79.8, 73.1, 52.8, 36.2.

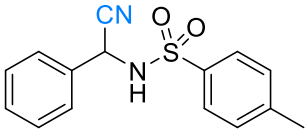

N-(cyano(phenyl)methyl)-4-methylbenzenesulfonamide (69j): The product **69j** (0.063 g, 88% yield) was obtained as pale-yellow solid. **^{1}H-NMR** (400 MHz, $CDCl_3$): δ= 7.84 – 7.77 (m, 2H), 7.49 – 7.32 (m, 7H), 5.47 (d, J = 9.0 Hz, 1H, CH), 5.23 (d, J = 9.0 Hz, 1H, NH), 2.46 (s, 3H, CH_3). **^{13}C-NMR** (101 MHz, $CDCl_3$): δ= 144.8, 136.1, 132.1, 130.1, 130.0, 129.4, 127.4, 127.1, 116.2, 48.3, 21.7.

2.8 Experimental section Part II

All reactions were carried out under aerobic conditions unless otherwise stated. All solvents and commercially available reagents were purchased from standard vendors and used without further purification unless otherwise stated. Electrolysis were performed using an IKA Electrasyn 2.0 using carbon graphite (C_{gr}) working electrode (**WE**) and platinum foil (**Pt**) counter electrode (**CE**) using a variable stirring rate between 400 - 1500 rpm. For the aromatic cyanation reactions the electrolysis were performed using an IKA Electrasyn 2.0 using platinum foil (**Pt**) working electrode (**WE**) and platinum foil (**Pt**) counter electrode (**CE**) using a variable stirring rate between 400 - 600 rpm. Analytical thin-layer chromatography (TLC) was performed using silica gel plates (0.25 mm thickness) on aluminum support. Visualization was accomplished by irradiation with a UV lamp and/or staining with either $KMnO_4$ or ninhydrin. Column chromatography was performed over Silica gel 60 Å (40-63µ mesh) using a Combi Flash Rf Lumen automatic flash chromatography system. Residual solvent was removed using a static oil pump (< 10 mbar). The cooling of reaction mixtures was achieved using an ice bath (0 °C).

NMR spectra were obtained using a JEOL ECZR 400 (^{1}H 399.78 MHz; ^{13}C 100.53 MHz) or ECA 500 (^{1}H 500.16 MHz; ^{13}C 125.77 MHz) spectrometer and are reported relative to the residual solvent resonances. All heteronuclear NMR spectra were ^{1}H decoupled and recorded at room temperature unless otherwise stated. Data for ^{1}H-NMR spectra are reported as follows: chemical shift (δ, ppm), coupling constant (Hz), multiplicity (s, singlet; d, doublet; t, triplet; m, multiplet; br, broad) and integration. Data for ^{13}C and ^{19}F NMR are reported in terms of chemical shift (δ, ppm). IR spectra were recorded on a Perkin Elmer Spectrum Two instrument as neat samples.

High Resolution Mass Spectrometry (HRMS) data were obtained by Dr. Iain Goodall and Bini Claringbold of the University of Greenwich Mass Spectrometry Service using a Waters Synapt G2 hybrid Quadrupole-orthogonal acceleration time-of-flight configuration (Waters, Manchester, UK) operating in Resolution Mode (M/ΔM ≥ 18,000), fitted with a Waters Acquity UPLC binary solvent chromatographic pump system. The column used was a reversed-phase Acquity BEH C18 2.1 x 50 mm, 1.7-micron bead, running a 3- minute

separation with an A:B eluent mixture comprising of either deionised water with 0.1% (v:v) formic acid and acetonitrile with 0.1% (v:v) formic acid (negative mode) respectively or deionised water with 0.1% (v:v) ammonium hydroxide and acetonitrile with 0.1% (v:v) ammonium hydroxide (positive mode) respectively. Mass calibration of the instrument was performed using sodium formate cluster ions, and an orthogonal Lock-SprayTM ESI probe was used with a lock mass calibrant, leucine-enkephalin. The pseudomolecular leucineenkephalin ion at *m/z* = 554.2615 (Negative Ion Mode), and *m/z* = 556.2771 (Positive Ion Mode), was used as the internal mass correction calibrant. Additional samples were analyzed on a Thermo LTQ Orbitrap XL coupled with a heated electrospray source (HESI). The capillary temperature was set to 275 °C and a voltage of 21 V. The sheath gas and auxiliary gas flow were set to 10 and 5 $L \cdot h^{-1}$ respectively and the source current and voltage set to 100 µA and 5 kV. A solution of analyte (0.1 mg/ml) and sodium formate (1% v/v) in acetonitrile was added by direct infusion (10 µL/min) into the mass spectrometer using a Hamilton syringe (250 µL). Flow chemistry experiments have been realized using an Asia® Electrochemistry Flow Chemistry System including Asia® Syringe Pump, FLUX Electrochemistry reactor with a carbon gasket electrode (WE) and a stainless-steel electrode (CE) (internal volume of the cell = 225 µL) and Pressure Controller. PTFE tubbings of 0.5 mm internal diameter have been used. Yields have been evaluated after reaching steady state.

Experimental procedures and characterization data of products 73 (Procedure A)

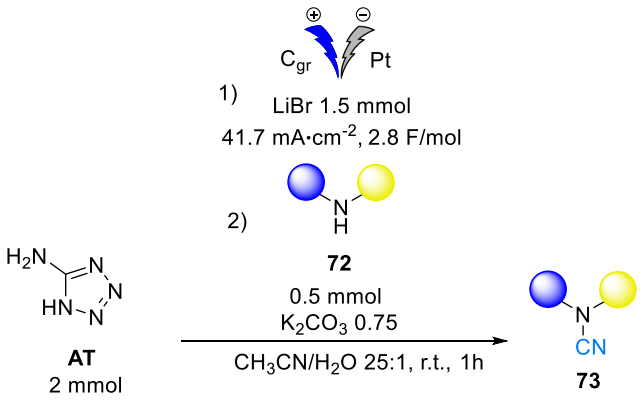

2 mmol of 5-aminotetrazole, 1.5 mmol of LiBr and 5 mL of CH_3CN/H_2O 25:1 are added to a 5 mL one compartment Electrasyn vial. The solution is then electrolyzed with a 41.7 $mA \cdot cm^{-2}$ current density for 2.8 F/mol using a carbon graphite anode (WE) and a platinum cathode (CE). At the end of the electrolysis, 0.5 mmol of amine and 1.5 mmol of K_2CO_3 are added and the solution is stirred for 1h at r.t. The reaction mixture is then quenched with a saturated aqueous solution of $NaHCO_3$, extracted with AcOEt and dried with Na_2SO_4. The solvent is removed under reduced pressure to afford the desired product without further purification.

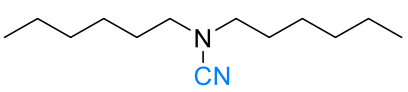

N,N-dihexylcyanamide (73a): Obtained following the general procedure A as colorless oil (90 mg, 0.43 mmol, 86 %). **^{1}H-NMR** (400 MHz,$CDCl_3$): δ= 3.00 – 2.92 (m, 4H), 1.69 – 1.57 (m, 4H), 1.32 (m, 12H), 0.96 – 0.84 (m, 6H). **^{13}C-NMR** (101 MHz, $CDCl_3$): δ= 118.1, 51.6, 31.5, 27.7, 26.2, 22.6, 14.1. **HRMS** (ESI) m/z: $[M+H]^+$ calcd for $C_{13}H_{27}N_2$ 211.2174, found 211.2175

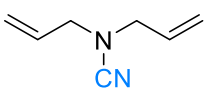

N,N-diallylcyanamide (73b): Obtained following the general procedure A as colorless oil (60 mg, 0.49 mmol, 98 %). **^{1}H-NMR** (500 MHz, $CDCl_3$): δ= 5.90 – 5.78 (m, 2H), 5.39 – 5.28 (m, 4H), 3.62 (m, 4H). **^{13}C-NMR** (126 MHz, $CDCl_3$): δ= 131.1, 120.7, 117.7, 53.5. **HRMS** (ESI) m/z: $[M+H]^+$ calcd for $C_7H_{11}N_2$ 123.0922, found 123.0931

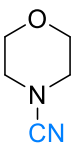

Morpholine-4-carbonitrile (73c): Obtained following the general procedure A as colorless oil (53 mg, 0.47 mmol, 95 %). **^{1}H-NMR** (400 MHz,$CDCl_3$): δ= 3.77 – 3.70 (m, 4H), 3.27 – 3.20 (m, 4H). **^{13}C-NMR** (101 MHz,$CDCl_3$): δ= 117.4, 65.8, 49.0. **HRMS** (ESI) m/z: $[M+H]^+$ calcd for $C_5H_9N_2O$ 113.0715, found 113.0714

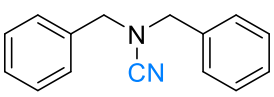

N,N-dibenzylcyanamide (73d): Obtained following the general procedure A as colorless oil (106 mg, 0.48 mmol, 95 %). **^{1}H-NMR** (500 MHz, $CDCl_3$): δ= 7.39 – 7.32 (m, 6H), 7.30 – 7.27 (m, 4H), 4.09 (s, 4H). **^{13}C-NMR** (126 MHz, $CDCl_3$): δ= 134.5, 129.1, 128.8, 128.8, 118.5, 54.4. **HRMS** (ESI) m/z: $[M+H]^+$ calcd for $C_{15}H_{15}N_2$ 223.1235, found 223.1248

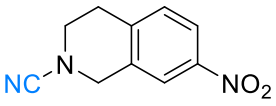

7-nitro-3,4-dihydroisoquinoline-2(1H)-carbonitrile (73e): Obtained following the general procedure A as colorless oil (99 mg, 0.49 mmol, 97 %). **^{1}H-NMR** (500 MHz,$CDCl_3$): δ= 8.07 (m, 1H), 7.96 (d, J = 2.3 Hz, 1H), 7.33 (d, J = 8.4 Hz, 1H), 4.51 (s, 2H), 3.54 (t, J = 5.8 Hz, 2H), 3.08 (t, J = 5.9 Hz, 2H). **^{13}C-NMR** (126 MHz,$CDCl_3$): δ= 146.8, 140.3, 132.4, 130.6, 122.4, 121.5, 117.2, 50.0, 46.4, 28.0. **HRMS** (ESI) m/z: $[M+H]^+$ calcd for $C_{10}H_{10}N_3O_2$ 204.0773, found 204.0779

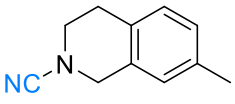

7-methyl-3,4-dihydroisoquinoline-2(1H)-carbonitrile (73f): Obtained following the general procedure A as colorless oil (74 mg, 0.43 mmol, 86 %). **^{1}H-NMR** (500 MHz,$CDCl_3$): δ= 7.02 (m, 2H), 6.85 (s, 1H), 4.37 (s, 2H), 3.47 (t, J = 5.9 Hz, 2H), 2.91 (t, J = 5.9 Hz, 2H), 2.31 (s, 3H). **^{13}C-NMR** (126 MHz, $CDCl_3$): δ= 136.5, 130.6, 129.6, 129.1, 128.1, 126.5, 118.2, 50.1, 47.0, 27.4, 21.1. **HRMS** (ESI) m/z: $[M+H]^+$ calcd for $C_{11}H_{13}N_2$ 173.1079, found 173.1085

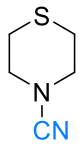

Thiomorpholine-4-carbonitrile (73g): Obtained following the general procedure A as colorless oil (63 mg, 0.49 mmol, 98 %). **^{1}H-NMR** (500 MHz, DMSO-d_6): δ= 3.47 – 3.36 (m, 4H), 2.70 – 2.61 (m, 4H). **^{13}C-NMR** (126 MHz, DMSO-d_6): δ= 117.5, 50.3, 25.4. **HRMS** (ESI) m/z: $[M+H]^+$ calcd for $C_5H_9N_2S$ 129.0486, found 129.0496

Experimental procedures and characterization data of products 75 (Procedure B)

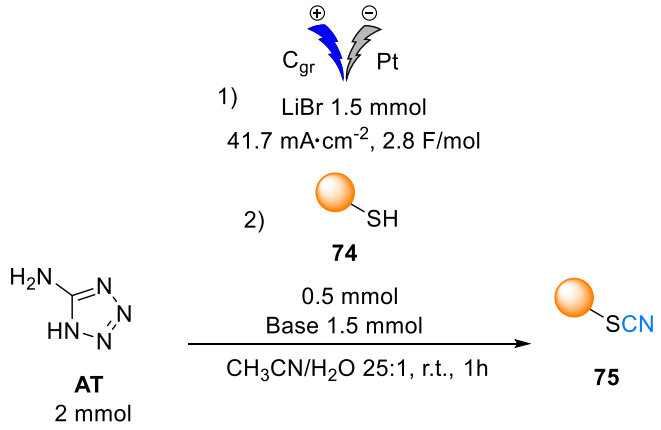

2 mmol of 5-aminotetrazole, 1.5 mmol of LiBr and 5 mL of CH_3CN/H_2O 25:1 are added to a 5 mL one compartment Electrasyn vial. The solution is then electrolyzed with a 41.7 $mA \cdot cm^{-2}$ current density for 2.8 F/mol using a carbon graphite anode (WE) and a platinum cathode (CE). At the end of the electrolysis, 0.5 mmol of thiol and 1.5 mmol of Base (Et_3N or DBU) are added dropwise at 0 °C and the solution is stirred at r.t. for 1h. The reaction mixture is then quenched with a saturated aqueous solution of $NaHCO_3$, extracted with AcOEt and dried with Na_2SO_4. The solvent is removed under reduced pressure to afford the desired product without further purification.

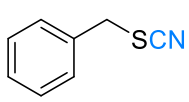

(thiocyanatomethyl)benzene (75a): Obtained following the general procedure B as colorless oil using Et_3N as base (62 mg, 0.42 mmol, 83 %). **^{1}H-NMR** (500 MHz, $CDCl_3$): δ= 7.45 – 7.31 (m, 5H), 4.17 (s, 2H). **^{13}C-NMR** (126 MHz, $CDCl_3$): δ= 134.5, 129.3, 129.1, 129.1, 112.1, 38.5.

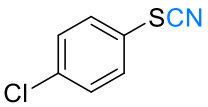

1-chloro-4-thiocyanatobenzene (75b): Obtained following the general procedure B as colorless oil using DBU as base (64 mg, 0.38 mmol, 75 %). **^{1}H-NMR** (400 MHz, $CDCl_3$): δ= 7.52 – 7.42 (m, 2H), 7.46 – 7.36 (m, 2H). **^{13}C-NMR** (101 MHz, $CDCl_3$): δ= 136.3, 131.6, 130.6, 122.8, 110.12. **HRMS** (ESI) m/z: $[M+H]^+$ calcd for C_7H_5NSCl 169.9831, found 169.9818

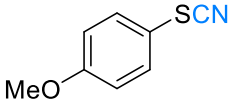

1-methoxy-4-thiocyanatobenzene (75c): Obtained following the general procedure B as colorless oil using DBU as base (33 mg, 0.2 mmol, 40 %). **^{1}H-NMR** (400 MHz, $CDCl_3$): δ= 7.54 – 7.44 (m, 2H), 6.99 – 6.88 (m, 2H), 3.82 (s, 3H). **^{13}C-NMR** (101 MHz, $CDCl_3$): δ= 161.4, 134.0, 116.0, 114.0, 111.7, 55.6. **HRMS** (ESI) m/z: $[M+H]^+$ calcd for C_8H_8NOS 166.0327, found 166.0326

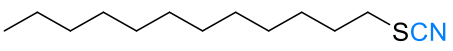

1-thiocyanatododecane (75d): Obtained following the general procedure B as colorless oil using Et_3N as base (64 mg, 0.28 mmol, 56 %). **^{1}H-NMR** (400 MHz, $CDCl_3$): δ= 2.96 – 2.89 (m, 2H), 1.80 (m, 2H), 1.41 (m, 2H), 1.35 – 1.19 (m, 16H), 0.86 (t, *J* = 6.8 Hz, 3H). **^{13}C-NMR** (101 MHz, $CDCl_3$): δ= 112.6, 34.2, 32.0, 30.0, 29.7, 29.6, 29.5, 29.4, 29.0, 28.1, 22.8, 14.2.

Experimental procedures and characterization data of products 77 (Procedure C)

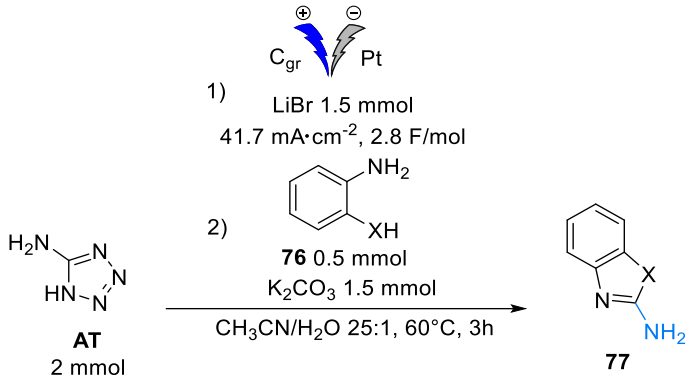

2 mmol of 5-aminotetrazole, 1.5 mmol of LiBr and 5 mL of CH_3CN/H_2O are added to a 5 mL one compartment Electrasyn vial. The solution is then electrolyzed with a 41.7 $mA.cm^{-2}$ current density for 2.8 F/mol using a carbon graphite anode (WE) and a platinum cathode (CE). At the end of the electrolysis, 0.5 mmol of amine and 1.5 mmol of K_2CO_3 are added and the solution is stirred for 3h at 60 °C. The reaction mixture is then quenched with a saturated aqueous solution of $NaHCO_3$, extracted with AcOEt, dried with Na_2SO_4 and the solvent is removed under reduced pressure. The crude mixture is purified via flash column chromatography using Hexane/AcOEt (from 9:1 to 0:10) as eluent to afford the desired product.

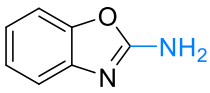

Benzo[d]oxazol-2-amine (77a): Obtained following the general procedure C as yellow oil (107 mg, 0.80 mmol, 80 %). **^{1}H-NMR** (500 MHz, $CDCl_3$): δ= 7.33 (m, 1H), 7.30 – 7.22 (m, 1H), 7.17 (m, 1H), 7.06 (m, 1H), 6.06 (s, 2H). **^{13}C-NMR** (126 MHz,$CDCl_3$): δ= 162.3, 148.7, 142.7, 124.1, 121.3, 116.4, 109.1. **HRMS** (ESI) m/z: $[M+H]^+$ calcd for $C_7H_7N_2O$ 135.0558, found 135.0558

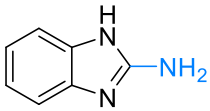

1H-benzo[d]imidazol-2-amine (77b): Obtained following the general procedure C as brown solid (76 mg, 0.57 mmol, 57 %). **^{1}H-NMR** (500 MHz, DMSO-d_6): δ= 7.15 – 7.10 (m, 2H), 6.92 – 6.87 (m, 2H), 6.44 (s,

2H). **^{13}C-NMR** (126 MHz, DMSO-d_6): δ= 155.1, 138.0, 120.1, 112.0. **HRMS** (ESI) m/z: $[M+H]^+$ calcd for $C_7H_8N_3$ 134.0718, found 134.0720

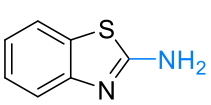

Benzo[d]thiazol-2-amine (77c): Obtained following the general procedure C as yellow oil (117 mg, 0.78 mmol, 78 %). **^{1}H-NMR** (500 MHz, DMSO-d_6): δ= 7.60 (d, J = 7.6 Hz, 1H), 7.47 (s, 2H), 7.30 (d, J = 7.9 Hz, 1H), 7.16 (t, J = 7.5 Hz, 1H), 6.96 (t, J = 7.4 Hz, 1H). **^{13}C-NMR** (126 MHz, $CDCl_3$): δ= 166.3, 152.1, 131.6, 126.1, 122.4, 121.0, 119.2. **HRMS** (ESI) m/z: $[M+H]^+$ calcd for $C_7H_7N_2S$ 151.0330, found 151.0331

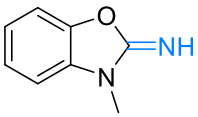

3-methylbenzo[d]oxazol-2(3H)-imine (77d): Obtained following the general procedure C as colorless oil (104 mg, 0.70 mmol, 70 %). **^{1}H-NMR** (500 MHz, DMSO-d_6): δ= 7.14 – 7.02 (m, 2H), 6.98 (m, 1H), 6.92 (m, 1H), 3.24 (s, 3H). **^{13}C-NMR** (126 MHz, DMSO-d_6): δ= 155.7,/ 143.8, 133.7, 123.3, 120.4, 108.1, 107.1, 28.3. **HRMS** (ESI) m/z: $[M+H]^+$ calcd for $C_8H_9N_2O$ 149.0715, found 149.0715

Experimental procedures and characterization data of products 79 (Procedure D)

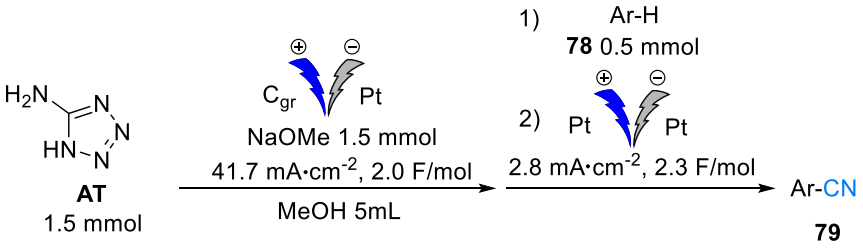

1.5 mmol of 5-aminotetrazole, 1.5 mmol of NaOMe and 5 mL of MeOH are added to a 5 mL one compartment Electrasyn vial. The solution is then electrolyzed with a 41.7 mA·cm^{-2} current density for 2.0 F/mol using a carbon graphite anode (WE) and a platinum cathode (CE). At the end of the electrolysis, 0.5 mmol of aromatic compound are added and the solution is electrolyzed with 2.8 mA·cm^{-2} current density for 2.3 F/mol using a platinum anode (WE) and a platinum cathode (CE). The reaction mixture is then quenched with a

saturated aqueous solution of $NaHCO_3$, extracted with Et_2O, dried with Na_2SO_4 and the solvent is removed under reduced pressure. The crude mixture is purified via flash column chromatography using Hexane/AcOEt (from 9:1 to 4:6) as eluent to afford the desired product.

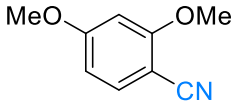

2,4-dimethoxybenzonitrile (79a): Obtained following the general procedure D as white solid (68 mg, 0.42 mmol, 83 %). **^{1}H-NMR** (500 MHz,$CDCl_3$): δ= 7.25 (d, J = 8.6 Hz, 1H), 6.30 (dd, J = 8.6, 2.3 Hz, 1H), 6.24 (d, J = 2.3 Hz, 1H), 3.68 (s, 3H), 3.64 (s, 3H). **^{13}C-NMR** (126 MHz, $CDCl_3$): δ= 164.8, 163.0, 135.0, 117.1, 105.9, 98.6, 94.1, 56.1, 55.8. **HRMS** (ESI) m/z: $[M+H]^+$ calcd for $C_9H_{10}NO_2$ 164.0712, found 164.0711

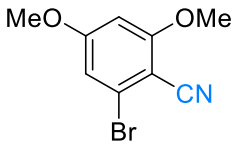

2-bromo-4,6-dimethoxybenzonitrile (79b): Obtained following the general procedure D as white solid (56 mg, 0.23 mmol, 46 %). **^{1}H-NMR** (500 MHz, $CDCl_3$): δ= 6.75 (d, J = 2.1 Hz, 1H), 6.40 (d, J = 2.2 Hz, 1H), 3.89 (s, 3H), 3.85 (s, 3H). **^{13}C-NMR** (126 MHz, $CDCl_3$): δ= 164.4, 164.0, 127.5, 115.4, 110.3, 98.3, 97.7, 56.5, 56.2. **HRMS** (ESI) m/z: $[M+H]^+$ calcd for $C_9H_9NO_2Br$ 241.9817, found 241.9837

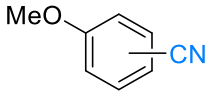

2-methoxybenzonitrile/ 4-methoxybenzonitrile (79c): Obtained following the general procedure D as mixture of isomers (*o*:*p* 1:1.2) and as colorless oil (29 mg, 0.22 mmol, 44 %). **^{1}H-NMR** (400 MHz, $CDCl_3$): δ= 7.63 – 7.53 (m, 4H, major + minor), 7.06 – 6.95 (m, 4H, major + minor), 3.95 (s, 3H, minor), 3.88 (s, 3H, major). **^{13}C-NMR** (101 MHz, $CDCl_3$): δ= 163.0, 161.4, 134.5, 134.1, 133.9, 120.9, 119.4, 116.6, 114.9, 111.4, 104.1, 101.9, 56.1, 55.7. **HRMS** (ESI) m/z: $[M+H]^+$ calcd for C_8H_8NO 134.0606, found 134.0619

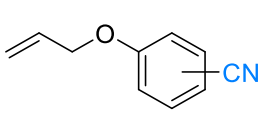

2-(allyloxy)benzonitrile/ 4-(allyloxy)benzonitrile (79d): Obtained following the general procedure D as mixture of isomers (*o*:*p* 1:1.5) and as colorless oil (38 mg, 0.24 mmol, 48 %). **^{1}H-NMR** (500 MHz,$CDCl_3$): δ= 7.65 – 7.48 (m, 4H, major + minor), 7.04 – 6.96 (m, 4H, major + minor), 6.06 (m, 2H, major + minor), 5.47 (m, 1H, minor), 5.35 (m, 1H, major), 4.68 (dt, J = 5.0, 1.6 Hz, 1H, minor), 4.61 (dt, J = 5.3, 1.5 Hz, 1H, major). **^{13}C-NMR** (126 MHz,$CDCl_3$): δ= 162.0, 160.4, 134.3,

134.1, 134.0, 132.2, 132.0, 121.0, 119.3, 118.6, 118.4, 116.6, 115.6, 114.9, 112.8, 104.2, 102.4, 69.6, 69.1. **HRMS** (ESI) m/z: $[M+H]^+$ calcd for $C_{10}H_{10}NO$ 160.0762, found 160.0777

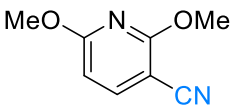

2,6-dimethoxynicotinonitrile (79e): Obtained following the general procedure D as white solid (66 mg, 0.40 mmol, 80 %). **^{1}H-NMR** (400 MHz, $CDCl_3$): δ= 7.67 (d, J = 8.3 Hz, 1H), 6.33 (d, J = 8.3 Hz, 1H), 4.01 (s, 3H), 3.95 (s, 3H). **^{13}C-NMR** (101 MHz, $CDCl_3$): δ= 165.8, 164.9, 144.3, 116.3, 102.9, 86.8, 54.4, 54.2. **HRMS** (ESI) m/z: $[M+H]^+$ calcd for $C_8H_9N_2O_2$ 165.0664, found 165.0680

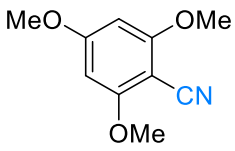

2,4,6-trimethoxybenzonitrile (79f): Obtained following the general procedure D with 25 mA as white solid (30 mg, 0.16 mmol, 31 %). **^{1}H-NMR** (400 MHz, $CDCl_3$): δ= 6.05 (s, 2H), 3.86 (s, 6H), 3.83 (s, 3H). **^{13}C-NMR** (101 MHz, $CDCl_3$): δ= 165.5, 163.9, 114.7, 90.5, 84.2, 56.2, 55.8. **HRMS** (ESI) m/z: $[M+H]^+$ calcd for $C_{10}H_{12}NO_3$ 194.0817, found 194.0824

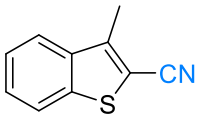

3-methylbenzo[b]thiophene-2-carbonitrile (79g): Obtained following the general procedure D as colorless oil (45 mg, 0.26 mmol, 52 %). **^{1}H-NMR** (500 MHz, $CDCl_3$): δ= 7.87 – 7.76 (m, 2H), 7.51 (m, 2H), 2.64 (s, 3H). **^{13}C-NMR** (126 MHz, $CDCl_3$): δ= 145.3, 141.0, 137.7, 128.0, 125.5, 123.7, 122.8, 114.7, 105.8, 13.9. **HRMS** (ESI) m/z: $[M+H]^+$ calcd for $C_{10}H_8NS$ 174.0377, found 174.0387

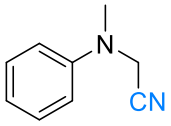

2-(methyl(phenyl)amino)acetonitrile (79h): Obtained following the general procedure D as colorless oil (26 mg, 0.18 mmol, 36 %). **^{1}H-NMR** (500 MHz, $CDCl_3$): δ= 7.36 – 7.26 (m, 2H), 6.98 – 6.88 (m, 1H), 6.90 – 6.84 (m, 2H), 4.17 (s, 2H), 3.01 (s, 3H). **^{13}C-NMR** (126 MHz, $CDCl_3$): δ= 147.9, 129.6, 120.3, 115.6, 115.0, 42.4, 39.4.

Experimental procedures and characterization data of products 81 (Procedure E)

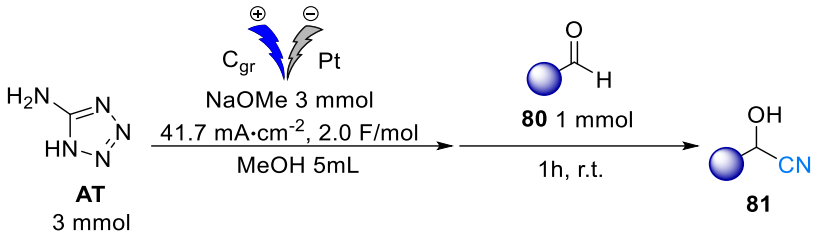

3 mmol of 5-aminotetrazole, 3 mmol of NaOMe and 5 mL of MeOH are added to a 5 mL one compartment Electrasyn vial. The solution is then electrolyzed with a 41.7 mA·cm^{-2} current density for 2.0 F/mol using a carbon graphite anode (WE) and a platinum cathode (CE). At the end of the electrolysis, 1 mmol of aldehyde are added and the solution is stirred at r.t, for 1h. The reaction mixture is then quenched with a saturated aqueous solution of $NaHCO_3$, extracted with AcOEt, dried with Na_2SO_4 and the solvent is removed under reduced pressure. The crude mixture is purified via flash column chromatography using Hexane/AcOEt as eluent to afford the desired product.

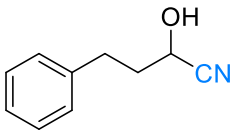

2-hydroxy-4-phenylbutanenitrile (81a): Obtained following the general procedure E as colorless oil (135 mg, 0.84 mmol, 84 %). **^{1}H-NMR** (400 MHz, $CDCl_3$): δ= 7.33 – 7.23 (m, 2H), 7.25 – 7.13 (m, 3H), 4.37 (m, 1H), 3.25 (d, J = 6.0 Hz, 1H), 2.80 (m, 2H), 2.20 – 2.08 (m, 2H). **^{13}C-NMR** (101 MHz, $CDCl_3$): δ= 139.7, 128.9, 128.6, 126.7, 120.1, 60.5, 36.6, 30.8. **HRMS** (ESI) m/z: $[M+H]^+$ calcd for $C_{10}H_{12}NO$ 162.0919, found 162.0929

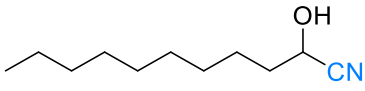

2-hydroxyundecanenitrile (81b): Obtained following the general procedure E as colorless oil (130 mg, 0.71 mmol, 71 %). **^{1}H-NMR** (500 MHz, $CDCl_3$): δ= 4.44 (t, J = 6.8 Hz, 1H), 3.06 (s, 1H), 1.89 – 1.77 (m, 2H), 1.53 – 1.41 (m, 2H), 1.39 – 1.18 (m, 12H), 0.91 – 0.81 (m, 3H). **^{13}C-NMR** (126 MHz, $CDCl_3$): δ= 120.3, 61.4, 35.2, 32.0, 29.5, 29.5, 29.3, 29.0, 24.7, 22.8, 14.2. **HRMS** (ESI) m/z: $[M+H]^+$ calcd for $C_{11}H_{22}NO$ calcd 184.1701, found 184.1720

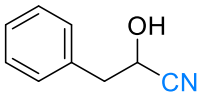

2-hydroxy-3-phenylpropanenitrile (81c): Obtained following the general procedure E as colorless oil (100 mg, 0.68 mmol, 68 %). **^{1}H-NMR** (500 MHz, $CDCl_3$): δ= 7.41 – 7.21 (m, 5H), 4.59 (t, J = 6.6 Hz, 1H), 3.09 (d, J = 6.7 Hz, 2H). **^{13}C-NMR** (126 MHz, $CDCl_3$): δ= 134.1, 129.8, 129.0, 127.8, 119.6, 62.2, 41.3. **HRMS** (ESI) m/z: $[M+H]^+$ calcd for $C_9H_{10}NO$ 148.0762, found 148.0763

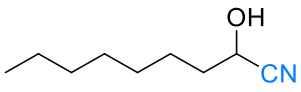

2-hydroxynonanenitrile (81d): Obtained following the general procedure E as colorless oil (115 mg, 0.74 mmol, 74 %). **^{1}H-NMR** (400 MHz, $CDCl_3$): δ= 4.44 (t, J = 6.8 Hz, 1H), 3.46 (s, 1H), 1.87 – 1.72 (m, 2H), 1.57 – 1.38 (m, 2H), 1.38 – 1.15 (m, 8H), 0.92 – 0.77 (m, 3H). **^{13}C-NMR** (101 MHz, $CDCl_3$): δ= 120.3, 61.3, 35.2, 31.8, 29.1, 29.0, 24.7, 22.7, 14.1. **HRMS** (ESI) m/z: $[M+NH_4]^+$ calcd for $C_9H_{21}N_2O$ 173.1654, found 173.1670

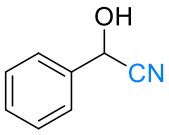

2-hydroxy-2-phenylacetonitrile (81e): Obtained following the general procedure E as colorless oil (90 mg, 0.68 mmol, 68 %). **^{1}H-NMR** (400 MHz, $CDCl_3$): δ= 7.51 – 7.45 (m, 2H), 7.41 (m, 3H), 5.47 (s, 1H), 4.00 (s, 1H). **^{13}C-NMR** (101 MHz, $CDCl_3$): δ= 135.3, 129.9, 129.3, 126.8, 119.1, 63.5. **HRMS** (ESI) m/z: $[M+H]^+$ calcd for C_8H_8NO 134.0606, found 134.0620

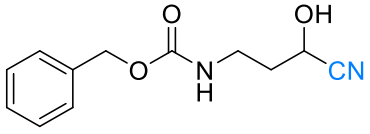

benzyl (3-cyano-3-hydroxypropyl)carbamate (81f): Obtained following the general procedure E as colorless oil (170 mg, 0.73 mmol, 73 %). **^{1}H-NMR** (500 MHz, $CDCl_3$): δ= 7.33 (m, 5H), 5.38 (t, J = 6.3 Hz, 1H), 5.09 (s, 2H), 4.81 (s, 1H), 4.50 (m, 1H), 3.46 – 3.28 (m, 2H), 1.97 (m, 2H). **^{13}C-NMR** (126 MHz, $CDCl_3$): δ= 157.7, 136.1, 128.7, 128.4, 128.2, 120.0, 67.4, 58.6, 36.5, 35.3. **HRMS** (ESI) m/z: $[M+H]^+$ calcd for $C_{12}H_{15}N_2O_3$ 235.1083, found 235.1097

83-85-68a-69a (Procedure F)

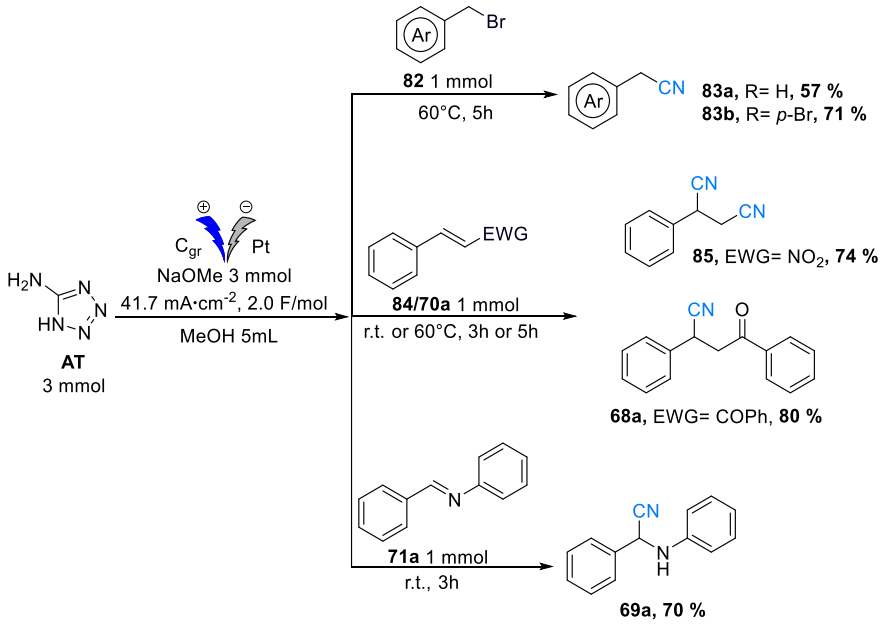

3 mmol of 5-aminotetrazole, 3 mmol of NaOMe and 5 mL of MeOH are added to a 5 mL one compartment Electrasyn vial. The solution is then electrolyzed with a 41.7 $mA \cdot cm^{-2}$ current density for 2.0 F/mol using a carbon graphite anode (WE) and a platinum cathode (CE). At the end of the electrolysis, 1 mmol of electrophile are added and the solution is stirred at r.t. or 60 °C for 3h-5h. The reaction mixture is then quenched with a saturated aqueous solution of $NaHCO_3$, extracted with AcOEt, dried with Na_2SO_4 and the solvent is removed under reduced pressure. The crude mixture is purified via flash column chromatography using Hexane/AcOEt as eluent to afford the desired product.

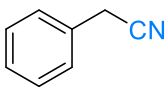

2-phenylacetonitrile (83a): Obtained following the general procedure F (60 °C, 5h) as colorless oil (66 mg, 0.56 mmol, 56 %). **^{1}H-NMR** (500 MHz, $CDCl_3$): δ= 7.44 – 7.27 (m, 5H), 3.74 (s, 2H). **^{13}C-NMR** (126 MHz, $CDCl_3$): δ= 130.0, 129.2, 128.1, 128.0, 118.0, 23.7. **HRMS** (ESI) m/z: $[M+H]^+$ calcd for C_8H_8N calcd 118.0657, found 118.0667

2-(4-bromophenyl)acetonitrile (83b): Obtained following the general procedure F (60 °C, 5h) as colorless oil (130 mg, 0.71 mmol, 71 %). **^{1}H-NMR** (500 MHz, $CDCl_3$): δ= 7.52 – 7.41 (m, 2H), 7.23 – 7.12 (m, 2H), 3.69 (s, 2H). **^{13}C-NMR** (126 MHz, $CDCl_3$): δ= 132.3, 129.7, 129.0, 122.2, 117.4, 23.2. **HRMS** (ESI) m/z: $[M+H]^+$ calcd for C_8H_7NBr calcd 195.9762, found 195.9774.

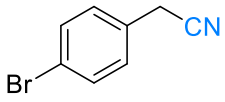

2-phenylsuccinonitrile (85): Obtained following the general procedure F (r.t, 3h) as yellow solid (115 mg, 0.74 mmol, 74 %). **^{1}H-NMR** (500 MHz, $CDCl_3$): δ= 7.32 – 7.23 (m, 5H), 4.02 (t, *J* = 6.8 Hz, 1H), 2.87 – 2.74 (m, 2H). **^{13}C-NMR** (126 MHz, $CDCl_3$): δ= 132.3, 129.7, 129.6, 127.3, 118.0, 115.5, 34.0, 24.7. **HRMS** (ESI) m/z: $[M-H]^-$ calcd for $C_{10}H_7N_2$ 155.0609, found 155.0618.

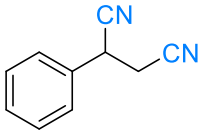

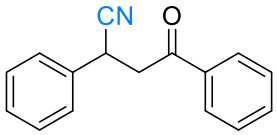

4-oxo-2,4-diphenylbutanenitrile (68a): Obtained following the general procedure F (60 °C, 5h) as yellow solid (188 mg, 0.80 mmol, 80 %). **^{1}H-NMR** (400 MHz, $CDCl_3$): δ= 7.95 – 7.89 (m, 2H), 7.62 – 7.55 (m, 1H), 7.48 – 7.30 (m, 7H), 4.55 (dd, J = 8.0, 5.9 Hz, 1H), 3.72 (dd, J = 18.0, 8.0 Hz, 1H), 3.50 (dd, J = 18.0, 5.9 Hz, 1H). **^{13}C-NMR** (101 MHz, $CDCl_3$): δ= 194.8, 135.7, 135.4, 134.1, 129.4, 129.0, 128.5, 128.2, 127.6, 120.8, 44.6, 32.0. **HRMS** (ESI) m/z: $[M+H]^+$ calcd for $C_{16}H_{14}NO$ 236.1075, found 236.1091.

2-phenyl-2-(phenylamino)acetonitrile (69a): Obtained following the general procedure F (r.t., 3h) as white solid (146 mg, 0.70 mmol, 70 %). **^{1}H-NMR** (500 MHz, $CDCl_3$): δ= 7.62 – 7.51 (m, 2H), 7.49 – 7.37 (m, 3H), 7.31 – 7.18 (m, 2H), 6.89 (m, 1H), 6.80 – 6.69 (m, 2H), 5.40 (s, 1H), 4.06 (s, 1H). **^{13}C-NMR** (126 MHz, $CDCl_3$): δ= 144.8, 134.0, 129.6, 129.6, 129.4, 127.3, 120.3, 118.3, 114.3, 50.3. **HRMS** (ESI) m/z: $[M+H]^+$ calcd for $C_{14}H_{13}N_2$ 209.1079, found 209.1097.

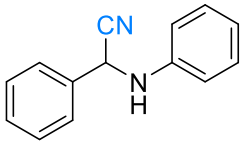

Flow experiment

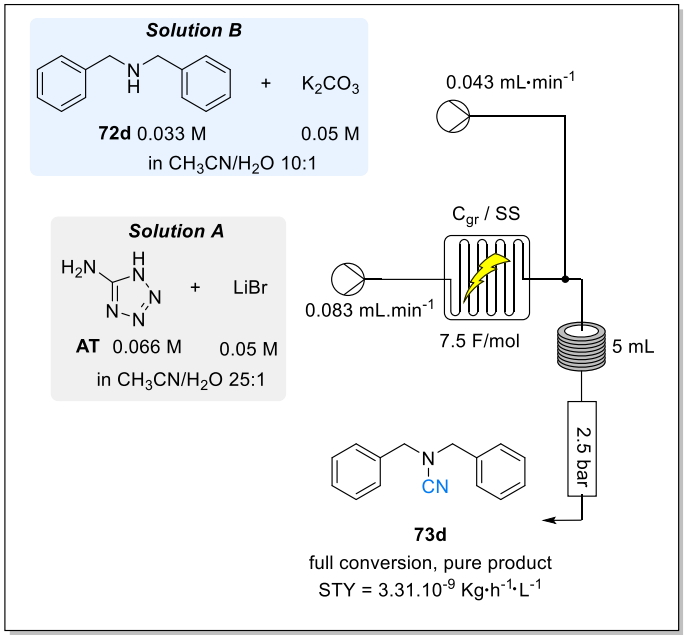

A solution LiBr (3 equiv., 0.05 M) and 5-aminotetrazole (4 equiv., 0.06 M) in a 25:1 mixture of CH_3CN/H_2O was pumped at 0.083 mL·min^{-1} through an Asia® FLUX reactor (225 µL, 50 mA) followed by a T-shaped mixer. A solution of substrate **72d** (1 equiv., 0.033 M) and K_2CO_3 (1.5 equiv., 0.05 M) in 10:1 mixture of CH_3CN/H_2O was pumped through the T-shaped mixer (180° from the first solution inlet). To the outlet of the mixer is plugged a 5 mL reactor followed by an Asia® Pressure Controller set at 2.5 bar. After the steady state was reached, the reaction mixture was collected for 1h 47 and then quenched with a saturated aqueous solution of $NaHCO_3$, extracted with AcOEt and dried with Na_2SO_4. The solvent is removed under reduced pressure to afford the desired product **73d** without further purification (0.15 mmol, 33 mg, 99 %).

2.9 Reference Chapter II

89) A. Rakshit, H. N. Dhara, A. K. Sahoo, B. K. Patel. The Renaissance of Organo Nitriles in Organic Synthesis. *Chem. Asian J.* 2022, *17*, e202200792.

90) Y. Xia, H. Jiang, W. Wu. Recent Advances in Chemical Modifications of Nitriles. *Eur. J. Org. Chem.* 2021, *48*, 6658-6669.

91) F. F. Fleming, L. Yao, P. C. Ravikumar, L. Funk, B. C. Shook. Nitrile-Containing Pharmaceuticals: Efficacious Roles of the Nitrile Pharmacophore. *J. Med. Chem.* 2010, *53*, 7902-7917.

92) Y. -S. Yen, Y. C. Hsu, J. T. Lin, C. W. Chang, C. P. Hsu, C. Tsai, D. -J. Yin. Pyrrole-Based Organic Dyes for Dye-Sensitized Solar Cells. *J. Phys. Chem. C* 2008, *112*, 19739-19747.

93) F. F. Fleming. Nitrile-containing natural products. *Nat. Prod. Rep.* 1999, *16*, 597-606.

94) M. Marzi, M. K. Vakil, M. Bahmanyar, E. Zarenezhad. Paxlovid: Mechanism of Action, Synthesis, and In Silico Study. *Biomed. Res. Int.* 2022, *2022*, 1-16.

95) D. McTavish, E. M. Sorkin. Verapamil. An updated review of its pharmacodynamic and pharmacokinetic properties, and therapeutic use in hypertension. *Drugs*, 1989, *38*, 19-76.

96) E. Kirino. Escitalopram for the management of major depressive disorder: a review of its efficacy, safety, and patient acceptability. *Patient Prefer Adherence* 2012, *6*, 853-861.

97) P. M. Irving, Y. Leung, M. C. Dubinsky. Guide to Tofacitinib dosing in patients with ulcerative colitis. *Aliment. Pharm. Ther.* 2022, *56*, 1131-1145.

98) G. P. Ellis and T. M. Romney-Alexander. Cyanation of aromatic halides. *Chem. Rev.* 1987, *87*, 779-794.

99) a) K. W. Rosenmund, E. Struck. Das am Ringkohlenstoff gebundene Halogen und sein Ersatz durch andere Substituenten. I. Mitteilung: Ersatz des Halogens durch die Carboxylgruppe. *Ber. Dtsch. Chem. Ges*. 1919, *52*, 1749-1755; b) J. Lindley. Copper assisted nucleophilic substitution of aryl halogen. *Tetrahedron* 1984, *4*0, 1433-1456.

100) **a)** T. Sandmeyer. Ueber die Ersetzung der Amidgruppe durch Chlor in den aromatischen Substanzen. *Ber. Dtsch. Chem. Ges.* **1884**, *17*, 1633-1635; **b)** H. H. Hodgson. The Sandmeyer reaction. *Chem. Rev.* **1947**, *40*, 251-277.

101) D. N. Deaton, A. M. Hassel, R. B. McFadyen, A. B. Miller, L. R. Miller, L. M. Shewchuk, F. X. Tavares, D. H. Willard, L. L. Wright. Novel and potent cyclic cyanamide-based cathepsin K inhibitors. *Bioorg. Med. Chem. Lett.* **2005**, *15*, 1815-1819.

102) B. G. Harvey, A. J. Guenthner, T. A. Koontz, P. J. Storch, J. T. Reams, T. J. Groshens. Sustainable hydrophobic thermosetting resins and polycarbonates from turpentine. *Green Chem.* **2016**, *18*, 2416-2423.

103) M. -J. Crawford, T. M. Klapötke, P. Klüfers, P. Mayer, P. S. White. CS_2N_3, A Novel Pseudohalogen. *J. Am. Chem. Soc.* **2000**, *37*, 9052-9053.

104) K. Okamoto, M. Watanabe, M. Murai, R. Hatano, K. Ohe. Practical synthesis of aromatic nitriles *via* gallium-catalysed electrophilic cyanation of aromatic C–H bonds. *Chem. Commun.* **2012**, *48*, 3127-3129.

105) W. E. Luttrell. Cyanogen bromide. *J. Chem. Health. Saf.* **2009**, *16*, 29-30.

106) "Announcement on the List of Toxic Chemicals Severely restricted on the Import and Export in China (Circular No. 65)", **2005** can be found under https://english.mee.gov.cn/Resources/Policies/policies/hazardouswaste/200712/t20071204_113792.shtml.

107) T. Schareina, A. Zapf, M. Beller. Potassium hexacyanoferrate(II)—a new cyanating agent for the palladium-catalyzed cyanation of aryl halides. *Chem. Commun.* **2004**, 1388-1389.

108) J. Vicario, J. M. Ezpeleta, F. Palacios. Asymmetric Cyanation of α-Ketiminophosphonates Catalyzed by *Cinchona* Alkaloids: Enantioselective Synthesis of Tetrasubstituted α-Aminophosphonic Acid Derivatives from Trisubstituted α-Aminophosphonates. *Adv. Synth. Catal.* **2012**, *354*, 2641-2647.

109) M. Pori, P. Galletti, R. Soldati, D. Giacomini. Asymmetric Strecker Reaction with Chiral Amines: a Catalyst-Free Protocol Using Acetone Cyanohydrin in Water. *Eur. J. Org. Chem.* **2013**, 1683-1695.

110) Y. -Q. Wu, D. C. Limburg, D. E. Wilkinson, G. S. Hamilton. 1-Cyanoimidazole as a Mild and Efficient Electrophilic Cyanating Agent. *Org. Lett.* **2000**, *2*, 795-797.

111) **a)** P. Anbarasan, H. Neumann, M. Beller. A Novel and Convenient Synthesis of Benzonitriles: Electrophilic Cyanation of Aryl and Heteroaryl Bromides. *Chem. Eur. J.* **2011**, *17*, 4217-4222; **b)** P. Anbarasan, H. Neumann, M. Beller. A General Rhodium-Catalyzed Cyanation of Aryl and Alkenyl Boronic Acids. *Angew. Chem., Int. Ed.* **2011**, *50*, 519-522.

112) **a)** N. Sato. A new efficient synthesis of *ortho*-cyanoarenes via directed lithiation followed by electrophilic cyanation. *Tetrahedron Lett.* **2002**, *43*, 6403-6404; **b)** N. Sato, Q. Yue. An efficient synthesis of cyanoarenes and cyanoheteroarenes via lithiation followed by electrophilic cyanation. *Tetrahedron* **2003**, *59*, 5831-5836.

113) G. Talavera, J. Peña, M. Alcarazo. Dihalo(imidazolium)sulfuranes: A Versatile Platform for the Synthesis of New Electrophilic Group-Transfer Reagents. *J. Am. Chem. Soc.* **2015**, *137*, 8704-8707.

114) X. Li, C. Golz, M. Alcarazo. 5-(Cyano)dibenzothiophenium Triflate: A Sulfur-Based Reagent for Electrophilic Cyanation and Cyanocyclizations. *Angew. Chem. Int. Ed.* **2019**, *58*, 9496-9500.

115) S. Kamijo, T. Hoshikawa M. Inoue. Photochemically Induced Radical Transformation of C(sp^3)–H Bonds to C(sp^3)–CN Bonds. *Org. Lett.* **2011**, *13*, 5928-5931.

116) H. Hu, S. Wu, F. Yan, M. Makha, Y. Sun, C.-X. Du, Y. Li. Recent developments in electrosynthesis of nitriles and electrocatalytic cyanations. *J. Energy Chem.* **2022**, *70*, 542-575.

117) Z. Fu, Y. Fu, J. Yin, G. Hao, X. Yi, T. Zhong, S. Guo, H. Cai. Electrochemical strategies for *N*-cyanation of secondary amines and α-*C*-cyanation of tertiary amines under transition metal-free conditions. *Green Chem.* **2021**, *23*, 9422-9427.

118) A. J. J. Lennox, S. L. Goes, M. P. Webster, H. F. Koolman, S. W. Djuric, S. S. Stahl. Electrochemical Aminoxyl-Mediated α-Cyanation of Secondary Piperidines for Pharmaceutical Building Block Diversification. *J. Am. Chem. Soc.* **2018**, *140*, 11227-11231.

119) H. Yang, Y. Shen, Z. Xiao, C. Liu, K. Yuan, Y. Ding. The direct trifluoromethylsilylation and cyanosilylation of aldehydes *via* an electrochemically induced intramolecular pathway. *Chem. Commun.* **2020**, *56*, 2435-2438.

120) Y. -T. Zheng, H. -C. Xu. Electrochemical Azidocyanation of Alkenes. *Angew. Chem. Int. Ed.* 2024, *63*, e202313273.

121) I. Yavari, S. Shaabanzadeh, S. Sheikhi. Electrochemical Synthesis of β-Ketonitriles from Aryl Methyl Ketones. *Chem. Sel.* 2020, *5*, 564-568.

122) S. S. Grishin, O. M. Mulina, V. A. Vil', A. O. Terent'ev. Electrochemical synthesis of CN-substituted imidazo[1,5-*a*]pyridines *via* a cascade process using NH_4SCN as both an electrolyte and a non-trivial cyanating agent. *Org. Chem. Front.* 2024, *11*, 327-335.

123) D. Hayrapetyan, R. K. Rit, M. Kratz, K. Tschulik, L. J. Gooßen. Electrochemical C-H Cyanation of Electron-Rich (Hetero)Arenes. *Chem. Eur. J.* 2018, *24*, 11288-11291.

124) M. Garbini, A. Brunetti, R. Pedrazzani, M. Monari, M. Marcaccio, G. Bertuzzi, M. Bandini. Reductive cyclodimerization of chalcones: exploring the "self-adaptability" of galvanostatic electrosynthesis. *Chem. Commun.* 2024, *60*, 404-407.

125) I. Chiarotto, L. Mattiello, M. Feroci. The Electrogenerated Cyanomethyl Anion: An Old Base Still Smart. *Acc. Chem. Res.* 2019, *52*, 3297-3308.

126) a) A. I. Lesnikovich, O. A. Ivashkevich, S. V. Levchik, A. I. Bala-banovich, P. N. Gaponik, A. A. Kulak. Thermal decomposition of aminotetrazoles. *Thermochim. Acta*, 2002, *388*, 233-251; b) J. -G. Zhang, L. -N. Feng, S. -W. Zhang, T. -L. Zhang, H. H. Zheng. The mechanism and kinetics of decomposition of 5-aminotetrazole. *J. Mol. Model.* 2008, *14*, 403-408; c) A. A. Paletsky, N. V. Budachev, O. P. Korobeinichev. Mechanism and kinetics of the thermal decomposition of 5-aminotetrazole. *Kinet Catal*. 2009, *50*, 627-635.

127) M. C. Leech, A. Petti, N. Tanbouza, A. Mastrodonato, I. C. A. Goodall, T. Ollevier, A. P. Dobbs, K. Lam. Anodic Oxidation of Aminotetrazoles: A Mild and Safe Route to Isocyanides. *Org. Lett.* 2021, *24*, 9371-9375.

128) Q. -W. Gui, Z. -Y. Xiong, F. Teng, T. -C. Cai, Q. Li, W. Hu, X. Wang, J. Yu, X. Liu. Electrochemically promoted oxidative α-cyanation of tertiary and secondary amines using cheap AIBN. *Org. Biomol. Chem.* 2021, *19*, 8254-8258.

129) K. Kiyokawa, T. Nagata, J. Hayakawa, S. Minakata. Straightforward Synthesis of 1,2-Dicyanoalkanes from Nitroalkenes and Silyl Cyanide Mediated by Tetrabutylammonium Fluoride. *Chem. Eur. J.* 2015, *21*, 1280-1285.

130) T. Noël, Y. Cao, G. Laudadio. The Fundamentals Behind the Use of Flow Reactors in Electrochemistry. *Acc. Chem. Res.* 2019, *52*, 2858-2869.

Chapter III: Ugi/Pictet-Spengler sequence as alternative for the synthesis of complex polycyclic scaffolds

3.1 Multicomponent Reactions (MCRs)

Multicomponent Reactions (MCRs) represent one of the most powerful and fascinating tools in organic synthetic chemistry.[131] These reactions are characterized by one-pot processes in which at least three reactants are combined to produce the desired product with high selectivity (**Figure 27**). Compared to traditional multi-step reactions, MCRs offer significant advantages in terms of atom economy, as the final products incorporate the majority of atoms from the starting materials, making them remarkably efficient. Additionally, the use of eco-friendly conditions and high convergence make multicomponent reactions an exceptional strategy, particularly aligned with the principles of "Green Chemistry".[132] Focusing in particular on the pharmaceutical industry, MCRs offer the opportunity to solve important issues regarding the synthetic preparations of complex molecular scaffolds, drastically reducing the costs, diminishing the reaction steps and also avoiding, in some case, the necessity of tedious purifications. Considering the high chemo-, regio-, and stereoselectivity,[133] MCRs typically result in excellent product yields, offering substantial benefits in terms of waste reduction.

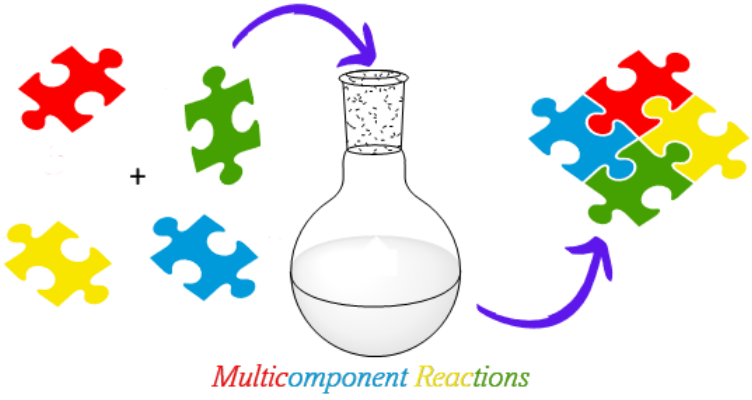

Figure 27: Multicomponent reactions.

Among the MCRs, the most widely utilized are the Passerini[134] and Ugi[135] reactions. The Passerini reaction has been firstly reported in 1921 by Mario Passerini and consists in a three-component reaction between isocyanides, a carbonyl source (aldehydes or ketones) and carboxylic acids to produce α-acyloxyamides (**Scheme 43**). The concerted mechanism of this reaction involves the formation of a hydrogen-bonded cluster, resulting from the interaction between the carboxylic acid and the carbonyl compound, which then reacts with the isocyanide in a single step. Since the initial step produces a non-polar cyclic transition state, the Passerini reaction is typically performed in non-polar solvents such as DCM, ethyl acetate, diethyl ether, and THF.

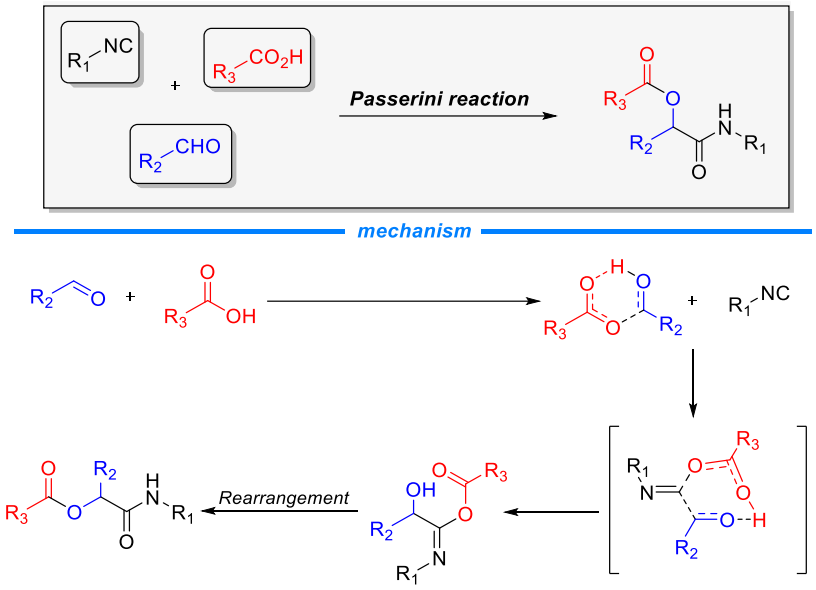

Scheme 43: Passerini reaction mechanism.

Although the Passerini reaction gives the possibility to easily synthesize different ester derivatives with a single reaction step, it has been neglected for several years. The potential of MCRs for the fast generation of complex products has been highlighted 40 years later, with the development of the Ugi reaction. Discovered in 1959,[136] The Ugi four-component reaction builds upon the Passerini procedure by

incorporating an additional amine into the mechanism, alongside the previously involved components. This modification adds complexity and versatility to the process (**Scheme 44**). In fact, while introducing an amide moiety typically requires multiple protection and deprotection steps, the Ugi reaction allows for the straightforward, one-pot preparation of various bis-amide products. Regarding the mechanism, the first step consists of the reaction between the carbonyl compound with the amine to form the corresponding imine. The imine is then protonated from the carboxylic acid, resulting in an activated iminium ion, which subsequently reacts with the isocyanide generating an imidate intermediate. Then, the nucleophilic addition of the carboxylate, followed by the Mumm rearrangement provide the formation of the final product. Contrary to the Passerini reaction, the Ugi reaction protocol is generally carried out in polar and protic solvents, such as methanol, ethanol and trifluoroethanol.[137]

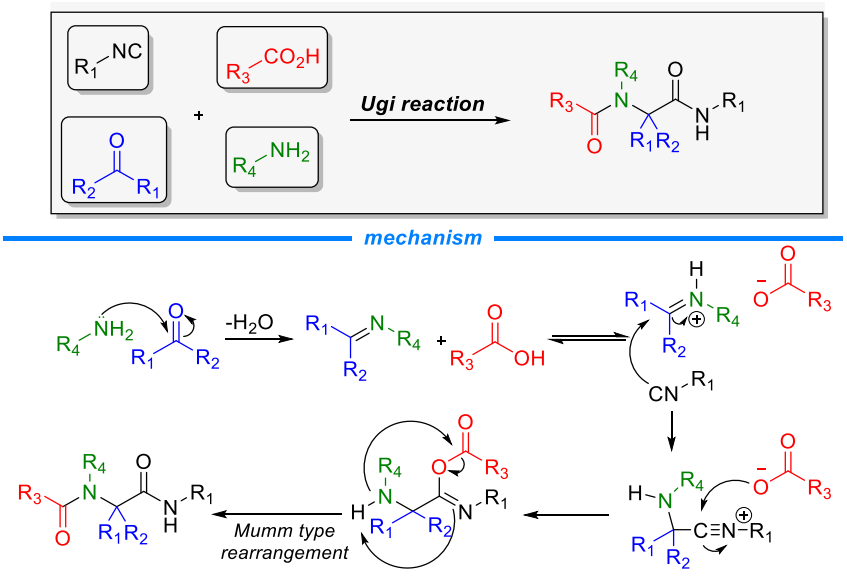

Scheme 44: Ugi reaction mechanism.

With only a molecule of water as byproduct, the Ugi reaction described perfectly the importance of the MCRs in terms of atom economy. In addition, due to the high

flexibility of the Ugi reaction with different functional groups, this protocol has been deeply investigated, especially in pharmaceutical research, with different variants developed, such as Ugi-3CR,[138] Ugi-Smiles[139] and others. The Ugi-4CR has in fact proved to be effective for the synthesis of many important drugs used for the treatment of several diseases.[133] Some examples are reported in **Figure 28**.

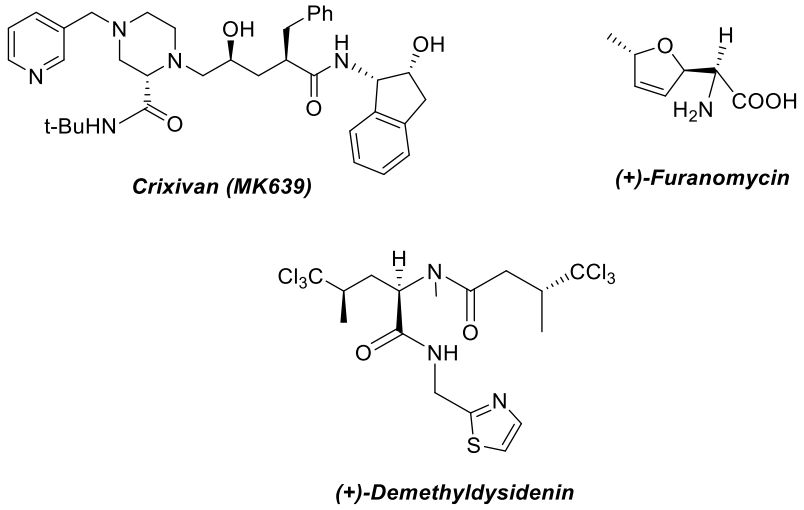

Figure 28: Biologically active compounds synthesized with Ugi-4CR.

3.2 Post-Ugi transformations

Given the importance of the Ugi-reaction in term of atom economy, mild reaction conditions and high structural variability, several studies have been conducted to combine this procedure with different post-transformations. In fact, by carefully choosing the four starting materials, the Ugi-adducts could be further manipulated to provide complex polyheterocyclic scaffolds. As a consequence, these synthetic sequences benefit from the convergence and versatility of MCRs, as well as from the diversity arising from post-Ugi transformations, including rearrangement, redox, addition, and substitution reactions (**Scheme 45**).[140] Owing to their broad

applicability, these combinations have been extensively utilized, with Ugi-products undergoing various transformations driven by either metal-mediated[141] catalysis or metal-free catalysis.[142]

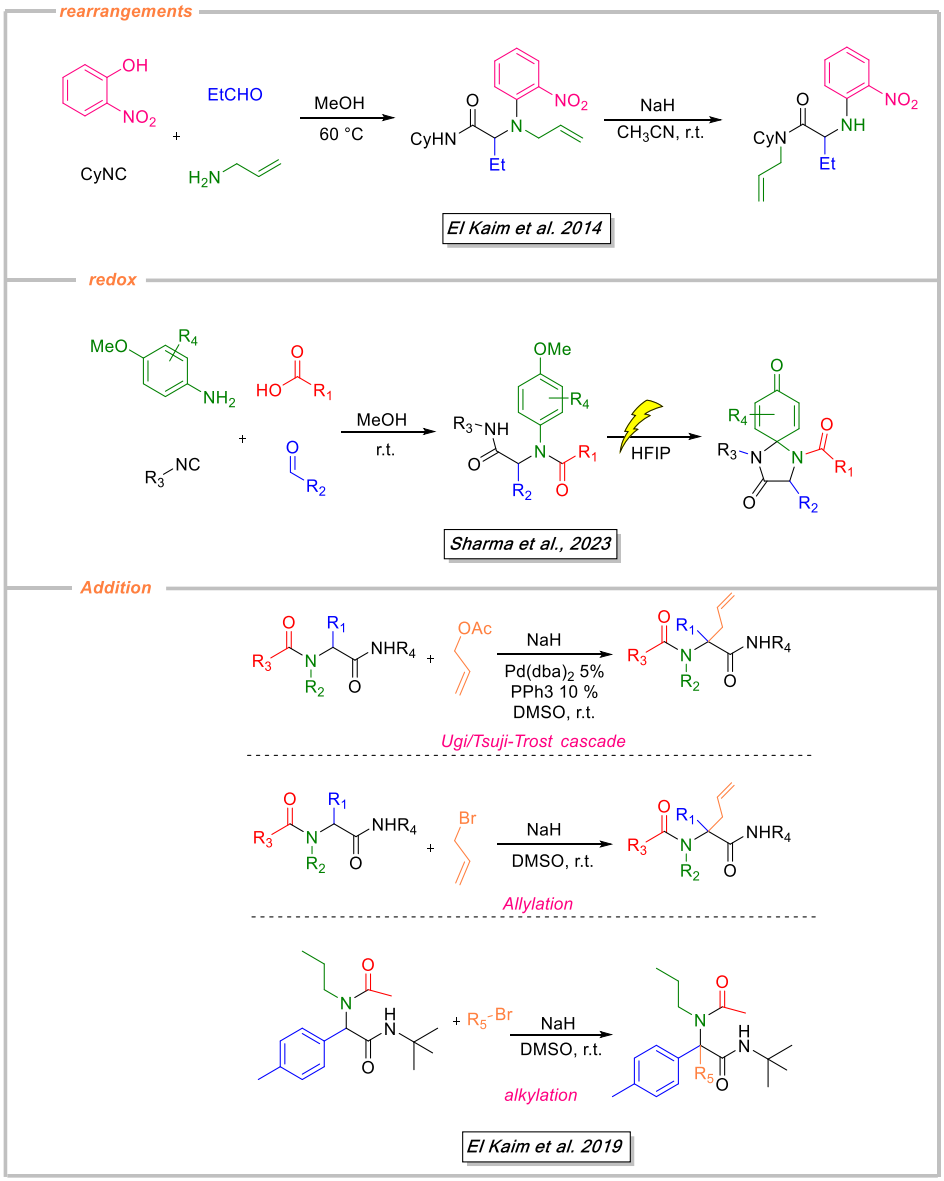

Scheme 45: Post-Ugi transformations.

Among the numerous examples of combining the Ugi reaction with subsequent transformations, one of the most widely applied sequences is the Ugi/Pictet-Spengler reaction. Pictet-Spengler reaction[143] (**Scheme 46**) has been developed in 1911 by the chemists Amè Pictet and Theodor Spengler, by heating β-phenylethylamine **86** and formaldehyde dimethylacetal in the presence of hydrochloric acid, resulting in a cycloaddition reaction.

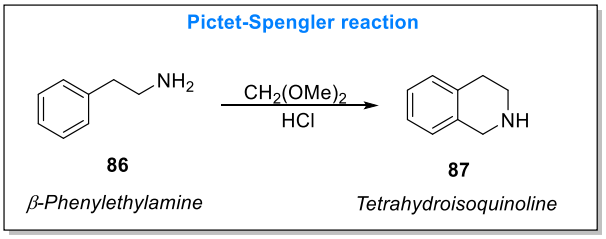

Scheme 46: First example of Pictet-Spengler reaction.

Twenty years after the discovery of PSR, Tatsui introduced an alternative application using tryptamine as the amine component.[144] This breakthrough led to the first synthetic generation of the 1,2,3,4-tetrahydro-β-carboline (THBC) skeleton (**Scheme 47**).

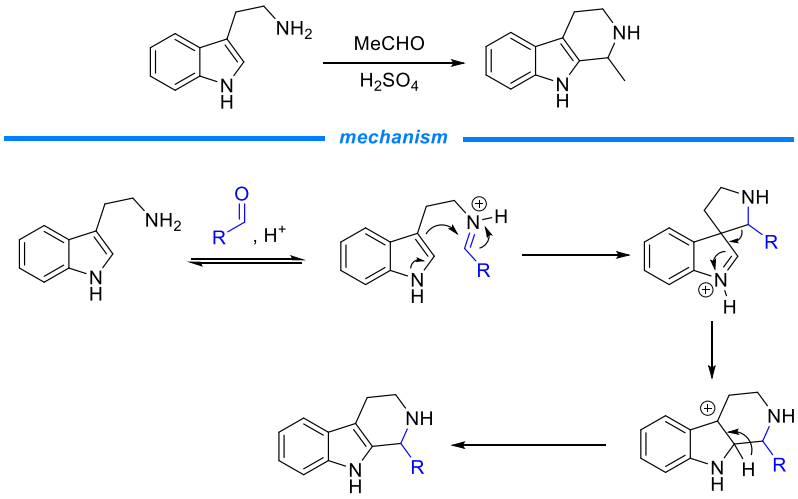

Scheme 47: P-S reaction with tryptamine.

Due to the high versatility of both reactions, the Ugi-Pictet-Spengler sequence has been extensively studied, leading to the synthesis of a wide range of structurally complex scaffolds. The first instance of combining the Ugi and Pictet-Spengler reactions was reported by Dömling and Ugi. Using phthalic aldehyde, t-butyl isocyanide, and the amino acid tryptophan, they successfully synthesized polycyclic products containing the THBC motif in a one-pot reaction.[145] This pioneering work underscored the synthetic significance of this combination, sparking numerous studies and publications that have demonstrated its applicability under various conditions and with diverse functional groups. Selected examples are shown in **Scheme 48.**[146]

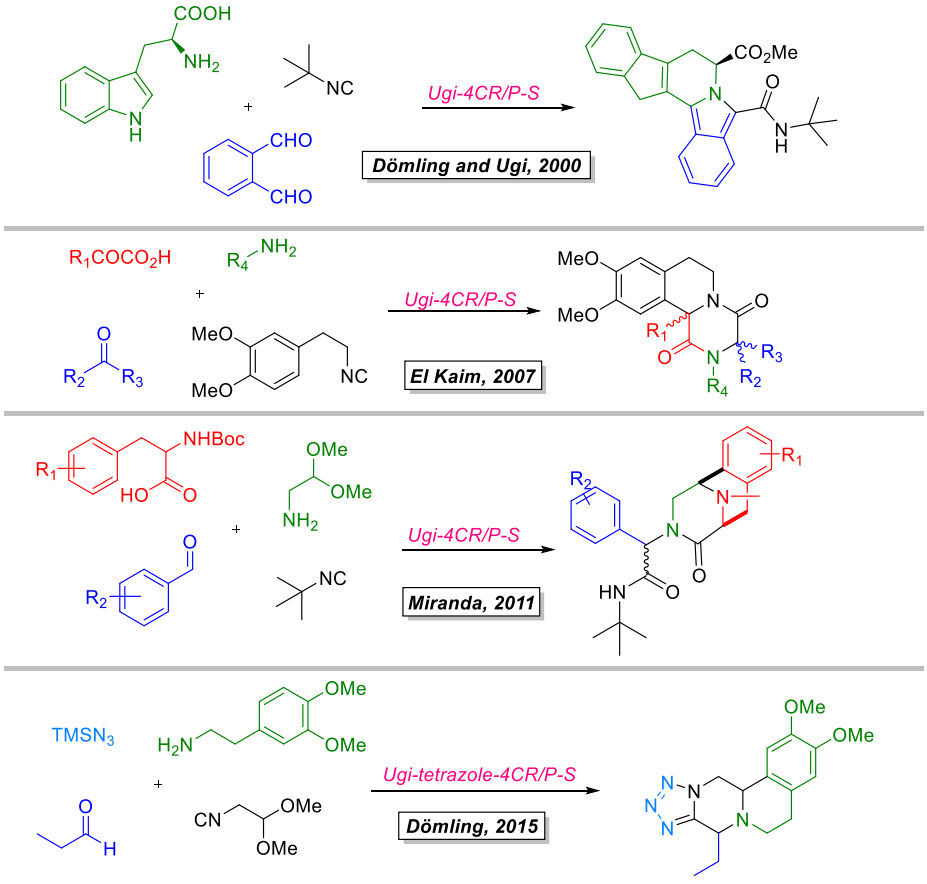

Scheme 48: Examples of Ugi/Pictet-Spengler reaction sequence.

3.3 Imidazopyridoindoles

Imidazopyridoindole, which consists in a β-carboline system fused with an imidazole ring, is a highly privileged scaffold found in various bioactive compounds. For example, Imidazopyridoindole-containing compounds have demonstrated efficacy as hypnotics-sedative and anticonvulsive drugs.[147] Additionally, a synthetic combinatorial library of Imidazopyridoindoles exhibited inhibition of β-amyloid-induced neurotoxicity.[148] Furthermore, the natural alkaloid *Peganumine A*,[149] a dimeric bridged tetrahydro-β-carboline fused with a 4-imidazolidinone ring, have demonstrated significant cytotoxic effects, resulting in an anticancer drug candidate (Figure 29).[150]

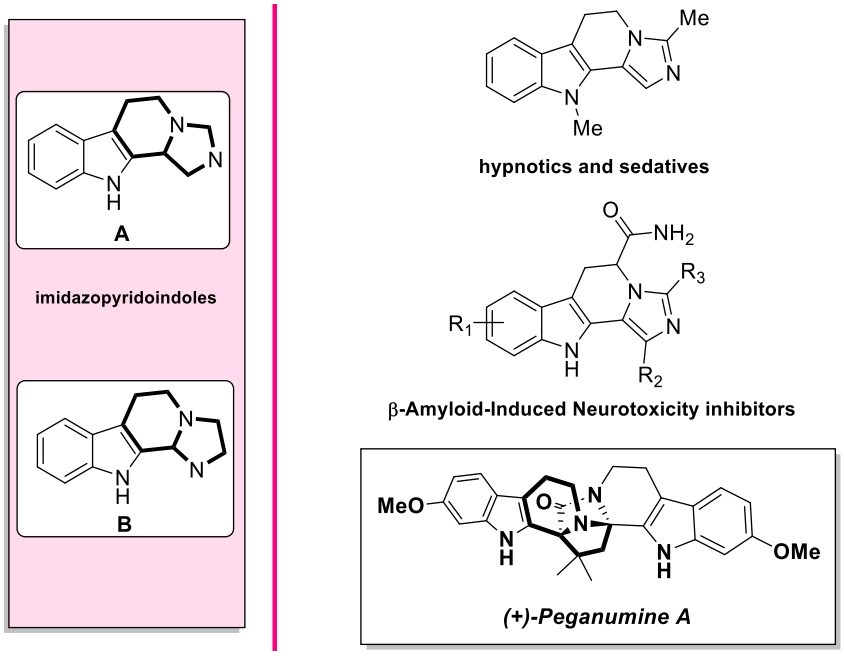

Figure 29: Imidazopyridoindoles and biologically active derivatives.

3.3 Diastereoselective Synthesis of High Functionalized 4-Imidazolidinone-Tetrahydro-β-Carboline Hybrids via Divergent Post-Ugi Transformation

Despite the promising biological activities exhibited by various derivatives, synthetic methods for the preparation of imidazopyridoindoles remain notably limited. In 2014, Lesma et *al.* introduced a classical approach to synthesize substituted imidazopyridoindoles, combining Ugi and Bischler-Napieralski (B-N) reactions using tryptamine isocyanide as the starting material.[151] More recently, Wu and coworkers developed a more efficient, one-pot method that directly employs tryptamine, streamlining the process by eliminating the need for multiple steps (**Scheme 49**).[152]

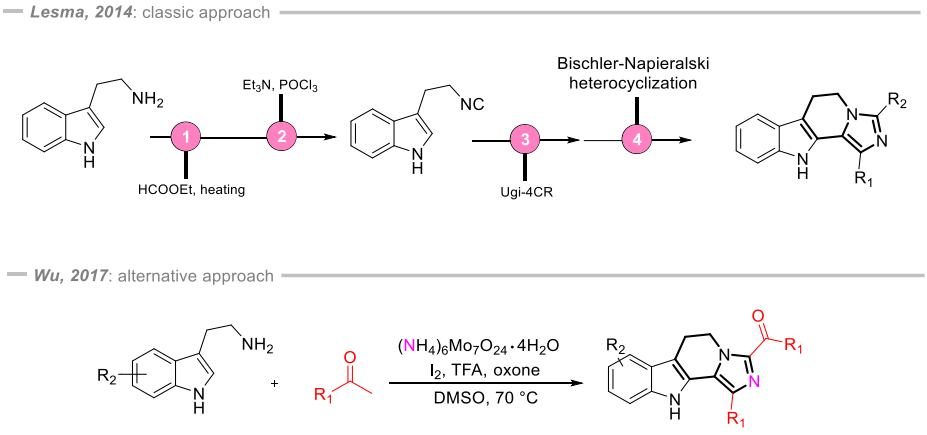

Scheme 49: Imidazopyridoindoles synthetic approaches.

However, the regioisomer **B** (**Figure 29**) of imidazopyridoindole has garnered significantly less attention compared to the other isomer. To bridge this gap, I focused my attention toward leveraging the high versatility of the Ugi-4CR adduct to promote an annulation/*N*-acylimidinium-mediated Pictet-Spengler cyclization reaction. Additionally, while P-S cyclizations involving iminium or *N*-acyliminium intermediates have been extensively studied,[153] the annulation reactions involving *N*-acylimidinium intermediates remain entirely unexplored (**Scheme 50**).

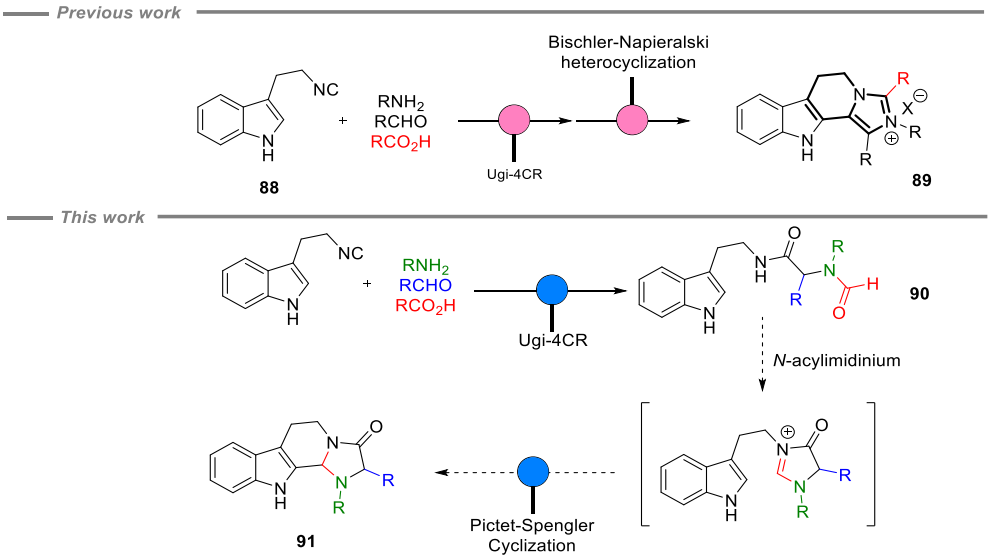

Scheme 50: Diastereoselective synthesis of 4-Imidazolidinone-Tetrahydro-β-Carboline Hybrids.

3.4 Results and discussion

I began the investigation by creating a library of Ugi-adduct building blocks for the subsequent cyclization. The starting materials were prepared using both aromatic and aliphatic aldehydes, along with anilines and alkylamines, reacting with 3-(2-isocyanoethyl)-1H-indole and formic acid under the conditions outlined in **Table 16**. The reaction led to good yields using aromatic aldehydes and anilines, also showing a general high tolerance with electron-donating and/or electron-withdrawing groups on the aromatic ring. Thus, various valuable halogen-substituted Ugi-adducts on the aromatic moieties, which can be further modified through secondary reactions, were smoothly synthesized with yields ranging from 45% to 54%.

Table 16: Synthesis of Ugi-4CR adducts.

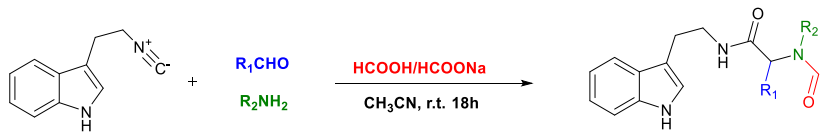

88 90

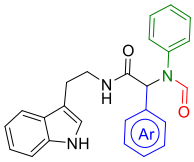

90a, Ar= p-OMe, 53 % yield, (1g, 52 %)
90b, Ar= p-Me, 53 % yield
90c, Ar= H, 50 % yield
90d, Ar= *p*-F, 55 % yield
90e, Ar= *m*-OMe, 51 % yield
90f, Ar= *m*-Br, 50 % yield
90g, Ar= *o*-CN, 44 % yield

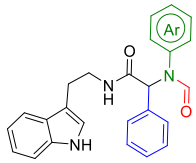

90h, Ar= *p*-F, 54 % yield
90i, Ar= *p*-Cl, 51 % yield
90j, Ar= *p*-NO_2, 41 % yield
90k, Ar= *p*-OMe, 52 % yield
90l, Ar= *p*-I, 45 % yield
90m, Ar= *p*-Me, 50 % yield

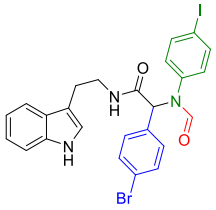

90n, 54 % yield

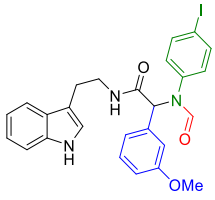

90o, 37 % yield

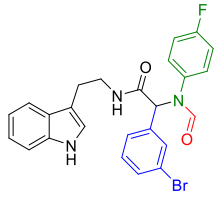

90p, 54 % yield

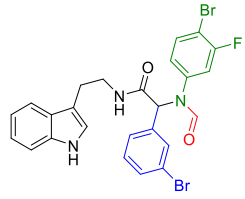

90q, 46 % yield

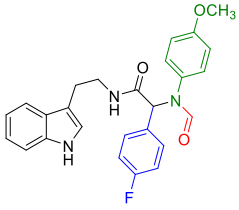

90r, 50 % yield

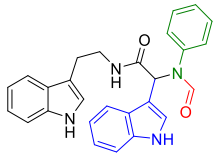

90s, 48 % yield

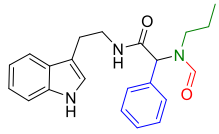

90t, 58 % yield

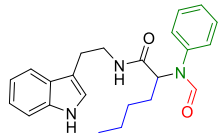

90u, 30 % yield

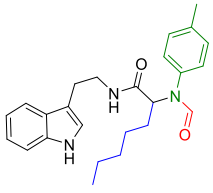

90v, 33 % yield

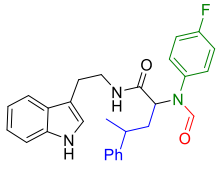

90w, 50 % yield

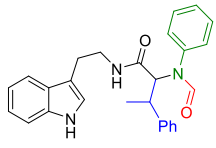

90x, 30 % yield

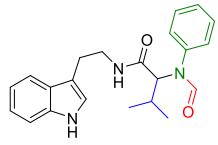

90y, 42 % yield

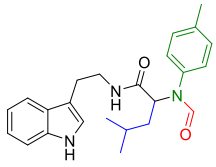

90z, 45 % yield

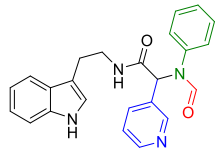

90ω, 51 % yield

Nicely, an unexpected 48% yield was achieved with 1H-indole-3-carbaldehyde despite the acidic reaction conditions. When using nicotinaldehyde, the desired product **90ω** was obtained with 51% yield. Finally, reactions employing aliphatic aldehydes and amines yielded moderate to good results.

With the desired set of Ugi-adducts in hand, I proceeded by evaluating the feasibility of the cyclization postulated in **Scheme 50** using **90a** as the model substrate. The heteroannulation has been tested with a diverse array of metal salts and complexes, resulting in the different entries reported in **Table 17**. The reactions carried out with catalytic amounts of JohnPhos Au(MeCN)SbF_6 and $Na_2PtCl_6 \cdot 6H_2O$ did not lead to any product, with the starting material recovered after 24h at 110 °C in 74% and 77% yield respectively (**Table 17, Entry 1-2**).[154] Disappointing results have been also obtained with other metal catalysts such as $Cu(OTf)_2$,[155] $Zn(OTf)_2$[156] and $Yb(OTf)_3$[157] (**Table 17, Entries 3–6**), instead favoring the hydrolysis of **90a** and the formation of α-ketoamide **92**. Among the different metal catalysts employed for the reaction, AgOTf has shown the best performance, resulting in a 48% isolated yield when it has been used in stoichiometric amount (**Table 1, Entry 8**).[158] The best results has been obtained using TMSOTf as Lewis acid promoter, in stoichiometric amount, achieving the desired cyclized product in 79% yield (**Table 17, Entry 11**).[159] Conversely, no reaction occurred by replacing TMSOTf with the Brønsted trifluoromethanesulfonic acid (TfOH) (**Table 1, Entry 12**).

Table 17: Optimization of the post Ugi hetero-annulation.

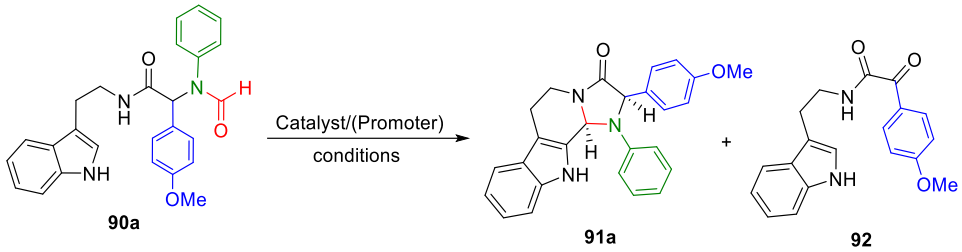

Es	Solvent 0.4 M	Catalyst/ Promoter	°C/h	Yield (%)[a] 91a	92
1	Toluene	JPAu(MeCN)SbF_6 (5%)	110/24	- (74)	-
2	Toluene	$Na_2PtCl_6 \cdot 6H_2O$ (5%)	110/24	- (77)	-
3	DMF	$Cu(OTf)_2$ (20%)	120/24	-	35%
4	Xylene	$Cu(OTf)_2$ (20%)	120/24	- (20)	22%
5	DMF	$Zn(OTf)_2$ (20%)	120/24	-	55%
6	DMF	$Yb(OTf)_3$ (20%)	120/24	-	74%
7	DMF	Ag(OTf) (20%)	120/24	<10	-
8	DMF	Ag(OTf) (100%)	120/48	48	-
9	DMF	TMSOTf (20%)	120/7	18 (61)	<5%[b]
10	DMF	TMSOTf (40%)	120/7	35 (52)	<5%[b]
11	DMF	TMSOTf (100%)	120/7	79	<5%[b]
12	DMF	TfOH (100%)	120/7	- (55)	-

[a]Isolated yields. Yields in parentheses refer to recovered starting material **90a**. [b] Determined by ^{1}H-NMR on crude mixtures.

Notably, despite the conditions used, the reaction with TMSOTf has shown a high diasteroselectivity, leading almost exclusively to the (R,R)/(S,S)-racemic mixture, assigned by 2D-NMR experiments and X-ray on the bromo-substituted derivative **91f**. In addition, DFT calculations show that the obtained diastereoisomer is 7 kJ/mole more stable than the other, both in gas-phase and in presence of solvents with different dielectric constants, such as toluene and DMSO.

With the optimized conditions in hand, I started the substrate scope of the reaction. The products reported in **Table 18** shown that the domino reaction proceeded quite smoothly with *para*- and *meta*-substituted arylaldehydes, resulting in the corresponding derivatives **91** with satisfactory to very good yields (71%-90%). Good yields (60-77%) have been also obtained with the Ugi-adducts with similar substituents on the aniline ring. Likewise, the simultaneous presence of *para*- and/or *meta*-substituents in both aromatic rings have been well tolerated. Also, the adducts generated with alkyl aldehydes have demonstrated a good reactivity, achieving the corresponding cyclized 5-alkyl-imidazolidin-4-ones **91u-z** in sufficient yield. Conversely, no reactivity has been observed with adduct **91t** incorporating the alkyl group on the amine moiety, as well as the reactions carried out with **90g**, **90s** and **90w**. The ^{1}H-NMR analyses on these crude mixtures have revealed in fact the complete degradation of the starting materials, with the formation of *N*-phenylformamide as the most abundant side product, isolated with a 30 % yield from the reaction of **90s**.

Table 18: Hetero-annulation substrate scope.

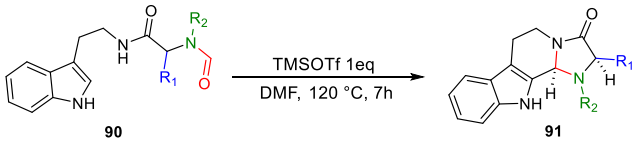

90 **91**

substrate scope

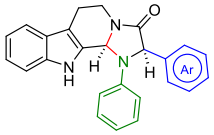

91a, Ar= *p*-OMe, 79 % yield, d.r.>20:1 (1g, 68%)
91b, Ar= *p*-Me, 71 % yield, d.r.>20:1
91c, Ar= H, 85 % yield, d.r.>20:1
91d, Ar= *p*-F, 90 % yield, d.r.>20:1
91e, Ar= *m*-OMe, 69 % yield, d.r.>20:1
91f, Ar= *m*-Br, 68 % yield, d.r.>20:1

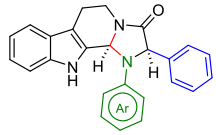

91h, Ar= *p*-F, 74 % yield, d.r.>20:1
91i, Ar= *p*-Cl, 77 % yield, d.r.>20:1
91j, Ar= *p*-NO_2, 64 % yield, d.r.>20:1
91k, Ar= *p*-OMe, 60 % yield, d.r.>20:1
91l, Ar= *p*-I, 55 % yield, d.r.>20:1
91m, Ar= *p*-Me, 76 % yield, d.r.>20:1

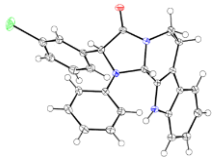

91f, CCDC 2311817

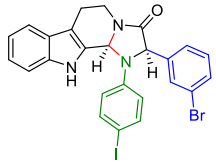

91n, 38 % yield, d.r.>20:1

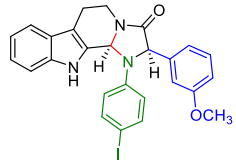

91o, 52 % yield, d.r.>20:1

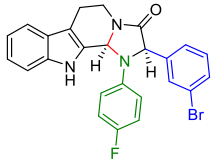

91p, 66 % yield, d.r.>20:1

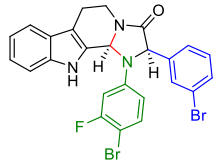

91q, 69 % yield, d.r.>20:1

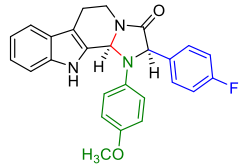

91r, 59 % yield, d.r.>20:1

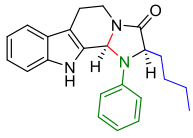

91u, 61 % yield, d.r.>20:1

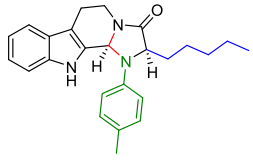

91v, 59 % yield, d.r.>20:1

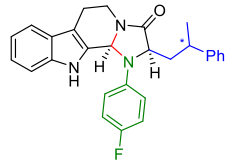

91w, 52 % yield, d.r.>20:1

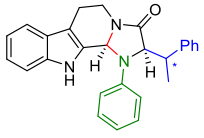

91x, 59 % yield, d.r.>20:1

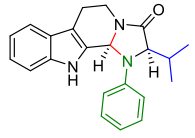

91y, 41 % yield, d.r.>20:1

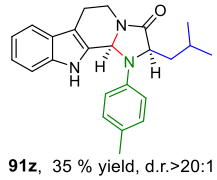

91z, 35 % yield, d.r.>20:1

Moreover, the gram-scale synthesis confirmed the practicability of this approach, with 68% isolated yield of the desired product using **90a** as starting material.

I also explored possible modifications of this new class of compounds, as shown in **Scheme 51**. Given the significance of *N*-substituted tetrahydro-β-carbolines as targeting μ-opioid receptors,[160] I attempted the reduction of the model substrate **91a**. Notably, with $LiAlH_4$ as the reducing agent, the opening of the imidazolidinone ring occurs simultaneously with the reduction of the carbonyl group, yielding the corresponding *N*-substituted tetrahydro-β-carboline **93** with a 57% yield (**Scheme 51, eq. a**).[161] Moreover, considering that Pd-catalyzed functionalization of haloaryl group could provide a practical and efficient approach for the diversity-oriented synthesis of various β-carboline-fused imidazolidin-4-ones, the representative iodo-derivative **91l** was submitted to the Sonogashira-Hagihara reaction with phenylacetylene. This approach allowed the synthesis of the alkynyl-derivative **94** with a good 73% isolated yield (**Scheme 51, eq. b**). These results pave the way for extensive structural modifications.[162]

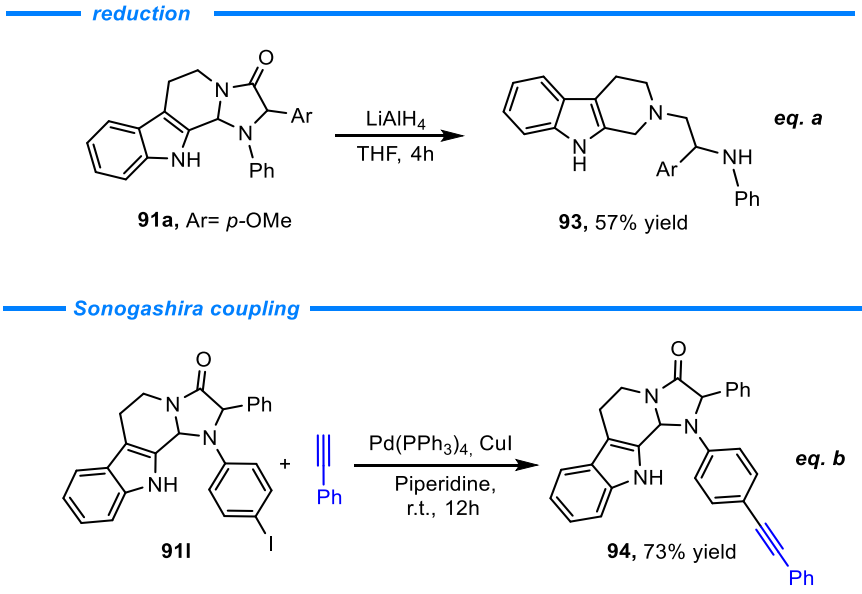

Scheme 51: Further elaborations.

The proposed reaction mechanism is depicted in **Scheme 52**. TMSOTf can facilitate the reaction either by activating the electrophilic moiety of the Ugi-adduct **90** to form intermediate **A**[163] or by activating the nucleophilic moiety to form intermediate **B**.[164] Both **A** and **B** can then generate the acylimidinium intermediate **C**, which undergoes a *P-S* reaction to produce the final product **91**. It has to be noted that the coordination of the formamide moiety like in **A**, as mentioned earlier, may also favor a degradation pathway, evidenced by the detection of *N*-phenylformamide.

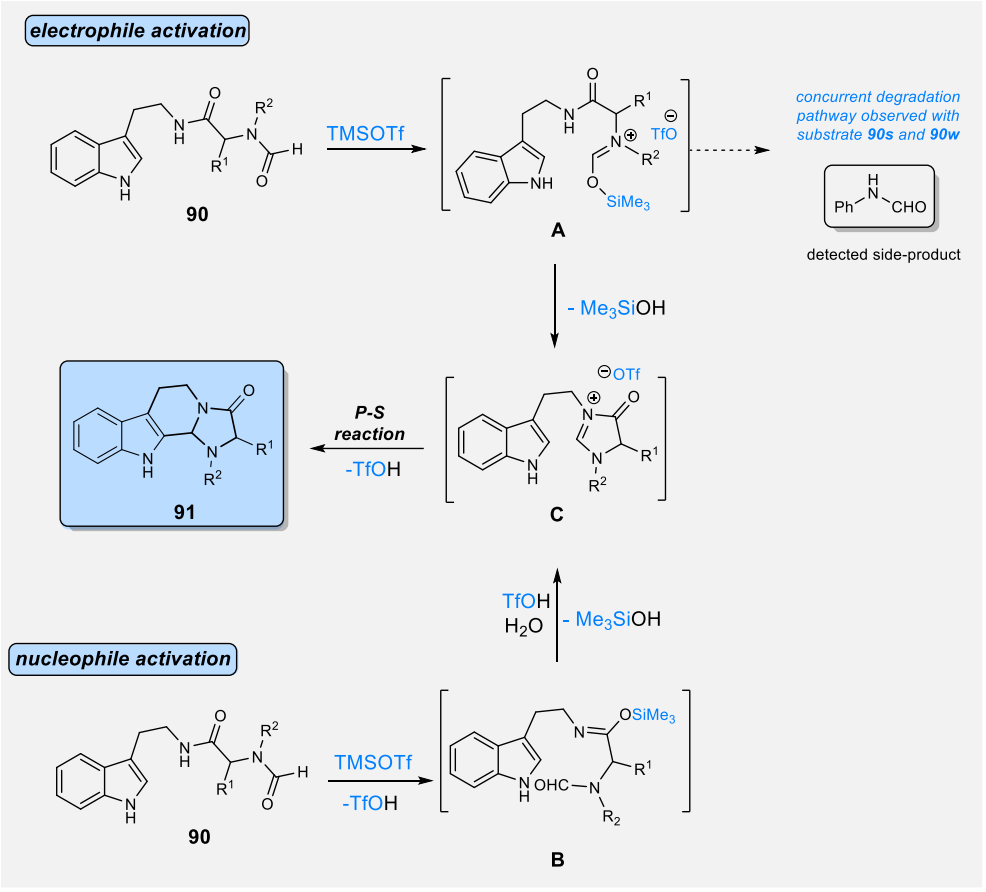

Scheme 52: Plausible reaction pathway.

3.5 Conclusions

In conclusion, in this work it has been established a divergent one-pot annulation/Pictet-Spengler sequence of novel *N*-formyl Ugi-4CR adducts, employing the cost-effective TMSOTf as a Lewis acid promoter under metal-free conditions. The presented method addresses the synthesis of challenging 4-imidazolidinone-tetrahydro-β-carboline hybrids, in good yields and high diastereoselectivity. The reaction exhibits a broad scope, and large-scale synthesis can be easily achieved. Notably, the resulting products also exhibited excellent potential for further synthetic modifications.

3.6 Experimental section

General materials and methods

Flash chromatography was carried out using silica gel 60 (70–230 mesh, Merck, Darmstadt, Germany). Yields are given for isolated products showing one spot on a TLC plate and no impurities were detectable in the NMR spectrum. ^{1}H NMR spectra were recorded at 400.13 MHz on a Bruker Avance III spectrometer using the standard Bruker "zg30" sequence. Chemical shifts (in ppm) were referenced to $CDCl_3$ (δ = 7.26 ppm) or Dimethyl sulfoxide-d_6 (δ = 2.50 ppm) as an internal standard. ^{13}C NMR spectra were taken on the same machine at 100.613 MHz, using the standard Bruker "zgpg30" sequence. Carbon spectra were calibrated with $CDCl_3$ (δ = 77.0 ppm) or Dimethyl sulfoxide-d_6 (δ = 39.50 ppm) as an internal standard. ^{19}F NMR spectra were taken on the same machine at 376.498 MHz, using the standard Bruker "zgfhigqn" sequence. Coupling constants (J) are quoted in Hertz. Mass measurements were performed using a MALDI-TOF spectrometer AB SCIEX TOF/TOF 5800 using matrix in combination with KI for the ionization.

Single crystal X-Ray diffraction data of **91f** (solvatomorphs a, b and g) were collected at the XRD2 beamline of the Elettra Synchrotron, Trieste (Italy). The crystals were soaked in NHV immersion oil (Jena Bioscience, Jena, Germany) and mounted on the goniometer head with kapton loops (MiTeGen, Ithaca, USA). Complete datasets were collected by the rotation method at 100 K (nitrogen stream supplied through an Oxford Cryostream 700). Data were acquired using monochromatic wavelengths of 0.620 Å on a Pilatus hybrid-pixel area detector (DECTRIS Ltd., Baden-Daettwil, Switzerland). The diffraction data were indexed and integrated using XDS. Semi-empirical absorption corrections, merging and scaling were performed exploiting multiple measures of symmetry-related reflections, using SADABS program. The structures were solved by the dual space algorithm implemented in the SHELXT code. Fourier analysis and refinement were performed by the full-matrix least-squares methods based on F_o^2 implemented in SHELXL (Version 2019/3). The molecular graphic program Coot was used for modeling. Anisotropic thermal motion refinement has been used for all atoms. Geometry restrains (SAME, DFIX and DANG) have been used on disordered solvent fragments. H-atoms were placed in geometrically calculated positions and refined using a riding model where to each H atom was assigned a fixed isotropic displacement

parameter with a value equal to 1.2Ueq of its parent atom or 1.5Ueq for the methyl and hydroxyl groups, U_{eq} being the equivalent isotropic thermal factor of the bonded non hydrogen atom. Drawings were prepared using Ortep-3, CCDC Mercury and Pymol.

General experimental procedure for the synthesis of acetamide derivatives 90

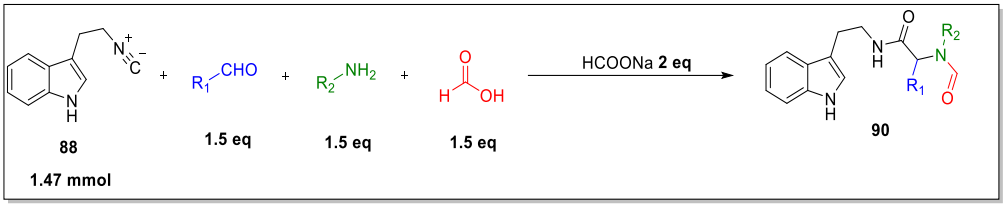

Formic acid (1.5 eq, 2.2 mmol) was added to a suspension of aldehyde (1.5 eq, 2.2 mmol), amine (1.5 eq, 2.2 mmol) and Sodium formate (2 eq, 2.94 mmol) in CH_3CN (3.7 mL). The solution was stirred for 2 minute and then 3-(2-isocyanoethyl)-1H-indole (250 mg, 1 eq, 1.47 mmol) was added. The mixture was stirred for 18 hours, at room temperature. Then, the mixture was extracted with DCM three times. The combined organic layer was dried over anhydrous Na_2SO_4 and concentrated under reduced pressure. The crude product was purified by column chromatography on silica gel (Petroleum ether/Ethyl acetate, 8:2 to 6:4) affording acetamide derivative **90** as a white solid.

General experimental procedure for the synthesis of imidazolidin-4-one derivatives 91

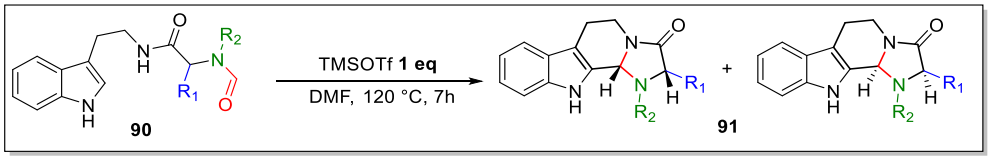

TMSOTf (1 eq, 0.4 mmol) was added to a solution of acetamide derivative (1 eq, 0.4 mmol) in DMF (1 mL). The solution was stirred at 120 °C for 7 hours. Then, the mixture was extracted with AcOEt three times. The combined organic layer was dried over anhydrous Na_2SO_4 and concentrated under reduced pressure. The crude product was purified by column chromatography on silica gel (Petroleum ether/Ethyl acetate, 85:15) affording 1,2-diphenyl-1,2,5,6,11,11b-hexahydro-3H-imidazo[1',2':1,2]pyrido[3,4-b]indol-3-one 1,2,5,6,11,11b-

hexahydro-3H-imidazo [1',2':1,2] pyrido[3,4-b] indol-3-one derivative **91** as a solid containing the racemic mixture of (2R,11bR)- and (2S,11bS)- for compound **91a**-**91f**, **91h**-**91r**, **91u**, **91v**, **91y** and **91z**, whereas compounds **91w** and **91x** were isolated as a diastereomeric mixture of the two epimers of isomer (2R,11bR)- and (2S,11bS)-, see below in the characterization section for more details.

N-(2-(1H-indol-3-yl) ethyl)-2-(4-methoxyphenyl)-2-(N-phenylformamido) acetamide (90a):

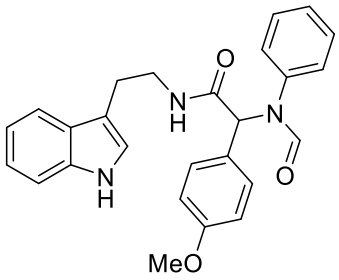

Prepared following general procedure **A** and isolated as a white solid in 53% yield (333 mg); mp 119-120°C. **^{1}H-NMR** (400 MHz, $CDCl_3$): δ= 8.26 (s, 1H), 8.00 (s, 1H), 7.46 (d, J = 7.9 Hz, 1H), 7.27 (d, J = 8.1 Hz, 1H), 7.21 – 7.06 (m, 4H), 7.03 – 6.93 (m, 5H), 6.89 (s, 1H), 6.60 (d, J = 8.4 Hz, 2H), 5.80 (t, J = 5.3 Hz, 1H), 5.77 (s, 1H), 3.66 (s, 3H), 3.56 (m, J = 13.5, 6.8 Hz, 2H), 2.90 (m, J = 7.2 Hz, 2H) ppm. **^{13}C-NMR** (101 MHz, $CDCl_3$): δ=169.0, 163.0, 159.6, 139.3, 136.3, 131.2, 129.0, 128.3, 127.8, 127.2, 125.9, 122.3, 122.1, 119.4, 118.6, 113.9, 112.7, 111.2, 63.4, 55.2 40.1, 25.0 ppm. **HRMS** m/z (MALDI-TOF) negative ion, calculated for $C_{26}H_{24}N_3O_3$: $[M-H]^-$ 426.1818, Found: 426.1820.

N-(2-(1H-indol-3-yl) ethyl)-2-(N-phenylformamido)-2-(*p*-tolyl) acetamide (90b): Prepared following general procedure **A** and isolated as a brown solid in 53% yield (320 mg); mp 116-117 °C. **^{1}H-NMR** (400 MHz, $CDCl_3$): δ= 8.35 (s, 1H), 8.06 (s, 1H), 7.53 (d, J = 7.9 Hz, 1H), 7.34 (d, J = 8.1 Hz, 1H), 7.25 – 6.95 (m, 12H), 5.91 (t, J = 6.0 Hz, 1H), 5.84 (s, 1H), 3.62 (m, 2H), 2.97 (m, 2H), 2.27 (s, 3H) ppm. **^{13}C-NMR** (101 MHz, $CDCl_3$): δ= 169.0, 163.1, 139.5, 138.4, 136.4, 131.0, 129.7, 129.3, 129.0, 128.1, 127.8, 127.3, 122.4, 122.1, 119.4, 118.7, 112.7, 111.2, 64.1, 40.2, 25.0, 21.1 ppm. **HRMS** m/z (MALDI-TOF) positive ion, calculated for $C_{26}H_{25}KN_3O_2$: $[M+K]^+$ 450.1584, Found: 450.1578.

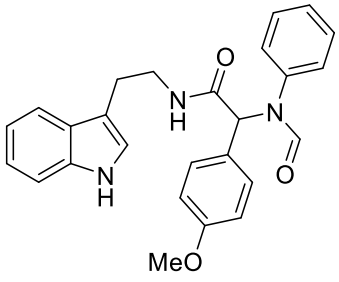

N-(2-(1H-indol-3-yl) ethyl)-2-phenyl-2-(N-phenylformamido) acetamide (90c): Prepared following general procedure **A** and isolated as a white solid in 50% yield (292 mg); mp 106-107 °C. **^{1}H-NMR** (400 MHz, $CDCl_3$): δ= 8.34 (s, 1H), 8.18 (s, 1H), 7.53 (d, J = 7.9 Hz, 1H), 7.33 (d, J = 8.1 Hz, 1H), 7.25 – 7.03 (m, 12H), 6.92 (s, 1H), 5.99 (t, J = 5.8 Hz, 1H), 5.89 (s, 1H), 3.63 (m, 2H), 2.97 (m, 2H) ppm. **^{13}C-NMR** (101 MHz, $CDCl_3$): δ= 168.8, 163.1, 139.4, 136.3, 134.0, 129.8, 129.0, 128.57, 128.55, 128.1, 127.9, 127.2, 122.4, 122.1, 119.5, 118.7, 112.6, 111.2, 64.2, 40.2, 25.0 ppm. **HRMS** m/z (MALDI-TOF) positive ion, calculated for $C_{25}H_{23}KN_3O_2$: $[M+K]^+$ 436.1427, Found: 436.1423.

N-(2-(1H-indol-3-yl) ethyl)-2-(4-fluorophenyl)-2-(N-phenylformamido) acetamide (90d): Prepared following general procedure **A** and isolated as a white solid in 55% yield (336 mg); mp 149-150 °C. **^{1}H-NMR** (400 MHz, $CDCl_3$): δ= 8.31 (s, 1H), 8.11 (s, 1H), 7.54 (d, J = 7.9 Hz, 1H), 7.34 (d, J = 8.1 Hz, 1H), 7.25 – 7.16 (m, 4H), 7.14 – 7.01 (m, 5H), 6.96 (s, 1H), 6.83 (t, J = 8.4 Hz, 2H), 5.98 (t, J = 5.6 Hz, 1H), 5.88 (s, 1H), 3.67 – 3.57 (m, 2H), 2.99 (m, 2H) ppm. **^{19}F-NMR** (376 MHz, $CDCl_3$): δ= -112.68. **^{13}C-NMR** (101 MHz, $CDCl_3$) δ = 168.6, 162.6 (d, $^1J_{C,F}$ = 248.3 Hz, CF), 161.4, 139.0, 136.4, 131.7 (d, $^3J_{C,F}$ = 8.4 Hz), 129.8 (d, $^4J_{C,F}$ = 3.67 Hz), 129.1, 128.2, 128.0, 127.3, 122.3, 122.2, 119.5, 118.6, 115.5 (d, $^2J_{C,F}$ = 21.3 Hz), 112.6, 111.2, 63.1, 40.2, 25.0 ppm. **HRMS** m/z (MALDI-TOF) negative ion, calculated for $C_{25}H_{21}N_4O_4$: $[M-H]^-$ 414.1618, Found: 414.1613.

N-(2-(1H-indol-3-yl) ethyl)-2-(3-methoxyphenyl)-2-(N-phenylformamido) acetamide (90e): Prepared following general procedure **A** and isolated as a white solid in 51% yield (320 mg); mp 115-116 °C. **^{1}H-NMR** (400 MHz, $CDCl_3$): δ= 8.34 (s, 1H), 8.28 (s, 1H), 7.53 (d, J = 7.9 Hz, 1H), 7.32 (d, J = 8.1 Hz, 1H), 7.25 – 7.20 (m, 3H), 7.19 – 7.03 (m, 5H), 6.91 (d, J = 2.3 Hz, 1H), 6.80 – 6.67 (m, 3H), 6.02 (t, J = 5.8 Hz, 1H), 5.85 (s, 1H), 3.61 (m, 5H), 2.96 (m, 2H) ppm. **^{13}C-NMR** (101 MHz, $CDCl_3$): δ= 168.7, 163.1, 159.6, 139.5, 136.4, 135.5, 129.6,

129.0, 128.1, 127.9, 127.2, 122.5, 122.1, 122.0, 119.4, 118.6, 115.1, 114.5, 112.5, 111.3, 64.2, 55.2, 40.2, 25.0 ppm. **HRMS** m/z (MALDI-TOF) positive ion, calculated for $C_{26}H_{25}N_3NaO_3$: $[M+Na]^+$ 450.1794, Found: 450.1793.

N-(2-(1H-indol-3-yl) ethyl)-2-(3-bromophenyl)-2-(N-phenylformamido) acetamide (90f):

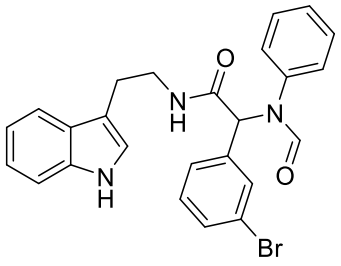

Prepared following general procedure **A** and isolated as a white solid in 50% yield (350 mg); mp 104-105 °C. **^{1}H-NMR** (400 MHz, $CDCl_3$) δ= 8.33 (s, 1H), 8.19 (s, 1H), 7.56 (d, J = 7.9 Hz, 1H), 7.41 – 7.33 (m, 3H), 7.27 (dt, J = 6.7, 3.2 Hz, 3H), 7.23 – 7.17 (m, 1H), 7.14 – 6.97 (m, 6H), 6.07 (t, J = 5.8 Hz, 1H), 5.83 (s, 1H), 3.66 (m, 2H), 3.01 (m, 2H) ppm. **^{13}C-NMR** (101 MHz, $CDCl_3$): δ= 168.1, 163.0, 139.1, 136.4, 136.3, 132.6, 131.6, 123.0, 129.2, 128.3, 128.0, 127.8, 127.2, 122.43, 122.40, 122.1, 119.4, 118.6, 112.4, 111.2, 63.6, 40.1, 24.9 ppm. **HRMS** m/z (MALDI-TOF) positive ion, calculated for $C_{25}H_{22}BrN_3NaO_2$: $[M+Na]^+$ 498.0793, Found: 498.0794.

N-(2-(1H-indol-3-yl) ethyl)-2-(2-cyanophenyl)-2-(N-phenylformamido) acetamide (90g):

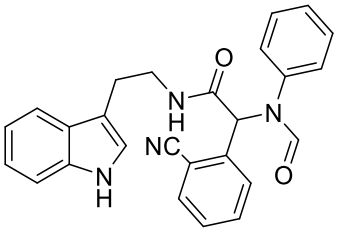

Prepared following general procedure **A** and isolated as a brown solid in 44% yield (270 mg); mp 120-121 °C. **^{1}H-NMR** (400 MHz, $CDCl_3$): δ= 8.32 (s, 1H), 8.12 (s, 1H), 7.46 (d, J = 7.9 Hz, 1H), 7.39 (d, J = 7.5 Hz, 1H), 7.28 (d, J = 7.8 Hz, 1H), 7.23 – 6.90 (m, 11H), 6.50 (t, J = 5.9 Hz, 1H), 6.26 (s, 1H), 3.60 (m, 2H), 2.91 (t, J = 6.6 Hz, 2H) ppm. **^{13}C-NMR** (101 MHz, $CDCl_3$): δ= 168.0, 163.3, 138.2, 137.8, 136.6, 133.3, 132.8, 131.1, 129.3, 129.0, 128.1, 128.0, 127.5, 123.2, 122.2, 119.5, 118.8, 117.4, 113.9, 112.4, 111.6, 61.2, 40.4, 25.2 ppm. **HRMS** m/z (MALDI-TOF) positive ion, calculated for $C_{26}H_{22}KN_4O_2$: $[M+K]^+$ 461.1380, Found: 461.1380.

N-(2-(1H-indol-3-yl) ethyl)-2-(N-(4-fluorophenyl) formamido)-2-phenylacetamide (90h):

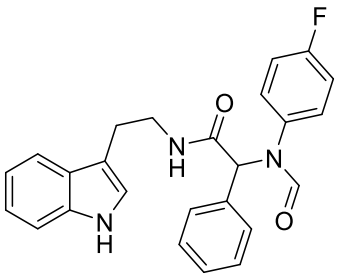

Prepared following general procedure **A** and isolated as a white solid in 54% yield (330 mg); mp 148-149 °C. **^{1}H-NMR** (400 MHz, $CDCl_3$): δ= 8.29 (s, 1H), 8.04 (s, 1H), 7.52 (d, J = 7.9 Hz, 1H), 7.34 (d, J = 8.1 Hz, 1H), 7.19 (m, 4H), 7.12 – 7.01 (m, 5H), 6.92 (s, 1H), 6.87 (t, J = 8.3 Hz, 2H), 5.93 (s, 1H), 5.83 (t, J = 6.0 Hz, 1H), 3.64 (m, 2H), 2.97 (m, 2H). **^{19}F-NMR** (376 MHz, $CDCl_3$): δ= -113.17. **^{13}C-NMR** (101 MHz, $CDCl_3$): δ= 168.9, 163.2, 161.9 (d, $^1J_{C,F}$ = 248.3 Hz, CF), 136.4, 134.8 (d, $^4J_{C,F}$ = 2.9 Hz), 133.7, 130.9, 130.8, 130.0, 128.7 (d, $^3J_{C,F}$ = 8.4 Hz), 127.2, 122.5, 122.0, 119.4, 118.6, 115.7 (d, $^2J_{C,F}$ = 22.7 Hz), 112.3, 111.4, 63.4, 40.2, 25.0 ppm. **HRMS** m/z (MALDI-TOF) positive ion, calculated for $C_{25}H_{22}FKN_3O_2$: $[M+K]^+$ 454.1333, Found: 454.1330.

N-(2-(1H-indol-3-yl) ethyl)-2-(N-(4-chlorophenyl) formamido)-2-phenylacetamide (90i):

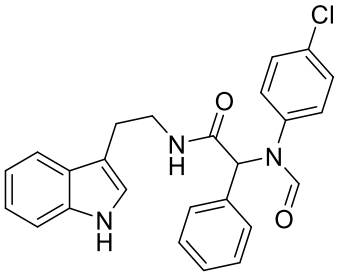

Prepared following general procedure **A** and isolated as a white solid in 51% yield (324 mg); mp 135-136 °C. **^{1}H-NMR** (400 MHz, $CDCl_3$): δ= 8.18 (s, 1H), 8.12 (s, 1H), 7.43 (d, J = 7.9 Hz, 1H), 7.24 (d, J = 8.1 Hz, 1H), 7.20 – 6.90 (m, 11H), 6.81 (s, 1H), 5.85 (m, 2H), 3.54 (m, 2H), 2.95 – 2.77 (m, 2H) ppm. **^{13}C-NMR** (101 MHz, $CDCl_3$): δ= 168.6, 162.8, 137.5, 136.3, 133.8, 133.6, 129.9, 129.8, 129.0, 128.7, 128.6, 127.2, 122.3, 122.0, 119.4, 118.5, 112.4, 111.2, 63.4, 40.1, 25.0 ppm. **HRMS** m/z (MALDI-TOF) negative ion, calculated for $C_{25}H_{21}ClN_3O_2$: $[M-H]^-$ 430.1322, Found: 430.1321.

N-(2-(1H-indol-3-yl) ethyl)-2-(N-(4-nitrophenyl) formamido)-2-phenylacetamide (90j):

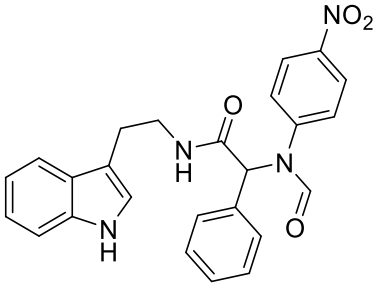

Prepared following general procedure **A** and isolated as a yellow solid in 41% yield (264 mg); mp 101-102 °C. **^{1}H-NMR** (400 MHz, $CDCl_3$): δ= 8.30 (s, 1H), 8.07 (s, 1H), 7.99 – 7.90 (m, 2H), 7.44 (d, J = 7.9 Hz, 1H), 7.24 (d, J = 8.2, 1H), 7.21 – 7.16 (m, 2H), 7.16 – 6.94 (m, 7H), 6.85 (s, 1H), 5.95 (s, 1H), 5.88 (t, J = 6.2 Hz, 1H), 3.57 (m, 2H), 2.89 (m, 2H) ppm. **^{13}C-NMR** (101 MHz, $CDCl_3$): δ=

168.2, 162.3, 146.4, 144.9, 136.3, 133.2, 129.5, 128.94, 128.87, 127.9, 127.2, 124.2, 122.3, 122.2, 119.5, 118.5, 112.4, 111.2, 63.3, 40.2, 25.0 ppm. **HRMS** m/z (MALDI-TOF) negative ion, calculated for $C_{25}H_{21}N_4O_4$: $[M-H]^-$ 441.1563, Found: 441.1558.

N-(2-(1H-indol-3-yl) ethyl)-2-(N-(4-methoxyphenyl) formamido)-2-phenylacetamide (90k):

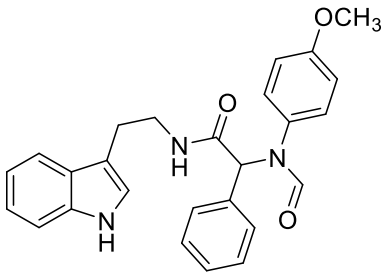

Prepared following general procedure **A** and isolated as a white solid in 52% yield (327 mg); mp 119-120 °C. **^{1}H-NMR** (400 MHz, $CDCl_3$): δ= 8.36 (s, 1H), 8.26 (s, 1H), 7.52 (d, J = 7.9 Hz, 1H), 7.32 (d, J = 8.1 Hz, 1H), 7.24 – 7.03 (m, 7H), 7.01 – 6.93 (m, 2H), 6.88 (d, J = 2.3 Hz, 1H), 6.71 – 6.64 (m, 2H), 6.00 (t, J = 5.8 Hz, 1H), 5.94 (s, 1H), 3.73 (s, 3H), 3.61 (m, 2H), 3.03 – 2.85 (m, 2H) ppm. **^{13}C-NMR** (101 MHz, $CDCl_3$): δ= 168.9, 163.3, 159.00, 136.3, 134.0, 131.6, 130.04, 129.95, 128.44, 128.42, 127.2, 122.4, 121.9, 119.3, 118.5, 113.9, 112.4, 111.2, 63.6, 55.3, 40.1 25.0 ppm. **HRMS** m/z (MALDI-TOF) positive ion, calculated for $C_{26}H_{25}KN_3O_3$: $[M+K]^+$ 466.1533, Found: 466.1536.

N-(2-(1H-indol-3-yl) ethyl)-2-(N-(4-iodophenyl) formamido)-2-phenylacetamide (90l):

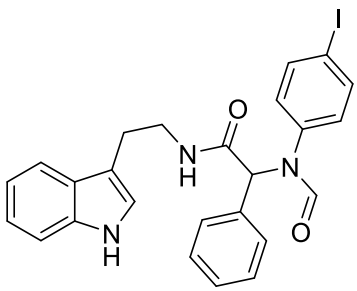

Prepared following general procedure **A** and isolated as a white solid in 45% yield (346 mg); mp 102-103 °C. **^{1}H-NMR** (400 MHz, $CDCl_3$): δ= 8.21 (s, 1H), 8.15 (s, 1H), 7.41 (m, 3H), 7.25 – 6.91 (m, 8H), 6.79 (d, J = 2.1 Hz, 1H), 6.72 (d, J = 8.1 Hz, 2H), 5.90 (t0, J = 5.7 Hz, 1H), 5.84 (s, 1H), 3.51 (m, 2H), 2.93 – 2.75 (m, 2H) ppm. **^{13}C-NMR** (101 MHz, $CDCl_3$) δ = 168.6, 162.7, 138.7, 138.0, 136.3, 133.5, 130.1, 129.7, 128.67, 128.63, 127.1, 122.4, 122.0, 119.3, 118.5, 112.3, 111.2, 93.2, 63.3, 40.1, 24.9 ppm. **HRMS** m/z (MALDI-TOF) negative ion, calculated for $C_{25}H_{21}IN_3O_2$: $[M-H]^-$ 522.0678, Found: 522.0675.

N-(2-(1H-indol-3-yl) ethyl)-2-phenyl-2-(N-*p*-tolylformamido) acetamide (90m): Prepared

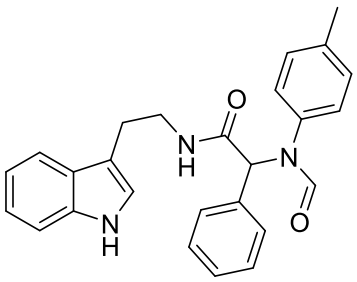

following general procedure **A** and isolated as a white solid in 50% yield (302 mg). mp 116-117 °C. **^{1}H-NMR** (400 MHz, $CDCl_3$): δ= 8.36 (s, 1H), 8.29 (s, 1H), 7.52 (d, J = 7.9 Hz, 1H), 7.32 (d, J = 8.1 Hz, 1H), 7.23 – 7.10 (m, 6H), 7.06 (t, J = 7.4 Hz, 1H), 7.02 – 6.93 (m, 4H), 6.89 (s, 1H), 6.05 (t, J = 5.9 Hz, 1H), 5.90 (s, 1H), 3.62 (m, 2H), 2.95 (m, 2H), 2.28 (s, 3H) ppm. **^{13}C-NMR** (101 MHz, $CDCl_3$): δ= 168.9, 163.3, 137.8, 136.7, 136.4, 134.2, 129.8, 129.6, 128.54, 128.50, 128.1, 127.3, 122.5, 122.0, 119.3, 118.6, 112.5, 111.3, 64.1, 40.2, 25.0, 21.0 ppm. **HRMS** m/z (MALDI-TOF) positive ion, calculated for $C_{26}H_{25}KN_3O_2$: $[M+K]^+$ 450.1584, Found: 450.1585.

N-(2-(1H-indol-3-yl) ethyl) -2-phenyl-2-(N-*p*-tolylformamido) acetamide (90n): Prepared

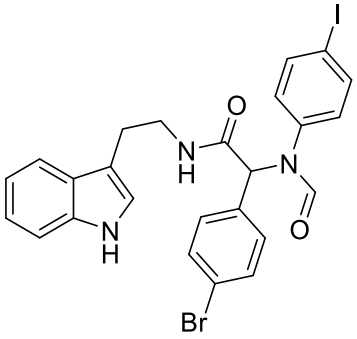

following general procedure **A** and isolated as a brown solid in 54% yield (478 mg), mp 110-111 °C. **^{1}H-NMR** (400 MHz, $CDCl_3$): δ= 8.24 (s, 1H), 8.11 (s, 1H), 7.52 (m, 3H), 7.35 (d, J = 8.1 Hz, 1H), 7.28 (m, 2H), 7.19 (t, J = 7.6 Hz, 1H), 7.07 (t, J = 7.5 Hz, 1H), 6.94 (m, 3H), 6.80 (d, J = 8.1 Hz, 2H), 5.89 (t, J = 5.8 Hz, 1H), 5.84 (s, 1H), 3.71 – 3.54 (m, 2H), 2.96 (m, 2H) ppm. **^{13}C-NMR** (101 MHz, $CDCl_3$): δ= 168.1, 162.7, 138.5, 138.3, 136.3, 132.6, 131.8, 131.4, 130.0, 127.1, 123.0, 122.3, 122.2, 119.5, 118.5, 112.4, 111.3, 93.5, 62.6, 40.1, 24.8 ppm. **HRMS** m/z (MALDI-TOF) positive ion, calculated for $C_{25}H_{21}BrIN_3NaO_2$: $[M+Na]^+$ 623.9760, Found: 623.9761

N-(2-(1H-indol-3-yl) ethyl)-2-(N-(4-iodophenyl) formamido)-2-(3-methoxyphenyl) acetamide (90o): 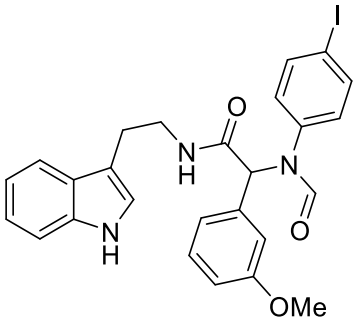 Prepared following general procedure **A** and isolated as a white solid in 37% yield (301 mg); mp 120-121 °C. **^{1}H-NMR** (400 MHz, $CDCl_3$): δ= 8.29 (s, 1H), 8.19 (s, 1H), 7.59 – 7.51 (m, 3H), 7.35 (d, J = 8.1 Hz, 1H), 7.23 – 7.05 (m, 3H), 6.94 (d, J = 2.3 Hz, 1H), 6.91 – 6.85 (m, 2H), 6.80 (dd, J = 8.4, 2.5 Hz, 1H), 6.76 – 6.66 (m, 2H), 5.94 (t, J = 5.8 Hz, 1H), 5.89 (s, 1H), 3.76 – 3.54 (m, 5H), 2.98 (m, 2H) ppm. **^{13}C-NMR** (101 MHz, $CDCl_3$): δ= 168.5, 162.7, 159.7, 139.0, 138.1, 136.4, 135.1, 130.2, 129.8, 127.2, 122.4, 122.11, 122.10, 119.5, 118.6, 115.3, 114.5, 112.5, 111.2, 93.3, 63.5, 55.3, 40.2, 25.0 ppm. **HRMS** m/z (MALDI-TOF) positive ion, calculated for $C_{26}H_{25}IN_3O_3$: $[M+H]^+$ 554.0941, Found: 554.0944.

N-(2-(1H-indol-3-yl) ethyl)-2-(3-bromophenyl)-2-(N-(4-fluorophenyl) formamido) acetamide (90p): 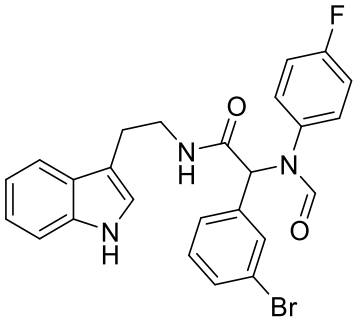 Prepared following general procedure **A** and isolated as a yellow solid in 54% yield (392 mg), mp 102-103 °C. **^{1}H-NMR** (400 MHz, $CDCl_3$): δ= 8.24 (s, 1H), 8.15 (s, 1H), 7.52 (d, J = 7.9 Hz, 1H), 7.41 – 7.29 (m, 3H), 7.17 (m, 1H), 7.12 – 6.98 (m, 5H), 6.96 (d, J = 2.4 Hz, 1H), 6.94 – 6.87 (m, 2H), 5.95 (t, J = 5.8 Hz, 1H), 5.84 (s, 1H), 3.73 – 3.54 (m, 2H), 2.98 (m, 2H) ppm. **^{19}F-NMR** (376 MHz, $CDCl_3$) δ -112.73 ppm. **^{13}C-NMR** (101 MHz, $CDCl_3$): δ= 168.1, 163.3, 162.1 (d, $^{1}J_{C,F}$ = 248.7 Hz, CF), 136.4, 136.0, 134.6 (d, $^{4}J_{C,F}$ = 2.9 Hz), 132.9, 131.9, 130.6 (d, $^{3}J_{C,F}$ = 8.8 Hz), 130.1. 128.5, 127.2, 122.5, 122.4, 122.2, 119.5, 118.6, 115.9 (d, $^{2}J_{C,F}$ = 22.7 Hz), 112.5, 111.3, 62.8, 40.2, 25.0 ppm. **HRMS** m/z (MALDI-TOF) negative ion, calculated for $C_{25}H_{20}BrFN_3O_2$: $[M-H]^-$ 492.0723, Found: 492.0720.

N-(2-(1H-indol-3-yl) ethyl)-2-(N-(4-bromo-3-fluorophenyl) formamido)-2-(3-bromophenyl) acetamide (90q): 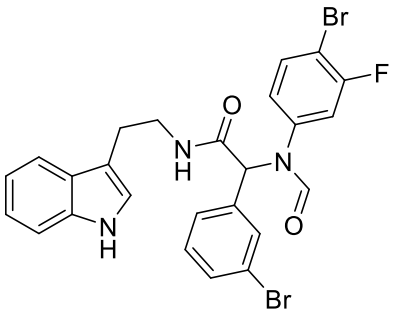

Prepared following general procedure **A** and isolated as a yellow solid in 46% yield (387 mg); mp 106-107 °C. **^{1}H-NMR** (400 MHz, $CDCl_3$): δ= 8.24 (s, 1H), 8.14 (s, 1H), 7.51 (d, J = 7.9 Hz, 1H), 7.43 – 7.29 (m, 4H), 7.21 – 7.13 (m, 1H), 7.11 – 6.93 (m, 5H), 6.76 (m, 1H), 5.94 (t, J = 5.9 Hz, 1H), 5.84 (s, 1H), 3.63 (m, 2H), 2.97 (m, 2H) ppm. **^{19}F-NMR** (376 MHz, $CDCl_3$): δ= -104.06 ppm. **^{13}C-NMR** (101 MHz, $CDCl_3$): δ= 167.8, 162.5, 158.8 (d, $^1J_{C,F}$ = 249.8 Hz, CF), 139.4 (d, $^3J_{C,F}$ = 8.4 Hz), 136.4, 135.6, 133.6, 132.7, 132.1, 130.3, 128.2, 127.2, 124.9 (d, $^4J_{C,F}$ = 3.7 Hz), 122.8, 122.4, 122.2, 119.5, 118.5, 116.6 (d, $^2J_{C,F}$ = 23.8 Hz), 112.4, 111.3, 108.9 (d, $^2J_{C,F}$ = 20.9 Hz), 62.7, 40.2, 24.9 ppm. **HRMS** m/z (MALDI-TOF) positive ion, calculated for $C_{25}H_{20}Br_2FKN_3O_2$: $[M+K]^+$ 609.9543, Found: 609.9539.

N-(2-(1H-indol-3-yl) ethyl)-2-(4-fluorophenyl)-2-(N-(4-methoxyphenyl) formamido) acetamide (90r): 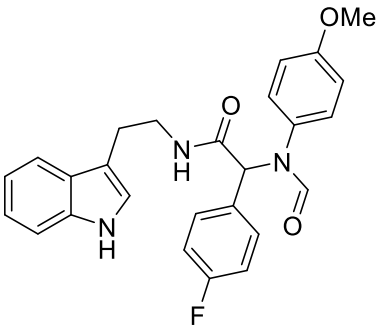

Prepared following general procedure **A** and isolated as a white solid in 50% yield (327 mg); mp 146-147 °C. **^{1}H-NMR** (400 MHz, $CDCl_3$): δ= 8.23 (s, 1H), 8.20 (s, 1H), 7.53 (d, J = 7.9 Hz, 1H), 7.34 (d, J = 8.1 Hz, 1H), 7.18 (t, J = 7.5 Hz, 1H), 7.11 – 7.02 (m, 3H), 6.96 – 6.88 (m, 3H), 6.83 (t, J = 8.6, 2H), 6.69 (d, J = 8.5 Hz, 2H), 5.97 (t, J = 5.8 Hz, 1H), 5.91 (s, 1H), 3.75 (s, 3H), 3.70 – 3.56 (m, 2H), 2.97 (m, 2H) ppm. **^{19}F-NMR** (376 MHz, $CDCl_3$) δ -112.67 ppm. **^{13}C-NMR** (101 MHz, $CDCl_3$): δ= 168.7, 163.2, 162.6 (d, $^1J_{C,F}$ = 248.7 Hz, CF), 159.2, 136.4, 131.9 (d, $^3J_{C,F}$ = 8.4 Hz), 131.2, 130.2, 129.8 (d, $^4J_{C,F}$ = 3.7 Hz), 127.2, 122.3, 122.1, 119.4, 118.6, 115.4 (d, $^2J_{C,F}$ = 21.6 Hz), 114.0, 112.5, 111.2, 62.5, 55.4, 40.1, 24.9 ppm. **HRMS** m/z (MALDI-TOF) negative ion, calculated for $C_{26}H_{23}FN_3O_3$: $[M-H]^-$ 444.1723, Found: 444.1720.

N-(2-(1H-indol-3-yl) ethyl)-2-(1H-indol-2-yl)-2-(N-phenylformamido) acetamide (90s):

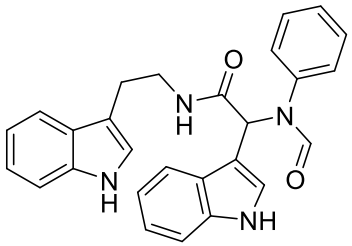

Prepared following general procedure **A** and isolated as a white solid in 48% yield (308 mg), mp 105-106 °C. **^{1}H-NMR** (400 MHz, $CDCl_3$): δ= 8.88 (s, 1H), 8.35 (s, 1H), 8.17 (s, 1H), 7.31 (d, J = 7.9 Hz, 1H), 7.22 (d, J = 8.0 Hz, 1H), 7.12 (m, 2H), 7.04 – 6.83 (m, 9H), 6.80 (d, J = 2.6 Hz, 1H), 6.48 (d, J = 2.3 Hz, 1H), 6.24 (s, 1H), 6.12 (t, J = 5.8 Hz, 1H), 3.48 (m, 1H), 3.32 (m, 1H), 2.71 (m, 2H) ppm. **^{13}C-NMR** (101 MHz, $CDCl_3$): δ= 169.4, 163.2, 139.5, 136.5, 135.8, 128.9, 127.7, 127.6, 127.2, 126.7, 126.3, 122.6, 122.5, 121.9, 120.2, 119.3, 118.6, 118.3, 112.1, 111.8, 111.4, 108.2, 56.0, 40.1, 24.9 ppm. **HRMS** m/z (MALDI-TOF) positive ion, calculated for $C_{27}H_{24}KN_4O_2$: $[M+K]^+$ 475.1536, Found: 475.1536.

N-(2-(1H-indol-3-yl) ethyl)-2-phenyl-2-(N-propylformamido) acetamide (90t): Prepared following general procedure A and isolated as a white oil in 58% yield (310 mg); mp 87-88 °C; The NMR spectra contain two sets of signals originating from different orientations of the formyl group. **^{1}H-NMR** (400 MHz, $CDCl_3$): δ= 8.59 (s, 1H, minor), 8.44 (s, 1H, major), 7.97 (s, 1H, major), 7.89 (s, 1H, minor), 7.44-7.39 (m, 1H+1H, major+minor), 7.25 – 7.12 (m, 5H+5H, major+minor), 7.10 – 7.01 (m, 2H+2H, major+minor), 7.00-6.93 (m, 1H+1H, major+minor), 6.77-6.76 (m, 1H+1H, major+minor), 6.24 (t, J = 5.8 Hz, 1H, mionr), 6.13 (t, J = 5.8 Hz, 1H, major), 5.54 (s, 1H, major), 4.81 (s, 1H, minor), 3.61 – 3.50 (m, 2H, minor), 3.49-3.37 (m, 2H, major), 3.16 – 2.96 (m, 2H+2H, major+minor), 2.92-2.84 (m, 2H, minor), 2.82-2.75 (m, 2H, major), 1.15 – 0.95 (m, 2H+2H, major+minor), 0.63 (t, J = 7.4 Hz, 3H, minor), 0.57 (t, J = 7.4 Hz, 3H, major) ppm. **^{13}C-NMR** (101 MHz, $CDCl_3$): δ= 169.1 (major), 168.9 (minor), 163.74 (minor), 163.69 (major), 136.54 (minor), 136.45 (major), 135.1 (minor), 134.7 (major), 129.3 (major), 129.07 (minor), 129.04 (major), 128.84 (major), 128.78 (major), 128.7 (minor), 128.6 (major), 128.3 (minor), 127.3 (major+minor), 125.3 (minor), 122.51 (major), 122.48 (minor), 122.1 (minor), 121.9 (major), 119.4 (minor), 119.3 (major), 118.6 (major), 118.5 (minor), 112.3 (major), 112.1 (minor), 111.5 (minor), 111.4 (major), 65.7 (minor), 61.0 (major), 48.8 (major), 46.0 (minor), 40.13 (minor), 40.09 (major), 25.05 (minor), 25.00 (major), 23.3

(major), 21.0 (minor), 11.3 (minor), 11.0 (major) ppm. **HRMS** m/z (MALDI-TOF) positive ion, calculated for $C_{22}H_{25}KN_3O_2$: [M+K]+ 402.1584, Found: 402.1583.

N-(2-(1H-indol-3-yl) ethyl)-2-(N-phenylformamido) hexanamide (90u) : Prepared following

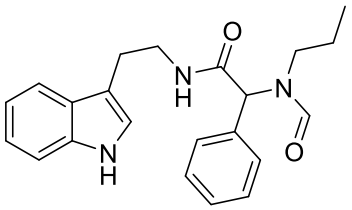

general procedure **A** and isolated as a white solid in 30% yield (166 mg); mp 92-93 °C. **^{1}H-NMR** (400 MHz, $CDCl_3$): δ= 8.38 (s, 1H), 8.23 (s, 1H), 7.60 (d, J = 7.8 Hz, 1H), 7.39 – 7.22 (m, 4H), 7.19 – 7.10 (m, 3H), 7.09 – 7.04 (m, 1H), 7.02 (d, J = 2.4 Hz, 1H), 6.65 (t, J = 5.8 Hz, 1H), 4.84 (m, 1H), 3.77 – 3.52 (m, 2H), 3.00 (t, J = 6.9 Hz, 2H), 1.92 – 1.78 (m, 1H), 1.55 (m, 1H), 1.37 – 1.06 (m, 4H), 0.78 (t, J = 6.8 Hz, 3H) ppm. **^{13}C-NMR** (101 MHz, $CDCl_3$): δ= 170.6, 163.8, 138.2, 136.4, 129.3, 127.6, 127.3, 126.1, 122.2, 121.9, 119.2, 118.6, 112.5, 111.2, 57.5, 39.9, 28.2, 27.2, 25.1, 22.1, 13.7 ppm. **HRMS** m/z (MALDI-TOF) negative ion, calculated for $C_{23}H_{26}N_3O_2$: $[M-H]^-$ 376.2025, Found: 376.2020.

N-(2-(1H-indol-3-yl) ethyl)-2-(N-*p*-tolylformamido) heptanamide (90v): Prepared following

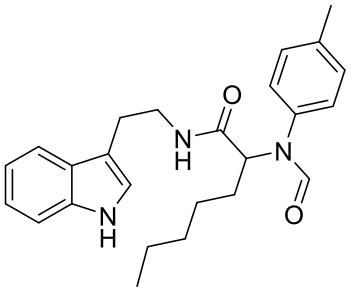

general procedure **A** and isolated as a white solid in 33% yield (197 mg); mp 92-93 °C. **^{1}H-NMR** (400 MHz, $CDCl_3$): δ= 8.21 (s, 1H), 8.11 (s, 1H), 7.61 (d, J = 7.9 Hz, 1H), 7.34 (d, J = 8.1 Hz, 1H), 7.22 – 6.97 (m, 7H), 6.60 (t, J = 6.0 Hz, 1H), 4.81 (t, J = 7.6 Hz, 1H), 3.76 – 3.53 (m, 2H), 3.00 (t, J = 6.9 Hz, 2H), 2.35 (s, 3H), 1.81 (m, 1H), 1.66 (m, 1H), 1.49 (m, 1H), 1.24 – 1.13 (m, 5H), 0.80 (t, J = 6.6 Hz, 3H) ppm. **^{13}C-NMR** (101 MHz, $CDCl_3$): δ= 170.7, 163.9, 137.7, 136.4, 135.7, 129.9, 127.4, 126.2, 122.15, 122.11, 119.4, 118.8, 112.8, 111.2, 57.5, 39.8, 31.3, 27.5, 25.8, 25.2, 22.3, 21.0, 13.9 ppm. **HRMS** m/z (MALDI-TOF) negative ion, calculated for $C_{25}H_{30}N_3O_2$: $[M-H]^-$ 404.2338, Found: 404.2340.

(4R)-N-(2-(1H-indol-3-yl)ethyl)-2-(N-(4-fluorophenyl)formamido)-4-phenylpentanamide

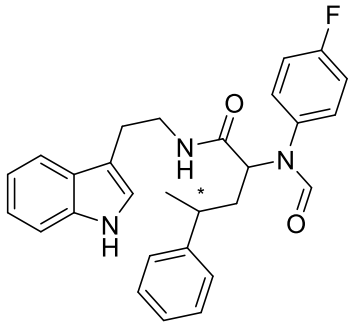

(90w): Prepared following general procedure **A** and isolated as a white solid in 50% yield (336 mg) and obtained as a mixture of diastereoisomers; mp 111-112 °C. The NMR spectra contain two sets of signals originating from different orientations of the formyl group and only for the ^{19}F NMR are evident the different shift for diastereoisomers. **^{1}H-NMR** (400 MHz, $CDCl_3$): δ= 8.29 – 8.26 (m, 1H+1H, major+minor), 8.02 (s, 1H, major), 7.92 (s, 1H, minor), 7.49 (d, J = 7.9 Hz, 1H, minor), 7.45 (d, J = 7.9 Hz, 1H, major), 7.22 – 7.00 (m, 5H+5H, major+minor), 7.00 – 6.80 (m, 8H+8H, major+minor), 6.40 (t, J = 5.8 Hz, 1H minor), 6.30 (t, J = 5.8 Hz, 1H major), 4.58 (m, 1H+1H, major+minor), 3.55 (m, 1H+2H, major+minor), 3.37 (m, 1H, major), 2.85 (m, 2H+2H, major+minor), 2.58 – 2.44 (m, 1H, minor), 2.41 (m, 1H, major), 2.05 – 1.90 (m, 1H+1H, major+minor), 1.76 (m, 1H, major), 1.55 (m, 1H, minor), 1.07 (d, J = 7.0 Hz, 3H, minor), 0.99 (d, J = 7.0 Hz, 3H, major) ppm. **^{19}F-NMR** (376 MHz, $CDCl_3$): δ= -113.32, -113.34, -113.39, -113.41 ppm. **^{13}C-NMR** (101 MHz, $CDCl_3$): δ= 170.5 (major), 170.3 (minor), 163.8 (major), 163.5 (minor), 161.9 (d, $^{1}J_{C,F}$= 248.3 Hz, CF, minor), 161.8 (d, $^{1}J_{C,F}$ = 248.3 Hz, CF, major), 145.8 (major), 145.3 (minor), 136.49 (minor), 136.45 (major), 134.2 (d, $^{4}J_{C,F}$ = 2.9 Hz, major), 134.1 (d, $^{4}J_{C,F}$ = 3.3 Hz, minor), 128.7, 128.6 (d, $^{3}J_{C,F}$ = 8.8 Hz, minor) 128.1 (d, $^{3}J_{C,F}$ = 8.4 Hz, major), 127.39 (minor), 127.38 (major), 127.1 (major), 126.8 (minor), 126.6 (major), 126.5 (minor), 122.3 (major+minor), 122.10 (minor), 122.07 (major), 119.41 (minor), 119.37 (major), 118.70 (minor), 118.66 (major), 116.3 (d, $^{2}J_{C,F}$= 22.7 Hz, major), 116.2 (d, $^{2}J_{C,F}$ = 22.7 Hz, minor), 112.49 (minor), 112.48 (major), 111.4 (minor), 111.3 (major), 55.6 (major), 55.5 (minor), 40.0 (major), 39.9 (minor), 36.7 (major), 36.5 (minor), 36.4 (major), 36.0 (minor), 25.2 (minor), 25.0 (major), 22.3 (major+minor) ppm. **HRMS** m/z (MALDI-TOF) positive ion, calculated for $C_{28}H_{28}FKN_3O_2$: $[M+K]^+$ 496.1803, Found: 496.1800.

N-(2-(1H-indol-3-yl)ethyl)-3-phenyl-2-(N-phenylformamido)butanamide (90x): Prepared

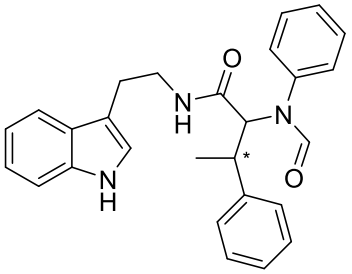

following general procedure **A** and isolated as a white solid in 30% yield (188 mg) and obtained as a mixture of diastereoisomers; mp 109-110 °C. **^{1}H-NMR** (400 MHz, $CDCl_3$): δ= 8.25 (s, 1H), 7.98 (s, 1H), 7.43 – 7.02 (m, 13H), 6.96 (m, 1.0 Hz, 1H), 6.69 (d, J = 2.3 Hz, 1H), 6.36 (s, 1H), 4.84 (d, J = 11.8 Hz, 1H), 3.47 (m, 1H), 3.36 – 3.23 (m, 2H), 2.63 (m, 2H), 1.03 (d, J = 6.8 Hz, 3H) ppm. **^{13}C-NMR** (101 MHz, $CDCl_3$): δ= 169.1, 164.5, 142.7, 139.5, 136.3, 129.5, 128.5, 127.9, 127.5, 127.3, 126.9, 125.8, 122.0, 119.3, 118.7, 112.7, 111.2, 65.1, 39.6, 37.9, 24.9, 19.2 ppm. **HRMS** m/z (MALDI-TOF) positive ion, calculated for $C_{27}H_{27}KN_3O_2$: $[M+K]^+$ 464.1740, Found: 464.1739.

N-(2-(1H-indol-3-yl) ethyl)-3-methyl-2-(N-phenylformamido) butanamide (90y): Prepared

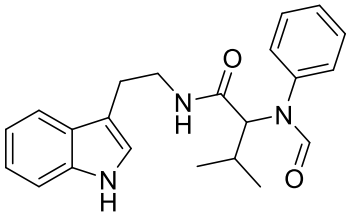

following general procedure **A** and isolated as a white solid in 42% yield (224 mg); mp 90-91 °C. **^{1}H-NMR** (400 MHz, $CDCl_3$): δ= 8.73 (s, 1H), 8.25 (s, 1H), 7.62 (d, J = 7.8 Hz, 1H), 7.43 – 7.27 (m, 6H), 7.18 (t, J = 7.5 Hz, 1H), 7.08 (t, J = 7.4 Hz, 1H), 7.04 – 6.96 (m, 2H), 4.33 (d, J = 11.4 Hz, 1H), 3.68 (m, 2H), 3.01 (t, J = 7.0 Hz, 2H), 2.49 (m, 1H), 0.99 ((d, J = 6.5 Hz, 3H), 0.83 (d, J = 6.6 Hz, 3H) ppm. **^{13}C-NMR** (101 MHz, $CDCl_3$): δ= 170.3, 164.2, 139.8, 136.3, 129.3, 127.3, 127.2, 125.3, 122.1, 121.9, 119.2, 118.6, 112.6, 111.1, 66.9, 39.7, 26.0, 25.2, 19.7, 19.3 ppm. **HRMS** m/z (MALDI-TOF) positive ion, calculated for $C_{22}H_{25}KN_3O_2$: $[M+K]^+$ 402.1584, Found: 402.1579.

N-(2-(1H-indol-3-yl) ethyl)-4-methyl-2-(N-*p*-tolylformamido) pentanamide (90z): Prepared

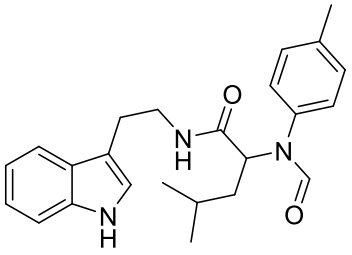

following general procedure **A** and isolated as a white solid in 45% yield (259 mg); mp 86-87 °C. **^{1}H-NMR** (400 MHz, $CDCl_3$): δ 8.60 (d, J = 9.2 Hz, 1H), 8.21 (s, 1H), 7.60 (d, J = 7.8 Hz, 1H), 7.36 – 7.26 (m, 1H), 7.21 – 7.03 (m, 4H), 7.04 – 6.96 (m, 3H), 5.05 – 4.95 (m, 1H), 3.76 – 3.53 (m, 2H), 3.00 (t, J = 6.5 Hz, 2H), 2.34 (s, 3H), 1.76 – 1.63 (m, 1H), 1.57 – 1.41 (m, 2H), 1.13 – 0.89 (m, 3H), 0.85 (d, J = 6.5 Hz, 3H), 0.78 (d, J = 6.5, 3H)

ppm. **^{13}C-NMR** (101 MHz, $CDCl_3$): δ= 170.7, 163.8, 137.6, 136.3, 135.4, 129.8, 127.2, 126.0, 122.2, 121.8, 119.1, 118.5, 112.3, 111.2, 55.4, 39.9, 36.2, 25.0, 24.5, 22.6, 21.9, 20.8 ppm. **HRMS** m/z (MALDI-TOF) positive ion, calculated for $C_{24}H_{29}N_3NaO_2$: $[M+Na]^+$ 414.2157, Found: 414.2155.

N-(2-(1H-indol-3-yl)ethyl)-2-(N-phenylformamido)-2-(pyridin-3-yl)acetamide (90ω):

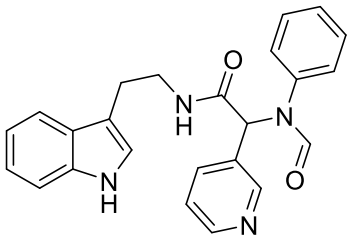

Prepared following general procedure **A** and isolated as a white solid in 51% yield (57 mg); mp 114-117 °C. **^{1}H-NMR** (400 MHz, $CDCl_3$): δ 8.32 (d, J = 4.6 Hz, 1H), 8.30 (s, 1H), 8.27 (s, 1H), 8.21 (s, 1H), 7.45 (d, J = 8.1 Hz, 1H), 7.34 (dt, J = 8.0, 1.9 Hz, 1H), 7.23 (d, J = 8.2 Hz, 1H), 7.15 – 7.11 (m, 3H), 7.08 (td, J = 7.3, 0.9 Hz, 1H), 6.98 (td, J = 7.4, 0.9 Hz, 1H), 6.95 – 6.91 (m, 3H), 6.88 (d, J = 2.2 Hz, 1H), 6.29 (t, J = 5.6 Hz, 1H), 5.85 (s, 1H), 3.61 – 3.55 (m, 2H), 2.93 – 2.88 m, 2H) ppm. **^{13}C-NMR** (101 MHz, $CDCl_3$): δ = 168.0, 163.1, 150.8, 149.6, 138.5, 137.5, 136.4, 130.0, 129.3, 128.3, 128.2, 127.2, 123.1, 122.4, 122.1, 119.5, 118.6, 112.4, 111.3, 61.2, 40.2, 25.0 ppm. **HRMS** m/z (MALDI-TOF) positive ion, calculated for $C_{24}H_{22}N_4NaO_2$: $[M+Na]^+$ 421.1640, Found: 421.1644.

2-(4-methoxyphenyl)-1-phenyl-1,2,5,6,11,11b-hexahydro-3H-imidazo[1',2':1,2]pyrido[3,4-b]indol-3-one (91a): Prepared following general procedure **B** and isolated as a brown solid in 79% yield (129 mg), mp 227-228 °C (dec). **^{1}H-NMR** (400 MHz, $CDCl_3$): δ= 8.23 (s, 1H), 7.54 (d, J = 7.8 Hz, 1H), 7.36 (m, 3H), 7.30 – 7.23 (m, 1H), 7.20-7.15 (m, 1H), 7.07 (d, J = 8.3 Hz, 2H), 6.93 (m, 1H), 6.86 (d, J = 8.2 Hz, 2H), 6.73 (d, J = 8.6 Hz, 2H), 6.49 (s, 1H), 5.06 (s, 1H), 4.63 (dd, *J* = 13.4, 6.4 Hz, 1H), 3.69 (s, 3H), 3.39 (td, J = 12.3, 5.4 Hz, 1H), 2.98 (m, 1H), 2.84 (m, 1H) ppm. **^{13}C-NMR** (101 MHz, $CDCl_3$): δ= 168.9, 159.5, 146.1, 136.5, 132.7, 130.31, 129.95, 127.6, 126.4, 123.1, 120.2, 119.3, 119.0, 114.5, 111.9, 111.7, 110.3, 69.6, 66.8, 55.2, 38.4, 20.5 ppm. **HRMS** m/z (MALDI-TOF) negative ion, calculated for $C_{26}H_{22}N_3O_2$: $[M-H]^-$ 408.1712, Found: 408.1710.

1-phenyl-2-(*p*-tolyl)-1,2,5,6,11,11b-hexahydro-3H-imidazo[1',2':1,2]pyrido[3,4-b]indol-3-one (91b): 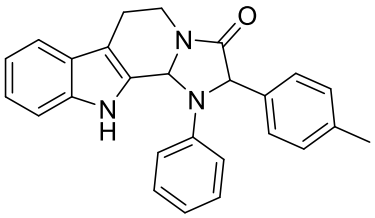

Prepared following general procedure **B** and isolated as a brown solid in 71% yield (111 mg); mp 261-262 °C (dec). **^{1}H-NMR** (400 MHz, $CDCl_3$): δ= 8.21 (s, 1H), 7.53 (d, J = 7.9 Hz, 1H), 7.36 (m, 3H), 7.30 – 7.22 (m, 1H), 7.18 (m, 1H), 7.03 (m, 4H), 6.93 (t, J = 7.4 Hz, 1H), 6.87 (d, J = 8.1 Hz, 2H), 6.50 (s, 1H), 5.08 (s, 1H), 4.63 (dd, *J* = 13.4, 6.4 Hz, 1H), 3.40 (td, J = 12.3, 5.4 Hz, 1H), 2.97 (m, 1H), 2.83 (m, 1H), 2.24 (s, 3H) ppm. **^{13}C-NMR** (101 MHz, $CDCl_3$) δ= 168.8, 146.1, 137.9, 136.5, 134.9, 132.7, 130.3, 129.6, 126.4, 126.3, 123.1, 120.2, 119.3, 118.9, 111.9, 111.6, 110.3, 69.6, 67.0, 38.4, 21.0, 20.4 ppm. **HRMS** m/z (MALDI-TOF) negative ion, calculated for $C_{26}H_{22}N_3O$: $[M-H]^-$ 392.1763, Found: 392.1767.

1,2-diphenyl-1,2,5,6,11,11b-hexahydro-3H-imidazo[1',2':1,2] pyrido[3,4-b] indol-3-one (91c)

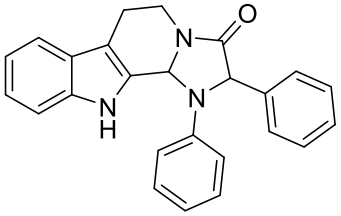

Prepared following general procedure **B** and isolated as a white solid in 85% yield (129 mg), mp 239-240 °C (dec). **^{1}H-NMR** (400 MHz, $CDCl_3$): δ= 8.28 (s, 1H), 7.54 (d, J = 7.8 Hz, 1H), 7.36 (m, 3H), 7.31 – 7.14 (m, 7H), 6.94 (t, J = 7.4 Hz, 1H), 6.85 (d, J = 8.1 Hz, 2H), 6.50 (s, 1H), 5.10 (s, 1H), 4.63 (dd, J = 13.4, 6.4 Hz, 1H), 3.40 (td, J = 12.4, 5.4 Hz, 1H), 3.04 – 2.91 (m, 1H), 2.84 (m, 1H) ppm. **^{13}C-NMR** (101 MHz, $CDCl_3$): δ= 168.6, 146.1, 137.9, 136.5, 132.6, 130.3, 129.0, 128.1, 126.46, 126.44, 123.1, 120.2, 119.4, 119.0, 112.0, 111.7, 110.3, 69.7, 67.3, 38.4, 20.5 ppm. **HRMS** m/z (MALDI-TOF) negative ion, calculated for $C_{25}H_{20}N_3O$: $[M-H]^-$ 378.1606, Found: 378.1606.

2-(4-fluorophenyl)-1-phenyl-1,2,5,6,11,11b-hexahydro-3H-imidazo[1',2':1,2]pyrido[3,4-b] indol-3-one (91d): 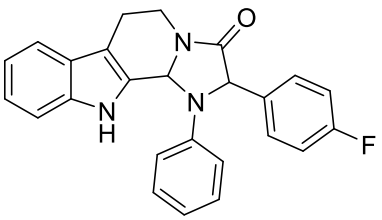

Prepared following general procedure **B** and isolated as a brown solid in 90% yield (143 mg), mp 236-237 °C (dec). **^{1}H-NMR** (400 MHz, $CDCl_3$): δ= 8.26 (s, 1H), 7.54 (d, J = 7.9 Hz, 1H), 7.41 – 7.32 (m, 3H), 7.26 (m, 1H), 7.22 – 7.11 (m, 3H), 6.90 (m, 5H), 6.49 (s, 1H), 5.07 (s, 1H), 4.62 (dd, J = 13.4, 6.4 Hz, 1H), 3.40 (td, J = 12.3, 5.4 Hz, 1H), 2.98 (m, 1H), 2.84 (m, 1H) ppm. **^{19}F-NMR** (376 MHz, $CDCl_3$): δ= -114.22 ppm. **^{13}C-NMR** (101

MHz, $CDCl_3$): δ= 168.4, 162.7 (d, $^1J_{C,F}$ = 246.5 Hz, CF), 146.0, 136.5, 133.6 (d, $^4J_{C,F}$ = 3.3 Hz), 132.5, 130.4, 128.1 (d, $^3J_{C,F}$ = 8.1 Hz), 126.4, 123.3, 120.3, 119.6, 119.0, 115.9 (d, $^2J_{C,F}$ = 21.6 Hz), 112.0, 111.7, 110.4, 69.7, 66.7, 38.5, 20.5 ppm. **HRMS** m/z (MALDI-TOF) positive ion, calculated for $C_{25}H_{21}FN_3O$: $[M+H]^+$ 398.1669, Found: 398.1667.

2-(3-methoxyphenyl)-1-phenyl-1,2,5,6,11,11b-hexahydro-3H-imidazo[1',2':1,2]pyrido[3,4-b]indol-3-one (91e): 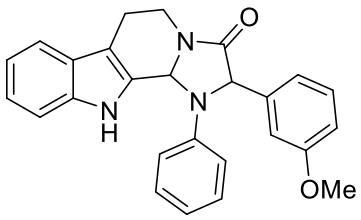

Prepared following general procedure **B** and isolated as a yellow solid in 69% yield (113 mg); mp 166-167 °C. **^{1}H-NMR** (400 MHz, $CDCl_3$): δ= 8.24 (s, 1H), 7.52 (d, J = 7.8 Hz, 1H), 7.42 – 7.28 (m, 3H), 7.23 (m, 1H), 7.19 – 7.09 (m, 2H), 6.97 – 6.80 (m, 4H), 6.72 (m, 1H), 6.51 (m, 2H), 5.08 (s, 1H), 4.63 (dd, J = 13.4, 6.4 Hz, 1H), 3.42 (m, 1H), 3.20 (s, 3H), 3.00 (m, 1H), 2.92 – 2.79 (m, 1H) ppm. **^{13}C-NMR** (101 MHz, $CDCl_3$): δ= 168.8, 160.1, 145.7, 139.7, 136.5, 132.8, 130.3, 129.9, 126.4, 123.2, 120.3, 119.2, 119.0, 118.8, 114.8, 111.6, 111.5, 110.5, 110.4, 69.4, 67.0, 54.5, 38.5, 20.4 ppm. **HRMS** m/z (MALDI-TOF) positive ion, calculated for $C_{26}H_{23}KN_3O_2$: $[M+K]^+$ 448.1427, Found: 448.1430.

2-(3-bromophenyl)-1-phenyl-1,2,5,6,11,11b-hexahydro-3H-imidazo[1',2':1,2]pyrido[3,4-b]indol-3-one (91f): 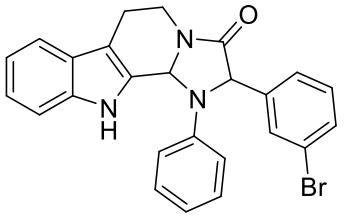

Prepared following general procedure **B** and isolated as a yellow solid in 68% yield (125 mg); mp 159-160 °C. **^{1}H-NMR** (400 MHz, $CDCl_3$): δ= 8.19 (s, 1H), 7.53 (d, J = 7.8 Hz, 1H), 7.40 – 7.30 (m, 5H), 7.28 – 7.24 (m, 1H), 7.17 (m, 1H), 7.08 – 7.00 (m, 2H), 6.97 (t, J = 7.4 Hz, 1H), 6.83 (d, J = 8.2 Hz, 2H), 6.51 (s, 1H), 5.06 (s, 1H), 4.62 (dd, J = 13.4, 6.4 Hz, 1H), 3.41 (m, 1H), 2.98 (m, 1H), 2.89 – 2.79 (m, 1H) ppm. **^{13}C-NMR** (101 MHz, $CDCl_3$): δ= 168.0, 145.8, 140.1, 136.5, 132.3, 131.3, 130.5, 130.4, 129.8, 126.4, 124.8, 123.3, 123.0, 120.3, 119.7, 119.0, 112.0, 111.6, 110.5, 69.7, 66.6, 38.5, 20.4 ppm. **HRMS** m/z (MALDI-TOF) negative ion, calculated for $C_{25}H_{19}BrN_3O$: $[M-H]^-$ 456.0711, Found: 456.0715.

1-(4-fluorophenyl)-2-phenyl-1,2,5,6,11,11b-hexahydro-3H-imidazo[1',2':1,2]pyrido[3,4-b]indol-3-one (91h): 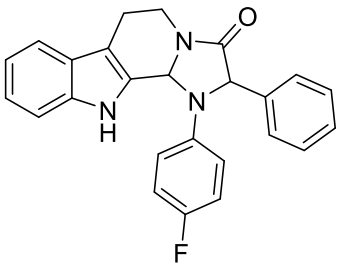

Prepared following general procedure **B** and isolated as a yellow solid in 74% yield (118 mg); mp 230-231 (dec). **^{1}H-NMR** (400 MHz, $CDCl_3$): δ= 8.34 (s, 1H), 7.65 (d, J = 7.8 Hz, 1H), 7.49 (d, J = 8.1 Hz, 1H), 7.46 – 7.23 (m, 7H), 7.14 (t, J = 8.5 Hz, 2H), 6.86 (m, 2H), 6.54 (s, 1H), 5.11 (s, 1H), 4.73 (dd, J = 13.4, 6.4 Hz, 1H), 3.50 (td, J = 12.4, 5.4 Hz, 1H), 3.14 – 3.02 (m, 1H), 2.95 (m, 1H) ppm. **^{19}F-NMR** (376 MHz, $CDCl_3$): δ= -125.20 ppm. **^{13}C-NMR** (101 MHz, $CDCl_3$): δ= 168.4, 156.7 (d, $^{1}J_{C,F}$ = 238.8 Hz, CF), 142.6 (d, $^{4}J_{C,F}$ = 2.2 Hz), 137.7, 136.5, 132.4, 129.0, 128.2, 126.40, 126.38, 123.2, 120.2, 118.9, 116.8 (d, $^{2}J_{C,F}$ = 22.4 Hz), 112.9 (d, $^{3}J_{C,F}$ = 7.3 Hz), 111.7, 110.4, 70.0, 67.8, 38.4, 20.4 ppm. **HRMS** m/z (MALDI-TOF) positive ion, calculated for $C_{25}H_{21}FN_3O$: $[M+H]^+$ 398.1669, Found: 398.1672.

1-(4-chlorophenyl)-2-phenyl-1,2,5,6,11,11b-hexahydro-3H-imidazo[1',2':1,2]pyrido [3,4-b]indol-3-one (91i): 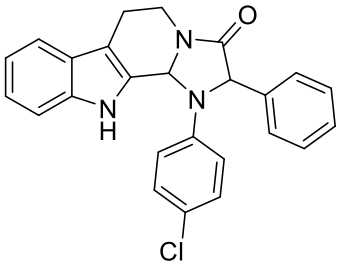

Prepared following general procedure **B** and isolated as a yellow solid in 77% yield (128 mg); mp 249-250 °C. **^{1}H-NMR** (400 MHz, $CDCl_3$): δ= 8.24 (s, 1H), 7.55 (d, J = 7.9 Hz, 1H), 7.40 (d, J = 8.1 Hz, 1H), 7.36 – 7.11 (m, 9H), 6.76 (d, J = 8.4 Hz, 2H), 6.49 (s, 1H), 5.02 (s, 1H), 4.64 (dd, J = 13.4, 6.4 Hz, 1H), 3.42 (td, J = 12.4, 5.3 Hz, 1H), 2.99 (m, 1H), 2.86 (m, 1H) ppm. **^{13}C-NMR** (101 MHz, $CDCl_3$): δ= 168.3, 144.6, 137.4, 136.5, 132.1, 130.1, 129.0, 128.3, 126.4, 126.3, 124.4, 123.3, 120.3, 119.0, 113.0, 111.7, 110.6, 69.7, 67.3, 38.4, 20.4 ppm. **HRMS** m/z (MALDI-TOF) negative ion, calculated for $C_{25}H_{19}ClN_3O$: $[M-H]^-$ 412.1217, Found: 412.1216.

1-(4-nitrophenyl)-2-phenyl-1,2,5,6,11,11b-hexahydro-3H-imidazo[1',2':1,2]pyrido[3,4-b]indol-3-one (91j): 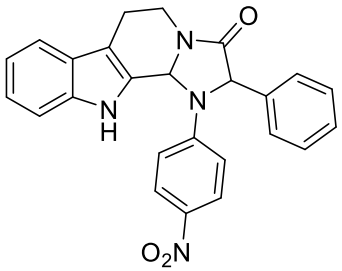

Prepared following general procedure **B** and isolated as a white solid in 64% yield (109 mg); mp 246-247 °C (dec). **^{1}H-NMR** (400 MHz, DMSO): δ= 10.83 (s, 1H), 8.26 (d, J = 9.2 Hz, 2H), 7.50 (t, J = 7.5 Hz, 2H), 7.27 – 6.92 (m, 10H), 5.55 (s, 1H), 4.45 – 4.35 (m, 1H), 3.51 (m, 1H), 2.88 – 2.73 (m, 2H) ppm. **^{13}C-NMR** (101 MHz, DMSO): δ= 168.4, 151.2, 139.2, 137.6, 137.3, 132.3, 129.1, 128.5, 126.9, 126.5, 126.4, 122.8, 119.7, 118.9, 112.8, 110.0, 79.7, 70.2, 65.6, 38.6, 20.3 ppm. **HRMS** m/z (MALDI-TOF) positive ion, calculated for $C_{25}H_{20}N_4NaO_3$: $[M+Na]^+$ 447.1433, Found: 447.1435.

1-(4-methoxyphenyl)-2-phenyl-1,2,5,6,11,11b-hexahydro-3H-imidazo[1',2':1,2]pyrido[3,4-b]indol-3-one (91k): 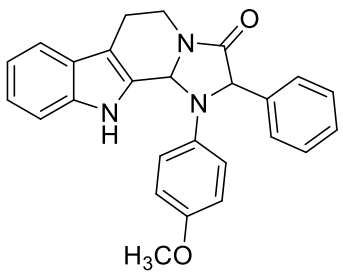

Prepared following general procedure **B** and isolated as a yellow solid in 60% yield (98 mg); mp 239-240 °C. **^{1}H-NMR** (400 MHz, $CDCl_3$): δ= 8.25 (s, 1H), 7.59 (d, J = 7.8 Hz, 1H), 7.42 (d, J = 8.1 Hz, 1H), 7.35 – 7.19 (m, 7H), 6.97 (d, J = 9.0 Hz, 2H), 6.86 (d, J = 9.0 Hz, 2H), 6.47 (s, 1H), 5.07 (s, 1H), 4.68 (dd, J = 13.4, 6.4 Hz, 1H), 3.83 (s, 3H), 3.44 (td, J = 12.4, 5.4 Hz, 1H), 3.09 – 2.96 (m, 1H), 2.89 (dd, J = 15.8, 5.3 Hz, 1H) ppm. **^{13}C-NMR** (101 MHz, $CDCl_3$): δ= 168.6, 153.5, 140.5, 138.3, 136.5, 132.8, 128.9, 128.1, 126.54, 126.49, 123.0, 120.1, 118.9, 115.8, 113.5, 111.6, 110.0, 70.0, 68.1, 55.8, 38.3, 20.5 ppm. **HRMS** m/z (MALDI-TOF) positive ion, calculated for $C_{26}H_{24}N_3O_2$: $[M+H]^+$ 410.1869, Found: 410.1870.

1-(4-iodophenyl)-2-phenyl-1,2,5,6,11,11b-hexahydro-3H-imidazo[1',2':1,2]pyrido[3,4-b]indol-3-one (91l): 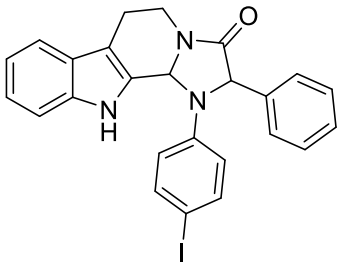

Prepared following general procedure **A** and isolated as a white solid in 55% yield (111 mg); mp 229-230 °C. **^{1}H-NMR** (400 MHz, $CDCl_3$): δ= 8.24 (s, 1H), 7.55 (m, 3H), 7.38 (d, J = 8.3 Hz, 1H), 7.27 (m, 1H), 7.18 (m, 4H), 7.10 (d, J = 7.1 Hz, 2H), 6.59 (d, J = 8.3 Hz, 2H), 6.46 (s, 1H), 5.00 (s, 1H), 4.61 (dd, J = 13.5, 6.3 Hz, 1H), 3.40 (td, J = 12.5, 5.3 Hz, 1H), 2.96 (m, 1H), 2.83 (m, 1H). **^{13}C-NMR** (101 MHz, $CDCl_3$): δ= 168.3, 145.5,

138.9, 137.3, 136.6, 132.0, 130.3, 129.1, 128.3, 126.3, 123.3, 120.3, 119.0, 114.1, 111.8, 110.7, 80.7, 69.6, 67.1, 38.5, 20.4. **HRMS** m/z (MALDI-TOF) negative ion, calculated for $C_{25}H_{19}IN_3O$: $[M-H]^-$ 504.0573, Found: 504.0575

2-phenyl-1-(*p*-tolyl)-1,2,5,6,11,11b-hexahydro-3H-imidazo[1',2':1,2]pyrido[3,4-b] indol-3-one (91m): 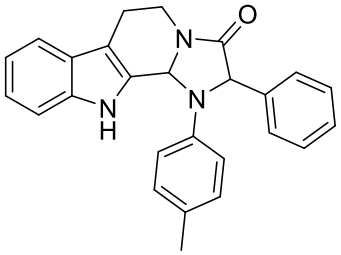
Prepared following general procedure **B** and isolated as a brown solid in 76% yield (120 mg); mp 232-233 °C (dec). **^{1}H-NMR** (400 MHz, $CDCl_3$): δ= 8.30 (s, 1H), 7.54 (d, J = 7.9 Hz, 1H), 7.37 (d, J = 8.1 Hz, 1H), 7.26 (m, 1H), 7.23 – 7.14 (m, 8H), 6.76 (d, J = 8.1 Hz, 2H), 6.46 (s, 1H), 5.07 (s, 1H), 4.62 (dd, J = 13.4, 6.4 Hz, 1H), 3.39 (td, J = 12.3, 5.4 Hz, 1H), 2.97 (m, 1H), 2.83 (m, 1H), 2.31 (s, 3H) ppm. **^{13}C-NMR** (101 MHz, $CDCl_3$): δ= 168.7, 144.0, 138.1, 136.5, 132.8, 130.8, 128.9, 128.8, 128.1, 126.5, 123.1, 120.2, 119.0, 112.1, 111.7, 110.1, 69.8, 67.5, 38.4, 20.5, 20.3 ppm. **HRMS** m/z (MALDI-TOF) negative ion, calculated for $C_{26}H_{22}N_3O$: $[M-H]^-$ 392.1763, Found: 392.1758.

2-(4-bromophenyl)-1-(4-iodophenyl)-1,2,5,6,11,11b-hexahydro-3H-imidazo[1',2':1,2]pyrido [3,4-b]indol-3-one (91n): 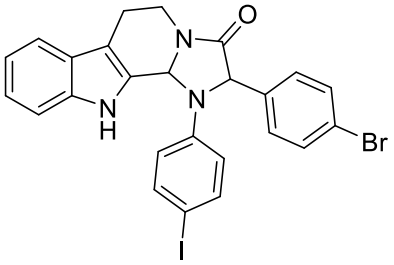
Prepared following general procedure **B** and obtained as a brown solid of an inseparable mixture of **3n** and the deiodinated derivative (vide infra the mass spectrum of mixture). The total mass obtained was 141 mg with 38% yield (89 mg) for **91n** as NMR yield (the major component of mixture was attributed to **91n** due to the relative intensity of the ^{13}C NMR peak of C-I, compared to the other peaks); The NMR spectra of the mixture are reported. **^{1}H-NMR** (400 MHz, $CDCl_3$): δ= 8.17 (s, 0.7H), 8.11 (s, 1H), 7.65 – 7.57 (m, 2H), 7.52 (d, J = 7.8 Hz, 1.4H), 7.41 – 7.25 (m, 9H), 7.18 (t, J = 7.5 Hz, 1.4H), 7.08 – 6.92 (m, 4H), 6.82 (d, J = 8.1 Hz, 1.4H), 6.59 (d, J = 8.6 Hz, 2H), 6.51 (s, 0.7H), 6.47 (s, 1H), 5.06 (s, 0.7H), 4.99 (s, 1H), 4.61 (m, 1.7H), 3.41 (m, 1.7H), 3.03 – 2.89 (m, 1.7H), 2.88 – 2.78 (m, 1.7H) ppm. **^{13}C-NMR** (101 MHz, $CDCl_3$): δ= 168.1, 167.8, 145.8, 145.3, 139.0, 136.9, 136.5, 136.4, 136.3, 132.4, 132.2, 132.1, 131.8, 130.4, 128.1, 128.0, 126.4, 126.3, 123.5, 123.3, 122.5, 122.3, 120.5, 120.3, 119.7, 119.0, 119.0, 114.1, 112.0, 111.7, 111.6, 110.8, 110.4, 81.1, 69.7, 69.5, 66.7, 66.4, 38.6, 38.5, 20.4,

20.4 ppm. **HRMS** m/z (MALDI-TOF) negative ion, calculated for $C_{25}H_{18}BrIN_3O$: $[M-H]^-$ 581.9678, Found: 581.9672.

1-(4-iodophenyl)-2-(3-methoxyphenyl)-1,2,5,6,11,11b-hexahydro-3H-imidazo[1',2':1,2]

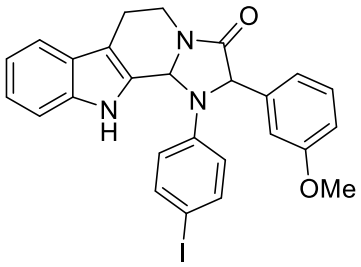

pyrido[3,4-b]indol-3-one (91o): Prepared following general procedure **B** and isolated as a yellow solid in 52% yield (111 mg); mp 229-230 °C (dec). **^{1}H-NMR** (400 MHz, $CDCl_3$): δ= 8.38 (s, 1H), 7.59 – 7.46 (m, 3H), 7.36 – 7.28 (m, 1H), 7.26 – 7.17 (m, 1H), 7.18 – 7.13 (m, 1H), 7.08 (t, J = 7.9 Hz, 1H), 6.78 – 6.67 (m, 2H), 6.62 – 6.54 (m, 2H), 6.50 – 6.38 (m, 2H), 4.92 (s, 1H), 4.58 (dd, J = 13.4, 6.2 Hz, 1H), 3.47 – 3.32 (m, 1H), 3.16 (s, 3H), 2.99 (m, 1H), 2.82 (m, 1H). **^{13}C-NMR** (101 MHz, $CDCl_3$) δ = 168.6, 160.1, 145.2, 139.1, 138.8, 136.6, 132.2, 130.1, 126.3, 123.4, 120.3, 119.0, 118.9, 115.0, 113.9, 111.7, 110.7, 110.5, 80.5, 69.4, 66.9, 54.5, 38.6, 20.4. **HRMS** m/z (MALDI-TOF) positive ion, calculated for $C_{26}H_{23}IN_3O_2$: $[M+H]^+$ 536.0835, Found: 536.0838.

2-(3-bromophenyl)-1-(4-fluorophenyl)-1,2,5,6,11,11b-hexahydro-3H-imidazo[1',2':1,2]

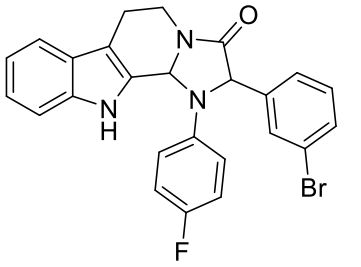

pyrido[3,4-b]indol-3-one (91p): Prepared following general procedure **B** and isolated as a yellow solid in 66% yield (126 mg); mp 205-206 °C (dec). **^{1}H-NMR** (400 MHz, $CDCl_3$): δ= 8.16 (s, 1H), 7.53 (d, *J* = 7.8 Hz, 1H), 7.42 – 7.29 (m, 3H), 7.29 – 7.23 (m, 1H), 7.22 – 7.13 (m, 1H), 7.13 – 6.98 (m, 4H), 6.80 – 6.70 (m, 2H), 6.43 (s, 1H), 4.96 (s, 1H), 4.61 (dd, J = 13.4, 6.4 Hz, 1H), 3.40 (m, 1H), 3.04-2.92 (m, 1H), 2.89 – 2.79 (m, 1H) ppm. **^{19}F-NMR** (376 MHz, $CDCl_3$): δ= -124.58 ppm. **^{13}C-NMR** (101 MHz, $CDCl_3$): δ= 167.8, 157.0 (d, $^1J_{C,F}$ = 239.5 Hz, CF), 142.3 (d, $^4J_{C,F}$ = 2.2 Hz), 140.0, 136.6, 132.1, 131.4, 130.5, 129.8, 126.4, 124.8, 123.3, 123.0, 120.3, 119.0, 116.9 (d, $^2J_{C,F}$ = 22.7 Hz), 113.1 (d, $^3J_{C,F}$ = 7.3 Hz), 111.6, 110.5, 70.1, 67.2, 38.5, 20.4 ppm. **HRMS** m/z (MALDI-TOF) negative ion, calculated for $C_{25}H_{18}BrFN_3O$: $[M-H]^-$ 474.0617, Found: 474.0620.

1-(4-bromo-3-fluorophenyl)-2-(3-bromophenyl)-1,2,5,6,11,11b-hexahydro-3H-imidazo [1',2':1,2]pyrido[3,4-b]indol-3-one (91q): Prepared following general procedure **B** and isolated as a yellow solid in 69% yield (153 mg); mp 212-213 °C (dec). **^{1}H-NMR** (400 MHz, $CDCl_3$): δ= 8.16 (s, 1H), 7.52 (d, J = 7.9 Hz, 1H), 7.49-7.41 (m, 1H), 7.38 (d, J = 8.2 Hz, 1H), 7.33 (dt, J = 8.1, 1.5 Hz, 1H), 7.29 – 7.22 (m, 2H), 7.17 (t, J = 7.5, 1H), 7.02 (t, J = 7.8 Hz, 1H), 6.95 (dt, J = 7.9, 1.4 Hz, 1H), 6.57 (dd, J = 10.9, 2.9 Hz, 1H), 6.48 (dd, J = 8.8, 2.9 Hz, 1H), 6.44 (s, 1H), 4.96 (s, 1H), 4.59 (dd, J = 13.4, 6.4 Hz, 1H), 3.40 (m, 1H), 2.97 (m, 1H), 2.88 – 2.78 (m, 1H) ppm. **^{19}F-NMR** (376 MHz, $CDCl_3$): δ= -103.52 ppm. **^{13}C-NMR** (101 MHz, $CDCl_3$): δ= 167.5, 160.2 (d, $^{1}J_{C,F}$ = 246.9 Hz, CF), 146.4 (d, $^{3}J_{C,F}$ = 9.5 Hz), 139.0, 136.6, 134.7 (d, $^{3}J_{C,F}$ = 2.2 Hz), 131.6, 131.2, 130.7, 129.6, 126.2, 124.6, 123.6, 123.2, 120.5, 119.0, 111.7, 111.1, 108.8 (d, $^{4}J_{C,F}$ = 2.9 Hz), 100.6 (d, $^{2}J_{C,F}$ = 27.1 Hz), 98.0 (d, $^{2}J_{C,F}$ = 21.3 Hz), 69.8, 66.4, 38.6, 20.3 ppm. **HRMS** m/z (MALDI-TOF) negative ion, calculated for $C_{25}H_{17}Br_2FN_3O$: $[M-H]^-$ 551.9722, Found: 551.9725.

2-(4-fluorophenyl)-1-(4-methoxyphenyl)-1,2,5,6,11,11b-hexahydro-3H-imidazo [1',2':1,2] pyrido[3,4-b]indol-3-one (91r): Prepared following general procedure **B** and isolated as a brown solid in 59% yield (101 mg); mp 227-228 °C (dec). **^{1}H-NMR** (400 MHz, $CDCl_3$): δ= 8.20 (s, 1H), 7.54 (d, J = 7.8 Hz, 1H), 7.37 (d, J = 8.1 Hz, 1H), 7.29 – 7.23 (m, 1H), 7.17 (m, 3H), 6.91 (m, 4H), 6.79 (d, J = 8.9 Hz, 2H), 6.40 (s, 1H), 4.99 (s, 1H), 4.61 (dd, J = 13.4, 6.3 Hz, 1H), 3.78 (s, 3H), 3.38 (m, 1H), 3.04 – 2.90 (m, 1H), 2.84 (m, 1H) ppm. **^{19}F-NMR** (376 MHz, $CDCl_3$): δ= -114.34 ppm. **^{13}C-NMR** (101 MHz, $CDCl_3$): δ= 168.4, 162.6 (d, $^{1}J_{C,F}$ = 246.1 Hz, CF), 153.6, 140.3, 136.5, 134.0 (d, $^{4}J_{C,F}$ = 2.9 Hz), 132.6, 128.2 (d, $^{3}J_{C,F}$ = 8.4 Hz), 126.4, 123.1, 120.2, 118.9, 115.8 (d, $^{2}J_{C,F}$ = 21.6 Hz), 115.7, 113.7, 111.6, 110.0, 70.1, 67.5, 55.7, 38.3, 20.5 ppm. **HRMS** m/z (MALDI-TOF) negative ion, calculated for $C_{26}H_{21}FN_3O_2$: $[M-H]^-$ 426.1618, Found: 426.1620.

2-butyl-1-phenyl-1,2,5,6,11,11b-hexahydro-3H-imidazo[1',2':1,2]pyrido[3,4-b]indol-3-one (91u): Prepared following general procedure **B** and isolated as a yellow solid in 61% yield (88 mg); mp 172-173 °C. **^{1}H-NMR** (400 MHz, $CDCl_3$): δ= 8.05 (s, 1H), 7.52 (d, J = 7.8 Hz, 1H), 7.43 (t, J = 8.0 Hz, 2H), 7.35 – 7.10 (m, 3H), 6.95 (dd, J = 18.6, 7.7 Hz, 3H), 6.28 (s, 1H), 4.66 (dd, J = 13.4, 6.4 Hz, 1H), 4.32 (m, 1H), 3.41 – 3.29 (m, 1H), 3.04 (m, 1H), 2.84 (m, 1H), 1.95 – 1.73 (m, 2H), 1.16 – 0.78 (m, 4H), 0.49 (t, J = 7.3 Hz, 3H) ppm. **^{13}C-NMR** (101 MHz, $CDCl_3$): δ= 171.2, 146.6, 136.4, 133.0, 130.4, 126.4, 122.9, 120.0, 118.9, 118.7, 111.4, 111.3, 110.0, 70.4, 62.1, 38.2, 31.2, 25.7, 22.4, 20.4, 13.5 ppm. **HRMS** m/z (MALDI-TOF) positive ion, calculated for $C_{23}H_{25}KN_3O$: $[M+K]^+$ 398.1635, Found: 398.1639.

2-pentyl-1-(*p*-tolyl)-1,2,5,6,11,11b-hexahydro-3H-imidazo[1',2':1,2]pyrido [3,4-b]indol-3-one (91v): Prepared following general procedure **B** and isolated as a yellow solid in 59% yield (91 mg); mp 180-181 °C (dec). **^{1}H-NMR** (400 MHz, $CDCl_3$): δ= 7.93 (s, 1H), 7.42 (d, J = 7.7 Hz, 1H), 7.21 (d, J = 8.1 Hz, 1H), 7.19 – 7.09 (m, 3H), 7.04 (m, 1H), 6.79 – 6.71 (m, 2H), 6.14 (s, 1H), 4.56 (dd, J = 13.4, 6.0 Hz, 1H), 4.20 (m, 1H), 3.25 (m, 1H), 2.93 (m, 1H), 2.74 (m, 1H), 2.27 (s, 3H), 1.84 – 1.62 (m, 2H), 1.03 – 0.72 (m, 6H), 0.39 (t, J = 7.3 Hz, 3H) ppm. **^{13}C-NMR** (101 MHz, $CDCl_3$): δ= 171.3, 144.5, 136.4, 133.2, 130.8, 128.4, 126.4, 122.9, 120.0, 118.7, 111.5, 111.3, 109.8, 70.6, 62.5, 38.2, 31.5, 31.3, 23.1, 22.2, 20.5, 20.3, 13.3 ppm. **HRMS** m/z (MALDI-TOF) negative ion, calculated for $C_{25}H_{28}N_3O$: $[M-H]^-$ 386.2232, Found: 386.2230.

1-(4-fluorophenyl)-2-(2-phenylpropyl)-1,2,5,6,11,11b-hexahydro-3H-imidazo[1',2':1,2]

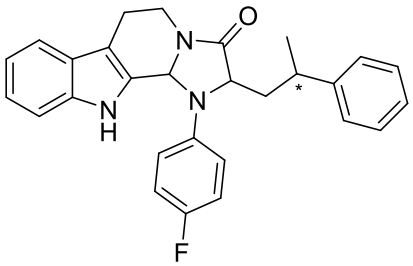

pyrido[3,4-b]indol-3-one (91w): Prepared following general procedure **B** and isolated as a white solid in 52% total yield (91 mg) of the epimers; The two epimers has been chromatographically separated.

91w less polar epimer mp 163-164 °C. **^{1}H-NMR** (400 MHz, $CDCl_3$): δ= 7.79 (s, 1H), 7.43 (d, J = 7.8 Hz, 1H), 7.24 (d, J = 8.1 Hz, 1H), 7.20 – 7.00 (m, 7H), 6.91 – 6.80 (m, 2H), 6.40 – 6.26 (m, 2H), 5.93 (s, 1H), 4.47 (dd, J = 13.4, 6.4 Hz, 1H), 3.77 (dd, J = 10.1, 2.9 Hz, 1H), 3.16 (m, 2H), 2.86 (m, 1H), 2.73 – 2.57 (m, 1H), 1.85 (m, 1H), 1.70 (m, 1H), 1.05 (d, J = 7.0 Hz, 3H) ppm. **^{19}F-NMR** (376 MHz, $CDCl_3$): δ= -125.44 ppm. **^{13}C-NMR** (101 MHz, $CDCl_3$): δ= 171.5, 156.7 (d, $^{1}J_{C,F}$ = 238.8 Hz, CF), 145.7, 143.0 (d, $^{4}J_{C,F}$ = 1.8 Hz), 136.5, 133.0, 128.4, 127.6, 126.7, 126.5, 123.1, 120.2, 118.9, 116.7 (d, $^{2}J_{C,F}$ = 22.4 Hz), 113.0 (d, $^{3}J_{C,F}$= 7.3 Hz), 111.5, 110.0, 70.9, 60.1, 41.5, 38.0, 35.9, 22.9, 20.3 ppm. **HRMS** m/z (MALDI-TOF) positive ion, calculated for $C_{28}H_{26}FKN_3O$: $[M+K]^+$ 478.1697, Found: 478.1695.

91w more polar epimer, mp 164-166 °C. **^{1}H-NMR** (400 MHz, $CDCl_3$): δ= 7.66 (s, 1H), 7.53 (d, J = 7.8 Hz, 1H), 7.33 (d, J = 8.1 Hz, 1H), 7.24 (m, 1H), 7.16 (m, 1H), 7.12 – 7.02 (m, 5H), 6.84 (m, 4H), 6.07 (s, 1H), 4.66 (dd, J = 13.4, 6.4 Hz, 1H), 4.18 (t, J = 5.5 Hz, 1H), 3.32 (m, 1H), 3.08 (m, 1H), 2.90 – 2.74 (m, 2H), 2.25 (m, 1H), 1.99 (m, 1H), 1.11 (d, J = 6.9 Hz, 3H) ppm. **^{19}F-NMR** (376 MHz, $CDCl_3$): δ= -123.60 ppm. **^{13}C-NMR** (101 MHz, $CDCl_3$): δ= 171.2, 157.4 (d, $^{1}J_{C,F}$ = 239.9 Hz), 146.7, 143.8 (d, $^{4}J_{C,F}$= 2.2 Hz), 136.7, 132.7, 128.2, 126.7, 126.6, 125.8, 123.1, 120.2, 118.9, 116.7 (d, $^{2}J_{C,F}$ = 22.4 Hz), 115.2 (d, $^{3}J_{C,F}$ = 7.7 Hz), 111.6, 110.1, 72.1, 62.1, 39.7, 38.3, 35.8, 23.5, 20.4 ppm. **HRMS** m/z (MALDI-TOF) negative ion, calculated for $C_{28}H_{25}FN_3O$: $[M-H]^-$ 438.1982, Found: 438.1983.

1-phenyl-2-(1-phenylethyl)-1,2,5,6,11,11b-hexahydro-3H-imidazo[1',2':1,2] pyrido[3,4-b] indol-3-one (91x): 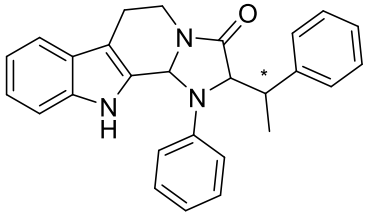 Prepared following general procedure **B** and isolated as a white solid in 59% total yield (96 mg) of the epimers; For the less polar epimer mp 152-153 °C. **^{1}H-NMR** (400 MHz, $CDCl_3$): δ= 7.71 (s, 1H), 7.37 – 7.27 (m, 2H), 7.21 (m, 2H), 7.17 – 7.06 (m, 1H), 7.06 – 6.98 (m, 1H), 6.91 – 6.81 (m, 3H), 6.71 (d, J = 8.1 Hz, 2H), 6.43 (t, J = 7.4 Hz, 2H), 6.38 – 6.30 (m, 1H), 5.96 (s, 1H), 4.41 – 4.30 (m, 2H), 3.29 (m, 1H), 3.02 (m, 1H), 2.40 (m, 1H), 2.22 (m, 1H), 1.47 (d, J = 7.4 Hz, 3H) ppm. **^{13}C-NMR** (101 MHz, $CDCl_3$): δ= 169.0, 146.6, 140.0, 136.4, 132.4, 130.3, 128.2, 127.1 126.9, 126.5, 122.7, 119.9, 119.1, 118.7, 111.3, 111.2, 110.0, 70.6, 68.1, 41.6, 37.8, 20.2, 15.6 ppm. **HRMS** m/z (MALDI-TOF) negative ion, calculated for $C_{27}H_{24}N_3O$: $[M-H]^-$ 406.1919, Found: 406.1917.

2-isopropyl-1-phenyl-1,2,5,6,11,11b-hexahydro-3H-imidazo[1',2':1,2]pyrido [3,4-b] indol-3-one (91y): 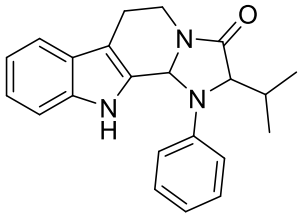 Prepared following general procedure **B** and isolated as a yellow solid in 41% yield (57 mg); mp 145-146 °C. **^{1}H-NMR** (400 MHz, $CDCl_3$): δ= 8.15 (s, 1H), 7.53 (d, J = 7.5 Hz, 1H), 7.43 (m, 2H), 7.35 (d, J = 8.1 Hz, 1H), 7.26 – 7.19 (m, 1H), 7.16 (m, 2H), 6.96 (t, J = 7.3 Hz, 1H), 6.91 (d, J = 8.2 Hz, 2H), 6.21 (s, 1H), 4.66 (dd, J = 13.4, 5.9 Hz, 1H), 4.19 (d, J = 3.1 Hz, 1H), 3.31 (m, 1H), 2.84 (m, 1H), 2.17 (m, 1H), 1.08 (d, J = 7.1 Hz, 3H), 0.59 (d, J = 6.8 Hz, 3H) ppm. **^{13}C-NMR** (101 MHz, $CDCl_3$): δ= 169.9, 147.0, 136.4, 133.0, 130.2, 126.4, 122.9, 120.0, 119.0, 118.8, 111.6, 111.5, 110.0, 71.2, 66.6, 38.0, 31.1, 20.6, 18.1, 16.7 ppm. **HRMS** m/z (MALDI-TOF) positive ion, calculated for $C_{22}H_{24}N_3O$: $[M+H]^+$ 346.1919, Found: 346.1922.

2-isobutyl-1-(*p*-tolyl)-1,2,5,6,11,11b-hexahydro-3H-imidazo[1',2':1,2]pyrido[3,4-b]indol-3-one (91z): 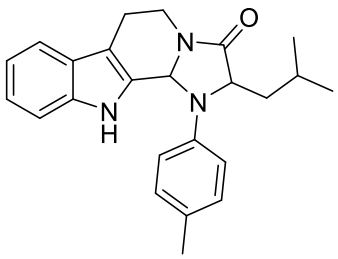 Prepared following general procedure **B** and isolated as a yellow solid in 35% yield (52 mg); mp 158-159 °C. **^{1}H-NMR** (400 MHz, $CDCl_3$): δ= 8.11 – 8.06 (m, 1H), 7.58 (d, J = 7.8 Hz, 1H), 7.38 (d, J = 8.1 Hz, 1H), 7.34 – 7.27 (m, 3H), 7.21 (t, J = 7.3 Hz, 1H), 6.93 (d, J = 8.6 Hz, 2H), 6.26 (s, 1H), 4.70 (dd, J = 13.4, 6.4 Hz, 1H), 4.30 (m, 1H), 3.40 (td, J

= 12.5, 5.4 Hz, 1H), 3.17 – 3.01 (m, 1H), 2.90 (m, 1H), 2.42 (s, 3H), 1.86 – 1.67 (m, 3H), 0.86 (d, J = 6.5 Hz, 3H), 0.79 (d, J = 6.6 Hz, 3H) ppm. **^{13}C-NMR** (101 MHz, $CDCl_3$): δ= 171.6, 144.8, 136.4, 133.2, 130.8, 128.8, 126.5, 122.9, 120.0, 118.8, 112.2, 111.4, 109.6, 70.8, 61.2, 41.2, 38.1, 24.3, 23.6, 22.4, 20.32, 20.29 ppm. **HRMS** m/z (MALDI-TOF) positive ion, calculated for $C_{24}H_{28}N_3O$: $[M+H]^+$ 374.2232, Found: 374.2229.

N-(2-(1H-indol-3-yl)ethyl)-2-(4-methoxyphenyl)-2-oxoacetamide (92): Known product and

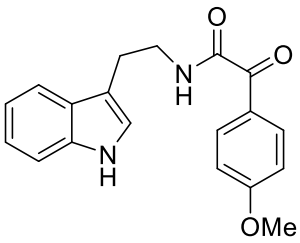

was identified by comparison of its physical and spectral data reported in the cited reference. **^{1}H-NMR** (400 MHz, $CDCl_3$): δ = 8.39 (d, J = 8.3 Hz, 2H), 8.12 (s, 1H), 7.64 (d, J = 7.8 Hz, 1H), 7.39 (d, J = 8.1 Hz, 1H), 7.28 – 7.05 (m, 3H), 6.94 (d, J = 8.3 Hz, 2H), 3.89 (s, 3H), 3.73 (dd, J = 7.1, 6.6 Hz, 2H), 3.08 (t, J = 6.8 Hz, 2H) ppm. **HRMS** m/z (MALDI-TOF) positive ion, calculated for $C_{19}H_{18}KN_2O_3$: $[M+K]^+$ 361.0954, Found: 361.0953.

N-(1-(4-methoxyphenyl)-2-(1,3,4,9-tetrahydro-2H-pyrido[3,4-b]indol-2-yl)ethyl)aniline (93):

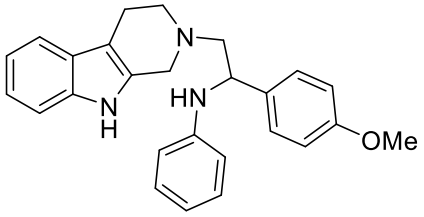

A flame-dried 10 mL round-bottom flask was charged with **91a** (150 mg, 0.366 mmol) and a stirbar. Anhydrous THF (2 mL) was added. Under a stream of N_2, $LiAlH_4$ in THF 1M (28 mg, 0.733 mmol) was added portion wise to control any exotherm. The solution was stirred at room temperature for 4 h. The reaction was cooled to 0 °C, and then slowly quenched by dropwise addition of 2M NaOH, and H_2O. The solution was extracted with CH_2Cl_2 and the organic layer were dried over Na_2SO_4, filtered, and concentrated in vacuo. The crude residue was purified by flash-chromatography (eluent: hexane/EtOAc, 95:5) afforded **93** (83 mg, 57 % yield). **^{1}H-NMR** (400 MHz, $CDCl_3$): δ = 7.77 (s, 1H), 7.50 (d, J = 7.5 Hz, 1H), 7.38 (d, J = 8.3 Hz, 2H), 7.30 (d, J = 7.8 Hz, 1H), 7.23 – 7.04 (m, 4H), 6.92 (d, J = 8.3 Hz, 2H), 6.68 (t, J = 7.3 Hz, 1H), 6.55 (d, J = 7.9 Hz, 2H), 5.35 (s, 1H), 4.42 (dd, J = 8.9, 6.3 Hz, 1H), 3.82 (s, 4H), 3.64 (d, J = 14.6 Hz, 1H), 3.01 (dd, J = 10.3, 5.6 Hz, 1H), 2.96 – 2.76 (m, 5H) ppm. **^{13}C-NMR** (101 MHz, $CDCl_3$): δ = 158.8, 148.2, 136.0, 134.4, 128.9, 127.4, 126.9, 121.5, 119.5, 117.9, 117.6, 114.2, 114.1, 110.8, 108.1, 64.0, 55.2, 55.1, 50.5,

49.7, 21.0 ppm. **HRMS** m/z (MALDI-TOF) positive ion, calculated for $C_{26}H_{26}N_3O$: $[M+H]^+$ 396.2076, Found: 396.2079.

2-phenyl-1-(4-(phenylethynyl)phenyl)-1,2,5,6,11,11b-hexahydro-3H-imidazo[1',2':1,2]

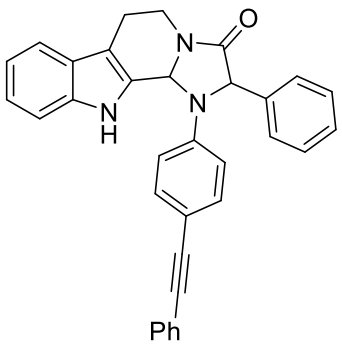

pyrido[3,4-b]indol-3-one (94): A mixture of **91l** (150 mg, 0.297 mmol), Phenylacetilene (65 µL , 0.594 mmol), $Pd(PPh_3)_4$ (34 mg, 0.029 mmol), CuI (6 mg, 0.029 mmol), in Piperidine (2 mL) was stirred at room temperature under nitrogen overnight. Then the solution was concentrated under reduce pressure and the mixture was extracted with AcOEt. The organic layer was washed with water, dried with sodium sulfate, filtered, and concentrated. The purification of the residue by flash chromatography (eluent: hexane/EtOAc, 95:5) afforded **94** (104 mg, 73 % yield). **^{1}H-NMR** (400 MHz, $CDCl_3$): δ = 8.32 (s, 1H), 7.51 (m, 5H), 7.36 (dd, J = 21.6, 7.4 Hz, 5H), 7.23 – 7.10 (m, 6H), 6.78 (d, J = 8.3 Hz, 2H), 6.54 (s, 1H), 5.07 (s, 1H), 4.62 (dd, J = 13.5, 6.3 Hz, 1H), 3.41 (td, J = 12.4, 5.3 Hz, 1H), 2.98 (m, 1H), 2.84 (dd, J = 15.8, 5.2 Hz, 1H) ppm. **^{13}C-NMR** (101 MHz, $CDCl_3$): δ = 168.3, 145.5, 137.3, 136.5, 133.7, 132.0, 131.4, 129.0, 128.3, 128.2, 128.0, 126.3, 123.5, 123.2, 120.2, 118.9, 113.8, 111.8, 111.7, 110.6, 89.2, 88.6, 69.5, 66.9, 38.5, 20.4 ppm. **HRMS** m/z (MALDI-TOF) positive ion, calculated for $C_{33}H_{26}N_3O$: $[M+H]^+$ 480.2076, Found: 480.2077.

N-Phenylformamide: The compound was isolated as a mixture of the tautomers. **^{1}H-NMR** (400 MHz, $CDCl_3$): δ = 8.62 (s, 2H), 8.28 (d, J = 1.5 Hz, 1H), 7.72 (br, 1H), 7.48 – 7.45 (m, 2H), 7.29 – 7.21 (m, 4H), 7.12 – 7.01 (m, 4H) ppm. **^{13}C-NMR** (101 MHz, $CDCl_3$): δ = 163.0, 159.4, 137.1, 137.0, 129.9, 129.2, 125.4, 125.0, 120.2, 119.0 ppm

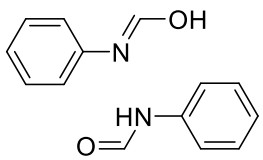

3.7 Reference Chapter III

131) R. C. Cioc, E. Ruijter, R. V. A. Orru. Multicomponent reactions: advanced tools for sustainable organic synthesis. *Green Chem.* **2014**, *16*, 2958-2975.

132) P. T. Anastas, J. C. Warner, *Green Chemistry*: Theory and Practice, Oxford University Press, New York, **1998**.

133) A. Dömling, W. Wang, K. Wang. Chemistry and Biology Of Multicomponent Reactions. *Chem. Rev.* **2012**, *6*, 3083-3135.

134) L. Banfi, A. Basso, C. Lambruschini, L. Moni, R. Riva. The 100 facets of the Passerini reaction. *Chem. Sci.* **2021**, *12*, 15445-15472.

135) M. A. Fouad, H. Abdel-Hamid, M. S. Ayoup. Two decades of recent advances of Ugi reactions: synthetic and pharmaceutical applications. *RSC Adv.* **2020**, *10*, 42644-42681.

136) I. Ugi, R. Meyr, C. J. A. C. Steinbruckner. Versammlungsberichte. *Angew. Chem.* **1959**, *71*, 373-388.

137) M. H. R. Carvalho, J. P. R. S. Ribeiro, P. P. De Castro, S. T. A. Passos, B. A. D. Neto, H. F. Dos Santos, G. W. Amarante. Solvent Dependent Competitive Mechanisms for the Ugi Multicomponent Reaction: A Joint Theoretical and Experimental Study in the α-Acyl Aminocarboxamides vs α-Amino Amidines Formation. *J. Org. Chem.* **2022**, *87*, 11007-11020.

138) J. C. Flores-Reyes, A. Islas-Jácome, E. González-Zamora. The Ugi three-component reaction and its variants. *Org. Chem. Front.* **2021**, *8*, 5460-5515.

139) L. El Kaïm, L. Grimaud. The Ugi–Smiles and Passerini–Smiles Couplings: A Story About Phenols in Isocyanide-Based Multicomponent Reactions. Eur. *J. Org. Chem.* **2014**, *35*, 7749-7762.

140) **a)** L. E. I. Kaim, L. Grimaud, S. R. Purumandla. Allyl and Benzyl Dance under Basic Conditions. *Synlett* **2011**, *13*, 1816-1820; **b)** D. Suwalka, B. K. Malviva, V. P. Verma, A. K. Jassal, S. Sharma. Merging Electrochemical Synthesis and Post-Ugi Cyclization for the Synthesis of Diverse 4-Imidazolidinones. *J. Org. Chem.* **2023**, *88*, 9199-9212; **c)** A. Zidan, A. M. El-Naggar, N. E. A. Abd El-Sattar, A. K. Ali, L. El Kaïm. Raising the Diversity

of Ugi Reactions Through Selective Alkylations and Allylations of Ugi Adducts. *Front. Chem.* **2019**, *7*, 20-28.

141) U. K. Sharma, N. Sharma, D. D. Vachhani, E. V. Van der Eychen. Metal-mediated post-Ugi transformations for the construction of diverse heterocyclic scaffolds. *Chem. Soc. Rev.* **2015**, *44*, 1836-1860.

142) X. Tang, L. Song. Recent Access to Polycycles via Post-Ugi Reactions. *Processes* **2023**, *11*, 699-718.

143) A. Pictet, T. Spengler. Über die Bildung von Isochinolin-derivaten durch Einwirkung von Methylal auf Phenyl-äthylamin, Phenyl-alanin und Tyrosin. *Ber. Dtsch. Chem. Ges.* **1911**, *44*, 2030-2036.

144) G. J. Tatsui. Preparation of 1-methyl-1,2,3,4-tetrahydro-β-carboline. *J. Pharm. Soc. Jpn.* **1928**, *48*, 453-459.

145) A. Dömling, I. Ugi. Multicomponent Reactions with Isocyanides. *Angew. Chem. Int. Ed.* **2000**, *39*, 3168-3210.

146) **a)** L. El Kaim, M. Gageat, L. Gaultier, L. Grimaud. New Ugi/Pictet-Spengler Multicomponent Formation of Polycyclic -Diketopiperazines from Isocyanides and α-Keto Acids. *Synlett* **2007**, *3*, 502-503; **b)** M. -A. Cano-Herrera, L. D. Miranda. Expedient entry to the piperazinohydroisoquinoline ring system using a sequential Ugi/Pictet–Spengler/reductive methylation reaction protocol. *Chem. Commun.* **2011**, *47*, 10770-10772; **c)** P. Patil, K. Khoury, E. Herdtweck, A. Dömling. MCR synthesis of a tetracyclic tetrazole scaffold. *Bioorg. Med. Chem.* **2015**, *23*, 2699-2715.

147) J. B. Fourtillan, M. Fourtillan, O. Karam, F. Zunino, J. C. Jacquesy, J. P. Tafani, U.S. PatentUS20060089372A1, **2006**.

148) N. Reixach, E. Crooks, J. M. Ostresh, R. A. Houghten, S. E. Blondelle. Inhibition of β-Amyloid-Induced Neurotoxicity by Imidazopyridoindoles Derived from a Synthetic Combinatorial Library. *J. Struct. Biol.* **2000**, *130*, 247-258.

149) C. Piemontesi, Q. Wang, J. Zhu. Enantioselective Synthesis of (+)-Peganumine A. *J. Am. Chem. Soc.* **2016**, *138*, 11148-11151.

150) K. -B. Wang, Y. -T. Di, Y. Bao, C. -M. Yuan, G. Chen, D. -H. Li, J. Bai, H. -P. He, X. -J. Hao, Y. -H. Pei, Y. -K. Jing, Z. -L. Li, H. -M. Hua. Peganumine A, a β-Carboline Dimer with a New Octacyclic Scaffold from *Peganum harmala*. *Org. Lett.* **2014**, *16*, 4028-4031.

151) A. Silvani, G. Lesma, S. Crippa, V. Vece. Multicomponent access to novel dihydroimidazo[1′,5′:1,2]pyrido[3,4-*b*]indol-2-ium salts and indoles by means of Ugi/Bischler–Napieralski/heterocyclization two step strategy. *Tetrahedron* **2014**, *70*, 3994-4001.

152) J. -C. Xiang, Z. -X. Wang, Y. Cheng, J. -T. Ma, M. Wang, B. -C. Tang, Y. -D. Wu, A. -X. Wu. A C–H Oxidation/Two-Fold Cyclization Approach toImidazopyridoindole Scaffold under Mild Oxidizing Conditions. *J. Org. Chem.* **2017**, *82*, 13671-13677.

153) **a)** A. Nash, X. Qi, P. Maity, K. Owens, U. K. Tambar. Development of the Vinylogous Pictet–Spengler Cyclization and Total Synthesis of (±)-Lundurine A. *Angew. Chem. Int. Ed.* **2018**, *57*, 6888-6891; **b)** B. de Carné-Carnavalet, J.-P. Krieger, B. Folléas, J.-L. Brayer, J.-P.Demoute, C. Meyer, J. Cossy. Diastereodivergent Pictet–Spengler Cyclization of Bicyclic *N*-Acyliminium Ions: Controlling a Quaternary Stereocenter. *Eur. J. Org. Chem.* **2015**, 1273-1282; **c)** W. Zhang, J. Franzén. Diverse Asymmetric Quinolizidine Synthesis: A Stereodivergent One-Pot Approach. *Adv. Synth. Catal.* **2010**, *352*, 499-518; **d)** B. E. Maryanoff, H.-C. Zhang, J. H. Cohen,I. J. Turchi, C. A. Maryanoff. Cyclizations of *N*-Acyliminium Ions. *Chem. Rev.* **2004**, *104*, 1431-1628.

154) **a)** N. Glinsky-Olivier, S. Shengwen Yang, P. Retailleau, V. Gandon, X. Guinchard. Enantioselective Gold-Catalyzed Pictet–Spengler Reaction. *Org. Lett.* **2019**, *21*, 9446-9451; **b)** N. Glinsky-Olivier, P. Retailleau, X. Guinchard. Gold-Catalyzed Synthesis of Spirofused Indoloquinuclidines. *Eur. J. Org. Chem.* **2018**, 5823-5829; **c)** S. W. Youn. Development of the Pictet–Spengler Reaction Catalyzed by $AuCl_3$/AgOTf. *J. Org. Chem.* **2006**, *71*, 2521-2523.

155) L. Zhang, F. Zhao, M. Zheng, Y. Zhai, H. Liu. Rapid and selective access to three distinct sets of indole-based heterocycles from a single set of Ugi-adducts under microwave heating. *Chem. Commun.* **2013**, *49*, 2894-2896.

156) V. Srinivasulu, S. McN Sieburth, R. El-Awady, N. M. Kariem, H. Tarazi, M. J. O'Connor, T. H. Al-Tel. Post-Ugi Cascade Transformations for Accessing Diverse Chromenopyrrole Collections. *Org. Lett.* **2018**, *20*, 836-839.

157) K. Manabe, D. Nobutou, S. Kobayashi. Catalytic Pictet–Spengler reactions using $Yb(OTf)_3$. *Bioorg. Med. Chem.* **2005**, *13*, 5154-5158.

158) M. Zaman, M. Hasan, A. A. Peshkov, K. Van Hecke, E. V. Van der Eycken, O. P. Pereshivko, V. A. Peshkov. Silver(I) Triflate-Catalyzed Protocol for the Post-Ugi Synthesis of Spiroindolines. *Adv. Synth. Catal.* 2020, *362*, 261-268.

159) A. Znabet, J. Zonneveld, E. Janssen, F. J. J. De Kanter, M. Helliwell, N. J. Turner, E. Ruijter, R. V. A. Orru. Asymmetric synthesis of synthetic alkaloids by a tandem biocatalysis/Ugi/Pictet–Spengler-type cyclization sequence. *Chem. Commun.* 2010, *46*, 7706-7708.

160) W. A. Alananzeh, M. N. Al-Qattan, Y. O. Ayipo, M. N. Mordi. *N*-substituted tetrahydro-beta-carboline as mu-opioid receptors ligands: in silico study; molecular docking, ADMET and molecular dynamics approach. *Mol. Divers*. 2023, *28*, 1273-1289.

161) I. T. Raheem, P. S. Thiara, E. A. Peterson, E. N. Jacobsen. Enantioselective Pictet–Spengler-Type Cyclizations of Hydroxylactams: H-Bond Donor Catalysis by Anion Binding. *J. Am. Chem. Soc.* 2007, *129*, 13404-13405.

162) J. Rayadurgam, S. Sana, M. Sasikumar, Q. Gu. Palladium catalyzed C–C and C–N bond forming reactions: an update on the synthesis of pharmaceuticals from 2015-2020. *Org. Chem. Front.* 2021, *8*, 384-414.

163) J. Ploog, J. Pongs, S. Weber, W. Maison. A Domino *Aza*-Prins/Friedel–Crafts Reaction for the Synthesis of Benzomorphans. *Synthesis* 2017, *49*, 693-703.

164) a) X.-Y. Yang, J.-M. Yang, B. Wu. TMSOTf-Promoted Cyclization of Indole-2-methyl-α-aminoketones: Access to 4-Aryl-Substituted β-Carbolines. *Org. Lett.* 2024, *26*, 1105-1109; b) C. Wade Downey, D. N. Confair, Y. Liu, E. D. Heafner. One-Pot Enol Silane Formation–Alkylation of Ketones with Propargyl Carboxylates Promoted by Trimethylsilyl Trifluoromethanesulfonate. *J. Org. Chem.* 2018, *83*, 12931-12938; c) S. Knapp, K. E. Rodriques, A. T. Levorse, R. M. Ornaf. A procedure for "iodolactamization". *Tetrahedron Lett.* 1985, *26*, 1803-1806.

Appendix

Electrochemical reactions

An electrochemical reaction is a process triggered or accompanied by the flow of electric current, typically involving the exchange of electrons between an organic species and an electrode.

From the early experiments conducted by Faraday in the 1800s to the advanced industrial applications of the 20th century, electrochemistry has undergone remarkable development (Figure 30). Faraday introduced fundamental concepts such as electrolysis, demonstrating that in certain cases, electrochemical processes can drive non-spontaneous reactions. This breakthrough paved the way for new synthetic approaches, including electrocatalysis and electrosynthesis.

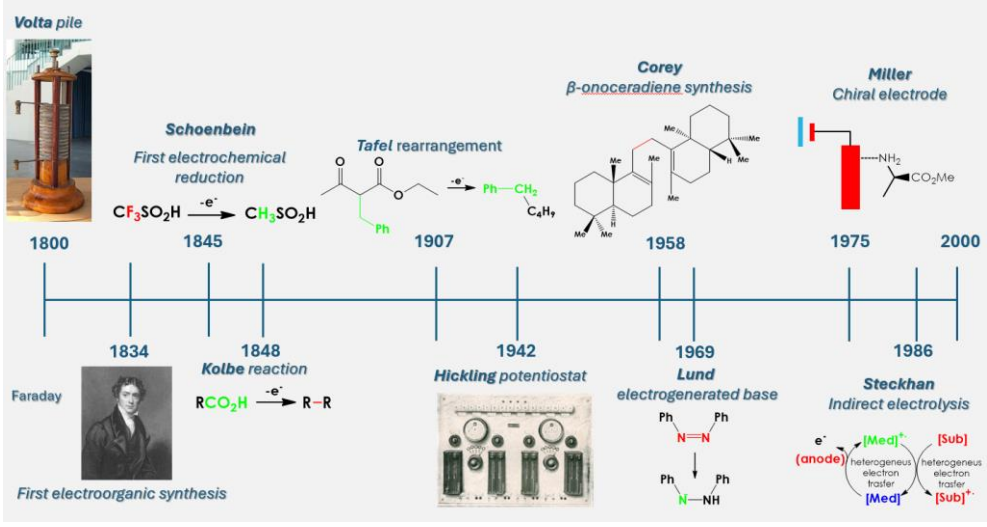

Figure 30: Selected milestones of representative electro-organic chemistry.

Electrosynthesis, in particular, plays a pivotal role in the field of green chemistry as it represents a cost-effective and environmentally friendly methodology. Some key features that define it as a green approach include:

- Avoidance of toxic oxidants and reductants: The ability to electrochemically generate reactive species in situ eliminates the need for harmful reagents. This reduces waste production and avoids exposure to toxic compounds.
- Use of a renewable and abundant resource—the electron: The electron acts as a reagent that does not need to be removed from the reaction environment, simplifying the work-up process and minimizing the disposal of by-products.
- Mild reaction conditions: Thanks to the high reactivity of electro-generated species, syntheses often require only ambient pressure, short reaction times, and do not involve extreme temperatures.
- Atom economy and energy efficiency: The electron, being a mass-free reagent, is readily available at low cost, contributing to both material savings and energy conservation.

Electrolysis

During an electro-organic reaction, the activation of the organic species occurs through a heterogeneous process involving the addition or removal of electrons at the electrode's surface. In particular, the power supply drives electrons from the cathode to the anode, creating a reducing environment at the cathode and an oxidizing environment at the anode. Each electrode is connected to the pole of a direct power source, which can control the potential or the current inside the electrochemical cell. The electrode where the reaction of interest takes place is referred as *working electrode*, while the other one is called *counter electrode*.

the addition or removal of electrons can result from two types of events:

- In the first case, **direct electron transfer** occurs between the electrode and the substrate, leading to the formation of radical cations at the anode (oxidation) and radical anions at the cathode (reduction).

- In the second case, a **mediator** is activated at the electrode interface, initiating a cascade of reactions involving the organic substrates, such as substitution, elimination, addition, or coupling reactions.

The indirect approach offers several advantages, such as the enhancement of the reaction efficiency and improvement of selectivity by avoiding side reactions. Furthermore, the ability to modify the structure of the mediator allows for precise control over the selectivity of the reactions.

Electrolysis can be performed under two different regimes: **constant current** or **controlled potential**. In the constant current approach, a simple direct current source (such as a battery or power supply) is sufficient to drive the reaction and convert the starting material. In contrast, the controlled potential method requires the use of a reference electrode to precisely monitor and control the potential applied. This technique is generally more selective, as it allows for the reduction or oxidation of the target species, minimizing the formation of unwanted side products.

Cell geometry

An important distinction in organic electrosynthesis lies in the cell geometry used for the reaction, which can be either a divided or undivided cell. The choice of cell depends on the specific requirements of the reaction. In an undivided cell, molecules are free to migrate between the cathode and anode, making it suitable for reactions where the substrate can undergo either reduction or oxidation without compromising selectivity. However, if the first electrolyzed product or the desired final product is prone to further reaction at the counter-electrode, the reaction selectivity can be significantly reduced/oxidized, resulting in lower yields. In such

cases, the use of a divided cell becomes advantageous. By separating the two electrodes with a diaphragm, this setup confines the reaction to a specific compartment, effectively preventing the formation of side products. Additionally, the diaphragm's porosity can be tailored to suit the specific reaction conditions or the current applied, allowing for further control over the electrochemical environment and enhancing the overall efficiency of the process. Some pictures of the different cell geometries are reported below.

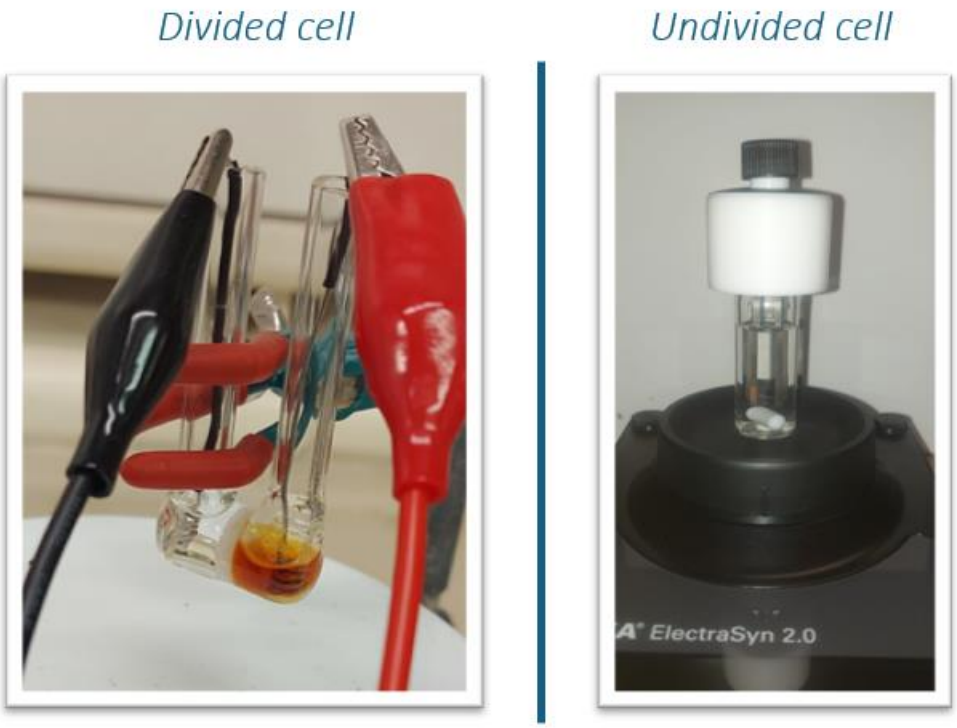

Figure 32: Divided cell *vs* undivided cell.

Electrode

The selection of electrode material, along with the applied potential, plays a key role in electrolysis and for the final product, as it can directly or indirectly influence the course of the reaction.

Commonly used electrodes for facilitating electron transfer include Platinum, Titanium, Palladium, Gold, Silver, Graphite, and Steel. In contrast, zinc, copper, and aluminum, which release Zn^{2+}, Cu^{2+}, and Al^{3+} ions during current flow, are typically used as **sacrificial electrodes**.

Solvent and supporting electrolyte

The choice of medium (solvent/supporting electrolyte) for electrolysis is highly dependent on the potential applied to the electrodes and plays a critical role, as it can influence the course of the reaction even more than the electrode material itself. For this reason, several factors are crucial when selecting a solvent, including:

- Solvent potential range (known as the electrochemical window) where the solvent remains stable.
- proton activity, related to the acidity of the solvent.
- ability to dissolve supporting electrolytes and substrates.
- accessible temperature range, viscosity, toxicity and cost.

Another important parameter to choosing the reaction solvent is the dielectric constant, which controls the dissociation of the electrolyte couple. The higher the dielectric constant of the solvent, the more conductive the solution will be.

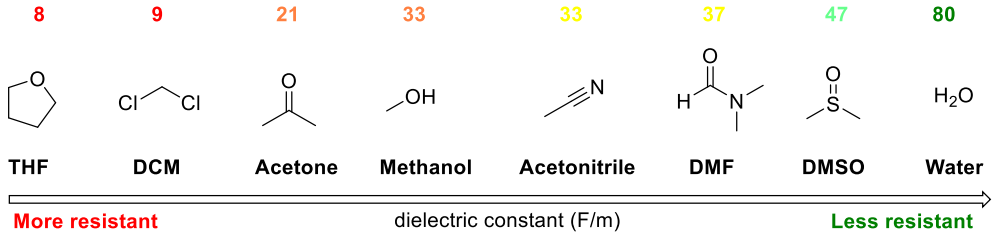

Figure 34: Solvent and dielectric constant.

Commonly used solvents include polar protic ones such as water and alcohols, including 1,1,1,3,3,3-hexafluoro-2-propanol (HFIP) and 2,2,2-trifluoroethanol, or

polar aprotic solvents like DMF, MeCN, and DMSO. However, even low-polarity solvents like THF, DCM, and acetone are applied in electrosynthesis.

Special mention should be made of ionic liquids, which, being molten salts at room temperature, provide an ideal reaction medium. They exhibit high conductivity (ranging from 1 to 10 mS/cm), a broad electrochemical stability window (up to 5 V), and sufficient ionic mobility, making them particularly well-suited for these processes.

For selected review on electrosynthesis:

- M. C. Leech, K. Lam. A practical guide to electrosynthesis. *Nat. Rev. Chem.* 2022, *6*, 275-286.
- C. Zhu, N. W. J. Ang, T. H. Meyer, Y. Qiu, L. Ackermann. Organic Electrochemistry: Molecular Syntheses with Potential. *ACS Cent. Sci.* 2021, *7*, 415-431.
- E. C. R. McKenzie, S. Hosseini, A. G. Couto Petro, K. L. Rudman, B. H. R. Gerroll, M. S. Mubarak, L. A. Baker, R. D. Little. Versatile Tools for Understanding Electrosynthetic Mechanisms. *Chem. Rev.* 2022, *122*, 3292-3335.
- J. Lodh, S. Paul, H. Sun, L. Song, W. Schöfberger, S. Roy. Electrochemical organic reactions: A tutorial review. *Front. Chem.* 2023, *10*, 956502.

Publications List

- C. Momoli, A. Arcadi, M. Chiarini, V. Morlacci, L. Palombi. ***in preparation.***
- C. Kiaku, S. Kaltenberger, D. Raydan, V. Morlacci, B. Claringbold, I. C. A. Goodall, L. Palombi, D. L. Poole, K. Lam. eEtherification: An electrochemical strategy towards the synthesis of sterically hindered dialkyl ethers from activated alcohols. *Org. Lett.* 2025, *27*, 147-152.
- V. Morlacci, M. Milia, J. Saiter, I. Pret Bhela, M. Leech, K. Lam. eCyanation using 5-aminotetrazole as a safer electrophilic and nucleophilic cyanide source. *JACS Au* 2024, 4, *11*, 4199-4205.
- C. Momoli, A. Lamenta, M. Charini, N. Demitri, D. Lamba, V. Morlacci, L. Palombi, A. Arcadi. Gold Salts as Alternative Catalysts in Sequential Reactions of 2-Aminobenzaldehydes. *J. Org. Chem.* 2024, 89, 16828-16837.
- V. Morlacci, M. Aschi, M. Chiarini, C. Momoli, L. Palombi, A. Arcadi. Product Selectivity Control in the Brønsted Acid-Mediated Reactions with 2-Alkynylanilines. *Molecules* 2024, *29*, 3693-3711.
- V. Morlacci, C. Momoli, M. Ndrita, M. Aschi, A. Arcadi, L. Palombi. Electrocatalytic Hydrogen Evolution Reaction Enabling Cyanation of Electron-poor Carbons with Acetone Cyanohydrin. *Eur. J. Org. Chem.* 2024, e202400236.
- L. Palombi, M. Monti, E. Scarel, V. Morlacci, M. Stener, M. Aschi. Unrevealing the Nitrogen Elusive Chirality of 3-Sulfanyl and 3-Sulfinyl N-Tosyl Isoindolinones by ECD Spectra: an Experimental and Theoretical Investigation. *Chem. Eur. J.* 2024, e202401618.

- V. Morlacci, A. Arcadi, M. Aschi, M. Chiarini, N. Demitri, D. Lamba, C. Momoli, L. Palombi, V. Vece. Diastereoselective Synthesis of High Functionalized 4-Imidazolidinone-Tetrahydro-β-Carboline Hybrids via Divergent Post-Ugi Transformation. *Adv. Synth. Cat.* 2024, *10*, 2376-2381.

- C. Momoli, V. Morlacci, M. Chiarini, L. Palombi, A. Arcadi. Friedländer-Type Reaction of 4-Cholesten-3-one with 2′-Aminoacetophenone: Angular versus Linear Quinoline-Fused Steroids. *Molbank* 2023, M1712.

- A. Arcadi, V. Morlacci, L. Palombi. Synthesis of Nitrogen-Containing Heterocyclic Scaffolds through Sequential Reactions of Aminoalkynes with Carbonyls. *Molecules* 2023, *28*, 4725-4767.

- V. Morlacci, T. Caruso, M. Chiarini, V. Marsicano, A. Arcadi, L. Palombi. On Route to Diverse Nitrogen-Bridged Polyhetero-cycles with an *N* (acyl), *N* (aryl)-acetal Core. *Chem. Sel.* 2023, e202301439.

- V. Morlacci, M. Aschi, M. Chiarini, A. Massa, A. Arcadi, L. Palombi. Ethyl 2-(12-Oxo-10, 12-dihydroisoindolo [1, 2-*b*] Quinazolin-10-yl) Acetate. *Molbank* 2023, M1628.

- V. Morlacci, T. Caruso, M. Chiarini, A. Arcadi, M. Aschi, L. Palombi. Electrochemical-Induced Cascade Reaction of 2-Formyl Benzonitrile with Anilines: Synthesis of *N*-Aryl Isoindolinones. *Molecules* 2022, *27*, 8199-8212.

Acknowledgements

I would like to begin this report by expressing my heartfelt gratitude to my supervisor, Prof. Laura Palombi, whose guidance, encouragement, and insightful advice have been invaluable throughout my doctoral journey. Her support has been instrumental in helping me navigate challenges and achieve milestones, and I am deeply thankful for her mentorship.

I am also sincerely grateful to Prof. Antonio Arcadi, whose expertise and feedback have significantly contributed to my academic and professional growth.

My warmest thanks go as well to my host supervisor, Prof. Kevin Lam, for the wonderful time I spent in his laboratory. His guidance and the fantastic lab environment made my experience immensely enriching and memorable.

Finally, I extend my appreciation to all the professors and colleagues in the department who have fostered an atmosphere of collaboration and learning, enriching my personal and professional development in countless ways. This period has given me the opportunity to meet true friends, whom I will always carry with me.

I would like to express my deepest gratitude to my girlfriend, Giulia, for her unwavering support, encouragement, and for standing by my side in all my choices. I am also profoundly thankful to my family, whose unconditional love and help have been the foundation of my perseverance.

This journey has been truly remarkable, and I am immensely grateful for the opportunity to work and grow alongside all of you.

valerio.morlacci@graduate.univaq.it

Viale di Pescina Gagliarda 102, Rome, Italy

+393317255761

VALERIO MORLACCI

Postdoctoral Researcher

PROFILE

I am a highly motivated and dynamic person with a strong work ethic and a high degree of adaptability. I actively seek out opportunities for learn and improvement, and I enjoy sharing my knowledge while collaborating in dynamic environments.

WORK EXPERIENCE

Postdoctoral Researcher - Università di Parma - SynCat Lab

Jan 2025– Present

Supervisors: Prof. Nicola Della Cà and Prof. Luca Capaldo

- Development of photochemical and electrochemical methods for carbonylation and decarbonylation reactions.

Researcher - Università degli Studi dell'Aquila

Dec 2024 – Jan 2025

Supervisor: Prof. Laura Palombi

- Development of new electrochemical pathways for the generation of carbocations.

PhD Candidate - Università degli Studi dell'Aquila

Nov 2021 – Nov 2024

Supervisor: Prof. Laura Palombi

- Development of new synthetic pathways for the preparation of heterocyclic derivatives *via* electrocatalysis and greener alternatives.
- Electro-induced cyanation reactions.

Visiting PhD Candidate - University of Greenwich

Jan 2024 – Jun 2024

Host Supervisor: Prof. Kevin Lam

- Electrochemical cyanation reactions using a new and safer cyanide surrogate, studying the scalability in flow-electrochemical system.
- Electrochemical etherification strategy to synthetise sterically hindered dialkyl ethers.

LANGUAGES

English: B2

SKILLS

- Multi-step synthesis
- Electrocatalysis/Electrosynthesis
- Flow chemistry
- Purification *via* flash chromatography, re-cristallization
- Characterization instruments: NMR, IR, HPLC, GC-MS, UV

DIGITAL SKILLS

- Microsoft Office
- MestreNova
- TopSpin
- ChemDraw
- Canva

SOFT SKILLS

- Team working
- Planning skills
- Problem solving
- Adaptability
- Communication skills

EDUCATION

Master's Degree in Chemistry - Università di Roma "La Sapienza"

2018-2021 (110/110 e Lode)
Supervisor: Prof. Andrea D'Annibale

- Multi-step synthesis of bile acid derivatives as potential ion receptors.

Bachelor's Degree in Chemistry - Università di Roma "La Sapienza"

2015-2018 (101/110)
Supervisor: Prof. Andrea D'Annibale

PUBBLICATIONS

- C. Momoli, A. Arcadi, M. Chiarini, V. Morlacci, L. Palombi, *under revision*.
- C. Kiaku, S. Kaltenberger, D. Raydan, V. Morlacci, B. Claringbold, I. C. A. Goodall, L. Palombi, D. L. Poole, K. Lam, *Org. Lett.* **2025**, *27*, 147–152.
- V. Morlacci, M. Milia, J. Saiter, I. Pret Bhela, M. Leech, K. Lam, *JACS Au* **2024**, 4, 4199–4205.
- C. Momoli, A. Lamenta, M. Charini, N. Demitri, D. Lamba, V. Morlacci, L. Palombi, A. Arcadi, *J. Org. Chem.* **2024**, *89*, 16828–16837.
- V. Morlacci, M. Aschi, M. Chiarini, C. Momoli, L. Palombi, A. Arcadi, *Molecules* **2024**, *29*, 3693.
- V. Morlacci, C. Momoli, M. Ndrita, M. Aschi, A. Arcadi, L. Palombi, *Eur. J. Org. Chem.* **2024**, e202400236.
- L. Palombi, M. Monti, E. Scarel, V. Morlacci, M. Stener, M. Aschi, *Chem. Eur. J.* **2024**, e202401618.
- V. Morlacci, A. Arcadi, M. Aschi, M. Chiarini, N. Demitri, D. Lamba, C. Momoli, L. Palombi, V. Vece, *Adv. Synth. Cat.* **2024**, 10, 2376-2381.
- C. Momoli, V. Morlacci, M. Chiarini, L. Palombi, A. Arcadi, *Molbank* **2023**, M1712.
- A. Arcadi, V. Morlacci, L. Palombi, *Molecules* **2023**, 28, 4725.
- V. Morlacci, T. Caruso, M. Chiarini, V. Marsicano, A. Arcadi, L. Palombi, *ChemistrySelect* **2023**, e202301439.
- V. Morlacci, M. Aschi, M. Chiarini, A. Massa, A. Arcadi, L. Palombi, *Molbank* **2023**, M1628.
- V. Morlacci, T. Caruso, M. Chiarini, A. Arcadi, M. Aschi, L. Palombi, *Molecules* **2022**, 27, 8199.

Parma, 10/02/2025

Valerio Morlacci